

Machinability Studies of Ti-6Al-4V Alloy Using Novel Minimal Solid Lubricant Mixture Application Method

THESIS

Submitted in partial fulfilment
of the requirements for the degree of

DOCTOR OF PHILOSOPHY

by

Rakesh Kumar G

ID. No. 2013PHXF0009H

Under the Supervision of

Prof. SURESH KUMAR REDDY NARALA



BITS Pilani
Pilani | Dubai | Goa | Hyderabad

BIRLA INSTITUTE OF TECHNOLOGY AND SCIENCE, PILANI

2018

BIRLA INSTITUTE OF TECHNOLOGY AND SCIENCE, PILANI

CERTIFICATE

This is to certify that the thesis entitled “**Machinability Studies of Ti-6Al-4V Alloy Using Novel Minimal Solid Lubricant Mixture Application Method**” and submitted by **Rakesh Kumar G**, ID No. **2013PHXF0009H** for award of Ph.D. of the Institute embodies original work done by him under my supervision.

Signature of the Supervisor:

Name in capital letters:

SURESH KUMAR REDDY NARALA

Designation:

Associate Professor

Department of Mechanical Engineering

BITS-Pilani Hyderabad Campus, Jawahar Nagar

Shameerpet (Mandal), Hyderabad – 500 078

Telangana, India.

Date:

Acknowledgement

I would like to express my sincere gratitude to my advisor **Prof. N. Suresh Kumar Reddy** for indispensable role, remarkable guidance, valuable suggestions, fruitful discussions, encouraging criticism and continuous support showered on me from the very first day I met him, till the final completion of the thesis. The greatest way to appreciate his generosity would be following the lessons I learnt from him which will be path maker of mine in future.

I am thankful to **Department of Science and Technology** (DST), Govt. of India for their project grant SR/S3/MERC/0031/2012, extending their financial support which helped me in procuring the work material and test facilities to conduct the research.

I am thankful to **Prof. Souvik Bhattacharyya** current Vice-Chancellor and **Prof. B. N. Jain**, former Vice-Chancellor, BITS-Pilani, Hyderabad Campus for providing me this opportunity to pursue the on-campus Ph.D. of this institute.

I am thankful to **Prof. G. Sundar**, current Director and **Prof. V. S. Rao**, former Director, BITS-Pilani, Hyderabad Campus for providing me this opportunity to pursue the on-campus Ph.D. of this institute.

My special thanks to **Prof. Amit Kumar Gupta**, current HOD and **Prof. Y. V. Daseswara Rao**, former HOD, for permitting me to carry out my research work in the Mechanical Engineering Department.

My sincere thanks to my Doctorial Advisory Committee (DAC) members, **Prof. Srinivas Prakash Regalla**, and **Dr. R. Sujith**, Mechanical Engineering Department, BITS Pilani, Hyderabad Campus for their time, comments and suggestions.

I am thankful to the entire faculty and staff of Mechanical Engineering Department BITS Pilani, Hyderabad Campus for their kind support and assistance.

I am thankful to **Prof. P. Yogeeswari**, Associate Dean, SRCD, **Prof. Vidya Rajesh**, Associate Dean, ARD and **Prof. Chittaranjan Hota**, Associate Dean, IPCD, BITS Pilani, Hyderabad Campus for their support to my research work.

I wish to express my sincere thanks to **Mr. J. Sravan Kumar** for his kind support, discussions and friendship throughout this study. I would like to acknowledge his contribution in performing experiments for lubricant film thickness measurement for this study. I would like to thank to **Dr. P. Umamaheshwera Reddy** for his co-operation and discussion for his support and suggestions to carry out this work effectively. I wish to extend my gratitude to **Mr. S.D. Amar** and **Mr. Pavandatta Jadhav** for proof reading.

I express my sincere thanks to **Mr. Praveen Kumar** and **Mrs. Bhagya Laxmi**, SRCD division for their cooperation during my Ph.D. work.

I extend my thanks to our lab technicians **Mr. C. Bali Reddy**, **Mr. M. Narsing Rao**, **Mr. P. Sridhar**, and **Mr. P. Mahender Chary** for helping me in conducting experiments in central workshop. My sincere thanks are due to all my colleagues at BITS Pilani, Hyderabad Campus, for their whole hearted support and cooperation who directly and indirectly contributed in the completion of this work.

I am extremely grateful to our laboratory assistants, **Mr. B. Suryanarayana**, **Mrs. N. Jagadishwar Reddy** and **Mr. B. Laxman**, Mechanical Engineering Department for their cooperation during my Ph.D. work

At the end, but from my heart, I thank and deeply appreciate my family **Mr. G. Rajalingam** (Father), **Mrs. G. Pushpamma** (Mother) and **Mrs. K. Uma Devi**, **Mrs. M. Anuradha** and **Mrs. G. Saritha** (Sisters) for their faith in me and for continuous support. It was under their influence I gained so much drive and an ability to tackle challenges head on. No words can express how grateful I am for their love and support.

Last but not the least, for the immense shower of blessings for timely accomplishment of the work in a presentable manner to the level of my satisfaction I must thank the “Almighty”, to whom I always surrender.

To those I may have Wronged,

I ask Forgiveness.

To those I may have Helped,

I wish I did More.

To those I Neglected to help,

I ask for Understanding.

To those who helped me,

I sincerely Thank you

So much...

Date:

Rakesh Kumar G

ABSTRACT

The growing demand for higher productivity, product quality and overall economy in manufacturing by machining, particularly to meet the challenges thrown by liberalization and global cost competitiveness, insists high material removal rate, high stability and long life of cutting tools. However, machining of advanced engineering materials like Ti-6Al-4V alloys is intrinsically associated with high heat and cutting temperatures. In modern industry, mechanical parts are subjected to friction and wear, leading to heat generation, which affects the reliability, life and power consumption of machinery. Although cutting fluids are employed to control the high machining zone temperatures, their usage possesses health hazards and in addition leading to higher machining cost. To encounter this problem, in recent years, solid lubricant assisted machining concept has been introduced to achieve enhanced lubricity and increased tool life in demanding tribological applications.

This work attempts to fill some of the gaps in contemporary research in improving the machining performance. On the experimental front, in the first phase an attempt has been made to investigate and evaluate the tribological (friction and wear) characteristics of various solid lubricants like molybdenum disulfide (MoS_2), graphite and boric acid at different sliding conditions. An experimental set-up has been developed for effective supply of solid lubricants to the pin-disc interface zone. The results show that friction coefficient increases with increase in applied load for all the considered environments. The tribological properties with MoS_2 solid lubricant exhibit larger load carrying capacity than that of graphite and boric acid. Very few and sparse efforts have been made to investigate the role of solid lubricant film thickness and its measurements during sliding condition. This research work is carried out with an aim to develop optimum MoS_2 solid lubricant suspension with different weight fractions and particle size to

analyze the tribological properties to assess its suitability for various industrial machining applications. To accomplish this, an experimental set-up has been developed to examine and measure the lubricant film thickness at various particle size and concentration of solid lubricants. A four-ball tester machine is used to assess the wear prevention (WP) and extreme pressure (EP) properties of lubrication oils. Experiments were performed on four-ball tester to determine WP properties and EP properties of solid lubricant additives of lubricated sliding surfaces using a variation of standard ASTM D2783 (WP test) and ASTM D4172 (EP test). The results obtained from the experiments showed that use of MoS₂ solid lubricants with lesser particle size provided effective thin film thickness in comparison to solid lubricants with large particle size. Results revealed that optimum particle size and concentration of suspended MoS₂ solid lubricants in base oil improve the tribological properties with an intended life time of the surfaces.

Hard turning is associated with high heat generation at tool-chip interface zone causing an adverse effect on the surface quality of the final product. The current investigation deals with studies concentrated on the usage of MoS₂ as solid lubricant in order to reduce friction coefficient for improving the machining process performance. In this direction, in the present research work, the feasibility of a novel approach for developing a new generation of machining technique namely electrostatic high velocity solid lubricant (EHVSL) experimental set-up has been envisaged with an aim to improve process performance and to eliminate cutting fluid usage in machining process. To investigate the role of developed EHVSL system, turning experiments are conducted on Ti-6Al-4V alloy at varying speed, feed and depth of cut considering surface roughness, cutting force and tool wear as performance indices. A detailed comparison has been made with other cooling techniques like minimum quantity solid lubricant (MQSL), minimum quantity lubricant (MQL), wet and dry cutting conditions using carbide cutting tool inserts with

an objective to reduce overall machining cost and improve machining performance. Results indicate that EHVSL with supplying MoS₂ solid lubricant mixture at a constant flow rate and lower volume results in a better penetration of solid lubricants into the tool-chip-workpiece interface, achieving improved surface roughness and long life of the cutting tool more effectively than MQSL, MQL, wet and dry machining at high cutting speed conditions.

In order to reduce the cutting temperature in the machining process, lubricant must adequately cover the tool-chip-workpiece interface. Different process parameters (air pressure, quantity of lubrication, position of nozzle, and nozzle distance) of the developed EHVSL spray method have various effects on the machinability performance. The cutting force and surface roughness, which are closely related to lubrication and coolant, play significant role in improving/reducing the machinability of a workpiece and extending/shortening the tool life. This work investigates the effect of optimum machining process parameters. The results revealed that the penetration ability of EHVSL spray system has a significant effect on cutting force and surface roughness. It was observed that when the nozzle tip spraying distance and compressor air pressure were either too large or too small, it is not effective for lubricant mist to penetrate into the tool-chip and tool-workpiece interface zone. The nozzle position (spraying angle) has found minimum impact on penetration ability of lubricants in the contact zone. Further, effective delivery of sufficient amount of solid lubricant to high temperature zone is the most important part of EHVSL application.

Modeling of machining process to associate/predict cutting parameters with cutting performance is very important for the manufacturing industry. Optimization of machining process is an essential part in improving the performance of machining since these parameters majorly influence on production cost, quality and time of the finished products. Due to wide

spread application of sophisticated and highly automated machine tools, manufacturing industries constantly seek for models and methods that are highly reliable for predicting the machining process performance. Group Method of Data Handling (GMDH) technique has been used for correlating interactions of various cutting parameters on surface roughness during turning operation. Consequently such a self-organizing modelling approach is useful in both modeling and prediction in an advanced manufacturing system where it is necessary to model and predict the surface roughness during machining operations.

The current research work also includes modeling of metal cutting process and its simulation to comprehend physical cutting process variables, such as, cutting force, and chip thickness by relating the same with practical conditions during dry and lubricant machining conditions. A 2D (two dimensional) finite element model was developed for orthogonal machining process for the current study. A Johnson-Cook material model with an energy-based ductile failure criterion is presented to predict Ti-6Al-4V alloy with the effect of different coolant supply strategy (dry, lubricant) on cutting performance in turning process. A comparison between experimental and predicted cutting force and chip thickness at varying speed and feed conditions was proposed and discussed. The results showed a good agreement with the predicted cutting force and chip thickness with varying friction coefficient at tool-chip interface.

The present research work is expected to form a scientific basis towards developing EHVSL technique for reducing the impact of difficulty in the machining of aerospace components made of difficult-to-machine materials like Ti-6Al-4V alloy in terms of both machinability and environmental perspectives.

Keywords: Ti-6Al-4V alloy, solid lubricant, friction, wear, FEM simulation, Abaqus/Explicit, cutting force, surface roughness, tool wear.

Table of Contents

CERTIFICATE.....	I
ACKNOWLEDGEMENTS.....	II
ABSTRACT.....	V
TABLE OF CONTENTS.....	IX
LIST OF TABLES.....	XIV
LIST OF FIGURES.....	XVI
LIST OF ABBREVIATIONS.....	XXII
LIST OF SYMBOLS.....	XXIV
CHAPTER 1 INTRODUCTION.....	1-17
1.1. BACKGROUND.....	1
1.2. AIM AND SCOPE OF PRESENT WORK.....	10
1.3. THE OBJECTIVES OF PRESENT WORK.....	12
1.4. METHODOLOGY.....	13
1.5. OVER VIEW OF THESIS.....	14
1.6. ORGANIZATION OF DISSERTATION.....	16
CHAPTER 2 LITERATURE REVIEW.....	18-54
2.1. INTRODUCTION.....	18
2.2. TYPES OF CUTTING FLUIDS AND THEIR PERFORMANCE.....	22
2.2.1. EFFECT OF WET LUBRICANT (FLOOD COOLING) IN THE MACHINING PROCESS.....	22
2.2.2. EFFECT OF DRY MACHINING.....	25
2.2.3 EFFECT OF MINIMUM QUANTITY LUBRICANT IN MACHINING PROCESS.....	27
2.2.4 EFFECT OF SOLID LUBRICANT ASSISTED MACHINING IN THE MACHINING PROCESS.....	31
2.3. TRIBOLOGICAL CHARACTERISTICS OF SOLID LUBRICANTS.....	39
2.4. GROUP METHOD OF DATA HANDLING.....	44
2.5. FINITE ELEMENT MODELLING APPROACH FOR MACHINING PROCESS.....	47
2.6. IDENTIFIED GAPS IN THE LITERATURE AND THESIS CONTRIBUTION.....	51
2.7. SUMMARY.....	53

CHAPTER 3 DEVELOPMENT OF ELECTROSTATIC HIGH VELOCITY SOLID LUBRICANT SPRAY SYSTEM.....	55-94
3.1. INTRODUCTION.....	55
3.2. DEVELOPMENT OF EHVSL EXPERIMENTAL SET-UP.....	58
3.2.1. ELECTROSTATIC HIGH VELOCITY SOLID LUBRICANT SET-UP.....	58
3.2.2. ELECTROSTATIC HIGH VELOCITY SOLID LUBRICANT PROCESS.....	60
3.2.3. NOZZLE.....	61
3.2.4. SYRINGE PUMP.....	63
3.2.5. HIGH VOLTAGE SYSTEM.....	63
3.3. STRUCTURE OF EHVSL SPRAY SYSTEM.....	64
3.4. ELECTROSTATIC CHARGED PROPERTIES.....	67
3.5. OTHER TOOLS AND EQUIPMENT.....	68
3.5.1. FORCE MEASUREMENT.....	68
3.5.1.1. DYNAMOMETER.....	68
3.5.1.2. CHARGE AMPLIFIER.....	70
3.5.1.3. ACQUIRING/ANALYZING SOFTWARE.....	71
3.5.2. PRECISION BALANCE.....	71
3.5.3. SURFACE ROUGHNESS MEASUREMENT.....	71
3.5.4. COMPUTER NUMERICAL CONTROL (CNC) TURNING MACHINE.....	73
3.5.5. INFRARED & THERMAL IMAGING CAMERA.....	73
3.6. EXPERIMENTAL DETAILS.....	74
3.6.1. WORKPIECE MATERIAL.....	75
3.6.2. SOLID LUBRICANT ADDITIVE.....	75
3.6.3. BASE OIL.....	76
3.6.4. PLANNING OF EXPERIMENTAL CONDITION.....	77
3.6.4.1. SELECTION OF PROCESS PARAMETERS.....	77
3.6.4.2. DESIGN OF EXPERIMENTS.....	77
3.6.5. EXPERIMENTAL PROCEDURE.....	78
3.6.6. SOFTWARE FOR ANALYSIS OF RESULTS.....	79
3.7. OPTIMAL PROCESS PARAMETERS FOR EHVSL ASSISTED MACHINING.....	80
3.8. EXPERIMENT DETAILS.....	81

3.9. RESULTS AND DISCUSSIONS.....	82
3.9.1. EFFECT OF AIR PRESSURE.....	82
3.9.2. EFFECT OF SPRAYING DISTANCE.....	84
3.9.3. EFFECT OF SPRAYING ANGLE.....	86
3.9.4. EFFECT OF SOLID LUBRICANT FLOW RATE.....	88
3.9.5. ANALYSIS OF DROPLET QUALITY WITH VARYING FLOW RATE.....	90
3.9.6. EFFECT OF ELECTROSTATIC VOLTAGE.....	91
3.10. SUMMARY.....	93
CHAPTER 4 TRIBOLOGICAL STUDIES TO ANALYZE THE EFFECT OF SOLID LUBRICANTS.....	95-138
4.1. INTRODUCTION.....	95
4.2. EXPERIMENTAL DETAILS AND OPERATING CONDITIONS.....	96
4.2.1. MATERIALS.....	96
4.2.2. BASE OIL.....	97
4.2.3. SOLID LUBRICANT ADDITIVES.....	97
4.2.4. PREPARATION OF SOLID LUBRICANTS.....	98
4.2.5. PROPERTIES OF LUBRICANTS.....	98
4.2.6. TRIBOLOGICAL STUDIES ON PIN-ON-DISK TRIBOMETER.....	99
4.2.7. ELECTRICAL CONTACT POTENTIAL.....	101
4.2.8. CHARACTERIZATION OF THIN FLUID FILM MEASUREMENT ON PIN-DISC INTERFACE....	102
4.2.8.1. SOLID LUBRICANT FILM THICKNESS MEASUREMENT PROCEDURE.....	102
4.2.8.2. SOLID LUBRICANT FILM THICKNESS OBSERVATION PROCEDURE.....	103
4.3. TRIBOLOGICAL STUDIES ON FOUR-BALL TESTER.....	104
4.3.1. MATERIAL.....	105
4.3.2. TEST FLUID.....	105
4.3.3. ADDITIVES.....	105
4.3.4. EXPERIMENTAL PROCEDURE.....	105
4.3.4.1. WEAR PREVENTION TEST.....	107
4.3.4.2. EXTREME PRESSURE TEST.....	107
4.4. RESULTS AND DISCUSSIONS.....	108
4.4.1. SOLID LUBRICANT SUSPENSION PROPERTIES.....	109

4.4.2. ANALYSIS OF FRICTION COEFFICIENT, WEAR RATE AND CONTACT TEMPERATURE.....	110
4.4.3. ANALYSIS OF WEAR MORPHOLOGY.....	117
4.4.4. CONTACT POTENTIAL MEASUREMENT OF SOLID LUBRICANT FILM THICKNESS.....	120
4.4.5. ANALYSIS OF MoS ₂ SOLID LUBRICANT FILM THICKNESS.....	122
4.4.6. ANALYSIS OF FRICTION COEFFICIENT AND WEAR.....	126
4.4.7. ELECTRICAL CONTACT POTENTIAL.....	130
4.4.8. ANALYSIS OF EXTREME PRESSURE PROPERTIES.....	132
4.4.9. ANALYSIS OF WEAR PROPERTIES.....	135
4.5. SUMMARY.....	137
CHAPTER 5 ELECTROSTATIC HIGH VELOCITY SOLID LUBRICANT MACHINING SYSTEM FOR PERFORMANCE IMPROVEMENT OF TURNING Ti-6Al-4V ALLOY.....	139-178
5.1. INTRODUCTION.....	139
5.2. RESULTS AND DISCUSSIONS.....	142
5.2.1. EFFECT OF EHVSL ON CUTTING FORCE.....	142
5.2.2. EFFECT OF EHVSL ON SURFACE ROUGHNESS.....	148
5.2.3. EFFECT OF EHVSL ON TOOL WEAR.....	154
5.2.4. EFFECT OF CHIP THICKNESS.....	162
5.3. SURFACE ROUGHNESS ESTIMATION BY GROUP METHOD OF DATA HANDLING (GMDH) TECHNIQUE FOR EHVSL MACHINING CONDITION.....	164
5.4. COMPARISON OF PREDICTED AND MEASURED SURFACE ROUGHNESS USING GMDH.....	170
5.5. SUMMARY.....	177
CHAPTER 6 FINITE ELEMENT MODELLING AND SIMULATION OF MACHINING Ti-6Al-4V ALLOY.....	179-200
6.1. INTRODUCTION.....	179
6.2. FE MODELLING OF THE ORTHOGONAL MACHINING PROCESS.....	182
6.2.1. MODELING OF WORKPIECE AND CUTTING TOOL MATERIALS.....	182
6.2.2. CONSTITUTIVE MODEL FOR WORK MATERIAL.....	183
6.2.3. DAMAGE MODEL.....	185
6.2.4. FE MACHINING SIMULATION PROCEDURE.....	186
6.2.5. FEA MODELLING AND SIMULATION OF ORTHOGONAL TURNING.....	187

6.3. SIMULATION RESULTS AND DISCUSSIONS.....	188
6.3.1. EFFECT OF CUTTING FORCE.....	188
6.3.2. EFFECT OF CHIP THICKNESS.....	195
6.4. SUMMARY.....	200
CHAPTER 7 CONCLUSIONS AND FUTURE WORK.....	201-203
7.1. SUMMARY.....	201
7.2. MAJOR CONTRIBUTION.....	203
7.3. SCOPE OF FEATURE WORK.....	207
REFERENCES.....	208-222
LIST OF PUBLICATIONS.....	223-220
BIOGRAPHY OF THE CANDIDATE.....	225
BIOGRAPHY OF THE SUPERVISOR.....	226

List of Tables

Table 3.1: Specifications of dynamometer	69
Table 3.2: Specifications of a charge amplifier	70
Table 3.3: Specifications of Talysurf profilometer	72
Table 3.4: Specifications of CNC lathe machine	73
Table 3.5: FLIR E60 Infrared Camera specifications	74
Table 3.6: Chemical composition of Ti-6Al-4V alloy	75
Table 3.7: Properties of base oil (SAE 40)	76
Table 3.8: Process variables and their levels	78
Table 3.9: 3 ³ Factorial design matrix for experimentation	78
Table 4.1: Chemical composition of Ti-6Al-4V alloy	97
Table 4.2: Spray parameters	100
Table 4.3: Film thickness test parameters	104
Table 4.4: Chemical composition of Chromium steel ball material	105
Table 4.5: ASTM D 2783 standards for extreme pressure condition	108
Table 4.6: Kinematic viscosity (cSt) of MoS ₂ solid lubricants with varying wt% concentrations	109
Table 4.7: Kinematic viscosity (cSt) of graphite solid lubricants with varying wt% concentrations	109
Table 4.8: Kinematic viscosity (cSt) of boric acid solid lubricants with varying wt% concentrations	110
Table 5.1: Machining performance of Ti-6Al-4V alloy under different cutting parameters	169
Table 5.2: Measured and predicted surface roughness estimation for different criteria using GMDH for Ti-6Al-4V alloy	173
Table 6.1: Mechanical and thermo-physical properties of workpiece and cutting tool used in FE simulations	183

Table 6.2: Ti-6Al-4V material constants for J–C constitutive model	184
Table 6.3: J-C failure parameters for Ti-6Al-4V alloy	186

List of Figures

Fig. 1.1: Structure of the thesis	17
Fig. 2.1: Heat generation in machining process in primary deformation and secondary deformation zone	19
Fig. 2.2: Flood cooling system in machining process	23
Fig. 2.3: Machining cost breakdown	24
Fig. 2.4: Machining with MQL system	28
Fig. 2.5: Schematic view of MQL technique	28
Fig. 2.6: Schematic diagram of MQSL experimental set-up	32
Fig. 3.1: Photographic view of developed electrostatic high velocity solid lubricant spray system	58
Fig. 3.2: Schematic illustration of the EHVSL spraying setup	59
Fig. 3.3: Schematic diagram of nozzle	62
Fig. 3.4: Photographic view of syringe pump	63
Fig. 3.5: High voltage power supply system	64
Fig. 3.6: Schematic view of nozzle with EHVSL spray system	65
Fig. 3.7: Components of typical electrostatic lubricant process	66
Fig. 3.8: Schematic view of EHVSL with cloud of tiny charged solid lubricant particles	67
Fig. 3.9: Schematic view of lathe tool dynamometer	69
Fig. 3.10: Photographic view of weighing balance during weighing solid lubricant samples	71
Fig. 3.11: A sample measure of surface finish on machined work material using surface profilometer (Taylor Hobson Surtronic S25)	72
Fig. 3.12: FLIR E60 Infrared thermal imaging camera	74
Fig. 3.13: Effect of cutting force with different air pressure	83
Fig. 3.14: Variation of surface roughness under different air pressure	83
Fig. 3.15: Effect of cutting force under different nozzle distance	85
Fig. 3.16: Variation of surface roughness under different nozzle distance	85
Fig. 3.17: Effect of cutting force under different nozzle positions	87

Fig. 3.18: Variation of surface roughness at different nozzle position	87
Fig. 3.19: Effect of cutting force with different flow-rates of solid lubricant	88
Fig. 3.20: Variation of surface roughness with different flow-rate of solid lubricant	89
Fig. 3.21: Average droplet particle size and number of droplets	91
Fig. 3.22: Effect of cutting force with different charging voltages	92
Fig. 3.23: Variation of surface roughness with different charge voltage	92
Fig. 4.1: Schematic view of Pin-on-disc wear and friction monitor	97
Fig. 4.2: Pin-on-disc experimental set-up	99
Fig. 4.3: Schematic drawing of the electric contact resistance	102
Fig. 4.4: Experimental set-up for lubricant film thickness measurement	103
Fig. 4.5: Stationary steel balls mounted on the cup	104
Fig. 4.6: A schematic view of four-ball test machine	106
Fig. 4.7: Coefficient of friction vs Normal load at various speed conditions (a) 100 m/min (b) 150 m/min (c) 200 m/min	112
Fig. 4.8: Wear rate vs Normal load at various speed conditions (a) 100 m/min (b) 150 m/min (c) 200 m/min	115
Fig. 4.9: Temperature vs Normal load at various speed conditions (a) 100 m/min (b) 150 m/min (c) 200 m/min	116
Fig. 4.10: Microscopic images of wear track of disc during MoS ₂ solid lubricants sliding condition (a) 10 N loads (b) 30 N load (c) 50 N load	118
Fig. 4.11: Microscopic images of wear track of disc during graphite solid lubricant sliding condition (a) 10 N (b) 30 N (c) 50 N	118
Fig. 4.12: Microscopic images of wear track of disc during boric acid solid lubricant sliding condition (a) 10 N (b) 30 N (c) 50 N	119
Fig. 4.13: Microscopic images of wear track of disc during dry sliding condition (a) 10 N (b) 30 N (c) 50 N	119
Fig. 4.14: Electric contact potential technique vs Normal load at various speed conditions (a) 100 m/min (b) 150 m/min (c) 200 m/min	121
Fig. 4.15: MoS ₂ lubricant film formation between pin and disc surface	123
Fig. 4.16: Average film thickness measurement for various particle size and concentration (a) 10 Microns, (b) 30 Microns (c) 50 Microns	124

Fig. 4.17: Friction coefficient vs sliding time with respect to particle size and concentration (a) 10 μm (b) 30 μm (c) 50 μm	127
Fig. 4.18: Wear vs sliding time of solid lubricants at different particle size and concentration (a) 10 μm (b) 30 μm (c) 50 μm	129
Fig. 4.19: Electrical contact potential vs sliding time of MoS ₂ with various particle size and concentration (a) 10 μm (b) 30 μm (c) 50 μm	131
Fig. 4.20: Effect of load (kg) carrying capacity of MoS ₂ at different particle size and concentration (a) 10 μm (b) 30 μm (c) 50 μm	133
Fig. 4.21: Friction coefficient and WSD for various concentrations of solid lubricant	135
Fig. 4.22: Microscopic images of worn surface of stationary steel balls at various concentrations	136
Fig. 5.1: Line diagram of developed Electrostatic High Velocity Solid Lubricant spray system	141
Fig. 5.2: Cutting force at cutting speed = 100, 150, 200 m/min, (a) Feed = 0.1, (b) Feed = 0.15, (c) Feed = 0.2 mm/rev under different environments (depth of cut = 0.5 mm)	143
Fig. 5.3: Cutting force at cutting speed = 100, 150, 200 m/min, (a) Feed = 0.1, (b) Feed = 0.15, (c) Feed = 0.2 mm/rev under different environments (depth of cut = 1 mm)	144
Fig. 5.4: Cutting force at cutting speed = 100, 150, 200 m/min, (a) Feed = 0.1, (b) Feed = 0.15, (c) Feed = 0.2 mm/rev under different environments (depth of cut = 1.5 mm)	145
Fig. 5.5: Surface roughness at cutting speed = 100, 150, 200 m/min, (a) Feed = 0.1, (b) Feed = 0.15, (c) Feed = 0.2 mm/rev under different environments (depth of cut = 0.5 mm)	149
Fig. 5.6: Surface roughness at cutting speed = 100, 150, 200 m/min, (a) Feed = 0.1, (b) Feed = 0.15, (c) Feed = 0.2 mm/rev under different environments (depth of cut = 1 mm)	150
Fig. 5.7: Surface roughness at cutting speed = 100, 150, 200 m/min, (a) Feed = 0.1, (b) Feed = 0.15, (c) Feed = 0.2 mm/rev under different environments (depth of cut = 1.5 mm)	151

Fig. 5.8: Tool wear at cutting speed = 100, 150, 200 m/min, (a) Feed = 0.1, (b) Feed = 0.15, (c) Feed = 0.2 mm/rev under different environments (depth of cut = 0.5 mm)	155
Fig. 5.9: Tool wear at cutting speed = 100, 150, 200 m/min, (a) Feed = 0.1, (b) Feed = 0.15, (c) Feed = 0.2 mm/rev under different environments (depth of cut = 1 mm)	156
Fig. 5.10: Tool wear at cutting speed = 100, 150, 200 m/min, (a) Feed = 0.1, (b) Feed = 0.15, (c) Feed = 0.2 mm/rev under different environments (depth of cut = 1.5 mm)	157
Fig. 5.11: SEM images of cutting tool in EHVSL machining condition at cutting speed 100 m/min	159
Fig. 5.12: SEM images of cutting tool in MQSL machining condition at cutting speed 100 m/min	160
Fig. 5.13: SEM images of cutting tool in wet machining condition at cutting speed 100 m/min	160
Fig. 5.14: SEM images of cutting tool in MQL machining condition at cutting speed 100 m/min	161
Fig. 5.15: SEM images of cutting tool in dry machining condition at cutting speed 100 m/min	161
Fig. 5.16: Chip thickness ratio at varying cutting speed and (a) Feed rate = 0.1 mm/rev, (b) Feed rate = 0.15 mm/rev, (c) Feed rate = 0.2 mm/rev	163
Fig. 5.17: Typical GMDH network	166
Fig. 5.18: GMDH network processing element 'm' of layer 'k'	167
Fig. 5.19: Input data for GMDH surface roughness model(R_a, v_c, f, a_p)	170
Fig. 5.20: Regularity criteria output obtained while modeling surface roughness at 75% of data	171
Fig. 5.21: Unbiased criteria output obtained while modeling surface roughness at 75% of data	171
Fig. 5.22: Combined criteria output obtained while modeling surface roughness at 75% of data	172
Fig. 5.23: Comparison of measured and predicted surface roughness at (a) 50%,	174

62.5% and 75% of experimental data in training set

Fig. 5.24: Regularity criterion model for estimation of surface roughness at 75% data in the training set at different speed, feed depth of cut conditions	176
Fig. 5.25: Unbiased criterion model for estimation of surface roughness at 75% data in the training set at different speed, feed depth of cut conditions	176
Fig. 5.26: Combined criterion model for estimation of surface roughness at 75% data in the training set at different speed, feed depth of cut conditions	177
Fig. 6.1: Input requirements for the FE model	183
Fig. 6.2: Flow chart of FEA prediction model of Ti-6Al-4V alloy machining	187
Fig. 6.3: The geometry of the 2D orthogonal cutting FE model	188
Fig. 6.4: FEM Simulation (a) chip formation (b) predicted cutting force under lubrication condition (c) comparison between experimental and simulation cutting force at different cutting speeds ($f = 0.1$ mm/rev)	189
Fig. 6.5: Comparison of experimental and FE simulated cutting force during Ti-6Al-4V alloy machining under lubricant at different cutting speeds ($f = 0.15$ mm/rev)	190
Fig. 6.6: Comparison of experimental and FE simulated cutting force during Ti-6Al-4V alloy machining under lubricant at different cutting speeds ($f = 0.2$ mm/rev)	191
Fig. 6.7: Distribution of (a) stress (b) strain and (c) temperature under lubricant condition while machining Ti-6Al-4V alloy at $V_c=100$ m/min and $f = 0.1$ mm/rev	192
Fig. 6.8: FEM Simulation (a) chip formation (b) predicted cutting force under dry condition (c) comparison between experimental and simulation cutting force at different cutting speeds ($f = 0.1$ mm/rev)	193
Fig. 6.9: Comparison of experimental and FE simulated cutting force during Ti-6Al-4V alloy machining under dry at different cutting speeds ($f = 0.15$ mm/rev)	193
Fig. 6.10: Comparison of experimental and FE simulated cutting force during Ti-6Al-4V alloy machining under dry at different cutting speeds ($f = 0.2$ mm/rev)	194

Fig. 6.11: Distribution of (a) stress (b) strain and (c) temperature under dry condition while machining Ti-6Al-4V alloy at $V_c=100$ m/min and $f = 0.1$ mm/rev	195
Fig. 6.12: (a) Comparison of simulated and experimental captured chip formation (b) comparison between experimental and simulation chip thickness under lubricant condition at different cutting speeds (cutting feed = 0.1 mm/rev)	196
Fig. 6.13: Comparison of experimental and FE simulated chip thickness during Ti-6Al-4V alloy machining under lubricant condition at different cutting speeds ($f = 0.15$ mm/rev)	197
Fig. 6.14: Comparison of experimental and FE simulated chip thickness during Ti-6Al-4V alloy machining under lubricant condition at different cutting speeds ($f = 0.2$ mm/rev)	197
Fig. 6.15: (a) Comparison of simulated and experimental captured chip formation (b) comparison between experimental and simulation chip thickness under dry condition at different cutting speeds (cutting feed = 0.1 mm/rev)	198
Fig. 6.16: Comparison of experimental and FE simulated chip thickness during Ti-6Al-4V alloy machining under dry condition at different cutting speeds ($f = 0.15$ mm/rev)	199
Fig. 6.17: Comparison of experimental and FE simulated chip thickness during Ti-6Al-4V alloy machining under dry condition at different cutting speeds ($f = 0.15$ mm/rev)	199

LIST OF ABBREVIATIONS

AISI	American iron and steel institute
ASTM	American society for testing and materials
BUE	Built up edge
CLF	Conventional cutting lubricant fluids
DEC	Dry electrostatic cooling
EHVSL	Electrostatic high velocity solid lubricant
EL	Electrostatic lubricant
EP	Extreme Pressure
FEM	Finite element method
FSL	Final Seizure Load
FSO	Full scale output
GMDH	Group Method of Data Handling
H ₃ BO ₃	Boric acid
HPC	High pressure cooling
HSM	High speed machining
HTMF	Hard turning with minimal fluid application
J-C	Johnson-Cook
LN ₂	Liquid nitrogen
MoS ₂	Molybdenum disulfide

MQL	Minimum quantity lubricant
MQSL	Minimum quantity solid lubricant
MRR	Material removal rate
MTS	Mechanical Threshold Stress
MVO	Minimum volume of oil
NDM	Near dry machining
PVD	Physical vapor deposition
S/N	Signal to noise ratio
SAE	Society of Automotive Engineers
SEM	Scanning electron microscope
SHPB	Split Hopkinson pressure bar
WP	Wear prevention
WSD	Wear scar diameter

LIST OF SYMBOLS

A, B, C, n, m	Johnson-Cook flow stress equation constants
$E, \epsilon_0, q, \epsilon_r$	Pauthenier's equation parameters
T	Current absolute temperature
kV	Kilovolt
f	Feed
\AA	Angstrom
F_c	Cutting force
F_f	Feed force
F_x	Radial thrust force
F_y	Tangential (main) cutting force
F_z	Feed force
R_a	Average surface roughness
T_m	Melting temperature
T_r	Reference temperature
V_b	Flank wear
a_p	Depth of cut
v_c	Cutting speed
σ	Flow stress
ϵ	Plastic strain
$\dot{\epsilon}$	Strain rate
μ	Coefficient of friction
τ	Shear stress

ρ	Density
γ	Rake angle
ϕ	Shear angle
μm	Micrometer
σ_n	Normal stress
$\frac{q_{\text{max}}}{m}$	Mean charge to mass ratio
$\dot{\epsilon}_0$	Reference strain rate
$\dot{\epsilon}^*$	Dimensionless strain rate

CHAPTER 1

INTRODUCTION

Contemporary manufacturing industries undergo rapid changes due to the ever increasing demands of customers for variety of reliable and sophisticated parts and products. Machining of advanced engineering materials like titanium alloys are used mostly in automobile and aerospace industries has been a topic of great curiosity for industrial production and scientific world. In modern industry, mechanical parts are subjected to friction and wear, leading to heat generation, which affects the reliability, life and power consumption of machinery. Effective cooling and lubrication in the machining zone are essential to improve friction and temperature by efficient heat dissipation which increases tool life and surface quality. New machining techniques are to be investigated to achieve this objective. Therefore, there is a need to concentrate efforts in this direction to overcome the above stated drawbacks and to look into new machining methods to achieve sustainable machining system. The current chapter describes the background, aim and scope of the present research. Research methodology, over view and organization of the thesis is also included.

1.1 Background

Machining is one of the most important and challenging tasks across the manufacturing community which involve controlled material removal from the workpiece using a cutting tool. Machining of advanced engineering materials like titanium alloys is receiving increasing attention in industrial production and scientific world. This is because of their superior physical and mechanical properties such as medium to high temperature strength, high strength-to-weight ratio, fracture and

corrosion resistance and bio-compatibility. This unique set of properties makes them ideal for a variety of engineering applications including automotive engine components, aerospace, turbines, biomedical devices, etc. However, great challenge is posed in the process of machining with poor thermal conductivity and low elongation-to-break ratio of Ti-6Al-4V alloys, because of the development of extreme temperature with relatively small tool-chip interface zone. Ezugwu and Wang [1] reported that high cutting temperature acting close to the tool-chip interface during high speed machining of Ti-6Al-4V alloy is the principal reason for rapid tool wear.

During past several decades in industries, low cutting speeds were used to reduce the possibility of high tempering of tool materials. The challenges imposed by liberalization and global cost competitiveness have led the contemporary manufacturing industries to meet the increasing demand of higher productivity, product quality and overall economy in machining processes like turning, grinding, milling, and drilling in terms of high material removal rate, high stability and long life of cutting tools [2]. With increasing demand for components with high accuracy and precision, the field of machining of high strength materials required to be significantly developed [3]. In order to achieve the present requirement of productivity and product quality, high cutting speed for hard-to-cut materials is now recognized as one of the key processes in advanced machining technology to achieve high material removal rate (MRR), increased machining accuracy, low cutting forces, decrease in workpiece distortion, increased part precision and better surface finish. Manufacturers continually strive for ways and means to achieve better quality and higher productivity in any machining operation to maintain their competitiveness. It is also required to reduce lead-time and manufacturing cost. Workpiece and cutting tool

surface undergo thermal damage due to the excessive temperature at the cutting zone. These high temperatures also have adverse effect on the metallographic properties of the machined surface.

Hard turning process is often associated with high heat generation at machining zone due to friction and plastic deformation of work material at tool-chip interface [4]. However, machinability of Ti-6Al-4V alloy is extremely complex due to its low thermal conductivity; high work hardening ratio and high chemical affinity with most of the tool materials accelerate tool wear, poor surface quality and diminish productivity [1]. Titanium alloys tend to adhere onto the tool surface due to high temperature presented at cutting edge during machining ($>1000^{\circ}\text{C}$), and at low cutting speed conditions, the built-up edge (BUE) is frequently observed [5]. High cutting forces acting in shearing zone promote high friction with high heat generation and consequently develop high temperature that accelerates tool wear [6]. Effective counter measures to govern heat generation at cutting interface is strongly required to ensure simultaneous improvement of productivity and product quality of machining operations. Thus, use of proper lubrication in machining processes is critically important to modify the conditions of contact area by effective control over frictional interaction which should ensure change in tool-chip interface and machining mechanics [7].

Application of cutting fluid in machining processes has two main objectives: (i) diminish friction by lubricating action and (ii) reduce cutting temperature by cooling action [6]. As lubricant is delivered in machining zone, cutting fluid must be present at tool-chip-workpiece interface and be active (preferably combining with the

materials) to form layers with reduced shearing strength and friction. Application of cutting fluid increases thermal convection. The combination of these lubri-cooling actions reduces tool wear, improves surface quality and augments productivity [6]. It is normal practice to use cutting fluids in large quantities while machining to exploit cooling, lubrication and chip removal. Using large quantity of cutting fluids leads to difficulties in procurement, disposal, storage and maintenance. Increase in pollution-preventing measures at a global level and consumer focus being directed towards environmental friendly products has increased pressure on industries to minimize or eliminate the cutting fluid usage [8]. Conventional metalworking fluids are not economic as they consume 7-17% of the total machining cost and eventually 16-20% of the total product cost. This percentage is quite high in contrast to the cost of cutting tool which accounts to 2-4% of total product cost. [9]. Cost of cutting fluid is often higher than cost of cutting tools. So, strict regulations on environmental protection are restrictive to the use of metalworking fluids.

Further, application of metalworking fluids extensively in machining process results in substantial volume of scrap/waste. In order to be friendly with environment like water bodies, water sources etc., use of cutting fluid and handling of its scrap/waste should be handled responsibly, through precautionary steps like prior treatment and proper handling of fluid wastes. It is worth mention the fact that the pre-treatment cost of the cutting fluid is often more than the price of the cutting fluid and since completely effective treatment is always not ensured, disposal may cause advertent contamination of water [10].

Besides the potential risk to environmental diseases caused by handling of

used cutting fluid waste stream, the use of fluids also pose serious threat to health as emphasized earlier. The statistics of National Institute for Occupational Safety and Health (NIOSH) reveal that around 12 lakh employees expose themselves to metal working fluids, working in areas like forming, machining and allied metal work. Use of cutting fluids in machining gives rise to airborne mist which has been medically linked to the workers' health concerns like respiratory illnesses and several types of cancer [11]. This makes cutting fluid usage a potential health concern of both long and short term consequences. Therefore, problems associated with these cutting fluids on environmental concerns forced manufacturers to seek possible elimination of them in order to meet the demands of environment free manufacturing. There is a tradeoff between using either dry machining or flood cooling machining [8]. In order to sustain the competition across the marketing community, one should focus on reducing the cutting cost and minimizing the associated environmental pollution [12].

However, machining without cutting fluid finds industrial acceptance only when it is possible to guarantee good surface quality without compromising the rate of MRR. Dry machining leads to poor outcome with rough surface finish and less accuracy, while cooling machining faces environmental issues and increased machining cost [8]. Few attempts were made to reduce the overall machining cost and to prevent environmental pollution while seeking to eliminate/minimize the usage of large quantity of cutting fluids and improve the machining properties (reduction in tool wear, friction, cutting force and surface roughness and improvement in metallurgical properties) during dry machining. However, cutting tools do not sustain the high heat generated at the machining zone during the machining of advanced engineering materials like Ti-6Al-4V alloy.

Machining without the use of large quantity of cutting fluid (green machining or sustainable machining or dry machining) as environmental protection is becoming increasingly important due to the apprehension about safety of environment. Dry/near dry cutting has the advantage of non-polluting atmosphere or water bodies, with reduced costs of cleaning and disposal; no hazard to health as they are non-allergic to skin [6]. To address cutting fluid penetration issue, high-pressure cooling (HPC) has been proposed for hard machining applications in which a high pressure spray of cutting fluid is directed to tool-chip interface [13]. However, HPC is a wasteful and energy-intensive cooling technique that requires both high pressures and flow rates of 70-160 bar and 2-20 l/min respectively.

To increase cooling potential beyond flood and high-pressure cooling, cryogenic cooling systems have been developed in which liquid nitrogen (LN₂) is sprayed into the tool-chip interface or into a pre-machined hole in the tool during titanium machining [14]. However, cryogenic cooling is often prohibitively expensive due to use of LN₂ which also requires high system flow rate (i.e. 0.75-4 l/min), making this process energy intensive requiring a specialized high flow rate pump [15]. Hence, there is a need to concentrate efforts in this direction to overcome the drawbacks mentioned above, and to look into new cooling and lubrication system that effectively penetrates cutting fluid into the tool-chip interface and increases tool life during titanium alloy machining while more efficiently utilizing cutting fluid and system energy. Hence, to achieve acceptable response level of cooling effect while maintaining flow rate at minimum, it is well sufficient to apply coolant to the tool-chip interface effectively by using controlled and focused jets. [6].

Increasing the productivity in any manufacturing industry through reduction in cost by the elimination of cutting fluids will decrease the environmental hazards and at the same time improving tribological properties are the main concerns. Accordingly, to overcome the above drawbacks and to look into new machining methods for controlling high heat generation, and for achieving sustainable machining system, there is a need for concentrated efforts in terms of applying lubricants effectively in the machining zone. In demanding, the improvement of productivity and product quality of machining process, use of solid lubricant in the machining zone is suggested as one of the necessary alternative machining technique to apply lubricants effectively to the high temperature zone [16].

Increasing demands for more accurate and precise components with high integrity and high machining technology of hard materials need to be significantly developed. Evolution in modern machining process has identified many economic and eco-friendly solid lubricants, which are able to withstand lubricity over a wide range of concentration and temperatures. Solid lubricants are also attractive in promoting as dry machining [6]. The application of solid lubricants include free from pollution of the atmosphere which result in reduced cleaning and disposal cost and cause no danger to health as they are non-allergic to skin [8]. During the machining of AISI 1040 steel workpiece with carbide cutting insert, parameters such as cutting force, specific energy and surface roughness are improved due to the usage of solid lubricants in the machining process [17]. Also, solid lubricant assisted machining produced lower rates of tool wear when compared with dry and wet machining conditions. MoS₂ and graphite are used as coolants during milling of AISI 1045 steel. It was observed that MoS₂ served as better coolant over graphite as it resulted in

significantly lower friction values at tool-workpiece interface. [18].

Internally layer structured solid lubricant additives have broadly been studied and offer excellent machining performance in terms of improved tool life and surface roughness [8]. Solid lubricants being used as anti-wear and extreme additives in base oil, graphite and MoS₂ [18] of small size were interacted more readily with the sliding surfaces of the friction pairs to form a thin protective film, which increases anti-wear ability of sliding surface. By virtue of low shear strength of materials and their intrinsic crystalline structures, good friction and wear reduction performances were noticed, where, bonding among molecules within each layer is a strong covalent whereas every two adjacent layers are bonded together by weak Van der Waals forces [6]. A good improvement in cutting force, tool wear reduction performances was observed due to the low shear strength of the materials as a result of their intrinsic crystal structure [17 &18]. Substantial improvement was observed in the tribological properties of the base-oil as a consequence of application of solid lubricants on the sliding interface [4].

Solid lubricants with thin film formation can adequately work under extreme conditions of temperature, load and speed [18]. Use of solid lubricant suspension with thin viscous lubricant along with sliding interface can effectively work under extreme conditions. [8]. To achieve improved performance in terms of better tool life and surface roughness, solid lubricants need to be applied effectively at the tool-chip interface [6,8 & 16-18]. Solid lubricants are also attractive in promoting dry machining and environment-friendly process.

Turning is of utmost importance in manufacturing industries like aerospace,

automotive, and forging sectors that give significant importance to surface roughness of the final product. Surface roughness plays a crucial role in the machining process as it significantly impacts on friction coefficient, fatigue strength and wear and corrosion resistance of the machined surface. However, there are several factors in the machining process that influence surface roughness, such as, feed rate, cutting speed, depth of cut, cutting tool, use of coolants etc. [19].

Modeling of turning process has been an important research issue for nearly a century. The prediction of surface roughness is a major task in the optimization of the cutting process. To develop a new model for predicting the surface roughness, it is vital to comprehend the various methods that are being used to estimate the surface roughness. Due to the extensive use of high automation in the machine tool industry, a system to predict machining parameters is important in manufacturing process.

The prediction of optimal cutting condition for higher productivity, good surface quality, dimensional accuracy and cost saving products plays a key role in process planning. Higher MRR would increase production but, if increased beyond a limit will affect surface roughness. Thus, it is necessary to determine machining conditions that result in high MRR while maintaining better surface finish. Therefore, accurate model of turning process is required both for the analysis and prediction of the quality of machining operations.

Finite element method (FEM) employs a scientific approach wherein the entire machining process can be simulated using various data inputs and simulated results can be further optimized to understand the physics involved in cutting process. In order to improve the efficiency and quality of the machining process before resorting

to costly and time consuming experimental trials, it is necessary to model and simulate the metal cutting process using finite element method. FEM simulations provide adequate information on various critical parameters such as angle of shear, chip generation and its thickness, interaction between flow stress and cutting tool, temperature profile at chip-tool interface, cutting forces, plastic deformation of the cutting edge and stresses acting on it that lead evaluation of tool wear [20].

1.2 Aim and scope of present work

Ti-6Al-4V alloys offer excellent properties such as high strength-to-weight ratio, fatigue strength, fracture toughness, corrosion resistance and ability to withstand higher working temperatures, due to which they are chosen over the conventional metals and alloys. Implementation of sustainable practices with an aim to minimize/eliminate the use of cutting fluids in machining process has always been a point of interest to the manufacturers. In the core machining phase, use of cutting fluids and energy consumption during the machining process directly influences the environmental impact of the cutting process involved in producing a certain feature.

Study of tribological properties which play significant role in manufacturing processes is primarily focused to reduce losses occurred by friction coefficient and wear of components of the tribo-mechanical system. In order to identify suitable solid lubricants for improving tribological properties, there is a need to test solid lubricant particles used in the current manufacturing applications. To characterize the same, an experimental setup has been developed to observe and measure the lubricant film thickness at various particles size and concentrations of solid lubricants. To determine the tribological properties of applied solid lubricant, EP (ASTM D2783) and WP

(ASTM D4172) tests will be performed on a four-ball tester.

In view of the above, the present research work shows the effective supply of micrometer sized MoS₂ solid lubricant suspensions on the rake and flank face of the cutting tool insert with novel EHVSL experimental set-up. Selection of the machining conditions effectively contributes to simultaneous improvement of quality and productivity. It is, therefore, vital to choose optimal machining parameters to enhance machinability for a given material without affecting the production timelines. The current research presents attempts made to investigate the influence of EHVSL on machining of Ti-6Al-4V alloy (grade 5) with tungsten carbide insert. Owing to its highly viscous and lubricating properties, SAE 40 oil is selected as base oil (i.e suspension medium for solid lubricant particles) for MQSL.

Surface roughness is an extremely complex phenomenon, affected by numerous factors such as cutting parameters, work material, cutting tool properties, structural rigidity of the machine, cutting temperature, status of lubrication etc., which are more difficult to detect and quantify. It is possible to apply Group Method of Data Handling (GMDH) technique to a great variety of areas for data mining and knowledge discovery, forecasting and systems modeling, optimization and pattern recognition. GMDH algorithms can automatically find inter-relations of data; it also selects an optimum structure of model or network in order to have better accuracy of existing algorithms.

FEM has been widely used to simulate metal cutting process. Numerous cutting force models have been established to predict the machining parameters. Although simulations were carried on dry machining conditions, very few attempts

were made to perform simulation on coolant assisted machining of hard to cut materials such as Ti-6Al-4V alloy. Metal cutting process involves high temperature and strain rates, which make Johnson-Cook (J-C) material, model the preferred material model that can simulate these exceptional conditions.

1.3 The objectives of present work

Applications of cutting fluids improve machinability and productivity by extending cutting tool life, due to its effective cooling and lubrication action. However, cutting fluids pose serious threats to ecology and operators health, and thus there is a great necessity to significantly concentrate for pollution-free and operator-friendly coolants/lubricant alternative for sustainable machining. The present research focuses on

- To develop a novel EHVSL assisted machining for sustainable machining of advanced engineering materials.
- To evaluate the effect of EHVSL cooling technique with application parameters, i.e lubricant flow rate, air pressure, angle impingement of nozzle, and spot distance on cutting force and surface roughness, while turning Ti-6Al-4V alloy.
- To investigate the performance of EHVSL assisted machining in terms of surface integrity and machining properties during machining of difficult-to-cut Ti-6Al-4V alloy and to compare the same with existing conventional and un-conventional techniques under the same operating conditions.
- To analyze the tribological performance of solid lubricants and to understand its influence in sliding conditions.

- To gain an understanding of the thin lubricant film development under sliding condition via experimental investigation.
- To perform EP tests and WP tests of applied solid lubricants using four-ball tester.
- To optimize the output response (surface roughness) during turning operation under EHVSL condition using GMDH technique and thus to identify a combination of most optimal parameters to obtain superior performance characteristics to achieve high productivity and MRR.
- To achieve development of 2D FE model for orthogonal cutting process to predict the chip thickness and cutting force.

1.4 Methodology

Investigations will be made to evaluate the tribological behaviour of various solid lubricants in depth at different sliding conditions and also, to investigate solid lubricant film thickness with respect to particle size and concentration on a pin-on-disc wear and friction monitor. Further, to check the extreme load capacity of the obtained solid lubricant with various particle size and concentration, EP and WP tests were performed on a four-ball tester.

The present work concentrates on the fabrication of a novel set-up in order to facilitate effective lubricant supply at tool-chip-workpiece interface. This system is specially designed, fabricated at Tribology Laboratory, Mechanical Engineering Department, BITS Pilani Hyderabad Campus, Hyderabad, India. Detailed procedure of the experimental set-up is discussed in Chapter 3. In the current study turning

operation was carried on Ti-6Al-4V alloy at different combinations of speed, feed and depth of cut machining parameters. Tungsten carbide tool was used to perform turning under

- Dry condition
- Flood cooling condition
- Minimum quantity lubricant (MQL)
- Minimum quantity solid lubricant (MQSL)
- Electrostatic high velocity solid lubricant (EHVSL)

The prediction of optimal cutting parameters is one of the major tasks to achieve good surface finish and dimensional accuracy and plays a key role in process planning. Due to the widespread use of highly automated machine tool in the industry, manufacturing requires methods for the prediction of machining processes. Machining conditions will further be optimized to improve MRR.

In addition to the above, Johnson-Cook constitutive equation with an energy-based ductile failure criteria is developed to create FEM for Ti-6Al-4V alloy. A series of FEM simulation of machining process will be carried out at various speed and feed conditions in dry and lubricant conditions to compare simulation results with the experimental results.

1.5 Over view of thesis

The thesis written in compilation format includes six sections divided into seven chapters and is outlined as below:

Section 1

Chapter 1 provides a brief introduction to the metal cutting process and possible lubrication approaches, importance of tribology in current industrial practice and FEM simulation of machining process that sets the stage for research objectives and methodology to be carried out for the current research work.

Section 2

Chapter 2 provides an overview of literature on the experimental and theoretical aspects of difficult-to-machine materials for understanding various process parameters like surface roughness, cutting force, tool wear, tool life, cutting temperature, tribological properties etc., for advanced engineering materials and summarizes with a review of the literature gaps.

Section 3

Chapter 3 describes the development of novel electrostatic high velocity solid lubricant spray system process and its working principle for sustainable machining process.

Section 4

In *Chapter 4*, sliding experiments are conducted on pin-on-disc tribometer to measure the tribological properties of various solid lubricant particles at different conditions. The thin lubricant film developed with solid lubricant spray system is empirically measured at various particle size and concentration of selected solid lubricant. Further, WP properties and EP properties tests were performed using four-ball tester.

Chapter 5 deals with detailed description of experimental tests conducted and the results obtained while machining Ti-6Al-4V alloy at various speed, feed and depth of cut conditions. A comparative study between EHVSL and wet, dry, MQL and MQSL environmental condition have been presented. GMDH technique is used to predict the boundary conditions of machining variables and machining performance.

Section 5

Chapter 6 presents the FEM predictions for cutting force, chip thickness and comparison of the same with experiments to assess the modeling capability of the material models in describing the machining deformation characteristics of Ti-6Al-4V alloy material during dry and EHVSL conditions.

Section 6

Chapter 7 concludes with providing the summary and specific contributions of the current study. Further, future scope has also been presented.

1.6 Organization of dissertation

Fig. 1.1 outlines the structure of the dissertation. It is organized in to six sections, with each covering various chapters. Each of the chapters presents the methodology adopted to achieve the objectives of the work.

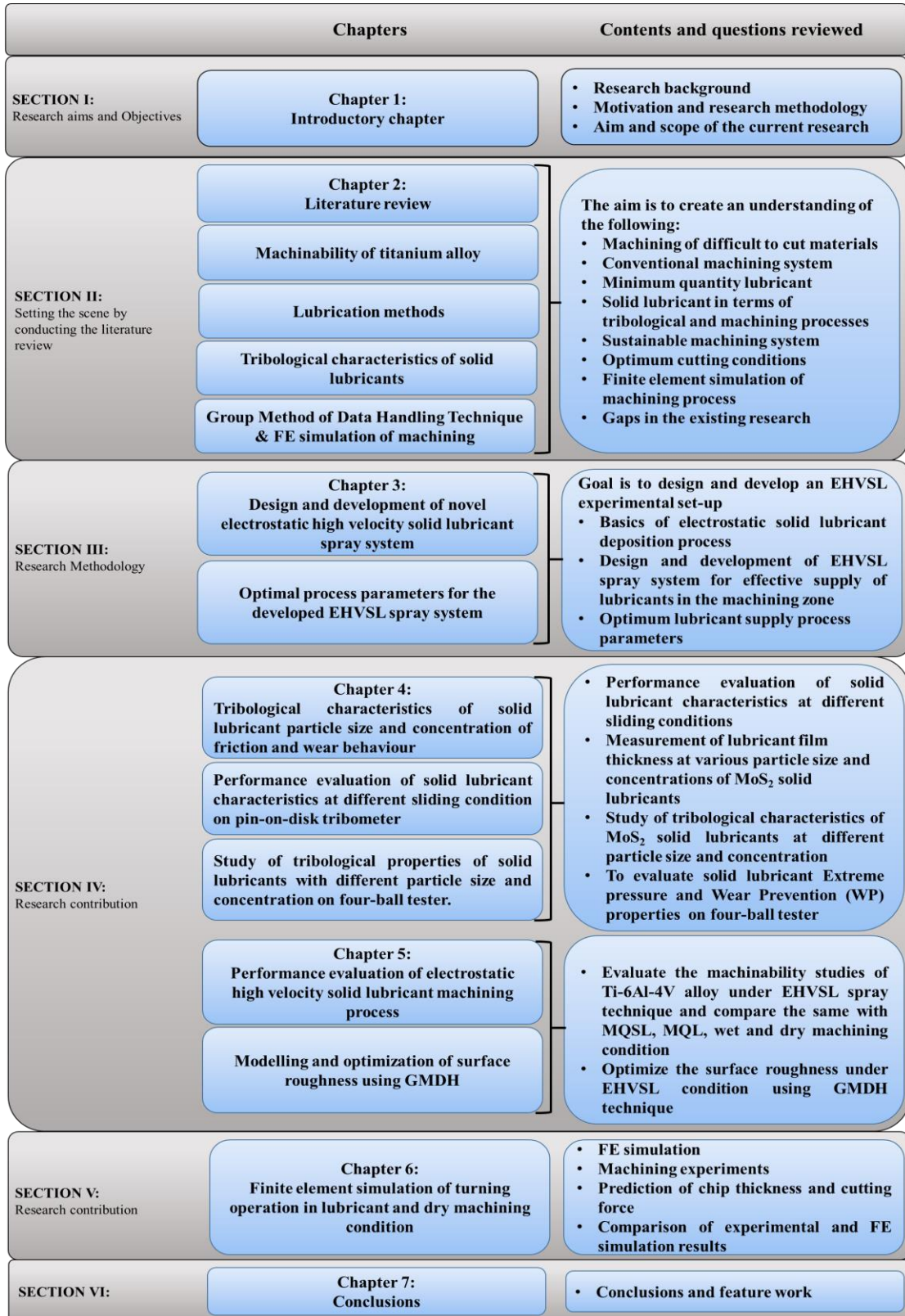


Fig. 1.1: Structure of the thesis

CHAPTER 2

LITERATURE REVIEW

This chapter provides an overview of the available literature concerning the application of cooling and lubrication in machining process, and available research concerning existing literature on wet, dry, MQL, and solid lubricant assisted machining. It includes the tribological studies on friction coefficient, rate of wear and physical characteristics of various solid lubricants at different sliding conditions. A reliable and structural identification method used to optimize cutting parameters has also been reported in the current chapter. The chapter also describes the FEM modeling and simulation studies of machining carried in the past. The chapter concludes with the review of literature gaps and summary of the chapter.

2.1 Introduction

Turning is one of the most widely used processes of removal of excess material from a component in order to impart the required dimension and quality in manufacturing industries. Surface roughness greatly influences the functional characteristics of the workpiece such as its compatibility, surface friction, fatigue resistance, etc., and thus, plays a crucial role in determining workpiece quality. Chip formation during metal cutting process consumes most of the energy and major information needed to evaluate the cutting parameters such as cutting force, surface roughness, tool life etc., is closely associated with it [10]. The energy supplied to deform the metal is dissipated in the form of heat in both primary and secondary deformation regions (shown in Fig. 2.1) [21]. In the manufacturing industry, machining performance is generally characterized by parameters like surface roughness, cutting force, tool wear, chip thickness, etc. Machining performance

through improved machinability parameters has long been recognized as they have considerable impact on productivity, product quality and overall economy. Such parameters largely depend on several parameters such as workpiece material properties, tool geometry, tool material, cutting fluid, method of applying coolants and cutting conditions [6].

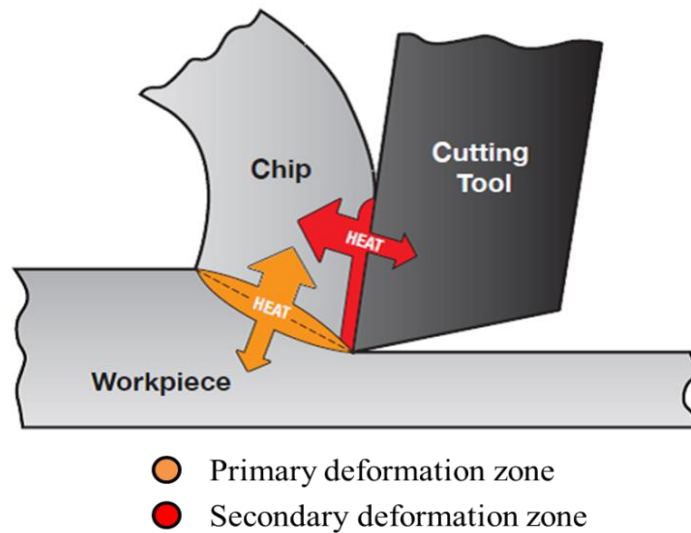


Fig. 2.1: Heat generation in machining process in primary deformation and secondary deformation zone [21]

In fact, the frictional interaction between the tool-chip at the rake face has major influence in determining tool wear and characteristics of the machined surface. It is believed that any change in contact conditions, as a means of better control over frictional interaction, results a change in the tool-chip contact interface and mechanics of machining, thereby influencing the contact temperatures, tool wear, cutting forces and energy consumption [18]. Research into this field is mainly driven by the need to improve sustainability performance of cutting processes. The challenge of modern machining industries has to fulfill increasingly high demands with regard to quality of machined workmaterial and productivity with a possible environmental impact. Among the several factors which intensely affect such goals, cutting fluids play

crucial role in reducing the contact temperature, friction, cutting force and tool wear during machining process.

During past decade in industries, low cutting speeds were used to minimize the possibility of high tempering the tool materials [4]. Increasing demand for more accuracy and precision components with high integrity components, the machining of hard materials need to be significantly developed. High speed machining technology for hard-to-cut materials is now recognized as one of the key processes in advanced manufacturing technology to achieve higher MRR, increased machining accuracy, decrease in workpiece distortion, increase part precision, low cutting force and better surface finish [22-24]. The high cutting forces acting in the shearing zones promote high friction with high heat generation and consequently develop high temperature that accelerates tool wear [22]. The friction arising during the machining operation and the wear on cutting tool is major loss factors. According to the German Society for Tribology [25], a loss of about 5% of gross social product arises annually in industrialized countries through the effects of friction and wear alone.

The quantity of heat developed as a result of higher temperature at tool-chip interface largely depends on cutting parameters i.e feed rate, cutting speed and depth of cut. Shaw [26] found that at a cutting speed of 1.5 m/min, the Built-up edge (BUE) was formed, but this can be retarded by employing cutting fluid. BUE is a small portion of the workpiece material that becomes the cutting edge during the machining process. However, considered cutting speed is too low for conventional machining.

Korkut and Dinertas [27] provided a more defined theory about the tendency for BUE formation in face milling process. They underlined that the BUE formation occurred at cutting speeds ranging from low to moderate. In this range, the

BUE tends to remain stable. Subsequently, if the cutting speed increases above the moderate magnitude then the BUE becomes less stable. In machining processes, cutting fluids are mainly required to serve two major purposes; (1) minimize/eliminate friction (i.e lubrication action) (2) reducing contact zone temperatures (i.e cooling action).

Therefore, use of cutting fluid in cutting operation is also beneficial in order

1. To serve the purpose of cooling the hot cutting zone by carrying away some of the heat generated.
2. To flush off chips on the machined surface thereby preventing them from causing scratches on machined surface.
3. To reduce friction for ensuring lower cutting force and minimize chatter.
4. To create a protection layer by creating thin film over the machining surface and to prevent chips from being welded onto the machined surface.
5. To minimize the effect of welding on the tool rake face to reduce its cause of failure.

Higher cutting speeds often cause cutting fluids to fail from being able to provide the necessary cooling and lubrication action at tool-chip interface effectively. As these high cutting speeds generate high temperatures, it is important to ensure the correct combination of the type of cutting tool material and cutting fluid to arrest a possible tool failure. Although proper cutting conditions can reduce chatter and work-hardening, they cannot effectively reduce the extreme cutting temperatures that accelerate tool wear. In order to resolve this problem, there is a need for cooling and lubrication systems that effectively penetrate the cutting fluid into the tool-chip interface and reduce the thermal wear during titanium alloy machining [1 & 5].

2.2 Types of cutting fluids and their performance

The process of machining involves a shearing mechanism to transform a workpiece to an end shape. This fundamental mechanism creates a high friction load between the cutting tool and the workpiece, which significantly increases the cutting temperature. In addition, friction dissipates energy thus generating heat, which if it is not properly controlled might have a detrimental effect on the cutting tool and machined component. The main sources of heat are normally generated at the (i) primary heat source from the a shearing zone, due to plastic deformation takes place, (ii) secondary heat source from a shearing zone along tool-chip interface and (iii) third source from rubbing zone along tool-workpiece interface. If proper and efficient cooling and lubrication methods are employed in the machining process, there is a possibility of lowering the temperature at machining zone which leads to reduction in frictional force. In order to improve the product quality and extend tool life, cutting fluids are applied in the high-temperature zone. Some of these are:

2.2.1 Effect of wet lubricant (flood cooling) in the machining process

In manufacturing industries, the common method to apply cutting fluids includes flooding, misting, spraying, dripping and brushing [28 & 29]. Among them, flood cooling is the most universal way. Flood cooling with nozzles or jets has been used as standard method for coolant application for more than a century [30]. The general machining of condition of flood cooling is shown in Fig. 2.2. The cutting fluids are arrayed out through nozzle to the workpiece and quantity of cutting fluid is pretty high. Using large quantity of cutting fluids leads to pose difficulties in procurements, storage, disposal and maintenance. As referred before, the disposal of the huge quantity of waste metalworking fluids brings about big problems to

environment and human health [31 & 32]. Although flood cooling delivers a relatively high volume flow rate of cutting fluid, studies have found that the cutting fluid fails to penetrate quickly and effectively upon to the critical location i.e tool-chip and tool-workpiece interface in a short period of time [33]. Abundant application of cutting fluids may increase production cost and cause environmental and health damages, particularly when not properly managed.



Fig. 2.2: Flood cooling system in machining process [26]

Traditionally, cutting fluids are used to provide cooling and lubrication in terms of improving the tool life by reducing tool temperature and the friction between the tool-chip-workpiece interfaces during cutting operation. In high speed machining process, conventional cutting fluid loses its cooling properties and fails to control high temperatures generated in cutting processes (as they get evaporated at the high temperatures that are generated close to the cutting zone) upon film boiling and that the boiling temperature of conventional coolants are lower than that of biodegradable coolants and coolant free machining [34]. The cost of cutting fluid is often higher than the cost of cutting tools.

Increasing pollution-preventing initiatives globally and consumer focus on environmentally conscious products has put increased pressure on manufacturing industries to minimize or eliminate the use of cutting fluids. Since, the cutting fluid application is not biological friendly, as the workers are continuously exposed to cutting fluids, they are mostly under the impact of toxic fluids, which cause severe health harms like genetic diseases, respiratory problems including occupational asthma and hypersensitive pneumonia [35 & 36], dermatological disorders such as irritation, oil acne and skin cancer [37].

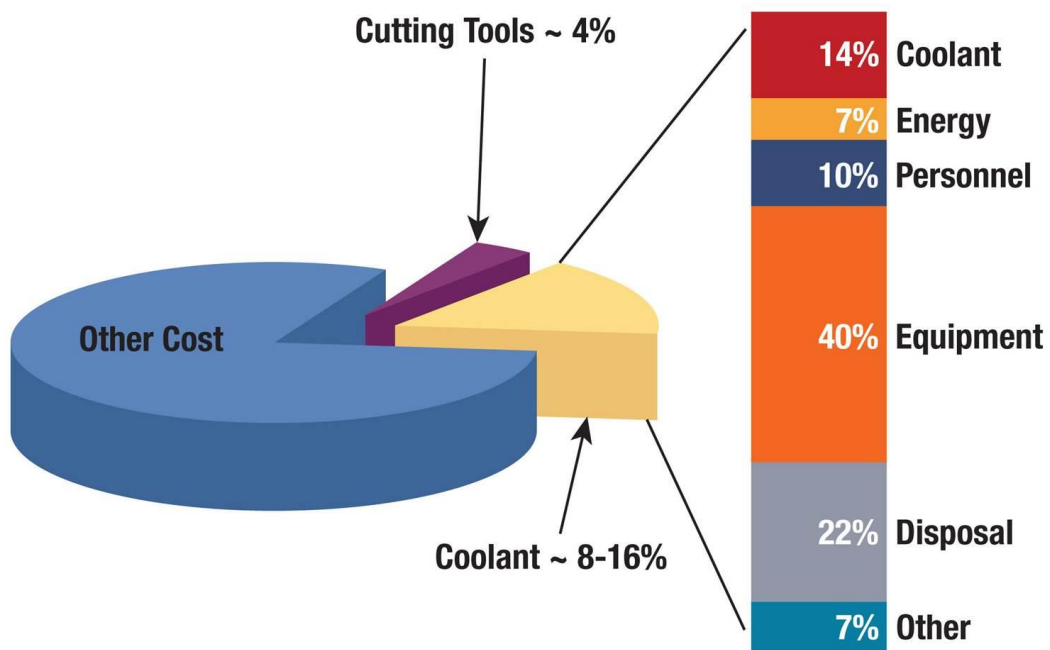


Fig. 2.3: Machining cost breakdown [21]

However, governments of most countries are demanding industries to reduce or if possible abolish the indiscriminate use of environmentally hazardous cutting fluids, due to possible environmental and health damages that they might cause [38]. Further, consuming large quantities of cutting fluids in cutting process leads not only to the above problems but also requires storage, disposal and maintenance.

Conventional metal working fluids are regarded as one of the top health risks in the machining processes [39 & 40]. Surveys carried out by German automotive industries show (Fig. 2.3) that the cost incurred on conventional metalworking fluids ranging from 8-16% of the total machined workpiece cost [22] and 16-20% of the total product cost [38] as compared to the tool cost which is only 2-4% [41]. The cost of cutting fluid is often higher than the cost of cutting tools. However, this flood lubrication technique has become obsolete due to its harmful impact on the environment [10]. Conventional lubricant fluids (CLF) in these applications are not effective in terms of decreasing the cutting temperature, reducing machining costs and improving environmental sustainability. Therefore, the significant improvement towards sustainability will be one of the most important challenges in near future. Manufacturers and researchers continuously strive to minimize or eliminate the usage of cutting fluids to make the processes eco-friendly and to achieve green manufacturing [4].

2.2.2 Effect of dry machining

The negative environmental impact of metalworking fluid, as previously discussed, has forced manufacturers to use alternative technique for more sustainable and economically feasible; particularly in industrialized countries with strict environmental regulations [42]. This leads to the implementation of dry machining which is ecologically desirable and reduces machining cost as fluids need not be disposed. Dry machining consumes less power and produces fine surface of the machined workmaterial than conventional machining [43]. The benefit of dry cutting includes: non-pollution of the atmosphere or water; no residue on the swarf which will be reflected in reduced cleaning and disposal costs, no danger to health and increased tool life by eliminating thermal shocks [44 & 45].

Decreasing the cost of the cutting process and associated reduction of environmental pollution by dry machining is the main key to remain competitive [46]. However, machining without cutting fluid finds industrial acceptance only when it is possible to guarantee good surface quality without compromising the rate of material removal [40]. Therefore, it is important to compare machining with and without using cutting fluids. However, higher friction between tool-chip and tool-workpiece leads to high machining zone temperatures in dry machining [46]. Due to high friction with heat generation and consequently develop high temperature in the machining zone, the workpiece is subjected to large thermal stresses leading to dimensional inaccuracy and the tool is also subjected to large thermal loads which can result in higher levels of oxidation, diffusion, etc., that accelerates tool wear.

The other primary solutions are using appropriated materials for tools (coated cutting tools). Those coated tools may withstand high temperatures, reduce cutting energy or even provide a lubricant effect for decreasing friction. For tool coating technologies, Schramm et al. [47] has tried to improve the properties of tool coating materials by reducing the spatial scale of the material system to nanometer dimensions. These studies include that nano-coating which significantly improve the hardness, toughness and modules of the tool so that they are able to behave better in friction, wear and lubrication.

Similarly, Umamaheshwar Reddy et al. [48] have developed coating electrostatic experimental set-up to coat the cutting tools. MoS₂ solid lubricants have been used as coated material. Further, in order to assess the performance of developed coated cutting tool, turning experiments were performed, in comprehending the results on cutting force, surface roughness, tool wear and compared the results with un-coated cutting inserts. Machining with coated cutting tools resulted in lower

frictional values at tool-chip interface zone leading to lower cutting force than those machining with un-coated cutting tools. Surface quality of the machined workpiece using coated cutting tool showed a much better improvement compare with uncoated cutting tool. There are still a lot of difficulties in the adoption of high-speed dry cutting of difficult-to-cut materials, because of the high cutting force and temperature in the machining area [2]. Without using cutting fluid, the function of cooling and lubrication will not exist, and this will cause severe friction and adhesion, reduce tool life and affect surface quality of workpiece [49].

2.2.3 Effect of minimum quantity lubricant in machining process

To overcome the economical and environmental related problems in the metal cutting process, manufacturing industries impose new demands and one possible solution is the use of MQL [50]. Being intermediate between dry machining and flood cooled machining; MQL is a plausible alternative to majority of machining processes [34]. While flood cooling machining uses excess of lubricant to achieve cooling by heat absorption, MQL uses limited quantity of lubricant which targets on reducing friction between tool and workpiece to obtain cooling. A cost effective alternative would be to reduce the consumption of cutting fluid whilst maintaining the same productivity and quality. Techniques to reduce the quantity of cutting fluids have been investigated during the last decade focused on MQL and near dry machining (NDM) [51]. The technique uses compressed air that carries oil droplets in a mixture that is pumped and directed to the cutting regions to exert its role adequately [52]. Fig. 2.4 shows the typical photographic view of machining with MQL system. The lubricating action is ensured by the oil droplets while the cooling action is given by the compressed air. The oil droplets are either of vegetable oil or mineral-based oils, and the flow rates are very small (usually ranging from 50 to 500 mL/h).



Fig. 2.4: Machining with MQL system [10]

MQL has been widely used in many machining processes such as turning, milling, drilling and grinding. Schematic view of MQL set-up is shown in Fig. 2.5. The small amount of oil is enough to reduce the tendency of work material to adhere onto the tool surfaces and diminish friction. Typically, the lubricants are sprayed through external supply system with one or more nozzles.

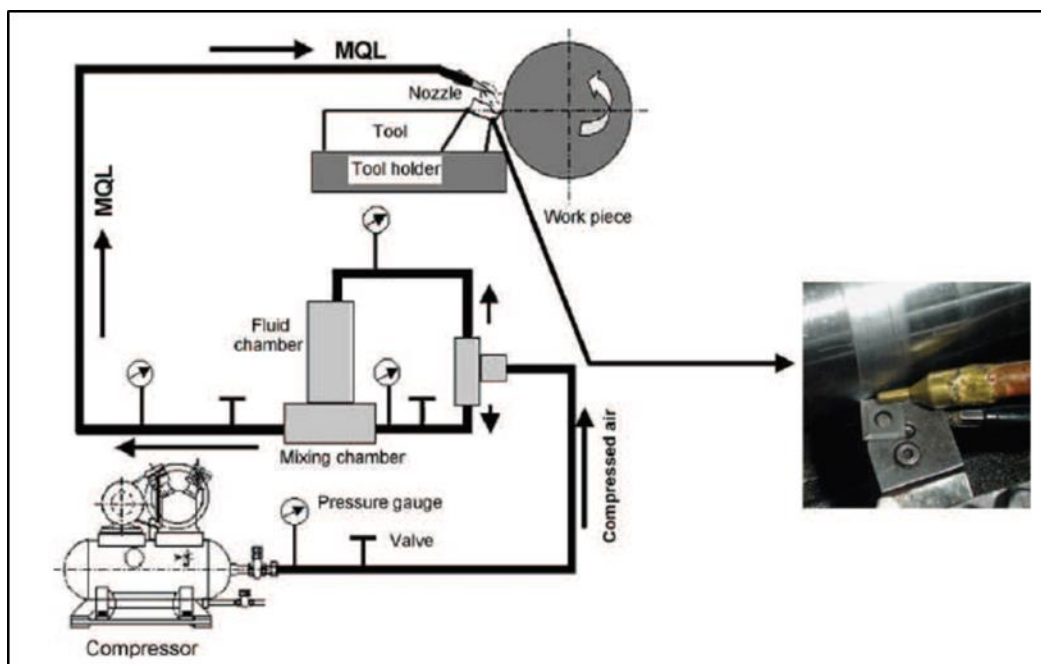


Fig. 2.5: Schematic view of MQL technique [2]

Test results indicate the amount of MWF's in MQL is nearly 3 to 4 order of magnitude lower than that of conventional system including flood cooling. Taking advantage of this technology, a little fluid can make a significant difference. In MQL, expert for cutting performance, secondary characteristics are also important including safety properties, biodegradability, and oxidation. Filipovic and Stephenson [53] summarize that external spray and through-tool are the two basic types of MQL delivery systems. In the external spray system, a cutting fluid reservoir is usually assembled besides the machine and nozzles are directed to the cutting zone and are connected to coolant reservoir through hoses. This kind of system of MQL is economical and portable for most of the machining operations. For through-tool system, there are two configurations available according to the way to create air-oil moisture. The first configuration is external mixing of oil and air and piping the mixture through the spindle or tool to the cutting zone. The other method is internal mixing of oil and air. The most common structure of it is two parallel tubes rotating through the spindle to bring to an external mixing device besides the tool holder where the mist can be created. The first method is simple and inexpensive. Nevertheless, the second way has less dropouts and dispersion and can deliver mist with larger droplets sizes. The internal system offers more effective cooling and lubrication for workpiece than the external spray [52].

Varadarajan et al. [54] have studied the performance of Hard Turning with Minimal Fluid application (HTMF) in comparison with that of conventional hard turning in wet and dry form. It was found that the obtained results of minimum cutting fluid are encouraging in terms of cutting force to that of conventional machining conditions. Rahman et al. [50] applied 42 l/min (flood coolant) as coolant; the results are compared with MQL of 8.5 ml/h and the comparative effectiveness was

investigated in terms of surface finish, cutting force and chip formation. From the obtained results, it is revealed that better surface finish has been found in MQL condition when compared with dry and flood cooling application. From the above studies it has been observed that MQL may be considered to be an economical and environmentally compatible lubrication technique. Machado and Wallbank [55] has performed experiment on turning using lubricant amounting to 200-300 ml/hr, which was applied in a fast-flowing air stream at a pressure of 2 bar. Results observed that, surface finish, chip thickness, and force variation are all affected beneficially compared to those obtained by flood coolant flow of 5.2 l/min.

Klocke and Eisenblatter [56] have investigated the cutting process without cutting fluids. According to Klocke et al. [45] cutting fluids help to achieve a specified result in terms of tool life, surface finish and dimensional accuracy, facilitate chip breaking and transport. However, they also impose problems related to waste disposal and environmental problems. Hence, with dry cutting, all the problems related with wet machining can be eliminated.

Another example is that Barczak et al. [57] conducted a study of plane surface grinding under MQL conditions comparing with traditional flood cooling. They found that low friction conditions, reasonable specific MRR and better workpiece quality can be achieved under MQL conditions. Although the findings above, MQL cannot be universally applied since it does not provide sufficient cooling for many operations [9]. Also, very hard materials and high cutting speed may not be suitable for MQL.

The main limitation of MQL is its limited effectiveness in cooling the cutting surface. This could be due to the fact that in high speed cutting conditions lubricants have difficulty in reaching the machining zone. If the fluid can be applied in a more

defined way, exactly to the machining zone, improved results can be expected [58]. Most of the researches have studied to control the effect of tool wear using different machining techniques; however, they were unable to achieve better results in increasing the tool life. In MQL there is a sudden vaporization of the water upon reaching the machining zone decreasing the cooling and lubrication aspects thereby affecting the tribological properties [8]. Hence, MQL may be considered as an economical and environmentally compatible lubrication technique for limited applications at low speed, feed, and depth of cut machining condition. Control of machining zone temperature is achieved by providing effective cooling and lubrication [2,6,8,16-18,38 & 50]. Machining without the use of any cutting fluid (dry or green machining or sustainable machining) is becoming increasingly more popular due to the concern regarding the safety of the environment [50]. Hence, there is a need for concentrated efforts in this direction to overcome the above stated drawbacks and to look into new machining methods to achieve sustainable machining system.

2.2.4 Effect of solid lubricant assisted machining in the machining process

High production machining of titanium alloys inherently generates high cutting zone temperature. Such high temperature causes dimensional deviation and premature failure of cutting tools [22]. It also impairs the surface integrity of the product by inducing tensile residual stresses and, surface and subsurface micro-cracks in oxidation and corrosion [59]. Due to the fact that the higher the tool temperature, the faster it wears. The use of cutting fluids in machining process has its main goal, the reduction of the cutting region temperature, either through lubrication, reducing friction, wear, or through cooling by conduction, or through the combination of these functions [60]. However, the application of conventional cutting fluids create several-

techno-environmental problems such as environmental pollution due to chemical disassociation of cutting fluids at high cutting temperatures, biological problems to operators, water pollution and soil contamination during disposal [61]. The initiatives of government to achieve anti-pollutant products are due to the interest of customers to have environmentally conscious products. This has increased the pressure to minimize waste streams. Hence, it is absolutely necessary to eliminate the use of cutting fluids and also to use an environmentally acceptable coolant in manufacturing industries. All the factors prompted investigations into the use of biodegradable coolants or coolant free machining. Hence, as an alternative to cutting fluids, researchers experimented with solid lubricants [8]. Minimum quantity solid lubricant assisted machining technique (shown in Fig. 2.6) has recently been proposed as an effective cooling and lubrication solution for a wide range of machining applications, including micromachining, and machining of hard-to-cut materials [6].

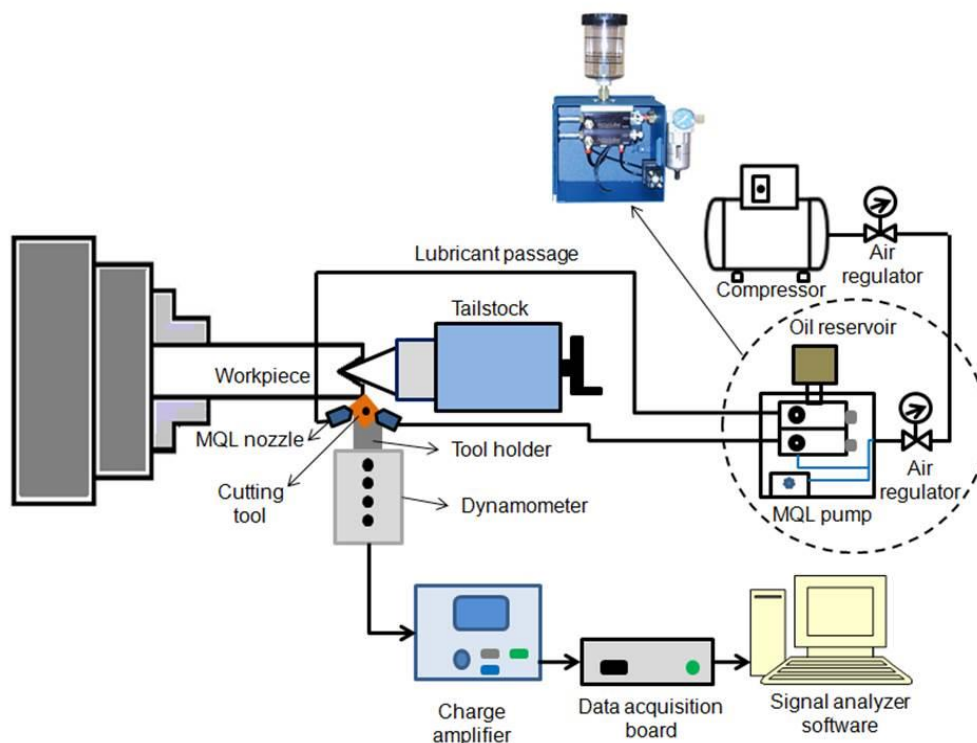


Fig. 2.6: Schematic diagram of MQL experimental set-up [6]

The use of solid lubricant in machining is one of the most effective strategies in this direction. In demanding the improvement of productivity and product quality of machining process, use of solid lubricant thin film were suggested as one of the necessary alternative machining technique to apply lubricants effectively to the high temperature zone [18, 62-64]. The solid lubricant spray system consists of a high-velocity compressed-air nozzle positioned inside a co-axial nozzle. The desire to control solid lubricant flow rate accurately and improve the particle size of lubricants sprayed from a spray nozzle has been a challenge for manufacturers to apply lubricants more effectively to the machining zone. Air atomizing spray nozzle produce fine mist spray with the help of compressed air, liquid breaks into small droplets as air provides shearing effects on liquid droplets. Liquid and air streams meet with in the nozzle and are mixed together and expelled through the same orifice. The solid lubricants are directed towards the exit of the nozzle where compressed-air inlet is fixed. When both the solid lubricant particles and compressed-air enters in to the mixing chamber, atomized solid lubricant particles entrain themselves with the high-velocity solid lubricant particles that are supplied via the nozzle tip to produce a focused axisymmetric jet of solid lubricant particles. During the machining process, the nozzle tip is directed towards the tool-chip interface to form a fast moving thin fluid film capability of effectively penetrating and cooling the tool-chip interface. The solid lubricant assisted machining does not require high-pressure pump and can run at a very low flow rate (i.e. 40 ml/hr) which is negligible amount of magnitude than that of flood, cryogenic and high-pressure cooling. The solid lubricants penetrate into the tool-chip interface by means of the thin fluid film appears to be the mechanism by which tool life is extended with solid lubricant spray system.

Solid lubricants assisted machining could be a viable alternative method to increase the life of the cutting tool. Solid lubricant additives with layered structure have been extensively studied and excellent machining performance has been observed in terms of improved tool life and surface finish [18]. The use of solid lubricant in powder form [63] can be applied in the machining process or solid lubricants suspended with base oils. Solid lubricants can be applied by different substrate such as graphite, by mixing with compressed air and directing the flow to the cutting region [65] or by an electrostatic field that attracts the solid lubricant powder onto the cutting region [58]. Good results were found in terms of reduction in cutting forces and improved surface roughness and tool lives when using these techniques. Using an automatic feeder, solid lubricants in a powder form have been applied directly to the machining zone [18]. Although sufficient coolant is applied in the machining zone, there is still a need for flushing action for cleaning of components which makes solid lubricants less attractive than conventional cooling techniques. Instead of using solid lubricant in powder form, semi-fluid lubricant containing a thickening agent of solid lubricant mixed with water-based soluble oil and grease has been used [68].

However, the application of solid lubricants in powder form produced significantly low cutting forces, due to the ineffective removal of semi-solid lubricant, and formed chips is the major limitation of this method. Finally, the application of water-based oils has been envisaged and successfully experimented under MQL conditions [62]. The mixture of solid lubricants (MoS_2 and graphite) with mineral based oils with an average particle size of 250 nm at various concentrations of solid lubricants (5% and 20wt% with respect to oils) has been used. The obtained results are very encouraging in terms of reduction in cutting force and better improvement in

tool life; however usage of solid lubricants (nano-materials) significantly increases the overall cost. The authors have investigated the possibility of using different solid lubricants as graphite, MoS₂ and boric by weight mixed with base oil SAE-40 as a minimum quantity lubricant, to reduce the heat generated in the machining zone (chip-tool interface) in turning process. Different process parameters like cutting forces, cutting temperatures, chip thickness, and surface roughness were observed and reported to be reduced as compared to dry machining. For the similar machining conditions higher reduction in the cutting forces, cutting temperatures, chip thickness and surface roughness in the presence of solid-liquid lubricant is possible, because the lubricant in the metal cutting process will provide the lubricating and cooling effects. They introduced a new concept of applying the solid-liquid lubricant with a brush to the work-piece surface that seeped with the cutting zone. It may be considered as real near dry machining condition.

Marques et al. [6] found that the size and quantity of the solid lubricant particles play a dominant role in the lubrication process. Further, the application process of solid lubricant at the tool-chip interface influences the lubrication characteristics during machining process. Mixed with oil, the solid lubricant can also be applied by the MQL technique. Some work has shown good results, for example, Rahmati et al. [64] applied the mixture of MoS₂ nanoparticles (20-60 nm) with oil at different concentrations (0, 0.2, 0.5 and 1.0%wt) with a flow rate of 20 mL/h, on Al6061-T6 (work material) and conducted experiments on end milling process. The results indicate that nanoparticles of MoS₂ at 0.5%wt, improved the surface quality of the workpiece when compared with other concentrations. The nanoparticles of MoS₂ improved the surface quality of the workpiece and the concentration of 0.5%wt presented the best result.

Dilbagh et al. [65] carried out experiment on turning operation and applied graphite and MoS₂ solid lubricant as coolants. Surface finish and cutting force results are all influenced beneficially under MoS₂ assisted machining and are compared with graphite assisted machining and flood coolant. The inferior results of surface roughness obtained by MoS₂ can be attributed to its strong adhesion tendency compared to graphite. Applying solid lubricants (graphite and MoS₂) as coolants in the machining operation is one alternative method to conventional wet and dry machining. Solid lubricant-assisted machining produces low value of cutting force and surface finish compared to dry turning process.

Deshmukh et al. [67] studied the performance of different solid lubricants like, MoS₂ based grease, graphite based grease and silicon compound mixed with SAE-20 base oil at different proportions while machining aluminium and brass with carbide cutting tool. The results showed that improved surface quality as compared to wet machining of aluminium and brass.

Vamsi et al. [68] studied the performance of solid lubricants like graphite and boric acid with SAE-40 oil while machining AISI 1040 steel with cemented carbide tool. After conducting one-factor-at-a-time experiment the results showed that minimum tool wear, surface roughness and cutting forces were observed during turning of AISI 1040 steel, when compared to wet and dry machining. Among the lubricants 20wt% boric acid in SAE-40 oil provided better performance for the selected work-tool material combination and cutting conditions. However, there was not much comparison between predicted chip-tool interface temperatures and measured chip-tool interface temperatures.

Increasing demands for more accurate and precision components with high integrity and the machining technology of hard materials need to be significantly developed. Reddy et al. [58] have been working in the area of MQL to achieve sustainable manufacturing using clean machining processes, such as graphite and MoS₂ [17,58 & 69]. The surface characteristic results obtained by MQL are in terms of reduction in cutting zone temperature due to its favorable changes in tool-chip and tool-workpiece interaction. In MQL process, the widely used solid lubricants are graphite and MoS₂ due to their crystalline lattice structure in the form of dry powder are effective lubricant additives. The layers of the structures can be easily sheared in the direction of motion over each other resulting in reduction in friction. Larger particle size has high number of layers which can be more suitable for relative rough surfaces at moderate speeds, whereas smaller particle sizes are suitable for smoother surfaces for low-speed conditions. Other components that is useful as solid lubricants in addition to the earlier widely used graphite and MoS₂ include boron nitride, polytetrafluorethylene (PTFE), talc, calcium fluoride, cerium fluoride and so on.

It is important that solid lubricant be applied effectively to the machining region in order to accomplish improved results. In view of this condition, Reddy et al. [58] has designed and developed electrostatic solid lubricant system with an aim to reduce eradicating the usefulness of cutting fluid when applying solid lubricants as a high velocity jet in machining at low flow rate. The authors did a relative evaluation analysis of wet machining and dry machining environments with the proposed method. An outstanding result obtained from the study is that solid lubricant machining used with the developed experimental set-up resulted in numerous improvements in surface roughness and tool life. Surface roughness and tool life improves intensely owing to the ability of the solid lubricant to be able to be

delivered appropriately into the tool-chip boundary region and achieve both lubrication and cooling tasks adequately.

The previous research work [6] clearly specifies that there is a need to concentrate efforts in the direction of applying high viscous lubricants effectively at the tool-chip and tool-workpiece interface to overcome high heat generation in machining of advanced engineering materials. It has been observed from research review that machining of advanced engineering materials like Ti-6Al-4V alloy causes high heat generation due to its poor thermal conductivity. It has also been revealed from the literature review that better cutting performance could be achieved when the lubricants are penetrated quickly and effectively upon to the critical location i.e tool-chip-work interface in a short period of time [70-73]. Evolution in modern machining process has identified many solid lubricants with low cost and eco-friendly, which can able to withstand high temperatures and pressures.

In order to overcome the tribological losses under machining condition, lubricants with high viscosities, lower evaporation loss and a potential to improve lubricity are used in the sliding interface zone, and the high viscosity lubricant should remain constant over the operating temperature range [74]. The better penetration ability of the lubricant is mainly determined by the lubricant viscosity to adhere onto the tool-workpiece interface, the velocity to impinge lubricants effectively into the tool-chip contact surface and the wetting ability to reduce the tool-chip contact temperature. The goal of the lubricant film is to establish an effective thin film which can support the applied load while reducing friction between the sliding surfaces [75]. To achieve better results in terms of tool wear and surface roughness, solid lubricants need to be supplied effectively to the machining zone [6,8,18,20,50,54,63 & 74].

Solid lubricants are also attractive in promoting dry machining, an environment-friendly process [8].

2.3 Tribological characteristics of solid lubricants

In modern industry, where mechanical parts are subjected to friction and wear, leading to heat generation, which affects the reliability, life and power consumption of machinery, the study of lubricant film formed between various geometric shapes is inherently complicated and interconnected [72 & 76]. Tribological characteristics quantify the performance of a system in terms of reliability, life and power loss, especially in case of automobiles and industrial machinery. Industrial lubricants are primarily used to improve quality of component life over decreased material wear rate and surface friction [77].

Since lower friction among sliding parts is a standout amongst most basic properties in manufacturing parts and tools, one conceivable solution to this is applying lubricant adequately in the sliding zone. A lubricant can significantly change the tribological properties of the sliding surface and is also capable of altering the nature of surface interaction between sliding conditions [78-80]. Majority of the bio-based oils was typically petroleum-based lubricants [77]. Environmental concerns call for the reduced use of environmental effective cutting fluids in machining processes due to hazards to operator's health. [72]. However, when temperature is elevated under extreme conditions, the failure of boundary films may cause direct contact with sliding surface and lead to adhesion, the surface damage may cause on the sliding components.

Liquid lubricants achieve this by forming a lubricant film which separates the sliding surface and thus limits their contact and adhesion [80]. The primary function

of the lubricant is to create and maintain a thin layer of lubricant between sliding surfaces, for which the viscosity of the base oil is the most significant property [81]. Many researchers have tried to improve the tribological lubrication characteristics to decrease coefficient of friction and wear rates. In order to overcome the tribological losses under sliding condition, lubricants with high viscosity, lower evaporation loss and potential to improve lubricity are used in sliding interface zone. The high viscosity property of the lubricant should remain constant and adhere over the operating temperature range [72]. The goal of the lubricant film is to establish an effective thin film that will support the applied load while reducing friction between the sliding surfaces [80]. To improve the lubricant characteristics for effective cooling and lubrication in the machining process, one approach is to use extreme pressure additives in the base oil [82]. Use of solid lubricant additives in the base oil can effectively work under extreme conditions. Effective lubricity with sufficient thin film thickness in the sliding zone depends on particle size [83-85]. The efficiency of solid lubricant particles strongly depends on the type of lubricant used, solid lubricant particle size, as well as filler concentration [86]. Also, lubricant lifetime is limited by the overlay thickness of solid lubricant particles supplied on the sliding interface [87]. The additive grain size and lubricant film formation are significant parameters to be matched to the surface finish of the substrate [84]. Size of the solid lubricant particles need to be optimal. Increase in particle size may result in abrasive wear due to abrasion caused by contamination in MoS₂, whereas smaller particles may result in accelerated oxidation [83]. Results showed that low size solid lubricant particles were expected to intermingle with surfaces of the sliding pairs to form a surface protective film, which increases the anti-wear ability.

Solid lubricant additives with layered crystal structure have been extensively studied and excellent tribological performance has been observed [88]. These solid lubricant additives, including graphite [89], MoS₂ [85], tungsten disulphide [90] and boron nitride [91], have a lamellar crystalline structure, in which bonding between molecules within each layer is strong covalent, while each two layers is bonded together by weak Van der Waal's forces. Good friction and wear reduction performances were observed due to low shear strength of materials as a result of their intrinsic crystal structure [88]. Results demonstrated that solid lubricants deposited on the sliding surface had improved the tribological properties of base oil. Micrometer sized particles of solid lubricants with certain hardness have also been reported to lead to abrasive friction [92]. MoS₂ and graphite are used as coolants and recognized to be good solid lubricants because of significant reduction in friction generation between sliding components. This could have contributed to reduction of cutting forces [18]. From the previous studies it was observed that MoS₂ (lamellar material) generally has good load carrying capability with a corresponding low friction coefficient under sliding condition [92 & 93]. If the lubricants are applied effectively to the sliding zone, there is a possibility of reducing the sliding temperature which leads to reduction in friction force [95]. Solid lubricants with thin film formation can adequately work under extreme conditions of temperature, loads and speeds [88]. According to Reddy and Nouari [96], lower friction coefficient and layered lattice structure of MoS₂ are key factors to this performance. Ease of chip formation increases due to reduction in tool-chip contact area; this change is driven by reduction in frictional force. The considerable reduction of machining force by applying MoS₂ and graphite assisted machining can be attributed to the formation of thin lubricant

film, thus, reducing material's shear strength in the interface zone and hence, making the machining easier [95].

Reddy et al. [96] performed experiments on turning of AISI 1040 steel applying MoS₂ as lubricant with varying particles (the particle sizes were 2, 6, 10, 20, 40, 70 and 75 μm). Results showed that tangential cutting force was constant for particle sizes of 2 to 20 μm. From the results it was concluded that solid lubricant with 20 μm is required MoS₂ particle size to impinge the solid lubricant in the interface zone for achieving better results in terms of improving cutting force. Though low sized particle i.e. below 20 μm, has also shown desirable performance, the reason for not selection is due to the possibility of excessive fineness that tends to work against performance in terms of difficulty to maintain constant and defined amount of powder flow to machining zone. Because, a constant and continuous supply of required solid lubricant powder to the machining zone can reduce friction coefficient.

Sentyurikhina et al. [97] has suggested that solid lubricants with particle size of 0.5-1, 2, 0.5-2, 6, 10, 40, 70 and 75 μm have been recommended for use in friction components. Dilbagh et al. [65] has observed the performance of solid lubricant assisted machining on AISI 52100 steel. The results showed that cutting force obtained while applying graphite was about 7% greater than that of MoS₂. The obtained performance influences the effect of lubricant and lubrication parameters, when the same size of solid lubricants is used. Richard et al. [95] has performed experiments with solid lubricant assisted machining considering 20% by weight ratio of MoS₂ (particle size of 6 μm), graphite mesh 625 (particle size of 20 μm), and graphite mesh 325 (particle size of 40 μm). Results were observed that superiority of MoS₂ solid lubricants has improved the life and quality of tool wear and surface roughness when compared with graphite 625 and graphite 325. The results also

indicate that solid lubricant assisted machining may be a viable alternative to dry and wet turning process. Experimental results show that among various types of soft layered solid lubricants, MoS₂ is the most commonly used solid lubricant in different process performance improvement applications. This is because it offers very low coefficient of friction, relatively high wear resistance and ability to withstand higher load conditions. It also requires low-maintenance requirement and accommodates wide range of operating temperatures up to 300°C [83-85].

Devine Lamson [98] and Stalling have investigated the effect of solid lubricant particle size and also examined the load carrying capacity of lubricating grease. It was observed that there was no significant difference between MoS₂ with mean particle sizes of 0.7 µm to 7 µm whereas particle of 0.3 µm caused a noticeably diminished load carrying capacity. In addition to low coefficient of friction, the deposited layer should have a long wear life which depends on additive concentration, particle size and distribution of solid lubricants [99]. Bartz [83] studied the effect of particle size on lubricating performance of MoS₂ solid lubricant and observed that using larger size solid lubricant particles at increasing load condition, wear rate increases; with low size particle at aggravating sliding conditions, lubricating effectiveness improved. The author also explained that at a given concentration, low size solid lubricants particles applied effectively to the sliding zone and form a complete and continuous film component of large size particles, due to availability of more number of particles.

It has been revealed from the literature review that minimum film thickness plays a vital role in improving tribological properties at any sliding condition [83]. The thickness of the lubricant film generated depends on operating conditions such as velocity, load, lubricant viscosity and relationship of pressure to viscosity. Very few

and sparse efforts have been made to investigate the role of lubricant film thickness and its measurements during sliding condition. Hence, there is a need to look into this direction.

2.4 Group Method of Data Handing

Surface roughness monitoring and estimation are essential for improved productivity of manufacturing systems. Surface finish of turned components has found to be influenced by various factors which include work material characteristics, tool material, work hardness, unstable BUE, machining time, tool geometry, cutting speed, feed rate, depth of cut, chatter, and use of cutting fluids. During such operations, the optimum process input parameters have to be used in order to have the best products that meet customer requirements. The GMDH [100], a heuristic self-organizing method of modelling, has been used to integrate evidence from different sensors and the cutting conditions to obtain estimations of surface roughness.

The prediction of surface roughness is very important in the optimization of the machining process. In order to develop a new model for predicting the surface roughness, it is essential to understand the various methods that are being used to predict the surface roughness [101 & 102]. Need for prediction in machining is necessitated by the widespread use of highly automated machine tool, and to have optimal cutting conditions for better finish, accuracy in dimensions etc. Hence, the need for determining machining conditions for maximum MRR during surface finish falls under the desired range.

Mukherjee and Basu [103] applied multiple regression technique in processing the results obtained from metal cutting experiments. By the use of multiple regression, the authors arrived at a general relationship between tool wear and various other

cutting parameters. The model was developed for turning operation by conducting the experiments on mild steel specimens. The expression shows the relations between flank wear of a single point cutting tool and the various cutting parameters. The experiments were conducted at very low speed and feed conditions using HSS tools. However, now a days 80% of machining tasks are conducted by coated inserts at very speed and feed conditions. The effect of tool geometry and cutting temperature has not been considered.

Godfrey C. Onwubolu et al. [104] developed a model for predicting the tool wear using GMDH technique. The experimental data was obtained by conducting the experiments on a milling machine by varying cutting speed, the engage angle, the width of workpiece and the net cutting time. The prediction error fell with in $\pm 10\%$ at more than 90% of predicting points. Ravinder et al. [105] conducted experiments for spheroidal graphite (SG) cast iron as the workpiece material and coated carbide as the tool material. The pattern regression technique was used to model progressive tool wear with dynamic tangential force and tool holder vibrations at different speeds and depth of cuts, keeping the feed constant.

Takesh Yoshida et al. [106] identified a grinding wheel wear equation by GMDH algorithm with successive determination of polynomial trend containing interactive terms, considering chemical composition and mechanical properties of work materials, abrasive grains, grain size, wheel speed and feed rate. The established model enables the grinding ratio to be predicted for all combinations of workpiece materials, grinding wheels and grinding conditions, and serves as an aid in the optimization of the grinding process.

In recent years, researchers [107-109] have concentrated in various methods for system identification. Among the widely used methods for empirical analysis of data and model building, multiple regression analysis is a well-known technique to identify and predict the linear systems based on input-output data. However, it is also well known that reliable mathematical models are not easy to express dynamic analysis of non-linear real systems have many problems in the selection of model structure and variables. Therefore, many methods for recognizing and modeling non-linear systems were projected. To estimate the parameters for identifying and modeling non-linear systems in higher order, most of the methods like genetic algorithm, fuzzy inference, neural networks and polynomial classifiers require large amount of data. Majorly, to predict and identify non-linear systems based on experiential data fuzzy logics and neural network methods were used. When building such model, the non-linear dynamically are not explicitly expressed as a mathematical model. Hence, to obtain a mathematical model for non-linear systems, polynomial classifiers and networks are introduced. On the other hand polynomial classifiers often require vast memory for storage and can lead to unpredictability when it uses higher order polynomials. Subsequently, the GMDH technique is introduced to predict metal cutting experimental results [19]. GMDH is based on a multilayered network of second order polynomial structure, with features that express non-linear dynamics as a mathematical model and stable polynomial of higher order. Therefore, GMDH provides an effective approach to identification of higher order non-linear systems [112]. Consequently, such a self-organizing modelling approach is useful in both modelling and prediction in an advanced manufacturing system where it is necessary to model and predict the surface roughness during machining operations [104].

2.5 Finite element modeling approach for machining process

Ti-6Al-4V alloys have attracted significant attention in recent years for applications in aerospace, automotive etc., due to their excellent combination of high specific strength (strength-to-weight ratio), their fracture-resistant characteristics, and their exceptional resistance to corrosion. Conversely, these materials are regarded as difficult-to-cut material because of their high chemical reactivity with cutting tool and low thermal conductivity of the material [112]. Theory of deformation process causing chip formation and tribological aspects of tool-chip contact and very high rate of plastic deformation in cutting operation are quite complex as it involves material, physical and thermo-mechanical issues. Clear understanding of physical phenomenon of cutting process needs a simplified machining model [113]. In the recent years, FEM based modeling and simulation of cutting operations is continuously attracting researchers for better understanding the chip formation mechanisms, heat generation in cutting zones, tool-chip interfacial frictional characteristics and integrity on the machined surfaces [114-115].

Many approaches have been used in order to predict the relation between these parameters and the resulting cutting coefficients. Some researchers used empirical models to estimate the cutting coefficients [116]; others used analytical models [117]. Over the last two decades researches used either mechanistic models [118] or FEM models [119]. FEM models have improved through years, and today it is showing relatively accurate and repeatable results when simulating metal cutting process. One advantage for using FEM models is the ability to include as many cutting parameters as possible including very complex parameters such as cutting edge radius. Therefore, FEM tool can help in modelling metal cutting process to understand the cutting

conditions, tool wear mechanisms, tool-chip temperature, residual stresses, etc., which cannot be measured directly.

Modelling and simulation of orthogonal machining process of Ti-6Al-4V alloy requires workmaterial flow characteristics such as high temperatures (1000 to 1400 °C), strain-rate factors (10^4 s^{-1} to 10^6 s^{-1}) and plastic strain ration of 0.5. These conditions can be usually obtained by SHPB bench equipped with high energy heating device [120 & 121]. Even though these devices can achieve higher temperatures, they fail to meet typical strain rate and plastic strain requirements. Hence, extrapolation material behaviour regulations to the cutting conditions must be valid.

The main differences observed between experimental and FEM results are the chip morphology, cutting force and feed force; which could be more than 50% for the variables when FEM results are compared with experimental results [122-125]. During orthogonal machining of AISI 4142 steel under dry condition, at a cutting speed of 50 m/min, feed rate of 0.1 mm/rev, depth of cut of 3 mm, a feed force of 920 N was observed. However, FEM analysis with the same cutting conditions resulted in a feed force of 340 N.

Owing to strong sensitivity to parameters like strain rate and temperature, the mechanical features observed in Ti-6Al-4V are quite complex. It is critical to understand these variations to have clarity of deformation modes and to interpret the relationship among microstructure and processing variables along with its properties in diverse loading conditions. To simulate the orthogonal cutting with accuracy, flow stress behaviour of workpiece material should be modelled with maximum accuracy.

Researchers have come out with constitutive material equations to precisely describe flow stress behavior of the workpiece.

The flow stress material model defines the flow stress as a function of strain, strain-rate and temperature such that, it not only considers the strain rates over a large range but also temperature changes due to thermal softening by large plastic deformation. These models include the Oxley model [126], the J-C model [127], Zerilli–Armstrong model [128], the Usui model [129], the Mechanical Threshold Stress model [130], Litonski–Batra model [131], Maekawa model [132], etc. J-C equation is a popular constitutive relation widely used in material modeling in theoretical and numerical terms defined in a wide range of strains, strain rates and temperatures.

Researchers like Ozel and Zeren [133] Umbrello et al. [134], choose to use J-C constitute equation for modelling Ti-6Al-4V alloy as workpiece material, because it is capable of accommodating high strain, strain rates and temperatures. According to Arrazola et al. [123] accuracy of predicted results largely depends on the modeling method, constitutive model for flow stress, boundary conditions (heat transfer) and sliding friction at tool-chip machining area.

In particular, the material J–C constants in model [120] were found under a constant strain rate of 2000 s^{-1} within the temperature range 700 to $1100 \text{ }^{\circ}\text{C}$ and a maximum true plastic strain of 0.3. In order to determine the basic mechanical properties, room temperature was also considered. Umbrello [134] carried out a finite element simulation-based study on high speed machining of Ti-6Al-4V alloy. The focus of study was on predictability of cutting forces, chip segmentation and chip morphology. The experimental results were in agreement with simulation results.

SHPB is used to assess values of J-C parameters. According to literature [133] SHPB should be considered the starting point for identifying J-C parameters. For accuracy in prediction, SHPB is recommended in combination with machining tests and segmentation models of analytical chip. A possible reason could be that the constants for J-C model in Lee and Lin [120] work are identified using both results from SHPB tests through high strain rate typically in the range of 10^2 – 10^4 s⁻¹ and plastic strain ratio of 0.5 which permit a good prediction in both for conventional machining and HSM.

Friction coefficient between tool and chip lubrication of machining, having been subjected to limited studies, is an important input for modeling the machining operations, and it affects chip formation and hence tool life, surface quality and energy consumption of cutting processes. Previously friction coefficient in finite element simulations was used as a constant term specifically to match results of experiments rather than study it by a tribological approach. Coolant is meant to enhance machinability conditions of work material. Also it should improve the tool life and surface quality of the workpiece by lubricating at tool-chip and tool-workpiece interface. Various efforts were taken to estimate the coefficient of friction at the tool-workpiece interface during difficult-to-cut material machining under both dry and lubricated conditions. In one of the recent investigation Wang et al. [135] studied the cutting forces with different coolant supply strategies, friction coefficient in the sliding region at the tool-workpiece interface and used in FEM to simulate metal cutting process. However, such studies have limitations in terms of lubrication condition governed by fluid flow parameters, and machining parameters.

Although many studies on Ti-6Al-4V alloy chip segmentation phenomenon have been published, including experimental, theoretical and FE simulation

[130-134], only a few accurate studies on FE modelling involving the prediction of both cutting force and chip thickness have been found under different cutting conditions. In addition, most of finite element analysis results under different cutting conditions which show good agreement with experimental results are proposed by modifying FE model such as critical failure criteria. Therefore, a method which can be used to accurately simulate same kind of material at different cutting conditions needs to be developed.

2.6 Identified gaps in the literature and thesis contribution

Literature from reputed national and international scientific journals and conference across the fields such as solid lubricant assisted machining, tribological characterization, FEM simulation has been made. The gaps identified and objectives proposed based on the literature establish a solid framework to carry research work. The literature review summarizes key research gaps as follows.

- Several investigations tried to achieve eco-friendly sustainable machining or green machining using minimum quantity of mineral based cutting fluids, vegetables oils based cutting fluids in machining processes. However, problems associated with these fluids on environmental concerns forced manufactures to seek possible elimination of them in order to meet the demands of sustainable manufacturing. Development of advanced machining method is one of the alternatives in this direction.
- To attain high production machining with high cutting speed, feed and depth of cut are inherently associated with generation of high cutting temperature. Sufficient amount of cutting fluid is important to achieve better process performance in terms of improving tool life and surface quality. Advancement in

modern tribology has identified use of solid lubricant in oil suspension with low cost and eco-friendly, which can sustain and provide lubricity over a wide range of temperature in controlling heat and frictional effects on machining zone.

- Literature survey indicates that MQSL spray system creates a thin fluid film that spreads on the pin-disk sliding surface interface; there has not been experimental investigation that defines solid lubricant film thickness with varying particle size and concentration. An experimental investigation will require a novel experimental set-up to collect the entire development of thin fluid film, from impingement to break-up as the current experimental techniques have narrow field of view.
- Solid lubricant spray system has demonstrated an improvement in surface roughness over flood cooling, dry, wet and MQSL during Ti-6Al-4V alloy machining. However, the effect of EHVSL spray system on the tool-chip interface cutting force and tool wear machining parameters during Ti-6Al-4V alloy machining has not yet been investigated.
- The literature studies reveal that optimization plays a key role at the end of any predictive modeling. Efficient handling of any machining process requires selection of optimal cutting conditions. Close study of literature reveal substantial evidence to support accuracy of surface roughness prediction which may be improved using GMDH technique.
- A series of finite element analysis for machining Ti-6Al-4V alloy in varying cutting speed and feed rate conditions is carried out under dry and lubricant condition. FEM chip formation has proved great sensitivity to tool-chip friction coefficient. There are only limited number of studies existing in machining applications due to its difficulties and complex nature of machining processes.

Hence, the current research gaps motivate the researchers and manufacturers to study and concentrate on efforts in this direction to overcome the above stated drawbacks and to look into new machining methods to achieve sustainable machining system and to study possible routes to achieve clean machining processes. Development of advanced machining method is one of the alternatives in this direction. In view of this, future research work should be carried out with an aim to identify ways of machining as well as machining without cutting fluids as the environmental protection is going to be the key issue in near future.

2.7 Summary

The continuous increasing demands for high productivity in modern industries have led to a need for high MRR, dimensional accuracy and high surface finish. High production requirements in the metal removal processes are met by incorporating high cutting velocity, depth of cut and tool feed. This leads to the development of high temperature and pressure in the primary and secondary cutting zones. If proper and efficient cooling methods are not employed, the heat developed will adversely affect the efficiency of cutting process.

The above literature survey clearly indicates that, there is a need to concentrate efforts in the direction of solid lubricant assisted machining to overcome the high heat generation in machining of advanced engineering materials. Further, if the lubricant can be applied in a more refined and defined way, just sufficient for effective lubrication, improved process results (reduction in machining cost, improvement in tribological properties, improvement in surface integrity; thereby overall increased productivity) may be expected. In addition, research studies highlighted that although the resulting lubrication is sufficient with solid lubricants,

there is still a need to look into flushing action and tool cleaning methods to make the solid lubricant more attractive than conventional liquid lubricant method. In this context, there is a need to look into novel development of electrostatic solid lubrication experimental setup. Among different solid lubricant materials highlighted in the review, MoS₂ is the most commonly used solid lubricant due to its highest load carrying capability with a corresponding low friction coefficient and easy of shearing action between contact surfaces. The study of lubricant film formed between various geometric shapes are inherently complicated and interconnected, making it necessary to understand the concepts of tribological phenomena. To overcome the tribological losses due to friction and wear, a significant portion of lubricant with high viscous properties allows very smooth relative motion between two sliding surfaces. Further, FEM and fundamental aspects of metal cutting simulations with existing constitutive material models and tool-chip contact friction modelling were discussed. It has been concluded here that in order to improve efficiency of metal cutting processes by lowering part cost and improving machining quality, it is necessary to model metal cutting processes and material behaviour. This research work aims at filling the gap with FE modelling and fundamental aspects of metal cutting simulations of Ti-6Al-4V alloy.

CHAPTER 3

DEVELOPMENT OF ELECTROSTATIC HIGH VELOCITY SOLID LUBRICANT SPRAY SYSTEM

The set objective of present research and impetus to overcome the research gaps in the existing literature (listed in chapter 2) establishes a framework to fabricate sustainable and innovative lubricant technology to facilitate the supply of solid lubricant particles effectively to the tool-chip interface at constant flow rate. In order to fulfill the objective of sustainable development, the current research work introduces a novel approach for developing effective minimal fluid application technique namely EHVSL assisted machining spray system. This chapter covers detailed information about the development of electrostatic spray system. The present chapter also presents the selection of work material used, cutting tool, experimental conditions, instrumentation, planning of experimental conditions and the procedures adopted for the study are described.

3.1 Introduction

The major challenge before modern machining industries is to achieve higher production rates by improving the quality of product in terms of closer tolerance, improved surface quality and enhanced performance while meeting the environmental and sustainable manufacturing principles. Manufacturers continually strive for ways and means to achieve better quality and higher productivity in any machining operation to maintain their competitiveness. Advanced studies in modern tribology have introduced several self-lubrication (or) solid lubricants with low cost and eco-friendly, which can withstand and provide lubricity over a broad spectrum of

temperatures [18]. It has been revealed from literature review that better cutting performance can be achieved when lubricants are penetrated quickly and effectively upon the critical location i.e. tool-chip-workpiece interface in a short period of time [58 & 136]. Development of advanced machining methods is one of the alternatives in this direction to apply lubricants effectively to high temperature cutting region to achieve better results.

Electrostatic spraying is advancement in atomization technology where droplets act as charge carriers when subjected to an electrostatic field of high-voltage. This technique is currently employed across various fields such as chemical, automotive, agriculture industries. Li et al. [137] made an effort to evaluate the impact of electrostatic spray technique on automobile finish mechanism and experimentally obtained reduction in exhaust emission rates with reduced average fuel droplets size. Ghanshyam et al. [138] developed electrostatic spray assisted system for coating thin films and unlike in chemical vapor deposition technique, obtained deposition efficiency as high as 80%. Law [139] presented a review on applications of electrostatic spray system in various sections of agriculture. The authors proposed that using this technique increased adsorption and penetration droplet rates can be achieved while minimizing waste. Besides, numerous researchers have developed novel machining systems where lubrication and cooling of cutting zone is done electrostatically [58, 136]. Reddy and Yang [58] developed an electrostatic lubrication (EL) technology to supply a defined quantity of cutting fluid at constant rate that uses on electricity to create droplets. Their study included a thorough comparison between MQL and dry drilling based on tool wear, diameter of the hole, thrust force and surface finish. The experimental results of the study proved EL to be an effective

technology and its potential to be used as a viable alternative. Studies were conducted by Liu et al. [140] on dry electrostatic cooling (DEC) assisted machining of hardened steel. The influence of DEC on cutting force and tool life were investigated and results showed that, unlike dry cutting, corona treated compressed air technique provides better lubrication and cooling and as a consequence, cutting force and tool wear decrease.

Keeping the necessary conditions in view, the current research work envisages the possibility of developing a novel experimental setup for effective supply of solid lubricant particles to the machining zone. In this direction, the present research work envisages the feasibility of developing a new generation of machining technique namely EHVSL spray system with an aim to abolish the application of cutting fluid and to minimize frictional force at tool-chip interface in the machining operation. This approach is based on the concept of supplying solid lubricant suspension (MoS_2 and base oil) as a thin lubricant film with high velocity jet along the cutting edge of inserts and with an aim to give a significant reduction in flow rate (20 ml/hr) while maintaining constant supply for specific hard turning of Ti-6Al-4V alloy, thus meeting environmental requirements. It is a novel technique introduced in the manufacturing process to supply micrometer sized solid lubricant particles effectively to the machining zone while satisfying sustainable issues in terms of enhancing tool life, resulting in higher productivity and ability of using higher cutting speeds, thus reducing surface roughness.

3.2 Development of EHVSL experimental set-up

Sufficient amount of cutting fluid and delivery method is very important in machining process to achieve better process performance in terms of improving tool life and surface quality [8 & 135]. The primary objective of the present research work is to fabricate the novel experimental set-up i.e. EHVSL system as shown in Fig. 3.1. It is a new technique introduced in the manufacturing process to improve process performance in turning operation. Detailed explanation about EHVSL supply system and nozzle design is explained below.

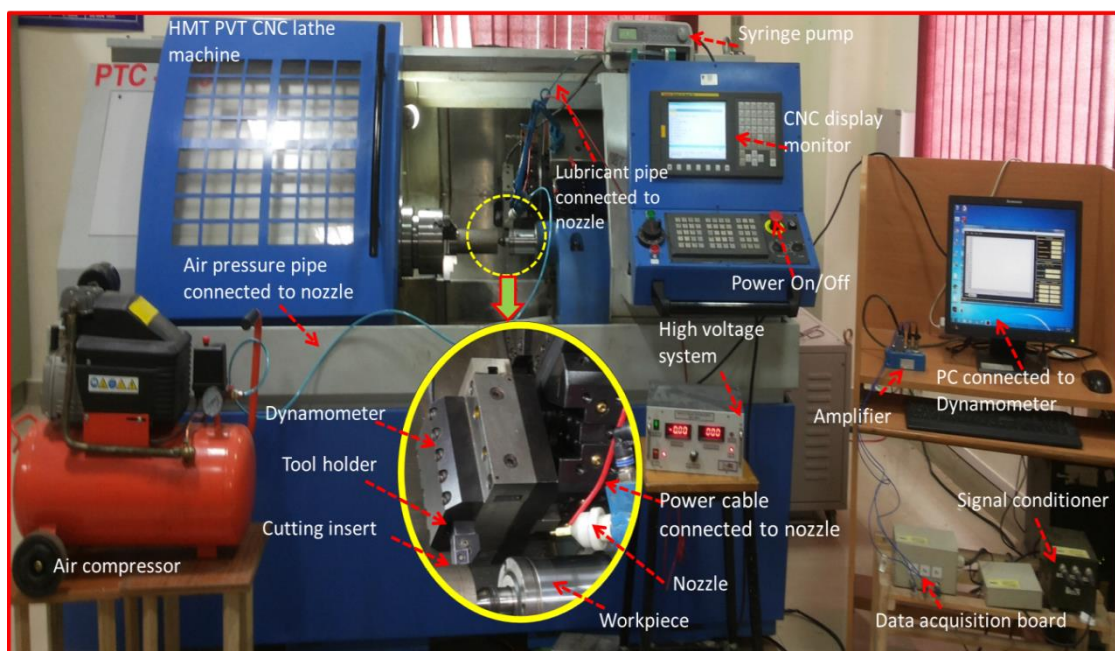


Fig. 3.1: Photographic view of developed electrostatic high velocity solid lubricant spray system

3.2.1 Electrostatic high velocity solid lubricant set-up

The EHVSL system consists of a syringe pump, high voltage power supply, spray nozzle, and air compressor as shown in Fig. 3.2. Effective cooling and lubrication in machining process is very crucial to control friction and extreme heat

generation involved in the process. In the present research work, the feasibility of the novel approach for developing a new generation of machining technique namely EHVSL with an aim to improve process performance and to eliminate the use of cutting fluids in machining process.

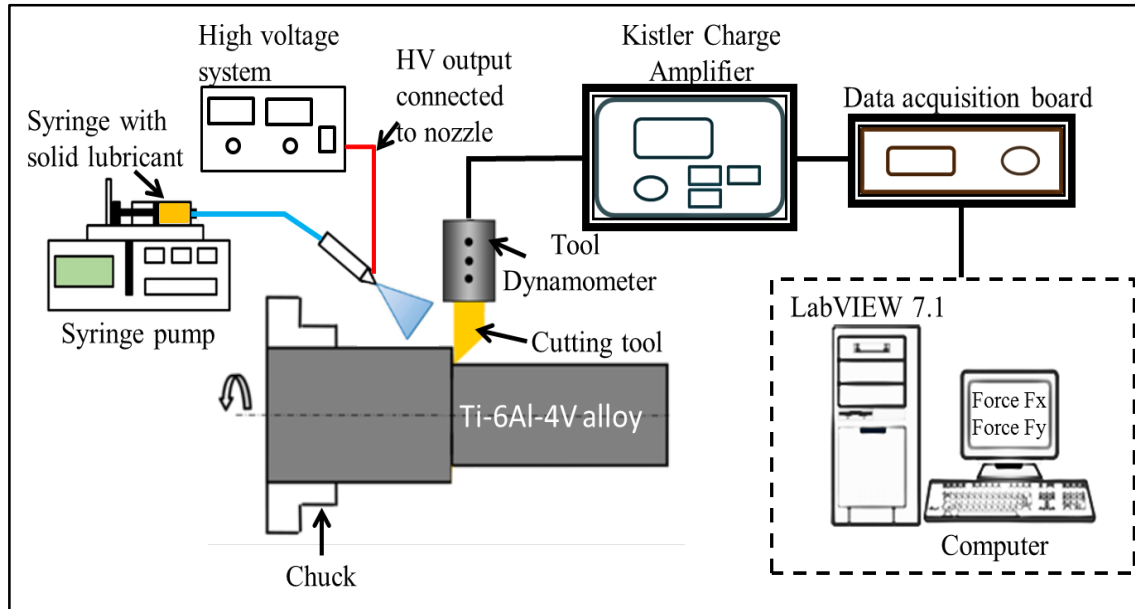


Fig. 3.2: Schematic illustration of the EHVSL spraying setup

The system uses contact electrification to charge lubricant in the nozzle and an electric field to aid in uniform lubrication at tool-chip-workpiece interface. It makes use of electrostatic charging principle to charge suspension of solid lubricants passing through specially developed nozzle. Syringe pump is used to maintain steady flow rate of lubricants. Air hoses were used to supply compressed air to the nozzle for lubricant atomization. To create a required electrostatic force within the sprayed solid lubricant particles, a high voltage (negative) potential of 0-10 kV was employed and connected by cable to the tip of the nozzle. The applied voltage is varied from 3 to 8 kV. When the lubricant particles reach the nozzle tip, they instantly get charged and are broken into smaller droplets by the compressed air. These charged-broken solid

lubricant particles quickly penetrate on to the rake and flank face of the tool-workpiece interface and create a thin lubricant film.

The electrostatic field created at tip of the nozzle, serves to ensure charging of lubricant particles owing to ionized air flow in the stream, and consequently, in-line air supply through nozzle provides easy transfer of solid lubricant particles towards the grounded tool-chip-workpiece interface. When solid lubricant particles come close to the grounded part (workpiece and cutting tool), an electrostatic attraction between the charged lubricant particles creates a temporary adhesion between solid lubricant particles and grounded tool-chip interface.

The function of high voltage supply is to create required electrostatic charge within sprayed lubricating particles to facilitate the adhesion of lubricant particles to the grounded part of tool-workpiece interface. The high velocity spray system is projected along cutting zone, so that solid lubricant suspension influences effectively on to the tool-chip-workpiece interfaces as possible. The electrostatic field created at the tip of the nozzle ensures charging of solid lubricants owing to ionized airflow in the stream, and consequently, the in-line air supply through nozzle provides easy transfer of lubricants towards the tool-workpiece interface.

3.2.2 Electrostatic high velocity solid lubricant process

Electric potential is a very important factor in the electrostatic lubrication process as it directly relate to the charge of lubricant particles. To achieve better process performance in terms of improving product quality and tool life, a spray of monodisperse solid lubricant particles (droplets) is achieved by passing a high viscous lubricant with necessary electrostatic charge within the sprayed lubricant particles to a high potential with a short distance away with respect to a ground electrode. In

supplying solid lubricants, a very small amount of lubricant particles will be applied in the form thin yet even lubricant mist droplets with high penetrability and wettability to the machining zone within a short time duration which is functionally important. Under the influence of an electrostatic field, solid lubricant particles meniscus takes the shape of a cone from the tip of which a thin lubricant film forms, primarily to cone-jet mode. These lubricant particles break into a stream of charged particle droplets that ultimately spread to form a uniform spray.

If the lubricants are uncharged, unlike in an electrostatically charged system, the process spray may lead to splash, spread, or rebound. Specifically, during high temperature condition, lubricant droplets tend to rebound because the pressure of the vapor below the liquid partially lifts the droplet. Because of this, the conventional spray cooling systems are not effective. Droplet coalescence is taken care by spray self-dispersion Columbic repulsion which also improves suspension by producing droplets of uniform size even at nanoscale [143]. The system uses contact electrification charge principle to charge the lubricant particles in the nozzle and an electric field to aid uniformly charged lubrication at chip-tool-workpiece interface surface. The nozzle tip diameter of spray system is 0.2 mm which is larger than the sprayed droplet particles, which diminishes the threat of clogging and intensely reduces the lubricant pressure drop.

3.2.3 Nozzle

Nozzle is one of the significant components of EHVSLS supply system, as seen in Fig. 3.3. For a developed experimental set-up, the nozzle is developed in such a way to effectively reach and cool/lubricate localized “hot-zones” (tool-chip-workpiece interface) in the cutting area with MQSL consumption as discussed early in

Chapter 2, Section 2.2.4. The nozzle tip is impinged onto the rake and flank face of the cutting tool. The nozzle fixture is attached to the tool holder support and so positioned that it applies charged solid lubricant mixture particles coming out of the nozzle reaches to machining zone with a constant flow rate of 20 ml/hr.

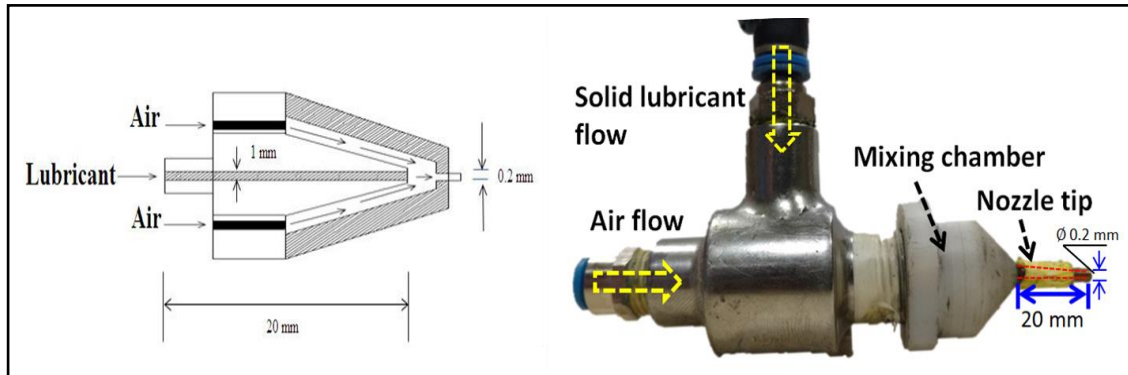


Fig. 3.3: Schematic diagram of nozzle

The impact energy of majority of solid lubricant particles is controlled by EHVSLS spray constraints (e.g. flow rate, air pressure, nozzle development, impingement angle, electrostatic voltage) to obtain ‘spreading’ droplet particles impingement regime, ideal for machining applications. Nozzle position is so adjusted as to supply charged solid lubricant suspension selectively to tool flank and rake face of cutting tool. Tool flank and rake face are the two important faces of cutting tool, where most flank wear and crater wear occur respectively. Enhancing its effectiveness as a lubricant, high velocity thin pulse jet electrostatic solid lubricant may create thin film that spreads over tool-chip-workpiece interface. Solid lubricants are firstly charged at nozzle tip and the charged solid lubricant particles are broken into micrometer sized droplets by the compressed air. The charged solid lubricant particles will quickly penetrate and adhere to the surface of tool-chip-workpiece interface to form thin lubricant film in the machining area.

3.2.4 Syringe pump

As the name indicates, the main component of syringe pump is syringe. Syringe pumps (Fig. 3.4) either pull the lubricant in or push it out via a syringe attached to it to obtain the volume quantity by the size of syringe. In this study, syringe pump is used for smaller quantity of lubricant and to maintain steady flow rate of solid lubricants. Using syringe pump it is quite easy to know the flow rate of lubricants. In order to allow the flow of lubricants from syringe pump, pressure is applied to the syringe plunger and syringe-pump-motor moves a block forward. It holds one syringe pump from micro-liter size up to 60 ml with a low flow rate of 1-1100 ml/hr.

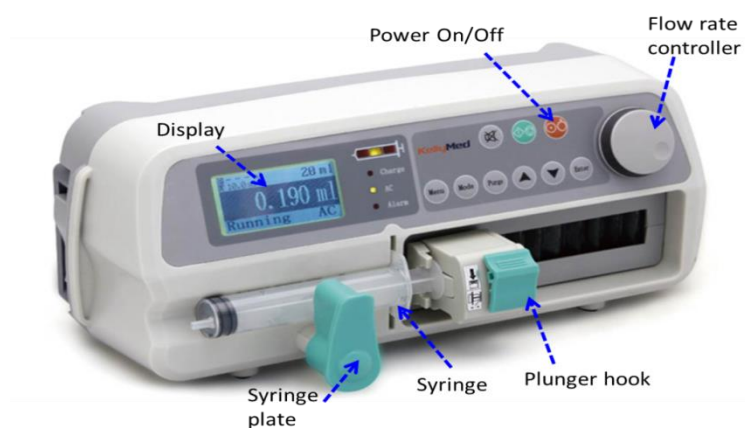


Fig. 3.4: Photographic view of syringe pump

3.2.5 High voltage system

High voltage power supply system is a key component in electrostatic application. The fundamental principle of operation of an electrostatic precipitator is that the lubricant particles are initially charged by passing them through an electric field; these charged lubricant particles get deflected across the particle collection field of the earthed plate. This basically comprises of a suitably designed and insulated setup transformer, from which the output can be controlled by adjusting incoming

mains supply voltage level. The transformer output is then rectified to produce a high negative voltage. In this study, a HV (High Voltage) DC power supply with output voltage range from 0 to 10 kV with output current up to 2000 A is used. The HV power supply is designed, developed and fabricated by Ionics Power Solutions Pvt. Ltd., Hyderabad (Fig. 3.5).

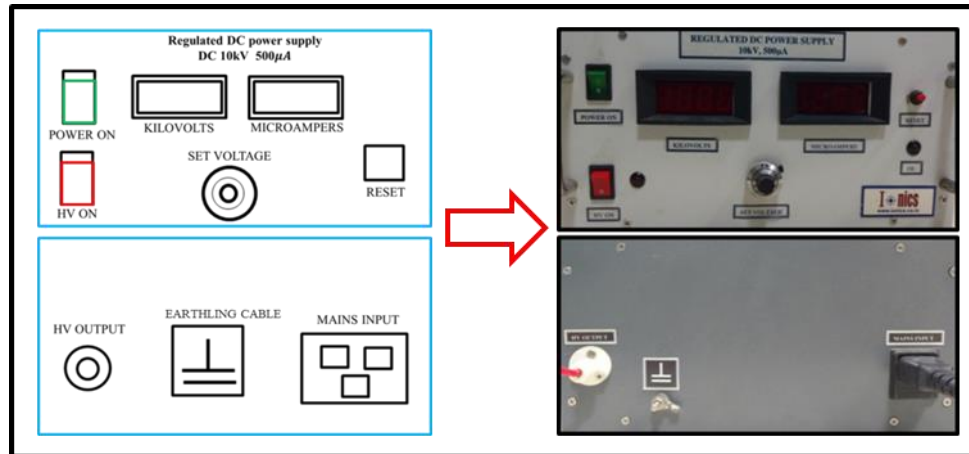


Fig. 3.5: High voltage power supply system

3.3 Structure of EHVSL spray system

Electrostatic spraying system has attracted great interest in recent studies for preparation of thin lubricant films. This supplies higher amount of lubricant at tool-chip-workpiece interface to enhance the process of adsorption film and oxide layer formation in the shortest available time. Developed EHVSL spray system comprises of a negative HV (High Voltage) power supply, spray nozzle, syringe pump, air pressure controller and air compressor. All the main components are connected with hoses and cables, with all necessary regulators and fittings. The technique uses compressed air that carries lubricant particles in a mixture that is pumped and directed to the cutting regions to exert its role adequately. The purpose of air compressor is to atomize solid lubricant particles by an air hose through the mixing chamber and then to supply the same to spraying nozzle. The high-velocity

thin pulse jet of EHVSL spray system nozzle was directed towards auxiliary cutting edge of the tool-chip interface, as indicated in a frame within Fig. 3.6. MoS₂ solid lubricant particles are initially charged at tip of the nozzle from where they are broken into droplets with air pressure to effectively cover tool-chip-workpiece interface. Electrostatically charged (negatively charged) solid lubricant particles will quickly penetrate and adhere on the surface of tool-chip interface to form thin solid lubricant film. However, larger particles give varying lubricant film thickness between the sliding interface zones. Particle size and voltage have significant effects on lubricant droplet particles and lubricant film thickness.

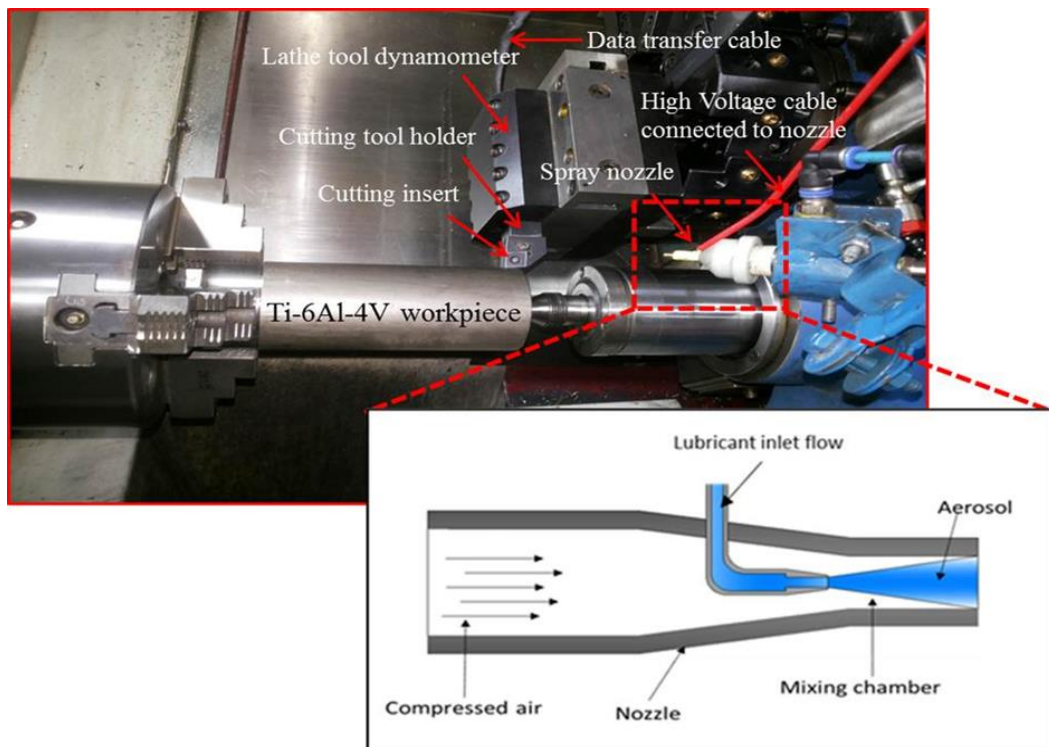


Fig. 3.6: Schematic view of nozzle with EHVSL spray system

For the developed EHVSL spray system, MoS₂ solid lubricant particles are used as lubricants. Solid lubricant particles were primarily charged at the nozzle tip and the charged lubricant particles were broken into lubricant droplets by air

compressor. To select the optimum value of charging voltage, trial experiments have been implemented, in order to attain a fine chargeability and uniform spray of solid lubricant droplets at the exit end of the nozzle tip.

The mechanism of charging particles will be discussed in detail in section 3.4. Solid lubricant particles are propelled by means of electrostatic force which transports the charged solid lubricants at the interface zone, which is earthed and enclosed. A component of typical electrostatic lubricant process is shown in Fig. 3.7. The charge on lubricant particle is attracted to the substrate where it is held by various adhesive forces. In order to accomplish a successful lubricating in the machining interface, this method uses a combination of the below listed elements.

- (i) Delivery of solid lubricants
- (ii) Charging of solid lubricants
- (iii) Transfer of solid lubricants from charging region (nozzle tip) to high temperature interface (tool-workpiece interface)
- (iv) Adhesion of solid lubricant particles at tool-chip interface

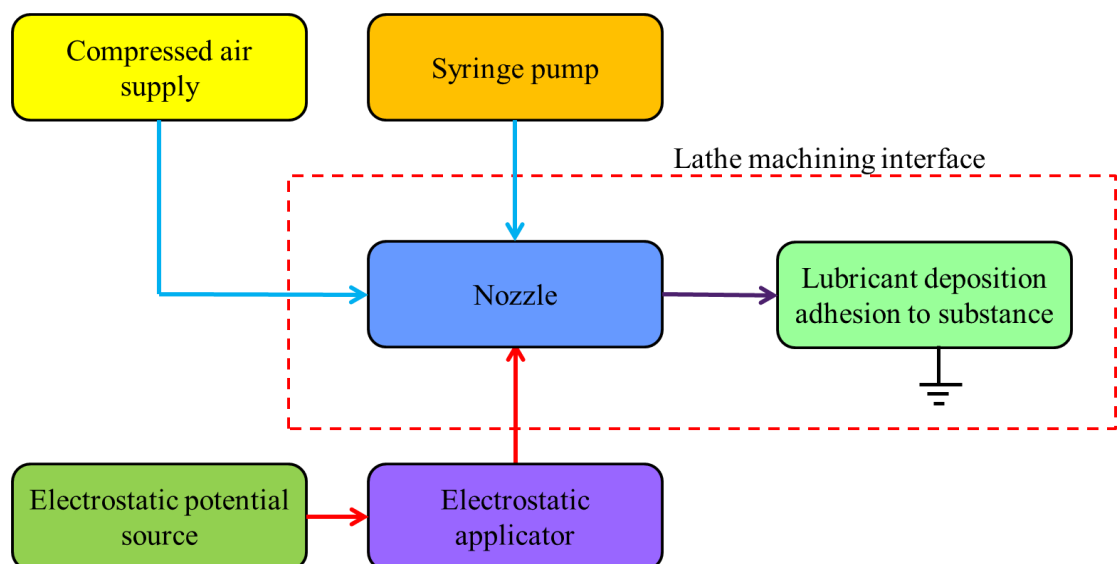


Fig. 3.7: Components of typical electrostatic lubricant process

3.4 Electrostatic charged properties

The function of high voltage supply is to generate necessary electrostatic charge within the sprayed lubricant particles and to facilitate adhesion of solid lubricant particles to tool-chip-workpiece interface (hot-zones). Strength of the electric field required to transfer lubricant particles towards the grounded workpiece is evaluated by calculating mean charge to mass ratio (q_{max}/m) of lubricant particles. Calculated particle mean charge to mass ratio and transfer efficiency of the developed lubricant spraying system are given by Eqn. 3.1. The particles pass through a highly charged and ionized electric field at the nozzle tip applying a strong negative charge to each particle. Schematic view of EHVSL with cloud of tiny charged solid lubricant particles is shown in Fig. 3.8.

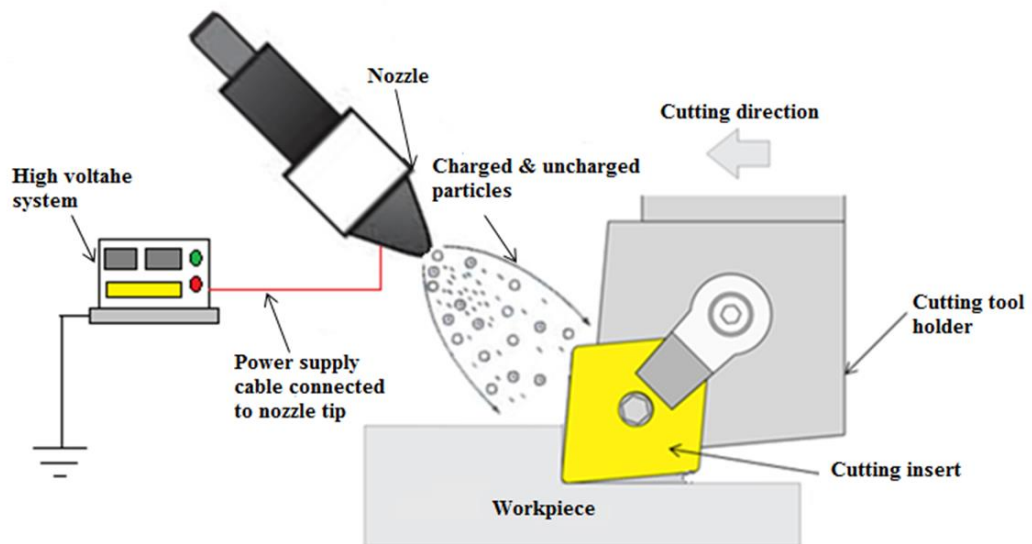


Fig. 3.8: Schematic view of EHVSL with cloud of tiny charged solid lubricant particles

In electrostatic charging spraying process, the amount of charge acquired by the solid lubricant particles not only determines their trajectories but also their adherence tendency to metal substrate [141 & 142]. Studies revealed that the particle

adherence tendency is the function of mean surface charge to mass ratio ($\frac{q_{max}}{m}$) of solid lubricant particles (Eqn. 3.1).

$$\frac{q_{max}}{m} = \frac{12 \pi r^2 \epsilon_0 E}{\left(\frac{4}{3}\right) \pi r^3 \rho} \text{-----} \quad (3.1)$$

Where q_{max}/m = mean charge to mass ratio, r = radius of the particles, ϵ_0 = permittivity of space, E = strength of electric field, ρ = density of the particle.

Measurement of this mean surface charge to mass ratio is very helpful in electrostatic solid lubricant process as it provides and indicates how effectively a particular lubricant experimental setup works, which in turn perhaps used to evaluate transfer efficiency of the system.

3.5 Other tools and equipment

Machining process is completely carried with dry, wet, MQL, MQSL and EHVSLS lubrication techniques. Tools and other equipment used in the present research work are as follows.

3.5.1 Force measurement

A considerable amount of investigation has been carried out for predicting and measuring the cutting forces. This owes to the fact that the developed cutting forces during machining have a direct impact on heat generation, which in turn has a direct influence on tool wear and surface roughness. In this study, piezoelectric lathe tool dynamometer is used for determining the machinability of the materials.

3.5.1.1 Dynamometer

The three component piezoelectric dynamometer helps to perform force

measurement in any machining processes (shown in Fig. 3.9). This is a multi-component transducer having three output channels with piezoelectric transducers designed to resolve the forces which are acting along the three mutually perpendicular axes. Dynamometer was mounted on specially designed fixtures as shown in Fig. 3.3. The cutting force is split into three namely the radial thrust force (F_x), tangential (main) cutting force (F_y), and feed force (F_z) which are taken as output. Table 3.1 shows the specifications of dynamometer used in the present work.

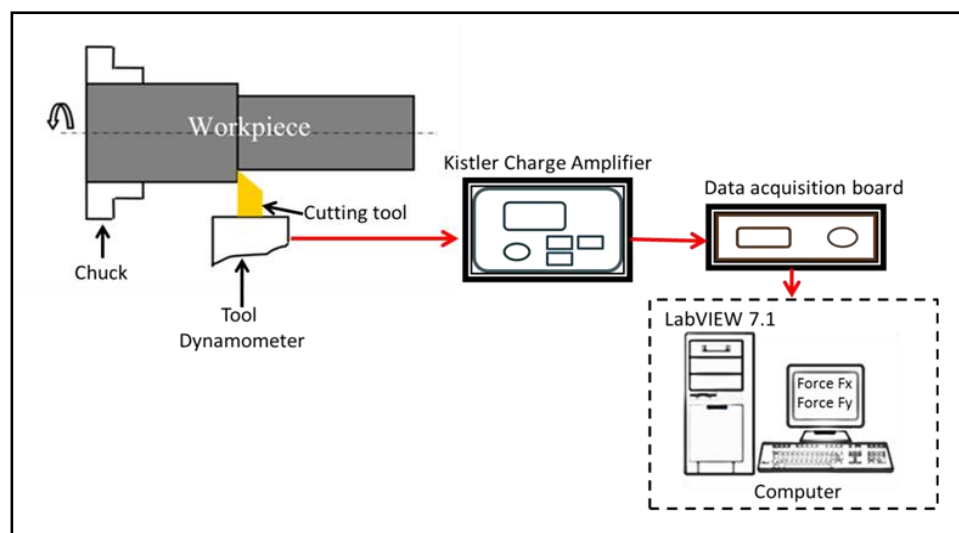


Fig. 3.9: Schematic view of lathe tool dynamometer

Table 3.1: Specifications of dynamometer

	F_x	F_y	F_z
Measuring Range (N)	2224	2224	4448
Sensitivity (Pc/N)	-7.78	-7.92	-3.72
Linearity $\leq \pm$ %FSO	0.3	0.3	0.3

For each of the three force components, a proportional charge signal is produced in the measuring element. These charge signals are fed to the charge amplifiers where they are converted into voltages that may be indicated or registered as desired. These low cross-talk sensors are highly sensitive and offer high stiffness

with excellent repeatability and long term durability. With the help of a tool holder, the tool insert is fixed to the dynamometer which is then placed on the machine tool turret using an adopter.

3.5.1.2 Charge amplifier

A charge amplifier is included in the setup for effective utilization charge difference that appears when piezoelectric sensors are loaded. It consists of an inner amplification unit which converts the input charge difference into voltage signals. A reliable connection is very essential between charge amplifier and dynamometer for a better quality of measured signals. Industrial charge amplifier 5007 A311 type is employed for amplifying the out of transducers into proportional voltage. The mechanical unit per unit volt for each channel is set according to force components connected to the channel. The specifications of the charge amplifier are as follows (Table 3.2). Ground-insulated cables are sealed with a metal hose to ensure safety when working in raw operative conditions on a machine tool. Stable connectors provided at both ends of the cable to achieve a protection of IP67 class at the connection to the stationary dynamometer.

Table 3.2: Specifications of a charge amplifier

Measuring ranges	± 100 to 1000000 pC
Voltage output full scale	-10 to ± 10 V
Output current	± 5 m A
Transducer sensitivity	0.1 to 11000 P _c /MU
Linearity	$< \pm 0.05\%$
Frequency response error, with standard filter 180 KHz (at 100 KHz)	$< \pm 5\%$

3.5.1.3 Acquiring/Analyzing software

NK Instruments offers optimized software for data acquisition and analysis with cutting force measurement. With the cutting force measurement (CFM) V 1.0.2, it is possible to set all of the constraints of the corresponding charge amplifiers that are important for data acquisition. The acquired data is presented in a graphics form and facilitate, together with various functions, the signal processing and analysis of the measurement signals. With Dyno Ware, it is easy to document and export the data.

3.5.2 Precision balance

A high-performance analytical balance (AUW 220D) measures sub-micron range masses with a minimum display 0.01 mg and has excellent response capabilities as shown in Fig. 3.10. In this study precision balance is used for measurement of total solid lubricant particles (maximum 20 g and minimum scale is 0.04 mg).

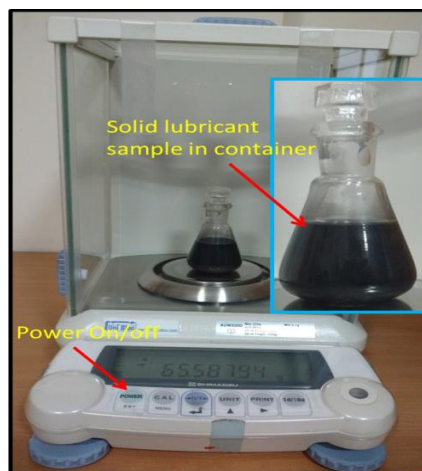


Fig. 3.10: Photographic view of weighing balance during weighing lubricant samples

3.5.3 Surface roughness measurement

In this investigation, surface roughness (R_a) measurements are taken using Talysurf-6; at an angle 90° to the direction of turning. Surface roughness is measured at three random points along the workpiece circumference. Average of these three

points is taken as the surface roughness of the machined workpiece. The specifications of surface roughness are shown in Table 3.3. A sample measure of surface finish on machined work material using surface profilometer (Taylor Hobson Surtronic S25) is shown in Fig. 3.11.

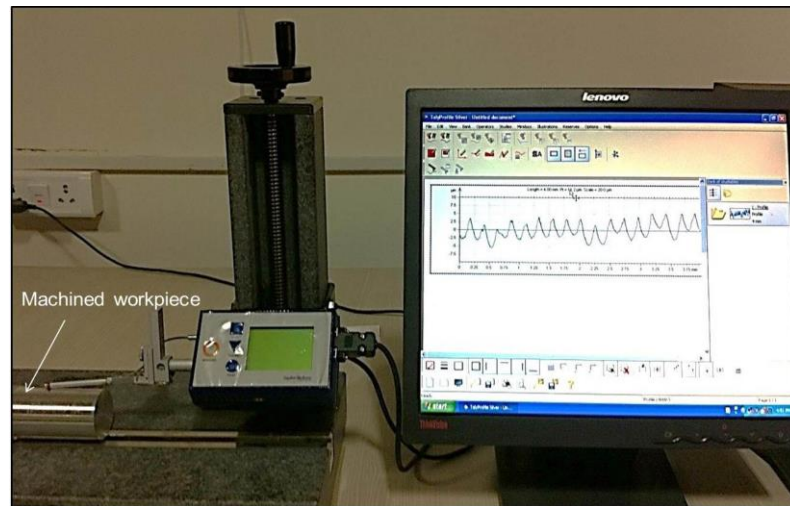


Fig. 3.11: A sample measure of surface finish on machined work material using surface profilometer (Taylor Hobson Surtronic S25)

Table 3.3: Specifications of Talysurf profilometer

Maximum height of stylus above traverse unit	340 mm
Work table	620x40 mm
Tee slots	Two (685x400x700)
Maximum length of traverse	120 mm between adjustable ends
Traverse speed	1 mm/s at Vh X5
Vertical magnification	X100, X200, X500, X1000, X 2000, X5000, X 10000, X100000.
Horizontal magnification	X2, X5, X20, X50 ... X1000.
Skid force (adjustable)	0.5 N maximum for all pick-up attitudes
Stylus tip size	2 μm (normal)
Skid radius	50.8 mm

3.5.4 Computer numerical control (CNC) turning machine

CNC is a special class of machine tool category used widely in turning, milling, drilling, grinding etc. CNC provides control over cutting tool and workpiece motions, and enables the operator to accurately employ the cutting condition such as feed, depth of cut, speed and miscellaneous functions. The basic objective behind the use of CNC turning machine is reduction of the cost of production and improvement in product quality. Machining by CNC turning can be done to very precise limits, which normally is very difficult by a conventional lathe. CNC turning machine (HMT PVT 260) used for experiments is (shown in Fig. 3.1) and its specifications are given in Table 3.4.

Table 3.4: Specifications of CNC lathe machine

Specifications	HMT-PRAGA PTC200
Spindle speed	100-4000 rpm
Maximum turning diameter	200 mm
Distance between centers	300 mm
Turning tool size	20x20 mm
Power cont/15min	5.5/7.5 kw
Tool holders	8

3.5.5 Infrared (IR) & Thermal Imaging Camera

The operation of an IR camera is based on the principle of conversion of heat into electrical signals. During operation the IR camera (shown in Fig. 3.12) detects infrared rays and suitably converts them into electronic signals. These signals are processed in the next step to generate thermal images on a small video monitor and to perform temperature measurements. IR camera precisely quantifies sensed heat and thus helps to monitor thermal performance. Besides it also helps to evaluate thermal-

related problems. The detailed specifications of IR camera are shown in Table 3.5. A thermal infrared camera (FLIR E60) with 320 x 240 pixels with thermal sensitivity of less than 0.05°C at 30°C is used to measure pin-disc contact temperature during the experimental conditions.



Fig. 3.12: FLIR E60 Infrared thermal imaging camera

Table 3.5: FLIR E60 Infrared Camera specifications

Resolution	320 x 240 pixels
Total pixels	76,800
Thermal sensitivity	< 0.05°C
Accuracy	± 2°C or ± 2% of reading
Temperature measurement range	-20 to 650°C
Display screen	3.5"
Video Camera w/Lamp	3.1 MP
Zoom	4x Continuous Digital

3.6 Experimental details

To assess the performance of developed EHVSL experimental set-up, experiments were carried out by properly selecting the concentration and flow rate of solid lubricant suspension in terms of improving machining properties, surface

integrity of machined part and comparing the same with existing cooling/lubrication methods.

3.6.1 Workpiece material

Each test to evaluate cutting performance was carried on Ti-6Al-4V grade 5 alloy bar of 300 mm length and 65 mm diameter. The chemical composition of Ti-6Al-4V alloy is given in Table 3.6.

Table 3.6: Chemical composition of Ti-6Al-4V alloy

Element	Al	V	Fe	C	Ti
Composition (wt. %)	5.560	4.070	0.185	0.022	89.997

During turning operation, possibilities of workpiece being subjected to vibrations are high. These vibrations may cause reduction in cutting speed which is not desirable. This negative effect can be minimized by properly supporting the workpiece at the tailstock by drilling a hole on its face before the start of the experiment. A 1 mm deep precut was made using tungsten carbide tool on each of the workpiece before the actual turning was performed to eliminate oxidation surface or top hardened surface. Prior to actual experiments, trials were conducted on CNC lathe machine at different cutting conditions. A dial indicator was used to check the extent of wobble in the workpiece during cut which was later minimized by proper adjustment of chuck.

3.6.2 Solid lubricant additive

Solid lubricant additives have gained significant popularity due to the excellent tribological performance they offer [14]. From the previous studies it was observed that, generally MoS₂ (lamellar material) possesses good load bearing

capacity corresponding to a low friction coefficient under sliding condition [19 & 21]. MoS₂ is one of the mostly well-known and widely used solid lubricants, although initially intended to be used for aerospace and military applications, now a days has increasingly been found in various lubrication techniques. Large particles may cause excessive abrasion wear due to impurities present in MoS₂; accelerated oxidation may result when smaller particles are used. It can be efficiently utilized to minimize wear and friction in fluid lubricants within the specified boundary conditions, to facilitate higher load bearing capability and during the instances of oil loss may slowdown/prevent any catastrophic seizure that may occur. In the present research work MoS₂ solid lubricant particles were chosen as an additive in the base oil with an average particle size of 10 μm . Thin films of MoS₂ added solid lubricants binds firmly to the sliding surfaces and effectively bring down friction and wear to lower levels.

3.6.3 Base oil

SAE 40 (Society of Automotive Engineers) oil has good lubricating properties owing to its higher viscosity. Thus, in the current study it is chosen as suspension medium for the solid lubricant. Table 3.7 lists out the properties of SAE 40 oil.

Table 3.7: Properties of base oil (SAE 40)

Flash point	260°C
Fire point	300°C
Kinematic viscosity at (40°C)	220 cSt
Kinematic viscosity at (100°C)	15.87 cSt
Specific density	865

3.6.4 Planning of experimental condition

An experimental program is designed to achieve the proposed objective in a simple manner. The planning and execution of the same has been discussed in the foregoing section.

3.6.4.1 Selection of process parameters

A large number of interacting variables increase the complexity of turning operation. Process variables such as feed, speed depth of cut etc., will have major influence on the geometry of the workpiece produced during turning operation. However, to ease the data collection process, only three of the variables are chosen for the experimental studies. From the review of the past literature, tool geometry (rake face and flank face) and cutting conditions (feed rate, cutting speed and depth of cut) were considered as process parameters and their effect on the cutting force, surface roughness, tool wear and chip thickness is investigated in the current research. Experiments were carried out keeping these factors at different levels. The range of individual factor was selected keeping in view the requirements of the present day industries.

3.6.4.2 Design of experiments

It is necessary to have a well-constructed design procedure to carry experiments since the way experimentation is designed majorly affects the number of experiments required. To investigate all the possible interactions occurring between independent variables such as feed, speed and depth of cut, a full factorial design of experimentation was employed to conduct the experiments. Responses measured were cutting force, tool wear, surface finish and chip thickness ratio. In the first stage of experimentation, each factor has three levels (shown in Table 3.8). Based on full

factorial design approach, 27 (3^3) experiments were conducted in all the considered environmental condition, each having a set of different factor levels, as given in Table 3.9.

Table 3.8: Process variables and their levels

Sl. No.	Parameter	Level-I (Low)	Level-II (Medium)	Level-III (High)
1	Cutting speed (v_c) m/min	100	150	200
2	Feed (f) mm/rev	100	150	200
3	Depth of cut (a_p) mm	0.5	1	1.5

Table 3.9: 3^3 Factorial design matrix for experimentation

Test No.	Cutting speed (V_c) m/min	Feed rate (f) (mm/rev)	Depth of cut (a_p) (mm)	Test No.	Cutting speed (V_c) m/min	Feed rate (f) (mm/rev)	Depth of cut (a_p) (mm)
1	100	0.1	0.5	15	150	0.15	1.5
2	100	0.1	0.5	16	150	0.2	0.5
3	100	0.1	0.5	17	150	0.2	0.5
4	100	0.15	1	18	150	0.2	0.5
5	100	0.15	1	19	200	0.1	1.5
6	100	0.15	1	20	200	0.1	1.5
7	100	0.2	1.5	21	200	0.1	1.5
8	100	0.2	1.5	22	200	0.15	0.5
9	100	0.2	1.5	23	200	0.15	0.5
10	150	0.1	1	24	200	0.15	0.5
11	150	0.1	1	25	200	0.2	1
12	150	0.1	1	26	200	0.2	1
13	150	0.15	1.5	27	200	0.2	1
14	150	0.15	1.5				

3.6.5 Experimental procedure

Turning experiments were carried on HMT PVT 260 CNC lathe machine at constant feed, speed and depth-of-cut. In the present study, the material used in all the experiments was Ti-6Al-4V alloy with an average hardness of 64 HRC. Cutting tool holder is attached to a piezoelectric dynamometer for measurement of cutting force

and three channel amplifiers was used to amplify signals for measuring cutting forces. Signals obtained from the sensor are sent to a PC where the data is processed by a data acquisition and analysis system and stored into the PC. Before actual machining, a pre-cut of 2 mm depth was carried on workpiece surface to remove irregularities if any, and to provide a similar surface for all tests. Photographic view of EHVSL system is shown in Fig. 3.1. Tungsten carbide tool inserts with ISO designation CNMG120412 were used as cutting tools. MoS₂ solid lubricant particles with 10 micrometer sized were used as solid lubricant substance. SAE 40 oil is used as base oil. Syringe pump is used to supply solid lubricant suspension through hose into the nozzle.

Based on the preliminary findings, and considering the influence of machining parameters, experiments for performance assessment of turning operation were done with constant feed rate, cutting speed, and depth of cut. Factors selected to carry performance studies were surface roughness, tool wear, cutting force and chip thickness ratio. Water-soluble cutting oil (Milacron ct 100, 10:1 dilution) was used in the conventional cooling condition i.e. wet machining (flood cooling). Variables like changes in set-up, machine condition etc., were kept constant throughout the experimentation. During MQL process, compressed air with minimum quantity of water-soluble cutting oil was used and applied at a flow rate of 500 ml/hr. In case of MQSL assisted machining, 20wt% concentration of MoS₂ solid lubricant particles (10 μ m) were selected as an additive in SAE 40 oil to prepare a solid lubricant suspension.

3.6.6 Software for analysis of results

ABAQUSTM/CAE, Computer Aided Engineering is a software used for

designing modelling, visualizing products and machinery in fields such as aerospace and automotive industries. Also, this software is widely used in academic and research organizations due to its capability to design and customize a wide range of materials models. ABAQUSTM offer a multi-physics platform making it suitable for simulations which require multiple fields. In the present work a two-dimensional (2D) FEA model is used to simulate orthogonal cutting of Ti-6Al-4V alloy using commercially available ABAQUSTM software and to analyze phase transformation of the cutting force and chip thickness during dry and EHVSL lubrication condition.

3.7 Operating process parameters for EHVSL assisted machining

It is essential in EHVSL assisted machining process that lubricant particles must effectively cover the hot-machining contact area. Another important variable is wettability of solid lubricant particles on tool-workpiece surface. Selection of machining conditions effectively contributes to the simultaneous improvement of quality and productivity. Therefore it is vital to choose optimal machining parameters of EHVSL spray system to enhance machinability for a given material without affecting production timelines. To achieve this goal, the current research work is carried to investigate the effect of high pressure cooling/lubrication with EHVSL technique and high velocity jet application parameters, i.e. concentration of lubricant to weight ratio, flow rate of lubricant, lubricant pressure, angle of the impingement of the jet, and spot distance of the nozzle on cutting force and surface roughness, while turning Ti-6Al-4V alloy. Experiments have been conducted to select the process parameters in hard turning with MoS₂ as a lubricant media and SAE 40 oil as a base lubricant. The smaller droplets, which can provide better penetration into the cutting surface, are more preferable especially in terms of applying lubricants effectively in

the machining zone.

3.8 Experimental details

Trial tests have been performed to select optimum values of charging voltage in order to achieve a fine chargeability and jet of lubricant droplets at the exit end of the nozzle. The selected trial domain is as follows: air pressure (1, 3, 5, 8, and 10 bar), nozzle spray distance (10, 20, 30, 40 and 50 mm), nozzle spray angle (30°, 60°), lubricant flow rate (5, 10, 20, 30, and 40 ml/hr), and electric potential (2, 4, 6, 8, and 10 kV). Huang et al. [84] observed an increase in surface adhesive force lubricant activity when the lubricants were charged. Further, reduction in surface tension and contact angle of lubricant droplets were also identified. A dramatic decrease in atomization resistance was also seen after charging the lubricants leading to reduction in their average diameter.

Further, in the present work attention has been made on effects of different process parameters in machining operation. EHVSL technique is a synergetic combination of electrostatic spraying and MQSL where a small quantity of lubricant is electrostatically charged (negatively) by contact charging method; these charged particles of the lubricant are directed into the machining zone in the form of thin yet even lubricant mist droplets with high penetrability and wettability. The focus of the present work is to identify the optimal spraying process parameters of EHVSL technique including compressed air pressure, lubricant flow rate, nozzle position, and nozzle distance on surface roughness and cutting force while machining Ti-6Al-4V alloy with portable low cost industrial equipment that can be easily installed, operated and maintained.

3.9 Results and discussions

For the effective application, the chargeability of electrostatic lubricant sprays can be improved by having a combination of electric voltage, lubricant flow rate and air pressure. The combined effect of these parameters further improves machinability performance i.e. cutting force and surface roughness. Within the framework of an optimization of cutting process, the knowledge of surface and subsurface characteristics is essential to understand machinability of any material. All the above cutting conditions are used to analyze the machinability characteristics of difficult-to-cut material considering surface roughness and cutting force. A cutting speed of 100 m/min with a feed rate of 0.1 mm/rev and a depth of cut of 0.5 mm was chosen based on the present industrial requirement and kept throughout the experiments.

3.9.1 Effect of air pressure

It is evident that fatigue life of a machine component depends strongly on surface of the workpiece which significantly affect its properties and characteristics. Fig. 3.13 and 3.14 compares the mean values of surface roughness and cutting force as a function of compressed air pressure under different air pressure conditions. It can be apparent that inferior surface roughness and cutting force is accomplished with increasing air pressure. This is due to decrease in cutting temperature in the interface zone. Fig. 3.13 and 3.14 shows, among all the considered air pressures employed, air pressure at 5 bar observed lowest cutting force and surface roughness. This may result due to the formation of smaller uniform droplets with high air pressure. Droplet with small size has a better ability to penetrate quickly and effectively in a short period of time into the machining zone [99]. This provides more wettability near the frictional

pair interface and helps to promote the formation of thin film of lubricant. It is very important in the cutting operation to reduce friction at tool-chip-workpiece interface, as reducing kinetic friction coefficient not only results in decreased frictional work, but also results in decreased shear work.

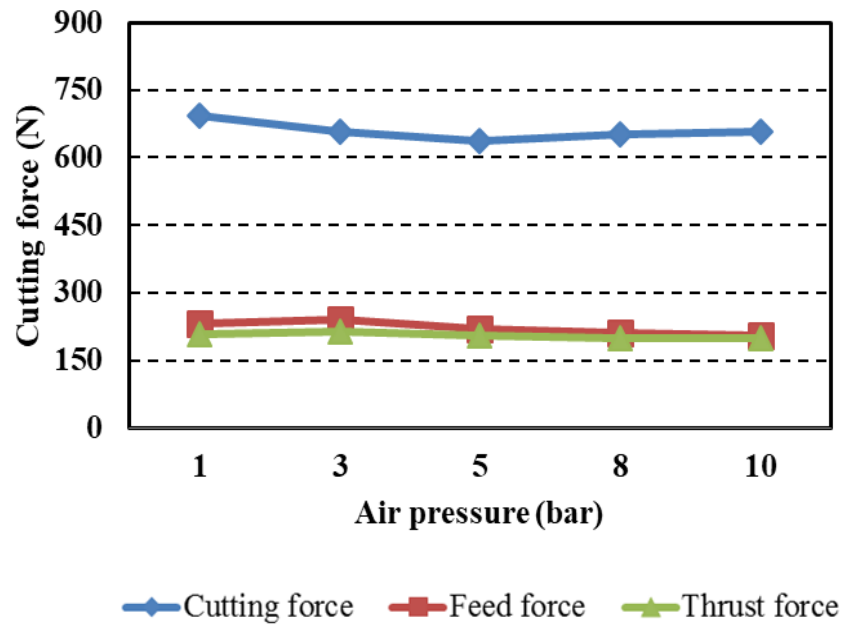


Fig. 3.13: Effect of cutting force with different air pressure

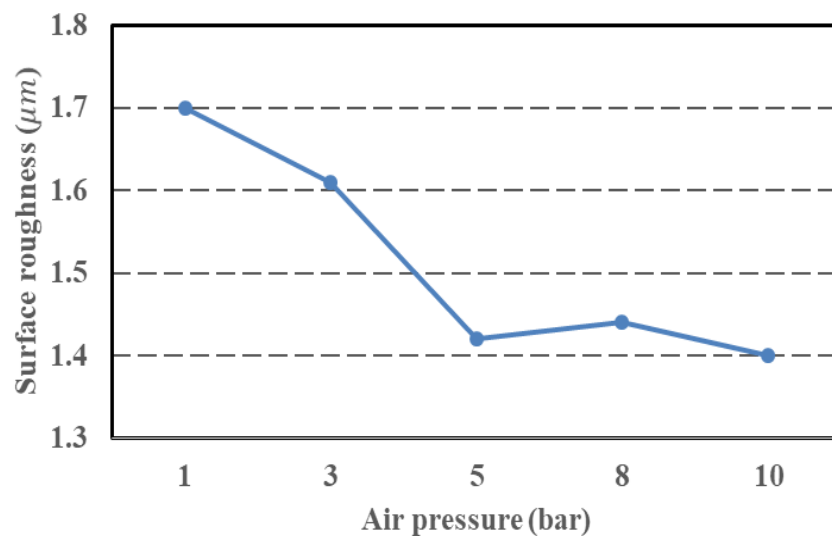


Fig. 3.14: Variation of surface roughness under different air pressure

However, it is evident that, higher pressure lubricant enables better surface finish primarily by governing the damage taking place due to abrasion, chipping and BUE formation at the auxiliary cutting edge. Consequently, the amount of blemishes caused by the cutting chips on the workpiece surface is reduced. In one of the previous study [6] it was observed that minimizing the main force and specific energy affected the surface quality and tool performance improved to a great extent. In fact, reducing the temperature by cooling action and friction by lubrication action eventually results in improving the surface roughness.

High pressure cooling in machining process is a very promising technology for enhancing tool life and productivity via appropriate cooling and lubrication. The continuous, high-velocity flow of the coolant breaks the chip into smaller segments. Increase in air pressure results in an adverse effect on the lubricant mist. According to momentum and mechanical energy conservation principle larger velocity causes spring back [10]. Because, higher air pressure produces higher speed droplets, which leads to spring-back of droplets from the surfaces of the workpiece and cutter, causing a lower effect on the form boundary of the lubricant film by physical adsorption on the surface of the metal.

3.9.2 Effect of spraying distance

Effective cooling and lubrication is necessary to ensure that temperature levels do not become excessive. This is because the lubricant mist fails to reach tool-chip contact region. During the machining process the behavior of average cutting force components under variant nozzle tip distance is shown in Fig. 3.15. Application of solid lubricants when targeted to rake face and flank face with varying distance, reduces the cutting force and surface roughness. Fig. 3.15 shows that the resultant

cutting forces for various nozzle distances range from 475 N to 574 N (10 mm to 50 mm). Further, the minimum cutting force (resultant force 468N) and surface roughness (1.48 microns) (as seen from Fig. 3.16) have obtained when the nozzle is positioned at the spraying distance of 20 mm. This is because, as the nozzle distance increases from interface zone the lubricant flow wide area increases, as the distance increases from interface zone, lubricant mist flow increases.

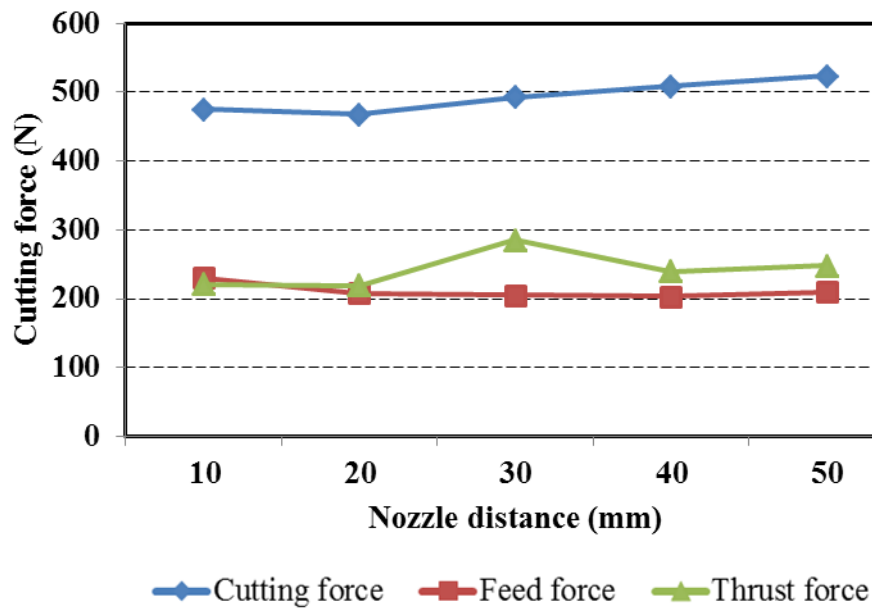


Fig. 3.15: Effect of cutting force under different nozzle distance

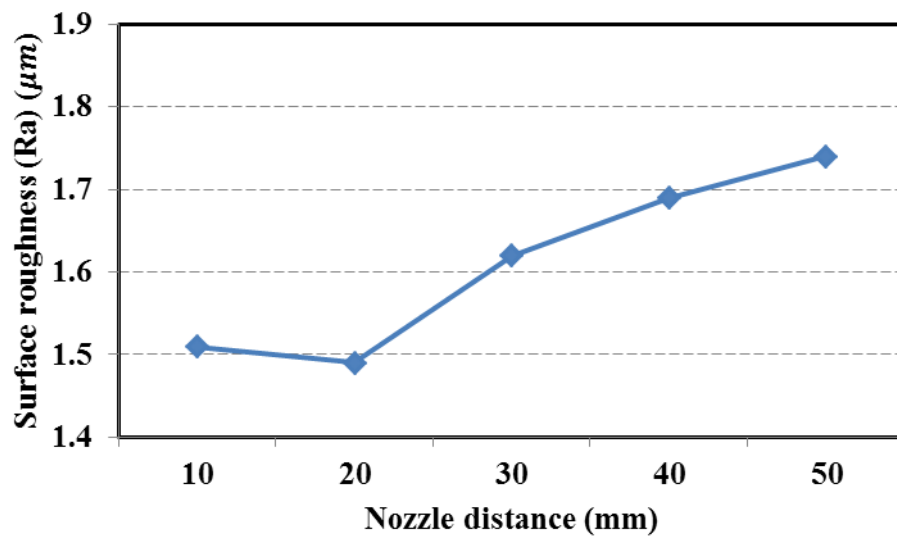


Fig. 3.16: Variation of surface roughness under different nozzle distance

Investigations by Park et al. [28] suggested that larger distances lead to smaller amount of droplets on the tool-chip interface. This is because larger spraying distances reduce the spraying velocity and penetration rates which ultimately results in increased friction [14]. It was also observed that with the increase of in-situ distance of nozzle tip to machining zone the lubricant is applied on the un-required portion wastage of lubricant takes place. The shorter distance has benefit for the droplets as it helps to effectively lubricate the contact area of the tool-chip-workpiece [57]. However too-short distance results in rebounding of droplets from obstacles leading to a poor physical adsorption of the lubricant film.

3.9.3 Effect of spraying angle

Effective cooling and lubrication is necessary to ensure temperature levels do not become excessive. Wetting angle plays an important role to elucidate lubricant performance as it is assumed that better wettability can be achieved with smaller wetting angles. The nozzle was located at two different position i.e. at 30° angle (nozzle position 1), 60° (nozzle position 2). The result showed that locating the nozzle at 30° angle (nozzle position 1) results in cutting force value of 440 N, lower than locating the nozzle at 60° angle (nozzle position 2). In addition, the cutting force has a similar tendency at two different positions of the nozzles. At the assumed positions 1 and 2, large amount of solid lubricant droplets adhered to the tool-workpiece interface during the cutting process. The high viscosity property of the lubricant should remain constant and adhere over the operating temperature range [1].

The variation of cutting force for different nozzle positions is shown in Fig. 3.17. From Fig. 3.17, it was observed that the wetting angle of the nozzle has a minimal impact on the penetration ability. The penetration ability of the lubricant mist

is mainly determined by the viscosity, the velocity and the wetting ability [27]. Therefore, when using high viscosity lubricant, the spraying angle of the nozzle has a minor effect on the cutting force (Fig. 3.17) and the surface roughness (Fig. 3.18).

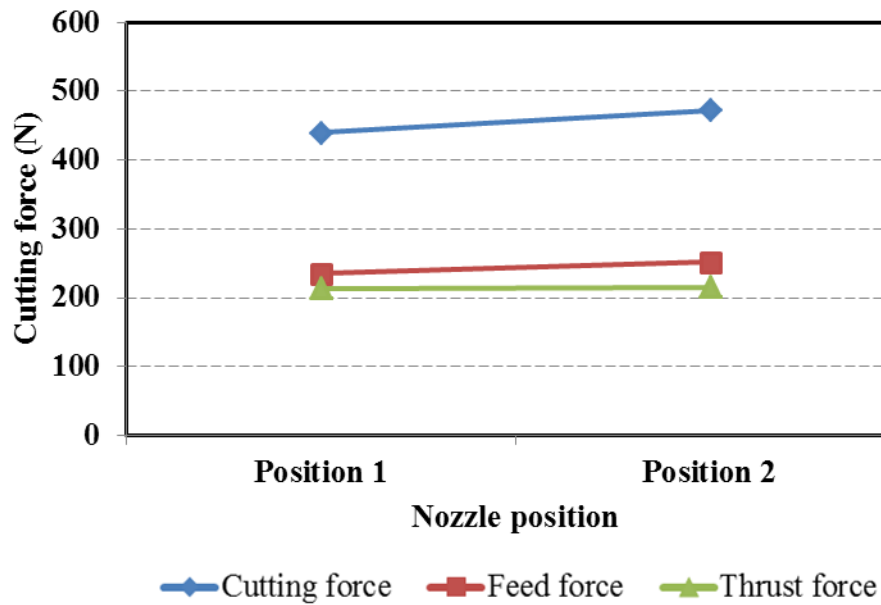


Fig. 3.17: Effect of cutting force under different nozzle positions

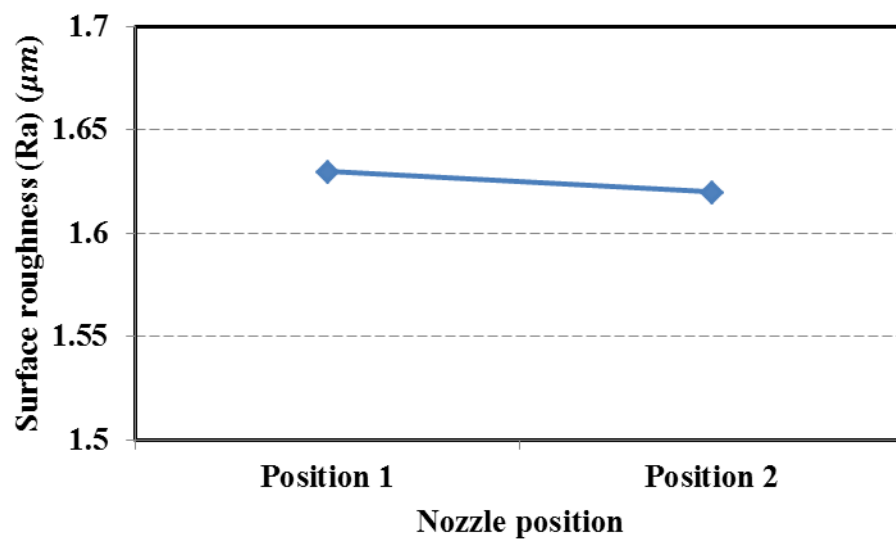


Fig. 3.18: Variation of surface roughness at different nozzle position

3.9.4 Effect of solid lubricant flow rate

The present investigation is an attempt to identify optimum flow rate of solid lubricant based machining. It is paramount in the machining process to supply sufficient amount of coolant/lubricant in the hot-machining zone (chip-tool-workpiece interface). Optimum supply of coolant/lubricant reduces the high temperature at cutting zone and friction forces, which subsequently improves the quality of the final product. The variation of cutting force and surface roughness with varying flow rate of solid lubricant conditions is shown in Fig. 3.19 and 3.20 respectively. A decrease in cutting force is observed with an increase in flow rate from 10 to 20 ml/hr. No significant variation was seen beyond the flow rate of 20 ml/hr. The applied lubricant (5 ml/hr) in the machining zone is not adhered for a long period, as the work piece rotates the applied lubricants slips away.

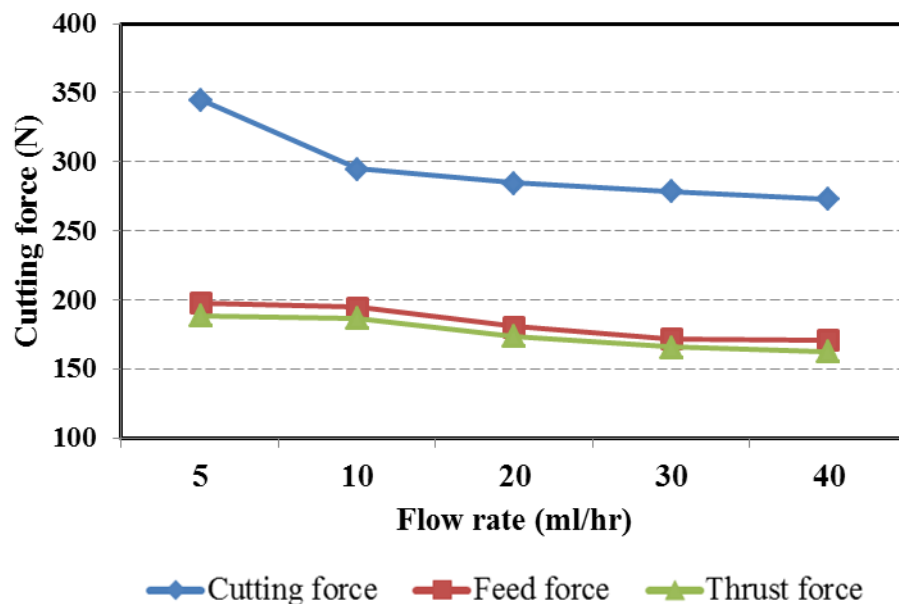


Fig. 3.19: Effect of cutting force with different flow-rates of solid lubricant

It has been clearly observed that the size of the droplets increases as the flow rate of the solid lubricant increases (Fig. 3.20). For an ideal lubrication system, it is

recommended to have a higher count of minimum sized droplets, covering the surface area as maximum as possible. It is found from the obtained results that for the selected base oil, a flow rate of 20 ml/hr is optimum to produce good quality lubricant mist. It was also observed that when high flow rate of lubricants applied in the machining zone, the lubricants applied on the tool-workpiece interface zone splashes (put away lubricant from work-tool interface zone). Hence from the obtained results it can be concluded that 20 ml/hr is the best flow rate for MoS₂ assisted machining of Ti-6Al-4V alloy. The cause of reduction in cutting force during increase in flow rate may reasonably be attributed that the cooling and lubrication effect of solid lubricants which results in improving the friction conditions at the machining interfaces.

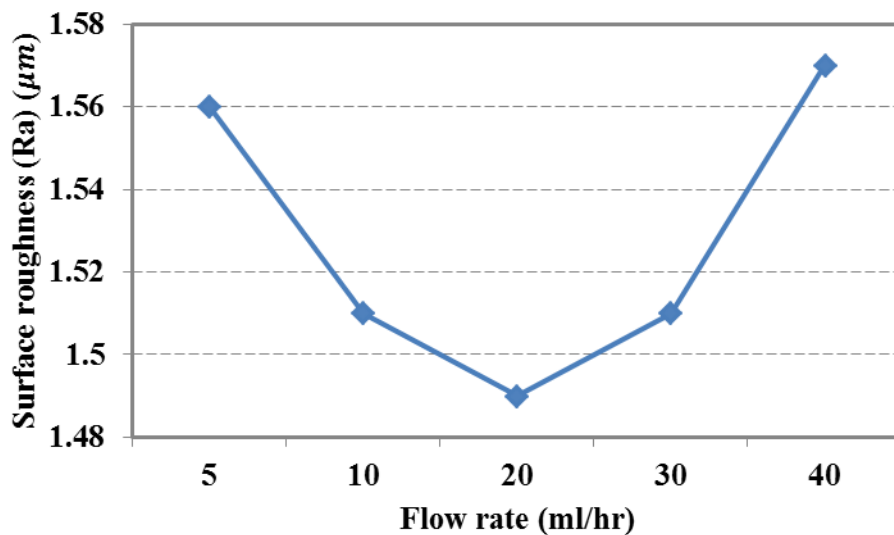


Fig. 3.20: Variation of surface roughness with different flow-rate of solid lubricant

Fig. 3.20 presents the variation of surface roughness with respect to the flow rate of solid lubricant. It can be seen from the Fig. 3.20 that, surface roughness decreases with increasing flow rate. However, surface roughness was not affected under lower flow rates. It was also revealed from experimental findings that there are no significant changes in the surface roughness when the flow rate of the solid

lubricant technique was increased from 20 to 40 ml/h. The lubricating action of the MoS₂ reduces the friction at tool-workpiece interface and thereby reduces the interface temperatures which subsequently results in improved tool life and surface roughness.

It was found that reducing the cutting force and specific energy will affect the surface quality to a great extent. In fact, reducing the temperature by cooling action and friction by lubrication action eventually results in improving the surface roughness. If the lubricant action prevails at chip-tool interface zone, the workpiece typically have a higher shear resistance, affecting the surface roughness. This phenomenon ultimately leads to easy chip removal and results in good surface finish. Better penetration of droplets was observed with the application of low quantity of cutting fluid. Also, lower cutting fluid quantities help droplets to adhere to the work surface and promote plastic flow on the rear side of the chip due to Rehbinder effect [15].

3.9.5 Analysis of droplet quality with varying flow rate

Fig.3.21 shows the droplet distribution with varying flow rate conditions. As observed, increasing flow rates result in droplets size expansion. For an ideal cooling/lubricating system, it is always recommended that there must be a higher count of minimum sized droplets, with the surface area being covered by the solid lubricant droplets to the maximum possible extent. It is found from the obtained results that for the selected base oil, a flow rate of 20 ml/hr is optimum to produce good quality lubricant mist.

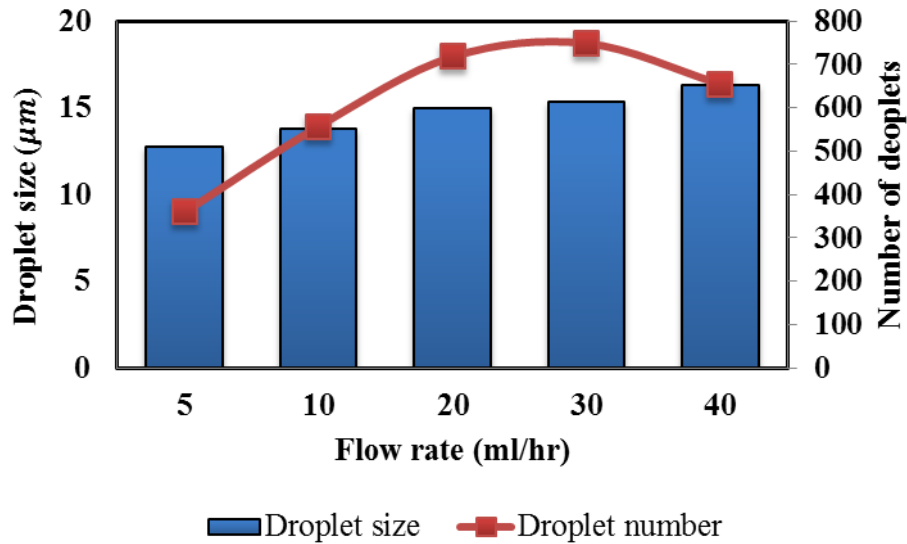


Fig. 3.21: Average droplet particle size and number of droplets

The high-velocity thin pulse jet of solid lubricant system was projected primarily to strike the rake and flank surface of the insert to protect the auxiliary cutting edge to enhance dimensional accuracy. The continuous, high-velocity flow of the coolant breaks the chips down into very small segments. Titanium and nickel-based alloys [16] have been machined to investigate the coolant's effect on machinability.

3.9.6 Effect of electrostatic voltage

The combined effect of the above parameters improves the machinability performance i.e. cutting force and surface roughness. Fig. 3.22 clearly shows that at higher charging voltages, the cutting force decreases compared with lower voltage. This perhaps attributed to the point that highly negative charge carrying lubricant droplets adhere and penetrate into the tool-chip interface, promoting plastic flow on the backside of the chip caused due to plasticization of crystals having basal orientation. Generally increased voltage results in a larger spray angle of the lubricant mists and smaller droplets [44]. This may impair the droplet distribution and adhesion

on the small machining area. In electrostatic machining process, a very small quantity of charged solid lubricant improves the flank wear rate. Electrostatic charging with 8 kV observed lower cutting force and surface roughness.

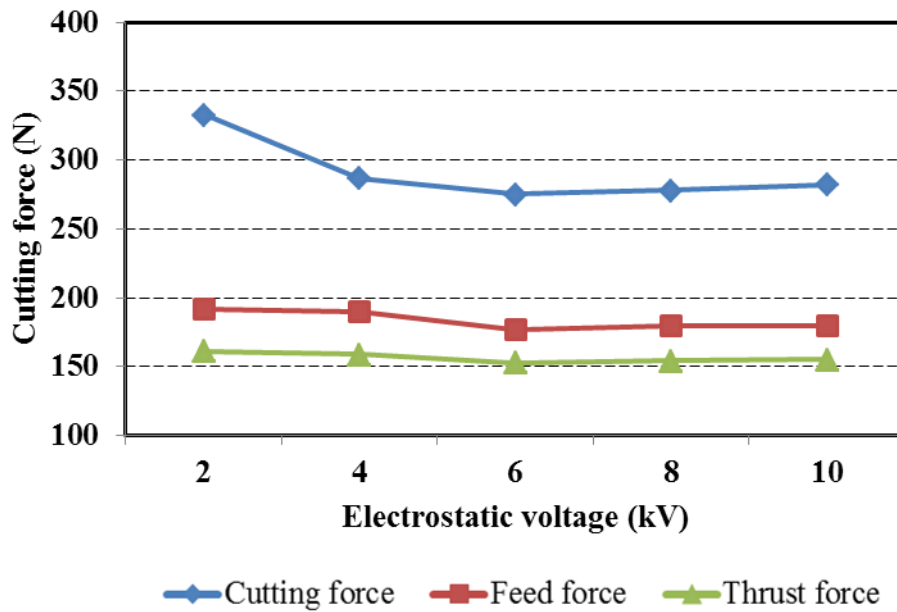


Fig. 3.22: Effect of cutting force with different charging voltages

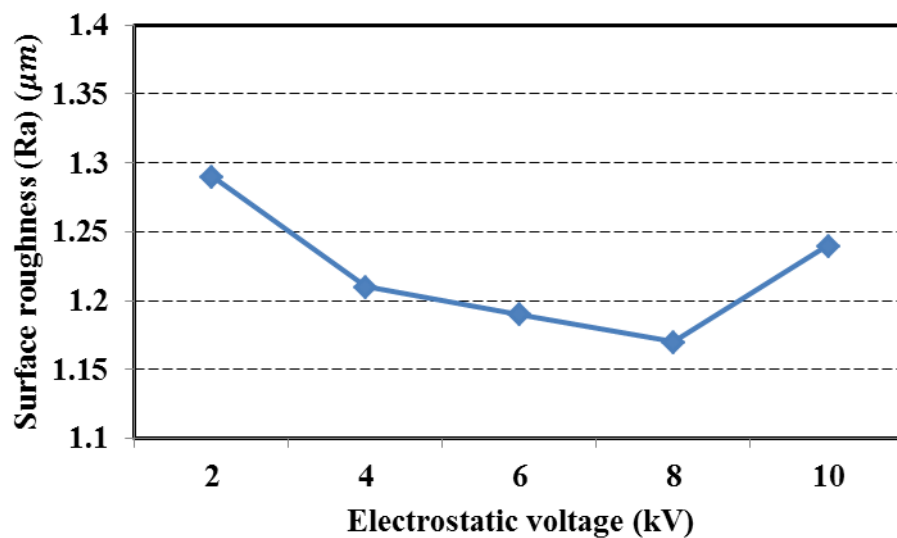


Fig. 3.23: Variation of surface roughness with different charge voltage

Fig.3.22 clearly shows that at higher charging voltages, the cutting force decreases compared with lower voltage. This is attributed to the improved

penetration, wetting, and spraying capabilities of the lubricant droplets, and their decreased average diameter, which facilitate a more effective entry of the charged lubricant into the machining area. Enhanced lubrication makes sure that cut chips slide easily on the surface of the tool and thus reduces chip-tool adhesion. Further, tool wear is prevented and as a result, tool life is increased with improved surface quality (Fig. 3.23). A reduction in cutting force is followed by a decrease in specific energy requirement and therefore improves the machinability. Li et al. [54] observed increase in tool life at higher charging voltages (20 kV). Park et al. [28] suggested that lubricant performance can be affected by droplet distribution. Obikawa et al. [66] reported that the lubricant droplets must escape from the stream of the air to reach the cutting interfaces.

3.10 Summary

The primary objective of the current investigation is to achieve the effective supply of solid lubricants in machining process through the development of novel EHVSL assisted machining set-up with overall machining performance enhancement and manufacturing cost by employing sustainable principles. The development of a novel near-dry experimental setup for effective supply of electrostatic micro-solid lubricant on cutting tool has been carried. Efforts have been made to evaluate the optimal process performance of EHVSL spray system during turning of Ti-6Al-4V alloy in terms of cutting force and surface roughness to obtain the most effective solution from the point of view of cost and energy consumption in machining process. The influence of EHVSL spray process parameters such as air pressure, flow rate, electrostatic voltage, nozzle position and nozzle distance is determined based on trial experimental study.

Air pressure and droplet deposition distance have been shown to be critical in order to enhance the effective application of electrostatic charged solid lubricant penetration into the tool-chip interface. It was observed that the spraying angle of the nozzle position has negligible impact on the mist penetration ability on machining zone. On the other hand with the reduction of cutting force and surface roughness, lower air pressure of 0.5 MPa is more effective in terms of higher deposition rate of lubricant droplet particles on the cutting interface. The lubricant flow rate and electrostatic voltage intensity are optimized at 20 ml/hr and 8 kV, respectively, so that the lubrication is achieved with the minimum possible lubricant usage and consequently the minimum cost and eco-friendly machining. In addition, it was concluded that under the influence of high electrostatic voltage (8 kV), with air pressure (5 bar), flow rate (20 ml/hr), nozzle distance (15 mm), solid lubricant particles meniscus takes the shape of a cone from the tip of which a thin lubricant film forms. The obtained results help in selecting the optimal machining parameters in turning Ti-6Al-4V alloy materials.

The research presented have characterizes the development of thin film created by solid lubricant spray system and investigates the resulting change in friction and wear during pin-on-disc sliding experiments. To accomplish this, an experimental set-up has to be developed to observe the nature of the spreading film with respect to particle size and concentration, sliding experiments are performed to determine the friction and wear reduction in sliding interface, respectively. To evaluate the performance of EHVSL process, tribological and machining studies have been carried out over a wide range of industrial test conditions and experimental investigations were presented in chapter 4 and chapter 5 respectively.

CHAPTER 4

TRIBOLOGICAL STUDIES TO ANALYZE THE EFFECT OF SOLID LUBRICANTS

4.1 Introduction

In modern industry, mechanical parts are subjected to friction and wear, leading to heat generation, which affects reliability, life and power consumption of machinery. Hence, study of lubricant film formed between various geometric shapes is inherently complicated and interconnected [76 & 144]. Tribological characteristics quantify the performance of a system in terms of reliability, life and power loss, especially in case of automobiles and industrial machinery. To overcome the tribological losses due to friction and wear, a significant portion of lubricant with high viscous properties allows very smooth relative motion between two sliding surfaces. In the boundary lubrication regime, tribological properties (friction and wear) are minimized by the development of a surface chemical reaction film. Advancement in modern tribology has facilitated the use of applying solid lubricants in various industrial applications. Solid lubricant additives with high viscous thin film formation between the sliding surfaces can adequately wet and adhere to a work surface.

It has been revealed from literature review that minimum film thickness plays a vital role in improving tribological properties at any sliding condition [76]. The lubricant film thickness relies on operating conditions like sliding velocity, input load, and viscosity of the lubricant and pressure-velocity relationship. Very few and sparse efforts have been made to investigate the role of lubricant film thickness and its measurements during sliding condition. The current research work carried with an aim

to develop optimum MoS₂ suspension with different weight fractions and particle size and to analyze tribological properties to assess its suitability for various industrial applications. Comparative studies have been made in terms of tribological characterization to illustrate the effectiveness of MoS₂ solid lubricant over graphite and boric acid. To characterize the lubricant film behavior between pin-disc interface zone, an experimental set-up has been developed to examine and measure lubricant film thickness at various particle size and concentrations of solid lubricants. To determine WP and EP properties of applied solid lubricants of varying particle size and concentration, WP (ASTM D4172), EP (ASTM D2783) experiments were performed on four-ball tester.

4.2 Experimental details and operating conditions

The aim of the current analysis is to understand the tribological characteristics of various solid lubricants at different sliding conditions. In the present work the factors considered for the study were sliding speed and normal load. Worn track observations on the surface of the disc were observed using tool maker's microscope.

4.2.1 Materials

Cylindrical Tungsten Carbide (WC) specimens of Ø6 mm and 30 mm length were used as pins against Ti-6Al-4V alloy disc specimen of Ø165 mm with 8 mm thickness to perform sliding experiments on pin-on-disc tribometer (Fig. 4.1). Pin and disc specimens were mirror polished and finished on a felt-polishing wheel using 0.6 µm diamond grit. The chemical composition of Ti-6Al-4V disc of the tested material is given in Table 4.1. Specimen surface topography was further not

quantified. Before the test, the specimens were thoroughly cleaned using an ultrasonic cleaner having anhydrous methyl alcohol.

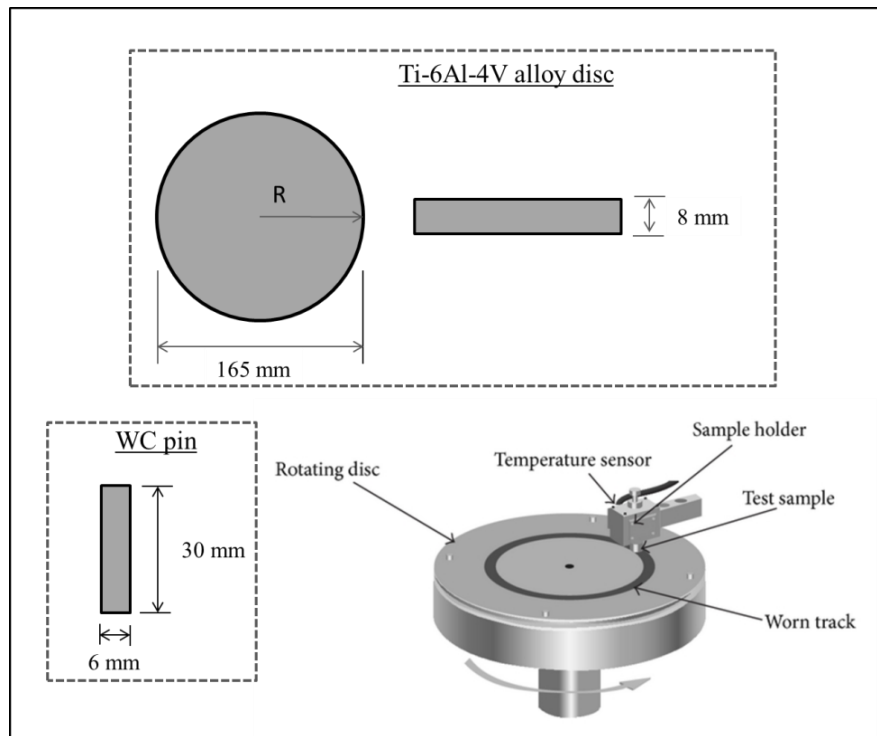


Fig. 4.1: Schematic view of pin-on-disc wear and friction monitor

Table 4.1: Chemical composition of Ti-6Al-4V alloy

Element	Al	V	Fe	C	Ti
Composition (wt. %)	5.560	4.070	0.185	0.022	89.997

4.2.2 Base oils

The base oil used in this study was SAE 40 oil with a viscosity of 220 cSt at 40°C. The detailed properties of the lubricants are shown in Table 3.7.

4.2.3 Solid lubricant additives

In recent years, due to the advent of new materials and processing techniques,

manufacturing industries have now focused its attention on solid lubricants for the cutting tool applications, because of their excellent tribological properties and good environmental friendly feature when compared with conventional lubricant additives. Solid lubricant additives find a variety of applications in manufacturing industries [10]. Solid lubricant as additives in base oil acts as key factor in influencing high performance anti-friction lubricant. Based on literature review, MoS₂, graphite, and boric acid solid lubricant particles were selected as an additive in base oil. Solid lubricant additives with varying concentration in the base oil were taken as 0%, 10%, 20%, 30%, 40% and 50% by weight ratio.

4.2.4 Preparation of solid lubricants

To overcome the tribological losses due to friction and wear, a significant portion of lubricant with high viscous properties allows very smooth relative motion between two sliding surfaces. An ultrahigh shear homogenizer was used at a speed of 10,000 rpm for about 10 minutes to suspend solid lubricant additives in base oil.

4.2.5 Properties of lubricants

The properties are important in determining of suitable additives for use of solid lubricant in sliding interface. The additives (MoS₂, graphite and boric acid) consist of different proportions of solid lubricants (0%, 10%, 20%, 30%, 40%, 50%) by weight ratio are suspended with SAE 40 oil. Measurement of kinematic viscosity (cooling and lubricating properties) of solid lubricant suspension is a key parameter to evaluate the effectiveness of a fluid as a lubricant. Subsequently, the blend was heated from room temperature to 55°C and the same temperature was maintained for 5 min while stirring using a rotor-stator homogenizer at a speed of 2000 rpm. Kinematic

viscosity is an important parameter to measure the effectiveness of a fluid (solid lubricant). In the current work a Capillary tube viscometer is used to determine kinematic viscosity of various lubricant mixtures.

4.2.6 Tribological studies on pin-on-disc tribometer

To investigate the tribological characteristics of various solid lubricants, experiments were performed on pin-on-disc wear and friction monitor as shown in Fig. 4.2, keeping all other test parameters constant. The tribometer consists of rotating disc (Ti-6Al-4V), stationary pin (WC) fixed at a specified location, loading system with a normal load applied by attaching weights along the pin's support arm, and friction and temperature measurement systems.

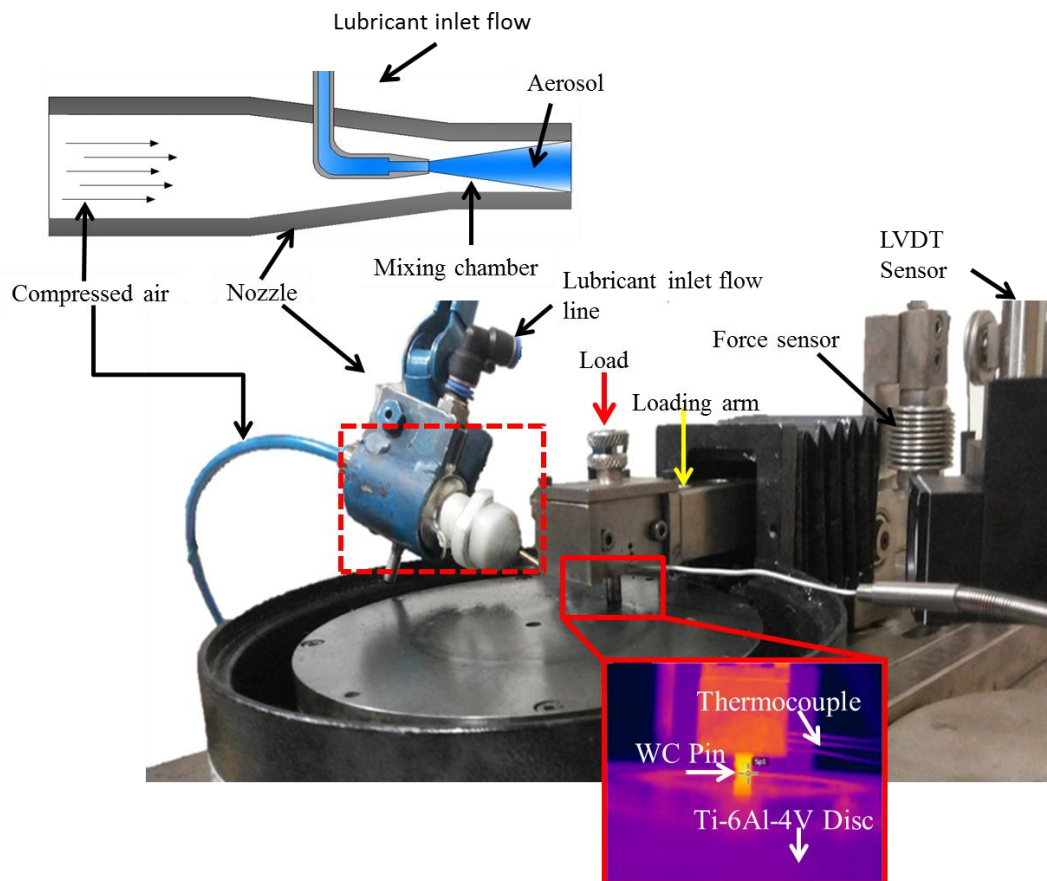


Fig. 4.2: Pin-on-disc tribometer experimental set-up

The details of the experiments have been shown in Table 4.2. Primarily, the micrometer sized solid lubricant particles were suspended in the base oil. Further, the prepared solid lubricant particles are used as lubricants in the sliding contact surface of pin-on-disc tribo-tester, and parallelly coefficient of friction was measured during the test. First experiment was performed at the initial track radius of 30 mm away from the center point. After each and every experiment the disc was cleaned with acetone. Suitable test conditions were selected based on the literature study.

Table 4.2: Spray parameters

Spray parameters	Value
Normal load (N)	10, 30, 50
Sliding time	300 sec
Sliding speed (m/min)	100, 150, 200
Solid lubricant	MoS ₂ , graphite, boric acid
Solid lubricant particle size	10 μ m
Air pressure	3 bar
Fluid flow rate	20 ml/hr
Impingement angle	30°
Spray distance	20 mm

Surfaces of discs were polished with diamond slurry. In the present test MoS₂, graphite, and boric acid solid lubricants were used as additives in the base oil and the obtained results are compared with dry sliding condition. By comparing the test results from various solid lubricant additives, identification of wear, friction coefficient and sliding temperature properties of the solid lubricants and the associate mechanisms becomes possible. Because of its superior viscosity and improved lubricating characteristics, SAE 40 oil was chosen as the suspension medium for solid

lubricant particles [95].

An experimental set-up (Fig. 4.2) has been developed to supply solid lubricants effectively to the pin-disc interface. Syringe pump is used to supply solid lubricant suspension with a constant flow rate of 20 ml/hr to the interface zone. To assist solid lubricants effectively in the sliding zone, a constant and continuous air pressure of 3bar is used. The stand-off distance of 20 mm was maintained from nozzle tip to pin-disc sliding interference throughout the experiments. To elude the impact of residual lubricant of previous experiment, the specimen was cleaned with acetone. All tests were performed at room temperature. Experimental apparatus working in combination with contact potential technique provides lubricant film thickness measurements in sliding point contact condition. A worn track on the surface of the disc was observed using tool maker's microscope. Further, to ensure and measure actual pin-disc contact temperatures, thermal infrared camera (FLIR E60) with 320 x 240 pixels with thermal sensitivity of less than 0.05°C at 30°C was employed.

4.2.7 Electrical contact potential

A device named electrical contact resistance (ECR) was designed to analyze the changes in contact conditions between pin and disc during the sliding test under lubrication process (shown in Fig. 4.3). It consists of two cables; one being connected to the pin holder and other being to the base plate. These two cables together are connected to resistance card. Output from the resistance card is connected to data acquisition card which is further displayed on software screen. When the top specimen makes a full contact with disc surface, the value is 100% indicating metal full contact, while in non-contact condition, the value displayed is 0%.

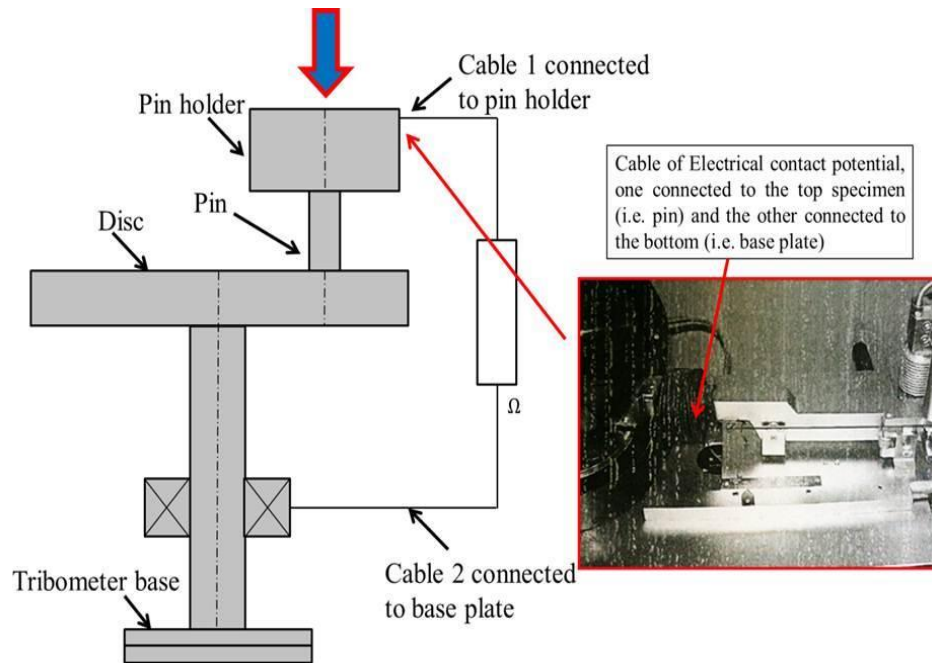


Fig. 4.3: Schematic drawing of the electric contact resistance

4.2.8 Characterization of thin fluid film measurement on pin-disc interface

On the sliding interface, solid lubricant particles form a thin film that penetrates into the pin-disc interface to improve the tribological properties. Investigation has to be conducted to characterize the solid lubricant film of various particle size and concentration. The experimental set-up has been developed to measure the MoS₂ solid lubricant film thickness.

4.2.8.1 Solid lubricant film thickness measurement procedure

In the present study solid lubricant film thickness deposited between two sliding surfaces was determined using the developed experimental set-up. A lighting scheme was applied to make the WC pin (orange) distinguishable from the fluid film (green) and the background (grey). Profile images of the thin fluid film taken by Canon slow motion camera represent the behavior of film along the pin-disc interface.

4.2.8.2 Solid lubricant film thickness observation procedure

Using the regulation provided by experimental set-up, the camera was arranged in a proper manner to capture the profile of thin fluid film formation, illuminating the lubricant film thickness development at various particle size and concentration. Using the adjustment provided by the experimental set-up the camera was adjusted in such a manner to capture the sliding zone of lubricant from a perspective normal to the pin and the disc surface (shown in Fig. 4.4) on which the thin lubricant film is obtained. In order to make formation of thin film during the sliding process, negligible (0.01g) amount of fluorescent was introduced into the solid lubricant. The resulting fluorescent lubricant film was illuminated using UV (Ultraviolet) light source [75]. Areas that are darker, experience a thinner film are brightly illuminated by the UV light. The details of the experiments have been shown in Table 4.3.

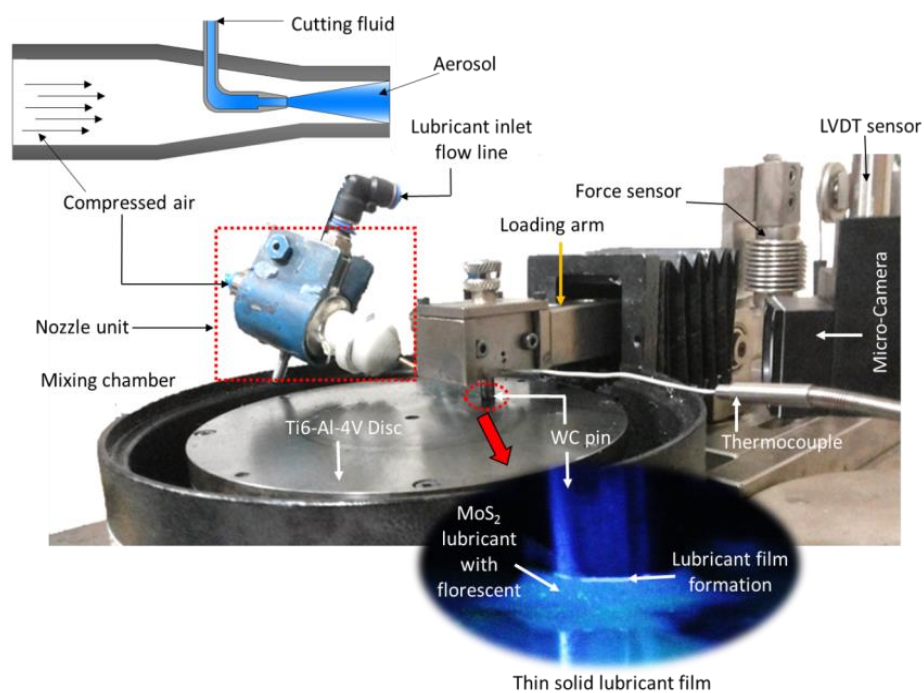


Fig. 4.4: Experimental set-up for lubricant film thickness measurement

Table 4.3: Film thickness test parameters

Spray parameters	Value
Spray distance	20 mm
Impingement angle	35 ⁰
Air pressure	3 bar
Fluid flow rate	20 ml/hr
Solid lubricant	MoS ₂
Particle size (μm)	10, 30, 50
Concentration (wt%)	0, 10, 20, 30, 40, 50

4.3 Tribological studies on four-ball tester

In trying to elucidate the effect of particle size and concentration on lubrication efficiency of MoS₂ solid lubricant, wide tests with different MoS₂ suspensions have been studied. Four-ball tester shown in Fig. 4.5 has been used to determine WP properties, EP properties and friction behavior of lubricants. The widely acceptable test results of four-ball tester make it an excellent choice to benchmark products.

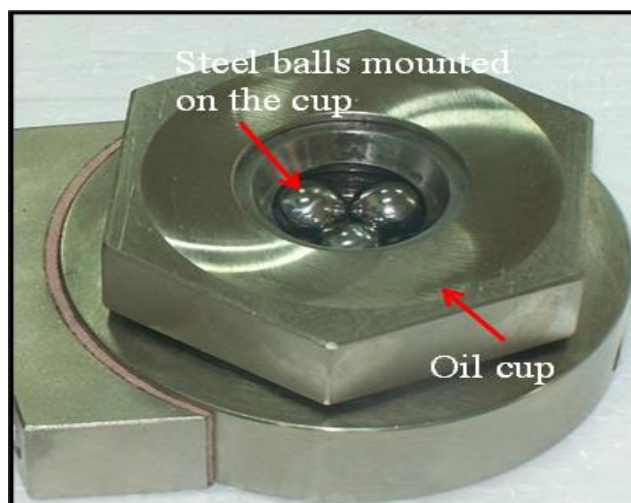


Fig. 4.5: Stationary steel balls mounted on the cup

4.3.1 Material

Test pieces consisting of four hard steel balls should be chromium alloy steel, made from AISI 52100, with ½ inch (12.7 mm) in diameter, Grade 25 EP (extra polish) and Rockwell C hardness 58 to 63 (Table 4.4).

Table 4.4: Chemical composition of Chromium steel ball material (AISI 52100)

Element	C	Mn	Si	P	S	Cr
Composition (wt. %)	0.95-1.10	0.20-0.50	0.35	0.025	0.025	1.30-1.60

4.3.2 Test fluid

The base oil used in this study was SAE 40 oil with a viscosity of 220 cSt at 40°C. Detailed properties of lubricants are shown in Table 3.7.

4.3.3 Additives

MoS₂ solid lubricant particles were chosen as an additive due to their higher load carrying capacity and excellent resistance to friction [85]. Three additives of MoS₂ solid lubricants with varying particle size were designed as 10 µm, 30 µm, and 50 µm. The concentrations of MoS₂ solid lubricant additive in the base oil were taken as 10%, 20%, 30%, 40%, and 50% by weight ratio.

4.3.4 Experimental procedure

The study examines tribological properties of different solid lubricant particle size and concentration of MoS₂ solid lubricants on four-ball tester (shown in Fig. 4.6). There is agreement relating to admirable performance of solid lubricant additives as dry lubricants; however, there exist controversies regarding effectiveness of solid

lubricant additive particles present in liquid lubricants. Therefore, efficient size of and proper concentration of solid lubricant particles in base oil is of major importance in terms of effective lubricant penetration in the machining zone. In the present study, 10, 30, 50 μm MoS_2 solid lubricant particles were suspended in base oil. Solid lubricant additives with varying concentration in the base oil were taken as 0%, 10%, 20%, 30%, 40% and 50% by weight ratio.

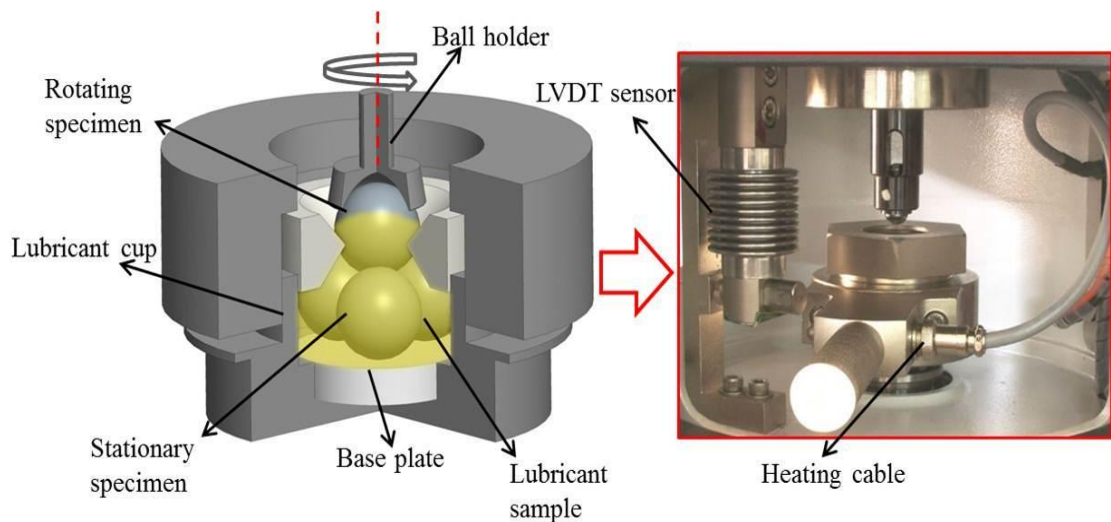


Fig. 4.6: A schematic view of four-ball test machine

In the current study, EP and WP tests were carried on a four-ball tester to evaluate the extreme pressure and wear prevention properties of solid lubricants. MoS_2 with varying particle size and concentration were suspended in SAE 40 oil. The assembly consists of four steel balls with three of them being coupled together to create point contact with the fourth ball that rotates on the top with respect to vertical axis; these four balls are covered by the lubricant oil under investigation and a load is applied and a timed test was performed (Fig. 4.6). Experimental parameters such as normal load, rotation speed and temperature were chosen as per the ASTM standards. The wear scar diameters (WSD) are measured and examined under microscope to

evaluate the WP behaviour of the lubricant. The applied load at which steel balls weld together is measured to evaluate the EP capacity of the lubricant. To elude the impact of residual lubricant of previous experiment, specimen was cleaned with acetone.

4.3.4.1 Wear Prevention test

The experiments are carried according to ASTM D4172 test standards. The contact surfaces of the ball specimens are completely covered with test lubricant i.e. MoS₂ solid lubricant. A timed test is performed with constant load of 40 kgf (392 N) and the upper ball is rotated at a constant speed of 1200 rpm for a period of 60 min. Temperature of the lubricating oil is regulated at 75°C (167°F). As per ASTM D4172 standards, the friction coefficient is then computed by taking the average normal and the tangential load (392 N, LC -1 N). Tool maker's microscope with a resolution of 0.01mm was used to measure WSD.

4.3.4.2 Extreme pressure test

According to ASTM D2783 standards, a set of tests were performed where each test was conducted for duration of 10 sec at a constant speed of 1200 rpm with increasing load until the balls get welded. Primarily the experiments were started at 160 kgf and additional runs were carried out consecutively at higher loads according to the ASTM D2783 (shown in Table 4.5) standards until the four balls get welded.

Table 4.5: ASTM D 2783 standards for extreme pressure condition

Sl. No	Load (kgf)
1	50
2	63
3	80
4	100
5	126
6	160
7	200
8	250
9	315
10	400
11	500
12	620
13	800

4.4 Results and discussions

In order to develop a method to assess the performance of solid lubricants, a set of pin-on-disc tribological tests were performed. Measured friction coefficient and rate of wear results were plotted as a function of applied load for all the considered lubricant conditions. To elucidate the impact of the particle size and concentration upon the lubricating effectiveness of MoS₂ solid lubricant, experimental set-up was developed to measure the lubricant film thickness at sliding interface. The measured friction coefficient and rate of wear plotted as a function of particle size and concentration of solid lubricant in all the lubricant conditions were considered. Further, to check the extreme load capacity and anti-wear properties of particle size

and concentration obtained, EP tests and WP tests were performed on four-ball tester.

4.4.1 Solid lubricant suspension properties

The effectiveness of the lubricant viscosity and required concentration of lubricants are of excessive importance in the presence of additives in base oil. As mentioned in the above section, to analyze the physical properties of suspension of solid lubricants in base oil, experiments have been carried out. From Table 4.6-4.8, it was observed that, there is an increase lubricant viscosity when the concentration of solid lubricant in the base oil increases. This shows that, lubricating property increases as the solid lubricant concentration in the base oil increases.

Table 4.6: Kinematic viscosity (cSt) of MoS₂ solid lubricants with varying wt% concentrations

Temperature (°C)	MoS ₂ concentration (wt%) in base oil					
	0%	10%	20%	30%	40%	50%
30	259	321	406	432	465	495
35	246	287	336	386	432	468
40	220	250	300	326	358	423
45	196	218	261	284	317	376
50	177	196	222	238	280	323

Table 4.7: Kinematic viscosity (cSt) of graphite solid lubricants with varying wt% concentrations

Temperature (°C)	Graphite concentration (wt%) in base oil					
	0%	10%	20%	30%	40%	50%
30	259	299	357	395	433	469
35	246	268	297	354	391	445
40	220	234	271	300	336	399
45	196	205	235	261	294	364
50	177	189	200	223	257	333

Table 4.8: Kinematic viscosity (cSt) of boric acid solid lubricants with varying wt% concentrations

Temperature (°C)	Boric acid concentration (wt%) in base oil					
	0%	10%	20%	30%	40%	50%
30	259	287	319	364	373	428
35	246	253	273	334	364	410
40	220	230	253	283	309	372
45	196	199	219	246	275	333
50	177	183	191	216	241	301

It is also evident from Table 4.6-4.8 that with the increase in the temperature of lubricant, viscosity of solid lubricant decreases. Subsequently viscosity of both solid lubricant and base oil is negatively affected by temperature [145]. Therefore, the obtained results indicate improved performance in terms of kinematic viscosity of solid lubricant upto 20wt% concentration of MoS₂, though, not much change was observed beyond 20wt%. However, in case of graphite and boric acid 30wt% concentration of solid lubricants shows better results compared to MoS₂ (20wt%). Hence, it can be concluded that the lubrication action suspension of 20wt% MoS₂ solid lubricant in SAE 40 oil is more efficient than graphite and boric acid lubricating conditions. In future, in following sections, to understand the tribological studies of solid lubricants, experiments were carried out with suspension containing 20wt% concentration of MoS₂ solid lubricant in SAE 40 oil, 30wt% concentration of graphite solid lubricant in SAE 40 oil and 30wt% concentration of boric acid solid lubricant in SAE 40 oil.

4.4.2 Analysis of friction coefficient, wear and contact temperature

Concentration of solid lubricant particles as additives in base oil (SAE 40 oil)

plays an important role to improve sliding conditions. Fig. 4.7 shows the sliding test results for solid lubricants and dry sliding condition. Prior to each sliding experiment, the instantaneous coefficient of friction between sliding surface increases until a certain maximum value and thereafter remains constant and attains a steady state condition. This perhaps attributed to the point that a certain amount of applied solid lubricant remains on friction pair surface which helps to the lubricant to create a thin film to provide effective lubrication. Fig. 4.7 shows the effect of sliding speed on the mean friction coefficient calculated from the acquired test results in condition of varying loads and in different solid lubricant. It was observed that there is a good difference in friction coefficient between MoS₂, graphite, boric acid and dry sliding condition. The general trend observed in all tested cases is that the friction coefficient decreases during increasing sliding speed condition. This could be due to the increase in contact temperature and energy dissipated by the friction in sliding contact [17 & 78].

In addition, MoS₂ solid lubricants exhibit lower friction coefficient compared to graphite and boric acid solid lubricants. This could be due to the fact that the highly viscous lubricants of MoS₂ solid lubricants exhibit larger load carrying capacity than that of graphite and boric acid. For MoS₂ solid lubricant conditions, the friction coefficient decreases to 0.023, 0.018 and 0.016 at 10 N load condition when the sliding speed increased from 100, 150, and 200 m/min. When graphite solid lubricants are applied to pin-disc interface zone, the friction coefficient decreases to 0.033, 0.028 and 0.025 at 10 N load when the sliding speed is increased from 100, 150, and 200 m/min. Similarly, for boric acid solid lubricants applied to the sliding zone, the friction coefficient decreases from 0.049, 0.041, and 0.038 respectively.

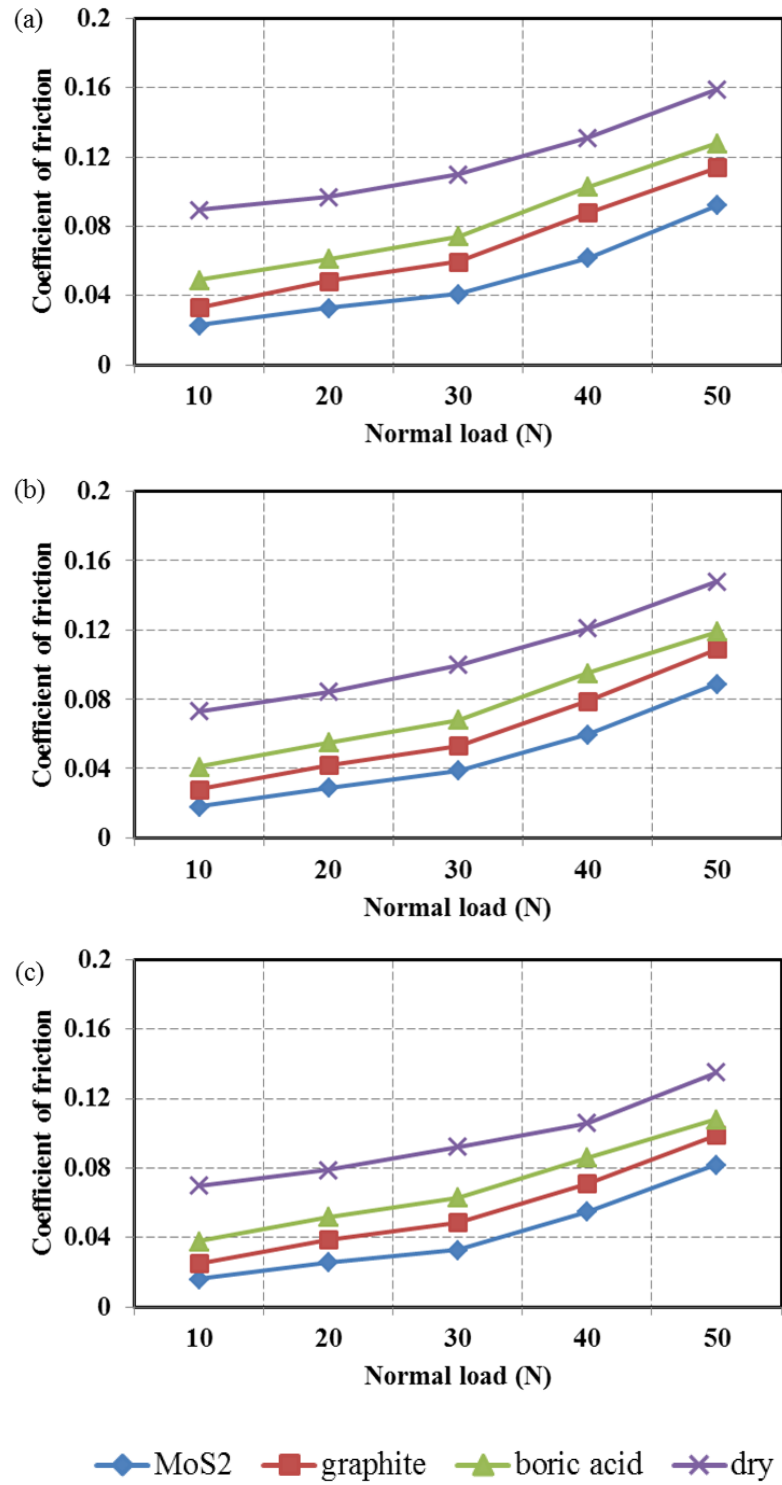


Fig. 4.7: Coefficient of friction vs Normal load at various speed conditions
 (a) 100 m/min (b) 150 m/min (c) 200 m/min

It was further observed that among all sliding conditions, MoS₂ with 20wt% demonstrated superior performance in terms of overall friction reduction property and a 25% and 39% and 56% reduction of friction coefficient was found, compared to graphite, boric acid and dry sliding conditions. Marques et al. [6] studied that during turning process, MQSL consisting of MoS₂ solid lubricant in base oil performed with better outcomes in terms of improved surface roughness, cutting force and tool wear as compared to graphite, and MQL conditions. A study by Guo Chen et al. [91] experimentally found that introduction of solid lubricant at tool-chip-workpiece interface resulted in reduced friction coefficient, lower tool-chip contact temperature and improved surface roughness.

Cambiella et al. [146] stated that the emulsifier concentration plays a key role on wetting behavior. Generally increase in MoS₂ concentration, in the base oil has a beneficial effect of reducing wear [10]. During sliding, heat develops at the pin-disc interface, and persuades high sliding temperature. Under such high sliding temperatures, applying solid lubricants in the pin-disc interference zone produces a thin film of lubricant on the pin-disc interface and reduces friction coefficient. Reduced coefficient of friction, shear resistance and sliding action within the contact zone are the main reasons for minimized flank wear [34]. One of the possible reasons for reducing coefficient of friction may be the layered lattice structure of the solid lubricant [99]. This may be due to the fact that solid lubricant additives with high viscous thin film formation between the sliding surfaces can adequately wet and adhere to a work surface. Hence, it may be concluded that the lubricant film formation of 20wt% MoS₂ with lesser particles is more effective, compared to graphite 30wt%, and boric acid 30wt% lubricating conditions.

Variation of wear coefficient of WC pin and Ti-6Al-4V disc with various solid lubricants at different sliding condition is illustrated in Fig. 4.8. Fig. 4.8 shows the effect of sliding speed on the wear coefficient acquired from test results under varying load conditions, and in different solid lubricant conditions. Minimum rate of wear coefficient was observed when MoS₂ solid lubricant additive particles were suspended in base oil. Lubrication reduces wear coefficient because of effective lubricant film formation at pin-disc contact region [73]. Solid additive particles of layered structure shear easily under traction to yield low friction coefficient. In addition, additives with MoS₂ particle exhibit less wear coefficient i.e. 11.2 μm at 10 N load conditions. Maximum wear coefficient is observed during dry sliding condition when 50 N load is applied i.e. 57.63 microns. It is clear from Fig. 4.8 that variation in sliding speed has little influence on wear coefficient of solid lubricants. Wear coefficient for graphite and boric acid was found to have negligible changes at 10 N load conditions. The first noticeable trend shows that, at all sliding conditions, MoS₂ with 20wt% overall exhibited superior friction reduction properties and a 17%, 25% and 40% reduction of wear coefficient, compared to graphite (30wt%), boric acid (30wt%) and dry sliding conditions. MoS₂ is generally known to have higher load bearing capacity with a low friction coefficient [99]. It was observed that during all solid lubricant conditions, wear coefficient increases with increase in normal load. From the Fig. 4.8, it was observed that though the applied lubricant films separate pin-disc sliding surfaces effectively, it was clear that the presence of thin viscous lubricants provide protection of contacting bodies against excessive friction coefficient and rate of wear. Fig. 4.9 shows the pin-disc sliding temperature.

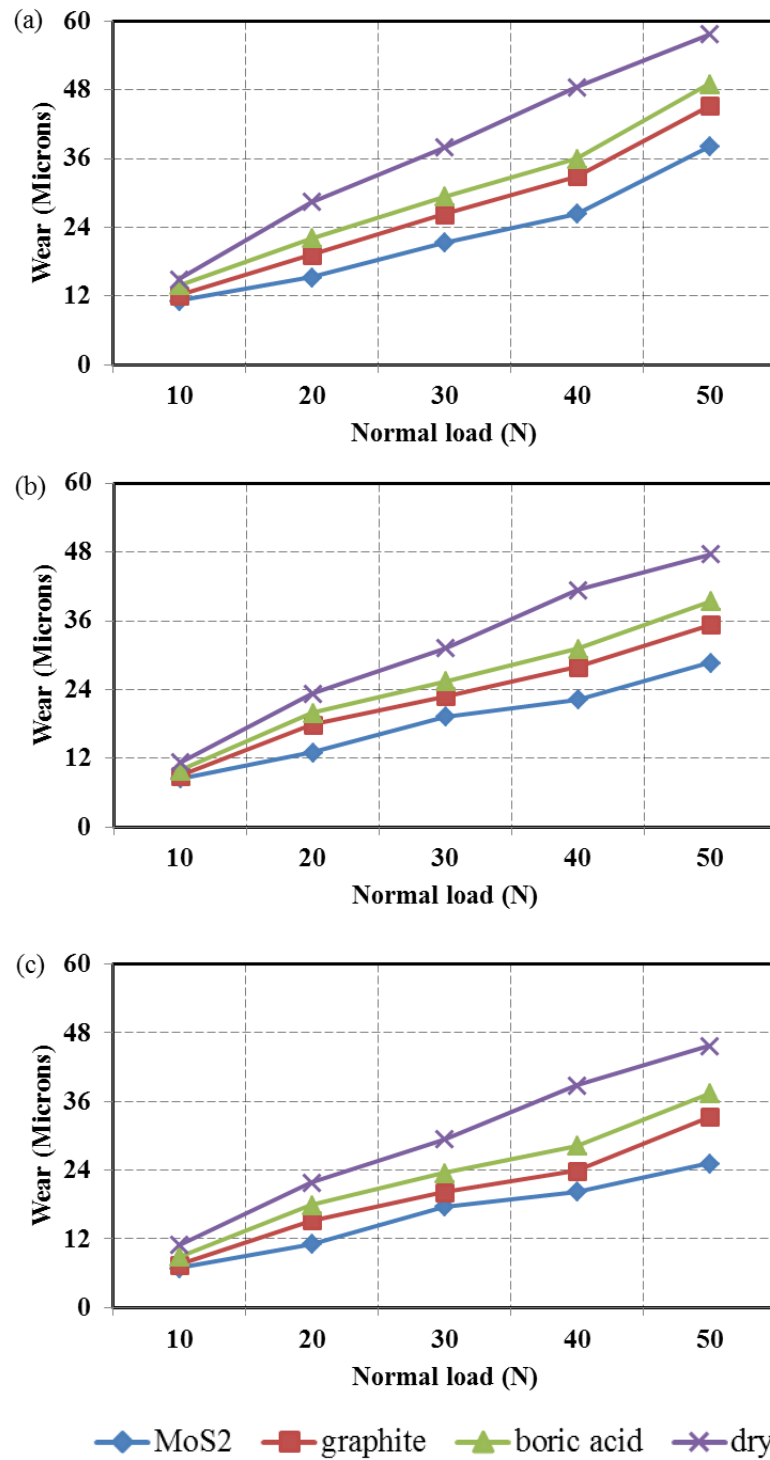


Fig. 4.8: Wear vs normal load at various speed conditions (a) 100 m/min (b) 150 m/min (c) 200 m/min

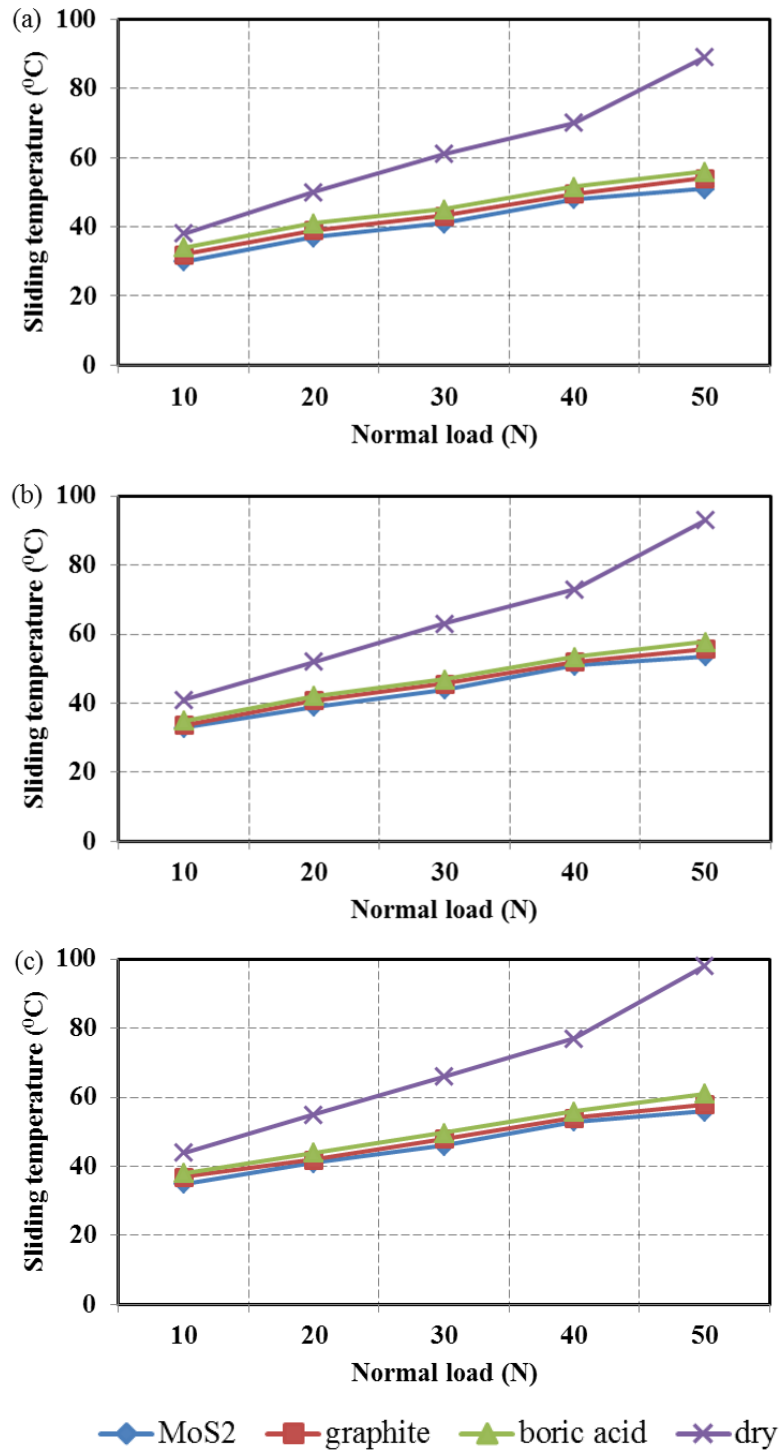


Fig. 4.9: Temperature vs normal load at various speed conditions (a) 100 m/min (b) 150 m/min (c) 200 m/min

Temperature of the pin-disc interface was measured (shown in Fig. 4.9) using

Infrared camera. When the graphite and boric acid solid lubricant mixture are used, temperature increases to 45°C and 47°C, whereas when using MoS₂, the temperature peaked to 43°C. This is due to the high rate of kinematic viscosity of MoS₂ solid lubricant. It was also found during the observation that in dry sliding condition, pin-disc interface temperature increased to 73°C.

4.4.3 Analysis of wear morphology

Tool Maker's Microscope was used to examine the lubrication mechanism of solid lubricant particles on worn surface of Ti-6Al-4V alloy disc. Quantification of wear track on the disc surface leads to better understanding of the effect of solid lubricant structure on lubricating properties. Fig. 4.10-4.13 show typical micrographs of worn disc surfaces lubricated by solid lubricant particles at varying load conditions and at 100 m/min speed condition. Fig. 4.10 shows the worn track surface of Ti-6Al-4V alloy disc during MoS₂ solid lubricant condition at normal loads and varying speed conditions. It was observed that when MoS₂ solid lubricants applied to the pin-disc interface during low load condition, wear on the disc surface was minimum (as shown in Fig. 4.10), when compared to graphite (Fig. 4.11) and boric acid (Fig. 4.12) solid lubricant conditions. In all environmental conditions, it was clearly observed that wear track surface increases when the normal load becomes higher. It was observed that, when the load increases in all solid lubricant conditions, rate of wear increases drastically. Delamination on the wear track was observed at high load conditions when graphite (Fig. 4.11 (b) & (c)) and boric acid (Fig. 4.12 (b) & (c)) solid lubricants were applied during sliding process. During the increase in applied load condition disc wears non-uniformly, wear track depth and width vary in longitudinal direction. Wear debris on the worn surface was observed during dry

sliding condition (Fig. 4.13), and wear track was too thin to be easily found.

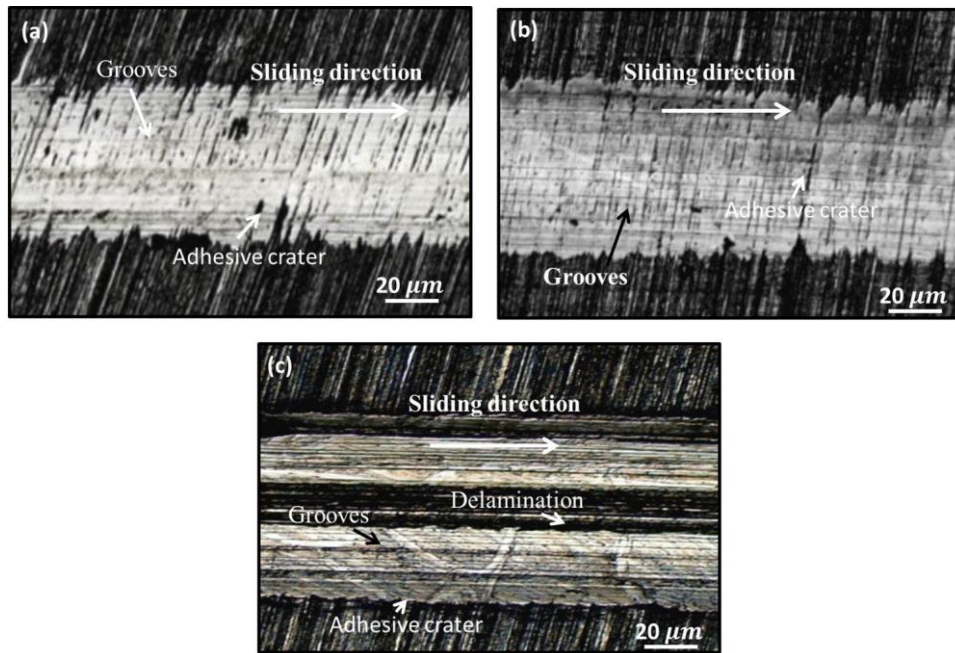


Fig. 4.10: Microscopic images of wear track of disc during MoS₂ solid lubricants sliding condition (a) 10 N (b) 30 N (c) 50 N

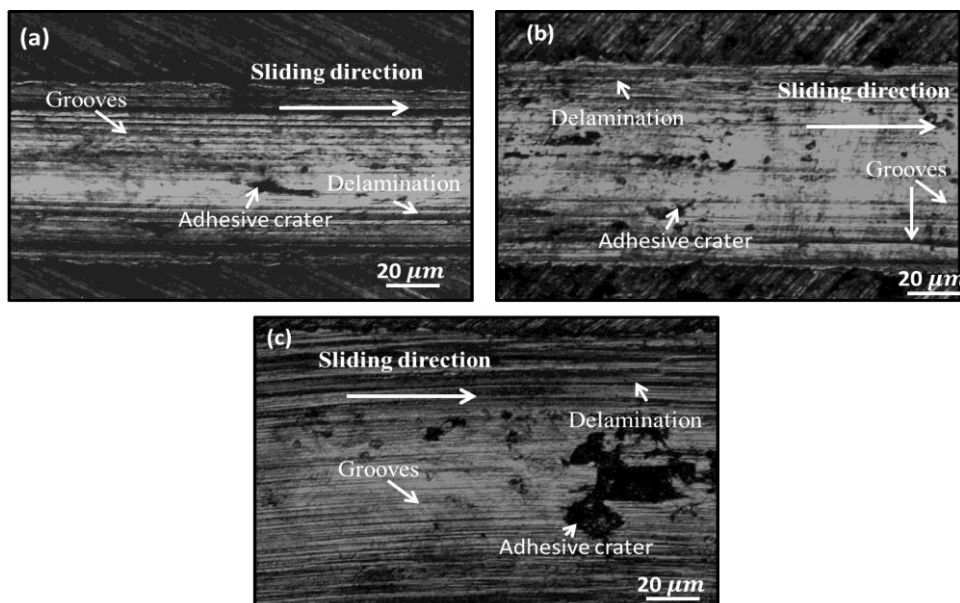


Fig. 4.11: Microscopic images of wear track of disc during graphite solid lubricant sliding condition (a) 10 N (b) 30 N (c) 50 N

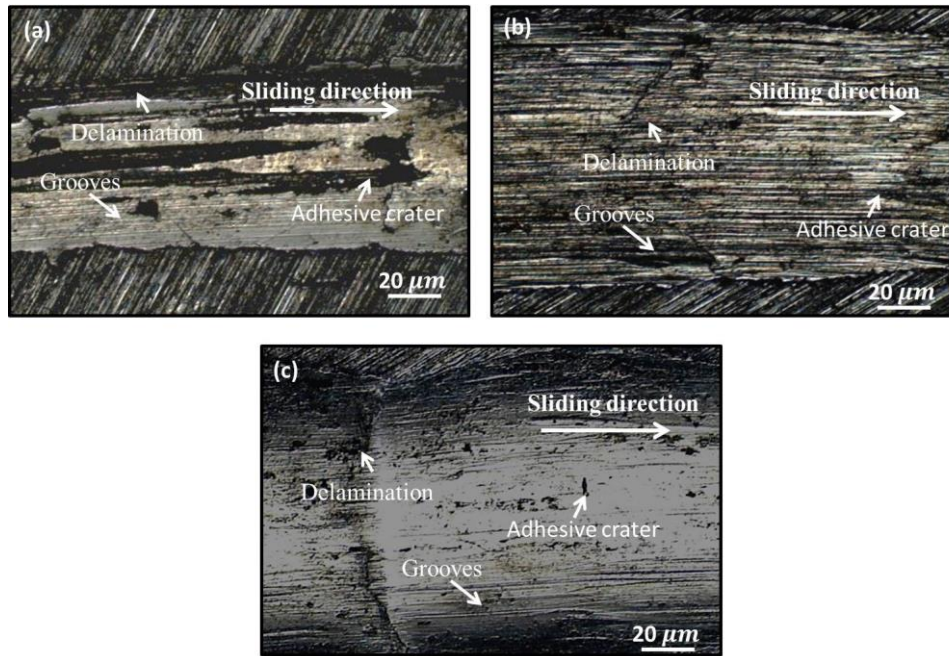


Fig. 4.12: Microscopic images of wear track of disc during boric acid solid lubricant sliding condition (a) 10 N (b) 30 N (c) 50 N

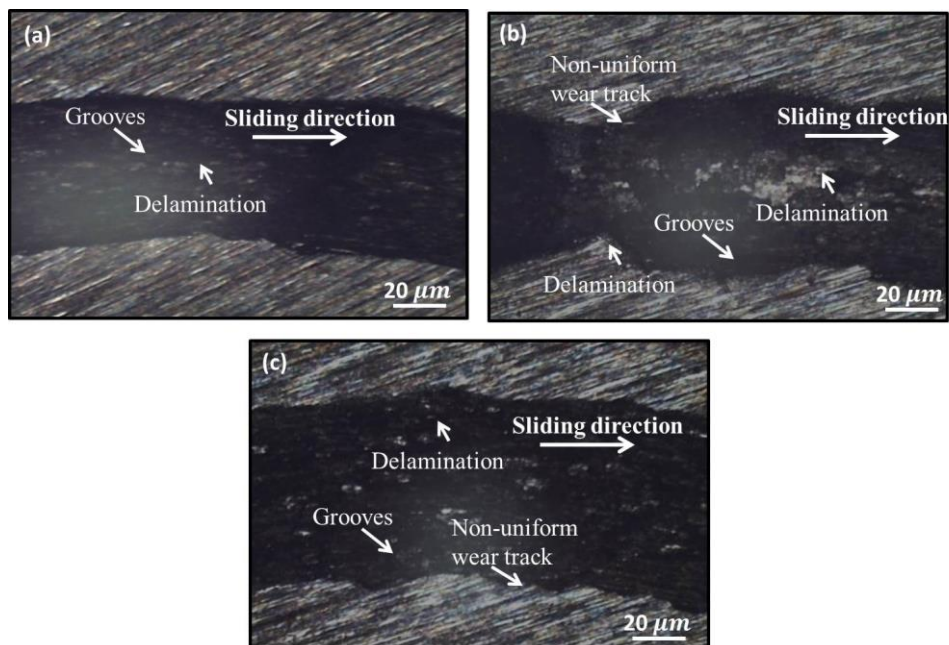


Fig. 4.13: Microscopic images of wear track of disc during dry sliding condition (a) 10 N (b) 30 N (c) 50 N

From Fig. 4.10-4.13, it was observed that as applied load increases, width of the wear track increases and many deep scratched grooves were observed on the wear track of the disc surface. When slid into the solid lubricant environment, wear debris on the wear track was difficult to found although higher rate of wear could be observed in boric acid and graphite environment compare to MoS₂ condition. The in-line air supply through nozzle provides easy transfer of lubricants towards the pin-disc interface. The compressed air supplied along solid lubricant will clean the pin-disc interface zone during the sliding process. It has been clear that the presence of thin viscous lubricants provides some protection to contacting bodies against excessive friction coefficient and wear. Combining the above test results, it was observed that, in all the environmental conditions as the load increases, rate of wear increases. Further, it was observed that when MoS₂ is applied as lubricant media to pin-disc interface zone, a stable and very low wear track (as shown in Fig. 4.10) is obtained at varying load conditions, and a uniform distribution of wear tracks has been observed at the contact area of disc.

4.4.4 Contact potential measurement of solid lubricant film thickness

With contact potential technique, as discussed in the previous section, when the top specimen (WC pin) makes complete contact on disc surface the contact potential value displayed is 100% indicating that pin and disc are in contact, and in the no-contact condition the value displayed is 0%. From Fig.4.14, it was observed that, for all solid lubricant environment conditions film thickness ranges between 91% - 96%. It was observed that when MoS₂ applied in the pin-disc interface during low load (10 N), the lubricant present in pin-disc interface was 90.89%.

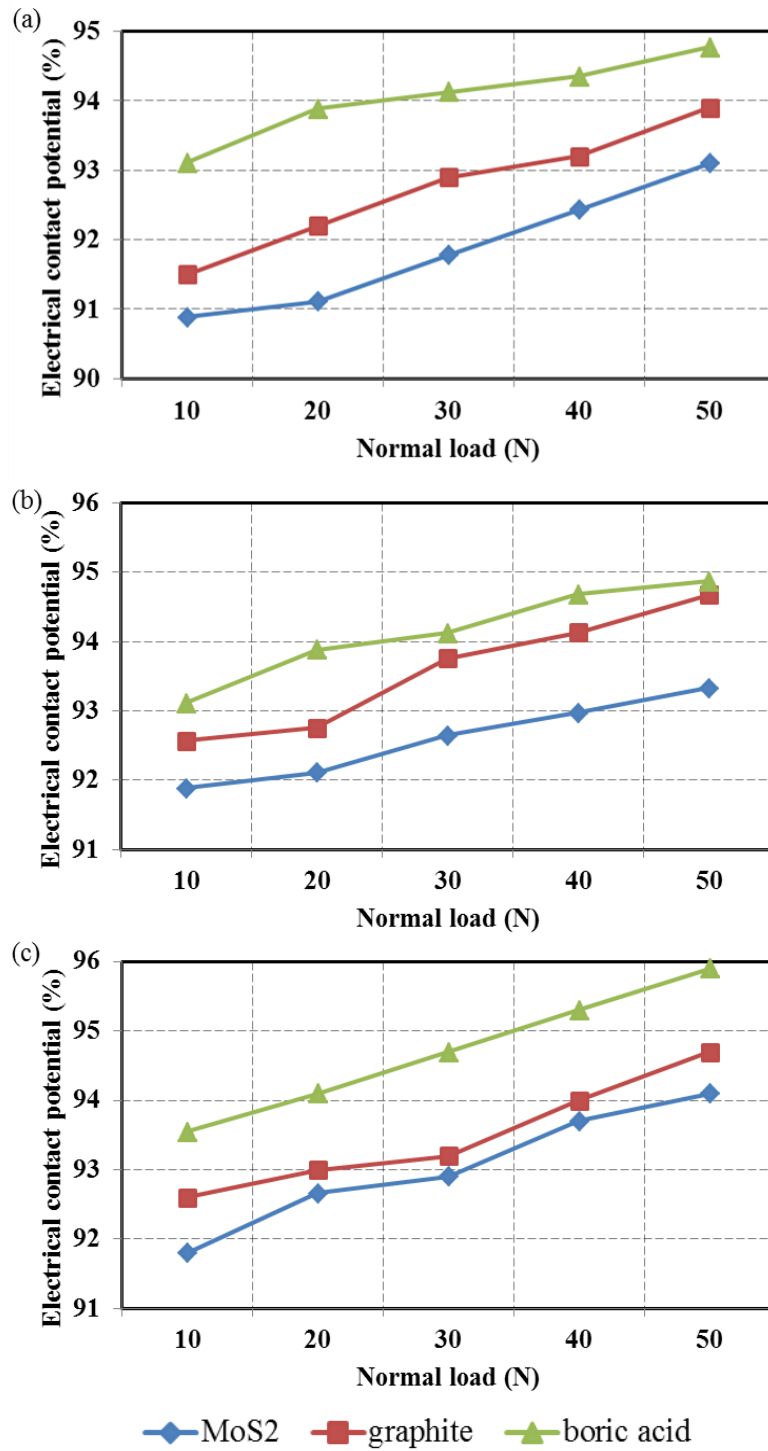


Fig. 4.14: Electric contact potential technique vs Normal load at various speed conditions (a) 100 m/min (b) 150 m/min (c) 200 m/min

With increase in the applied load to 30 N, the difference in ball disc interface

was 91.78%. With the significant increase in the applied load to 50 N, the difference in pin-disc interface was observed to be 93.1% approximately. When graphite is applied as lubricant, contact potential was found to be 91.5% at 10 N, and film thickness increases to 93.9% at 50 N load condition. Difference of 2.5% was observed with graphite condition during 10 N to 50 N load conditions. During boric acid lubrication condition, contact potential ranges from 93.11 – 94.78% at 10 N to 50 N. It was observed that with all applied solid lubricant conditions, as the load increases, the contact potential between pin-disc interface increases. As observed from Fig. 4.14, with an increase in the sliding speed, contact between the pin-disc interface increases. During dry sliding conditions debris particles were found to be accumulated at the pin-disc interface which eventually resulted in non-uniform contact potential.

4.4.5 Analysis of MoS₂ solid lubricant film thickness

Within the impingement zone, the focused high velocity lubricant is introduced on the lubricant film sliding surface that drives the fluid to sliding interface from the impingement point at high velocity. This fast moving fluid film is too thin to be detected with UV light. As highlighted in the previous section, an experimental apparatus was structured to characterize the thin lubricating film at various particles (size) and for concentration each combination of MoS₂ solid lubricants. The film thickness was measured between two sliding surfaces on pin-on-disc tribometer. In order to characterize the thin film formation, images were collected at varied particle size and concentration (Fig. 4.15). The film thickness (lubricant present between pin and disc surface) was measured in three dissimilar positions and then averaged for each combination of particle size and concentration.

The subsequent value of measured film thickness is shown in Fig. 4.16. Overall distribution process of the lubricant between the pin-disc surfaces was observed from the side view as shown in Fig. 4.4. Lubricant film thickness between pin and disc interface was observed in Fig. 4.15 as measured using tool maker's microscope.

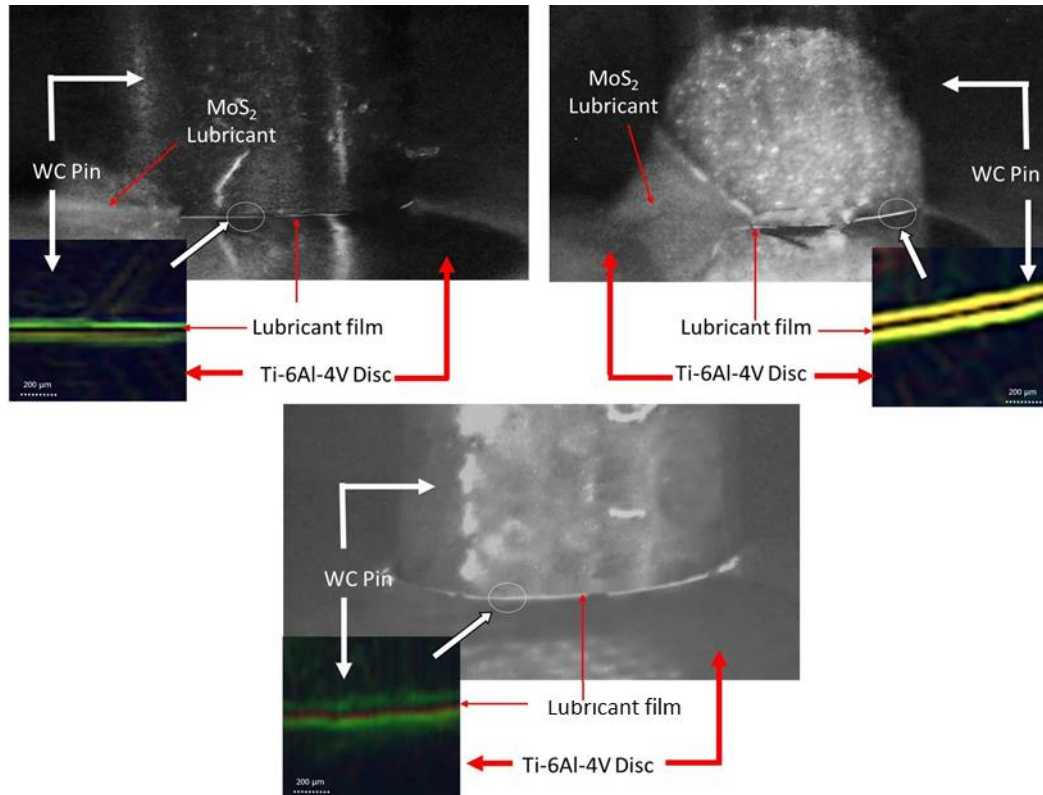


Fig. 4.15: MoS₂ lubricant film formation between pin and disc surface

Investigation has been carried out to select the film thickness obtained between pin-disc sliding surface when MoS₂ lubricant particles of different grain size and concentration were applied as lubricant. For applied particles and concentrations, average solid lubricant film thickness measurements indicate that there is not much difference when lesser particles with varying concentrations are applied.

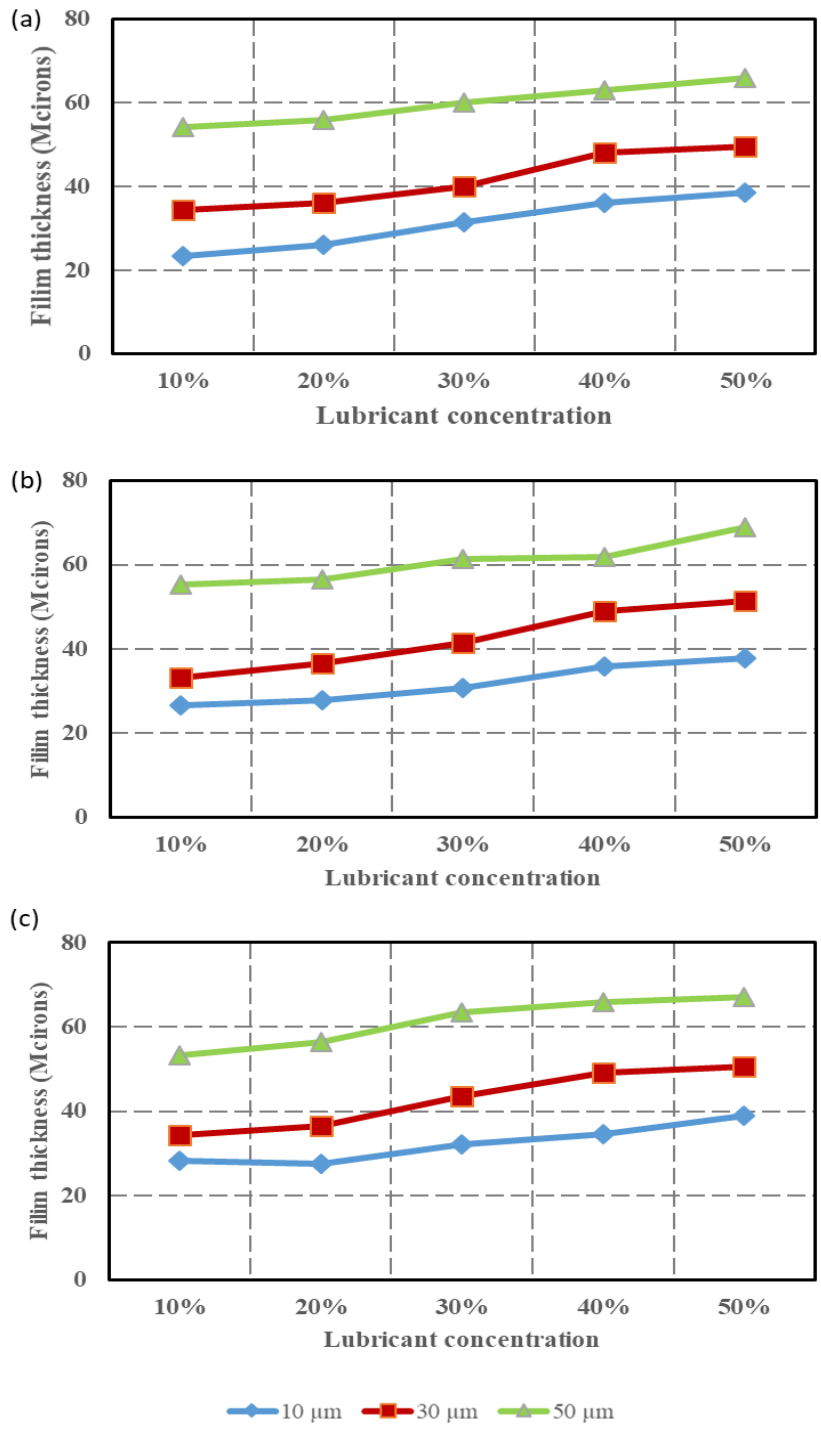


Fig. 4.16: Average film thickness measurement for various particle size and concentration (a) Trial 1 (b) Trial 2 (c) Trial 3

Fig. 4.16 shows lubricant film thickness observed between pin-disc interfaces.

As the additive particle size increases, the average lubricant film thickness tends to increase with increase in particle size. It was also evident from Fig. 4.16 that with increase in additive concentration in base oil lubricant film thickness also increases. Minimum value of film thickness measured was 23.4 μm . This is the thinnest film measured when particle size and concentration of 10 μm with 10wt% concentration was applied, the maximum lubricant film thickness measured was 69 μm observed at 50wt% concentration with 50 μm particle size of solid lubricant additive. Moderate film thickness was observed when additives with 30 μm particle size. Beyond 20wt% concentration, film thickness significantly increases with increase in reinforcement percentage. Bartz [83] observed that, as applied additive particle size increases, lubricant film thickness tends to increase.

Reddy et al. [18] found that more particles could be accommodated within a film of same thickness if size of the particles was reduced. Results from Fig. 4.16 also reveal that in all particle size conditions lubricant film thickness does increase with increasing particle size and concentration of solid lubricant. Compared to large sized particles, those with smaller size have demonstrated intrinsic advantages. The advantage of applying thin lubrication in the sliding interface is that the lubrication (additives) makes available a relatively plentiful supply of solid lubricant which, in turn reduces and is suitable for applications of long durability and high duty [85]. The obtained results of lubricant film formation reveals the range of thin lubricant film thickness developed between 10 μm grain size and 20wt% concentration in which the film thickness is least distributed.

4.4.6 Analysis of friction coefficient and wear

Tribological characterization was done on pin-on-disc wear and friction monitor to see the effect of particle size and concentration of solid lubricant. The effectiveness of particle size and correct concentration of MoS₂ is of great important in the presence of additives. Then, the mean value of friction coefficient is calculated from acquired test results. Fig. 4.17 shows friction coefficient versus solid lubricant concentration with different particle size. It was observed that there is a good difference in friction coefficient between 10 μm , 30 μm and 50 μm particle size. For all the available particle sizes, the friction coefficient was found to be decreasing with increasing MoS₂ concentration in base oil, as shown in Fig. 4.17. As MoS₂ has a lamellar structure, it can be easily sheared in the sliding direction [76]. In addition, additives with lower particle size exhibit less friction coefficient i.e. 0.036, and maximum friction coefficient was observed when 10wt% additive concentration was applied i.e. 0.062. The friction coefficient for other concentrations was found to have negligible changes when 10 μm particle sizes were applied.

The first noticeable trend shows that, for all sliding conditions and same concentration (20wt%), the reduction in coefficient of friction was more in case of MoS₂ with 10 μm particle size when compare to MoS₂ containing particles of 30 and 50 μm . Sentyurikhina et al. [97] suggested that solid lubricants with lesser particle size have greater tendency to interact with friction pair surfaces and to readily form a protective film to increase anti-wear characteristics of sliding surfaces [146].

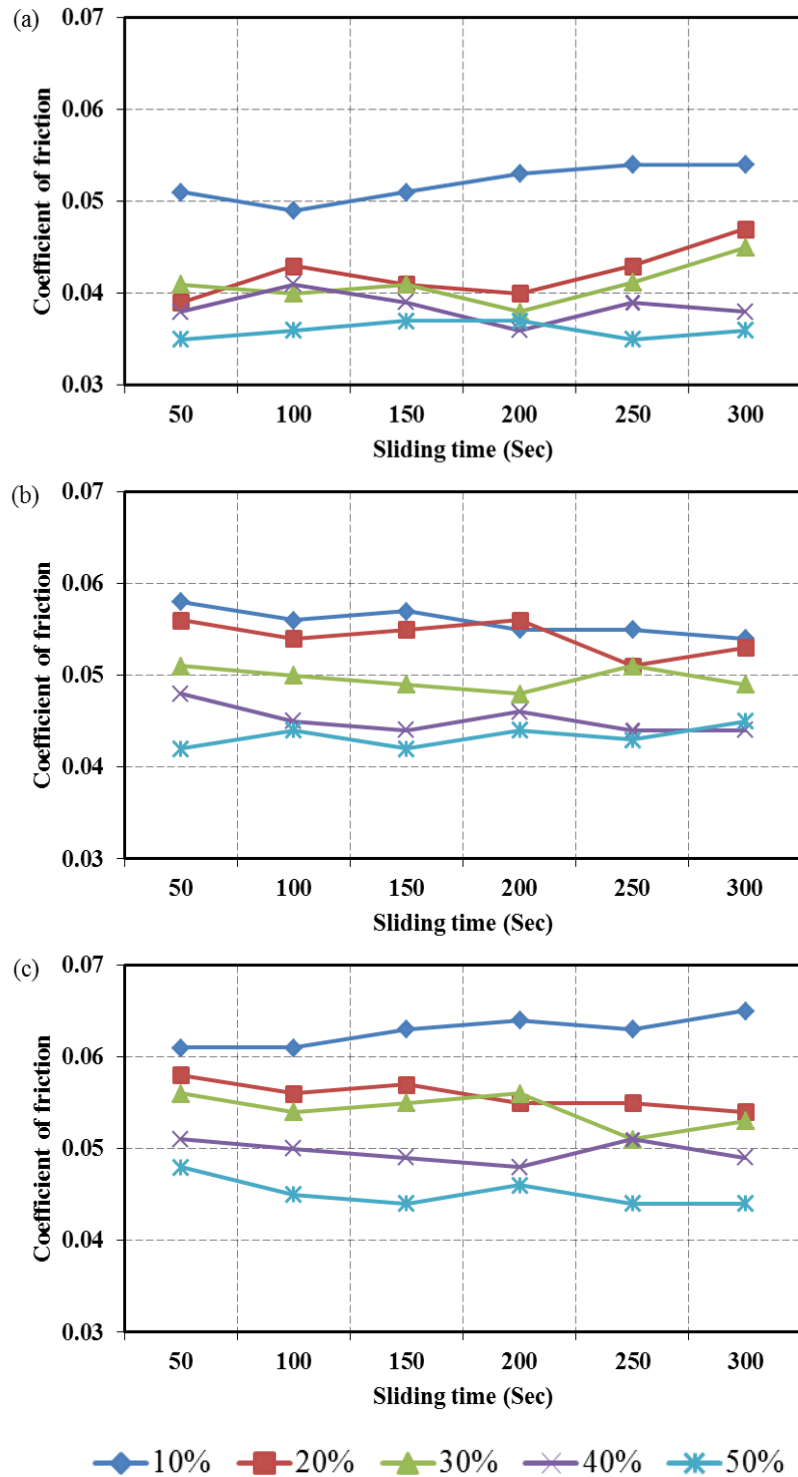


Fig. 4.17: Friction coefficient vs sliding time with respect to various particle size and concentration (a) 10 μm (b) 30 μm (c) 50 μm

Cambiella et al. [146] reported that emulsifier concentration plays a key role on the wetting behavior. Generally increase in the MoS₂ concentration in the base oil has a beneficial effect of reducing wear [10]. All the considered concentrations exhibited low friction coefficient with negligible changes except 10wt% concentration. Whereas, in 30 and 50 μm friction coefficient increases with increase in particle size. One of the possible reasons for reducing coefficient of friction may be the layered lattice structure of the solid lubricant [99]. This may be due to the fact that lubricants with high adhesion tendency and viscosity in the sliding zone decreases sliding nature between contact surfaces [65]. Variation of wear coefficient of WC pin and Ti-6Al-4V disc with different particle size and concentration is illustrated in Fig. 4.18.

Superiority of lesser particles (10 μm sized) is due to its continuous film formation and higher adhesion tendency as compared to coarse particles. Hence, it may be concluded that lubricant film formation of 20wt% MoS₂ with lesser particles is highly effective than other lubricating conditions. From Fig. 4.18, it was observed that though the applied lubricant films separate pin/disc sliding surfaces effectively, it is clear that the presence of thin viscous lubricants provides some protection of contacting bodies against excessive friction coefficient and rate of wear. Minimum rate of wear coefficient was observed when smaller additive particles were suspended on base oil. Lubrication reduces the wear coefficient because of effective lubricant film formation at contact region. The solid additive particles of layered structure shear easily under traction to yield low friction coefficient.

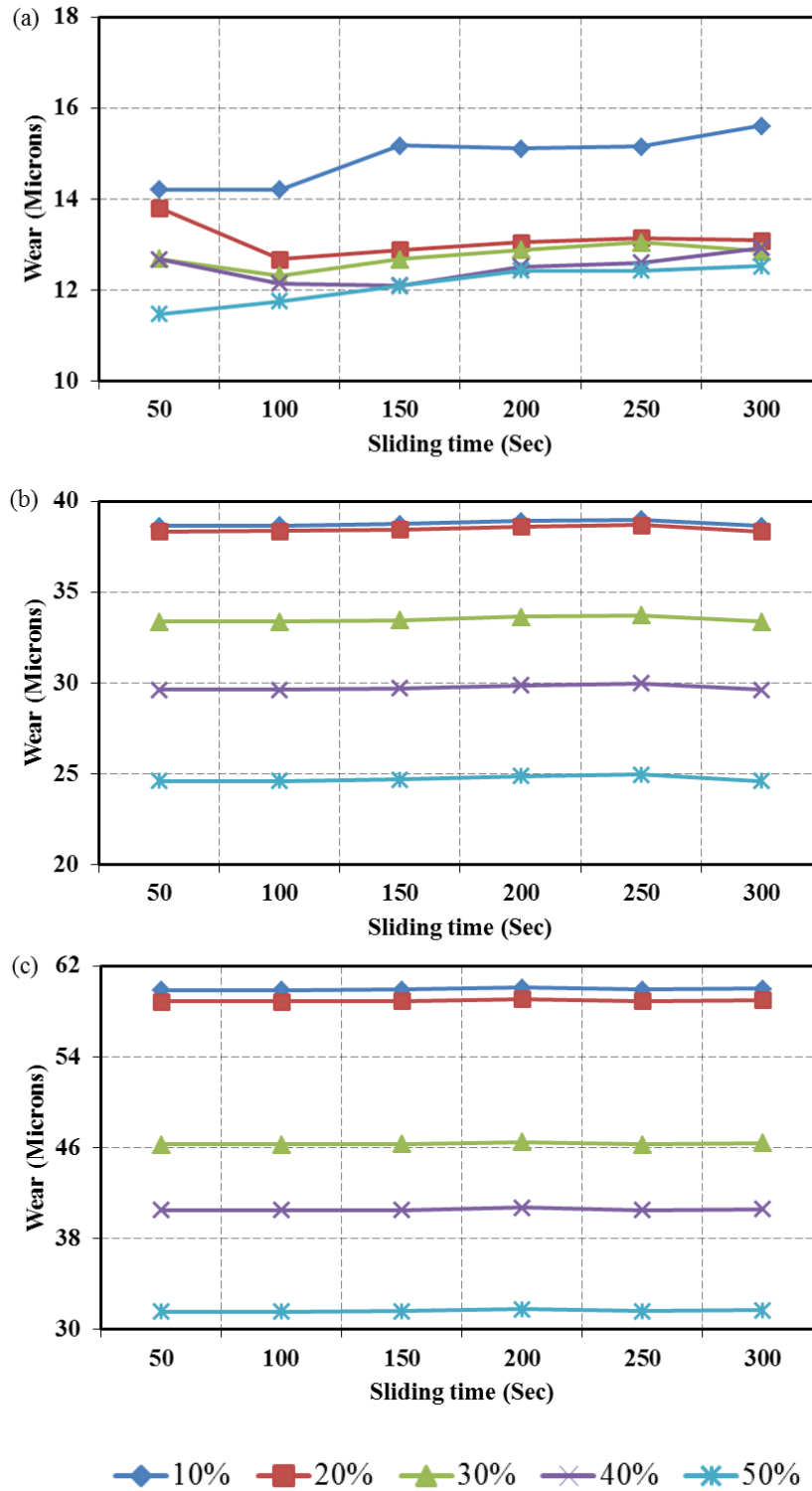


Fig. 4.18: Wear vs sliding time with respect various particle size and concentration

(a) 10 μm (b) 30 μm (c) 50 μm

Combining the above test results, it was observed that in all concentration conditions as the particle size increases, wear rate increases. It was found that the wear coefficient of WC pin is in the decreasing order of 50 μm , 30 μm , 10 μm under solid lubricant conditions. It was also observed that during all the particle size condition wear coefficient decreases with increase in additive concentration. Wear coefficient was reduced by 65% and 77% with lesser particles when compared to 30 μm and 50 μm . Solid lubricants with lesser particle size were more likely to interact with surfaces of the friction pairs to form a surface protection film, which increases anti-wear ability of sliding surfaces [146].

4.4.7 Electrical contact potential

To study the contact situation between pin-disc sliding surfaces, the electrical contact potential resistance was used in pin-on-disc tribometer. Fig. 4.19 shows that the contact gap between the pin-disc specimens increased when 30 μm and 50 μm particle size additives were applied. It was recorded that in all concentrations contact potential increased in the same order. Highest contact potential of 95% was found when a smaller particle with 10wt% suspension occurs in base oil. It was also observed that as the additive particle size increases, the contact potential increases with respect to increase in concentration. When 50 μm particle size additives are added to the base oil, contact potential technique results in increase in contact gap between sliding surfaces. Results from Fig. 4.19 conclude that with increase in the particle size and concentration the gap/contact between the sliding surfaces increases. From Fig. 4.19 it is evident that, for all the available particles sizes the electrical contact potential tends to increase for lower concentration of reinforcement. It is also seen from the graphs that as the reinforcement increase the electrical contact potential

decreases. Lower gap/contact is observed with lesser particles, whereas concentration with 20wt% - 50wt% results negligible difference.

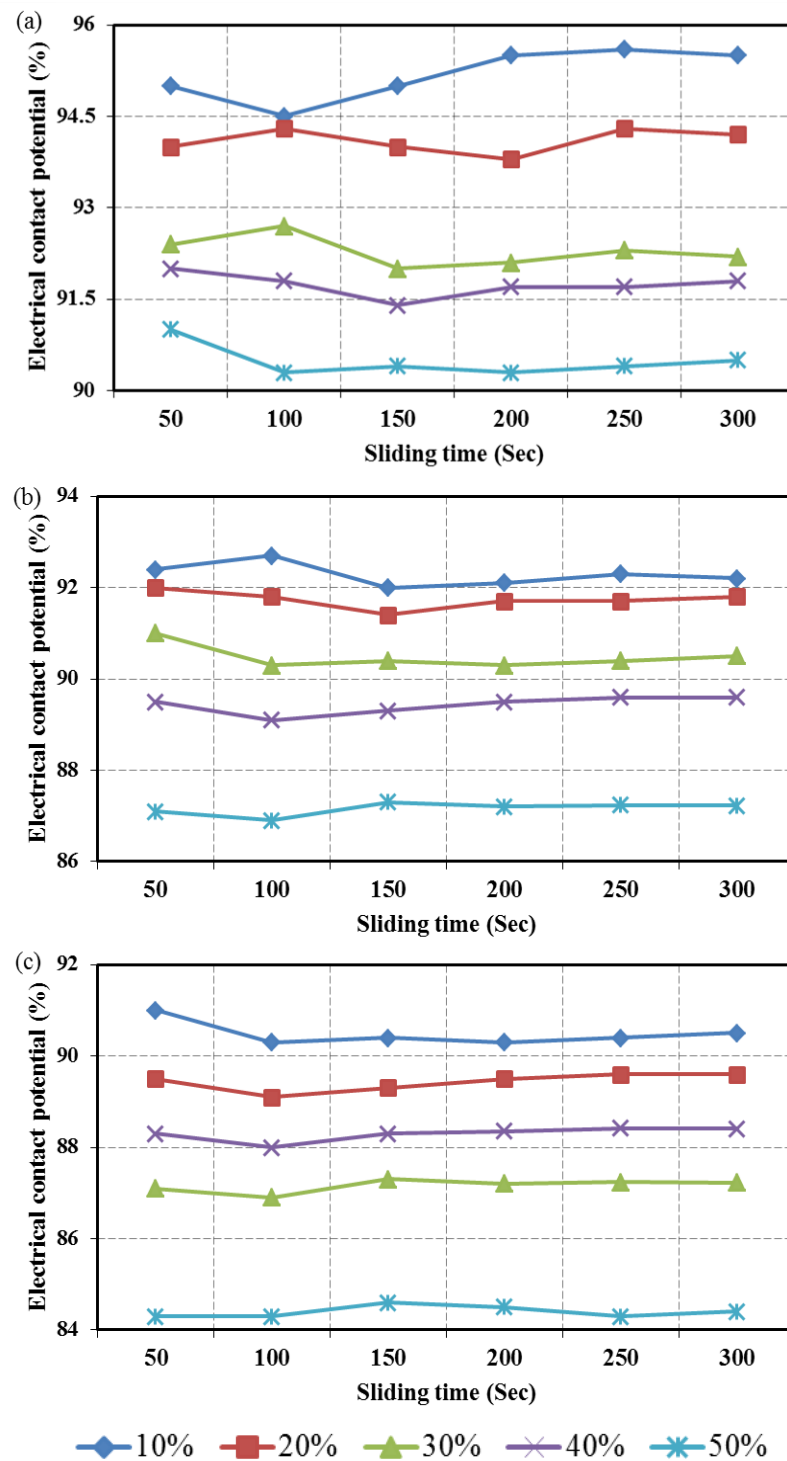


Fig. 4.19: Electrical contact potential vs sliding time of MoS₂ with various particle size and concentration (a) 10 μm (b) 30 μm (c) 50 μm

4.4.8 Analysis of extreme pressure properties

In order to examine the effect of load carrying property of varying solid lubricant particle size and emulsion composition of additive used in the base oil, EP tests were performed on Four-ball tester, following the ASTM D2783 standards. EP characteristics of MoS₂ solid lubricants were studied for a load of range 160 kgf until the ball specimen welded with each other as defined as Final Seizure Load (FSL). Fig. 4.20 shows variation in the friction coefficient under varying loads for varying MoS₂ solid lubricant concentration. Performances of the EP additives are dependent on three factors which are (i) strength of the tribo-film (ii) reaction rate between the additive and the sliding surface and (iii) finally the compatibility between the base oil and the additive [87]. Generally increase in MoS₂ concentration in the lubricant has a beneficial effect regarding wear.

The worn surface of the balls was examined using tool maker's microscope. In no case had any visible wear of the ball occurred. It is determined that wear scar under heavy load test diminishes as the concentration of MoS₂ increases [85]. Under light loads, particle size has no effect while under heavy loads larger grain sizes result in increased wear [86]. Fig. 4.20 shows critical failure load carrying capacity of MoS₂ solid lubricant particle size and concentration. Failure load was determined as average of the load at which the frictional force increased sharply and of the previous load at low friction [86]. Compared to additive particles size 30 μm and 50 μm , most of the additive particles (10 μm) presented lower friction coefficient. It clearly reveals that the friction coefficient for low sized particles (10 μm) is minimum as compared to 30 μm and 50 μm MoS₂ particles, which showed higher friction coefficient throughout

the load range.

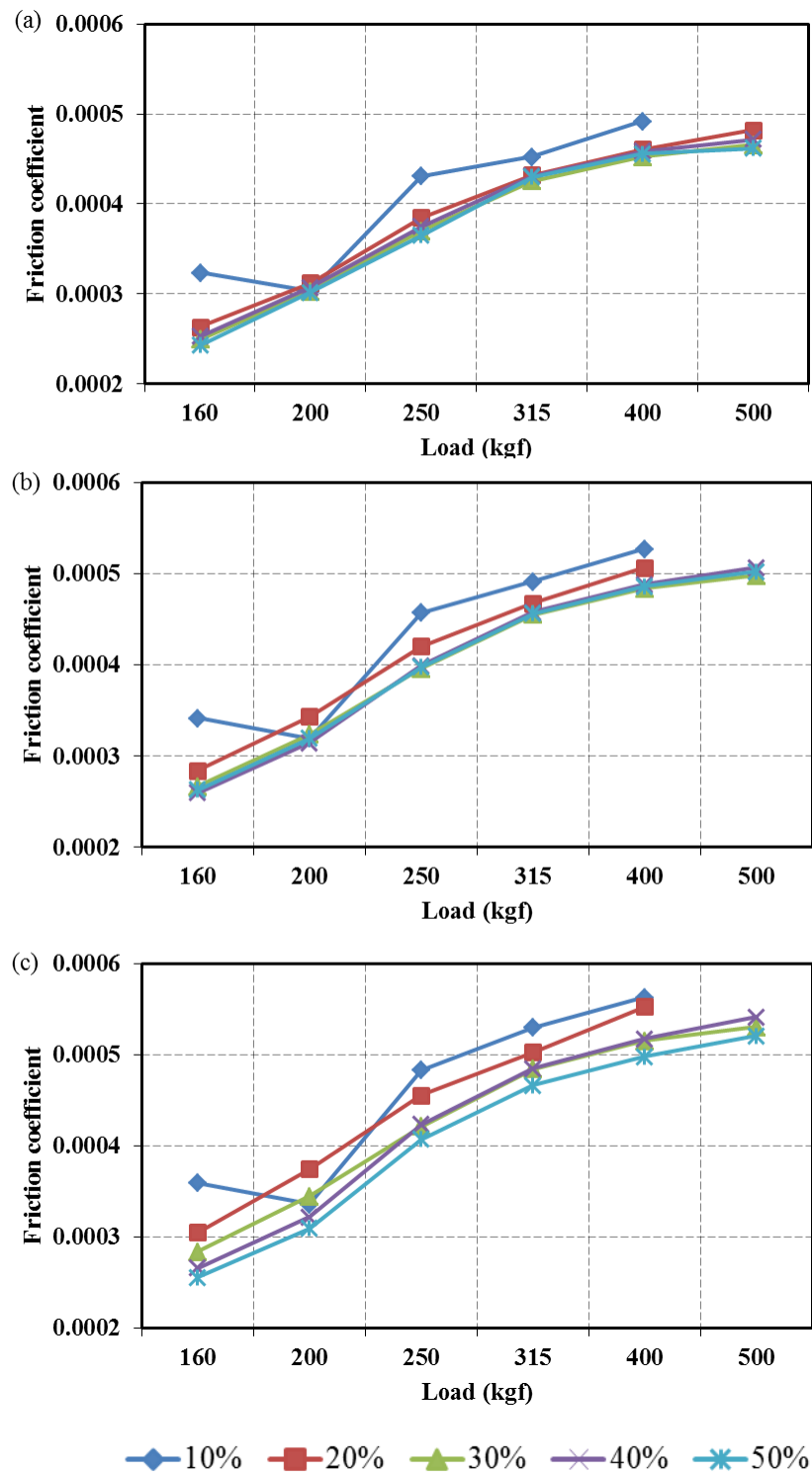


Fig. 4.20 Effect of load (kgf) carrying capacity of MoS₂ at different particle size and concentration (a) 10 μm (b) 30 μm (c) 50 μm

Solid particles of a layered structure shear easily under traction to yield low friction coefficient [85]. From Fig. 4.20, it was found that 20wt%, 30wt%, 40wt% were more stable in terms of final seizure load (FSL) which is defined as the load at which lubricant film totally break down and testing all material (four balls) becomes welded. It was observed that 20wt% of MoS₂ solid lubricant impaired lowest friction coefficient up to initial seizure load at which substantial amount of wear occurred and in final seizure load the lowest friction coefficient was found to be under 40wt% concentration. Fig. 4.20 implies that 20wt% and 40wt% with low size particles have extreme capability to retain its properties up to load of 620 kgf. It was observed from Fig. 4.20 that for MoS₂ particles of 10 μm mixed with oil in 10wt% concentration, the limiting load beyond which balls got fused was around 400 kgf. For higher concentrations 20wt% and above, balls got fused at a load of 620 kgf. For 30 μm particle size, it was observed that 10wt% and 20wt% concentrated solid lubricant based oil withstood a load of 400 kgf before getting fused. Higher concentrations of over 20wt% enabled fusing of balls at 620 kgf. Similarly, particle size of 50 μm showed similar load carrying characteristics as that of 30 μm . It is suggested from the obtained experimental results that the application of MoS₂ with lower particle size (10 μm) and a lower concentration with the base oil (i.e. up to 20wt%) gives rise to better load carrying capacities that too with lower friction coefficient. This can be justified by the fact that at higher loads lubricating film thickness becomes thinner than some of the properties present in the boundary lubrication regime. The suspensions of MoS₂ have been found to have good boundary lubricant conditions due to their larger surface area to volume ratio [85].

4.4.9 Analysis of wear prevention properties

The aim of the current work is to understand the better role of base lubricant and the additives in the boundary regime. Fig. 4.21 shows the variation of friction coefficient and WSD at varying additive concentration of MoS₂ solid lubricant. It is evident from Fig.4.21 that the coefficient of friction decreases with increase in MoS₂ concentration. The results revealed that for 0wt% additive contaminated lubricant exhibited higher friction coefficient than that of other contamination. The subsequent increase in friction coefficient was found for 10wt% MoS₂ suspended lubricant oil. Among the considered conditions, a solid lubricant with 20wt% provides better performance in terms of reducing friction coefficient and WSD. The change in friction coefficient for other concentrations was found with negligible changes.

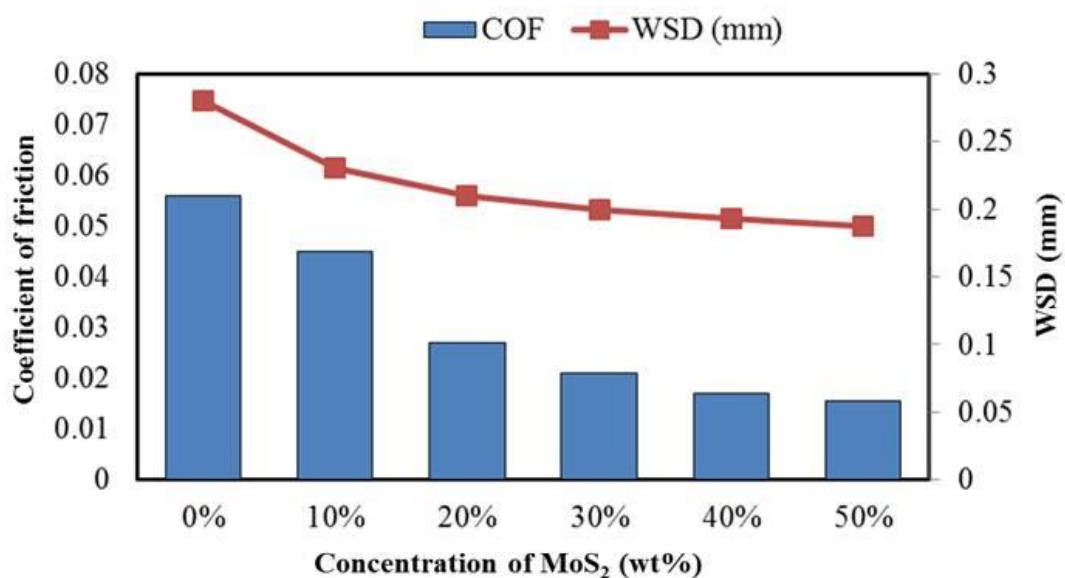


Fig. 4.21: Friction coefficient and WSD for various concentrations of solid lubricant

The results revealed that contamination of higher concentration of MoS₂ is effective in reducing friction. When pure lube oil was contaminated with 20wt% MoS₂, there is a decrease in friction coefficient. It can be observed in Fig 4.21, that

the increase in additive concentration in base oil yields, better friction-reduction behavior. One of the reasons might be the effect of viscosity [18]. This is because a certain quantity of applied solid lubricant accumulates on the surface of friction pairs, and is advantageous for the lubricant to form sufficient lubricant film in order to provide effective lubrication. The micrographs of the worn surfaces of the stationary ball specimen for varying suspension of MoS₂ concentration are shown in Fig. 4.22. It can be seen from the Fig. 4.22 that adhesive wear occurred on the ball surfaces in all considered conditions. The significant improvement in WSD was observed for 20wt% as compared to other concentrations. This is due to the increase in the suspension of additive in base oil leads to greater binding of the lubricants, which in turn provides an excellent resistance to shear force [28]. Though, an increase in concentration more than 20wt% in the base oil has shown negligible changes on WSD.

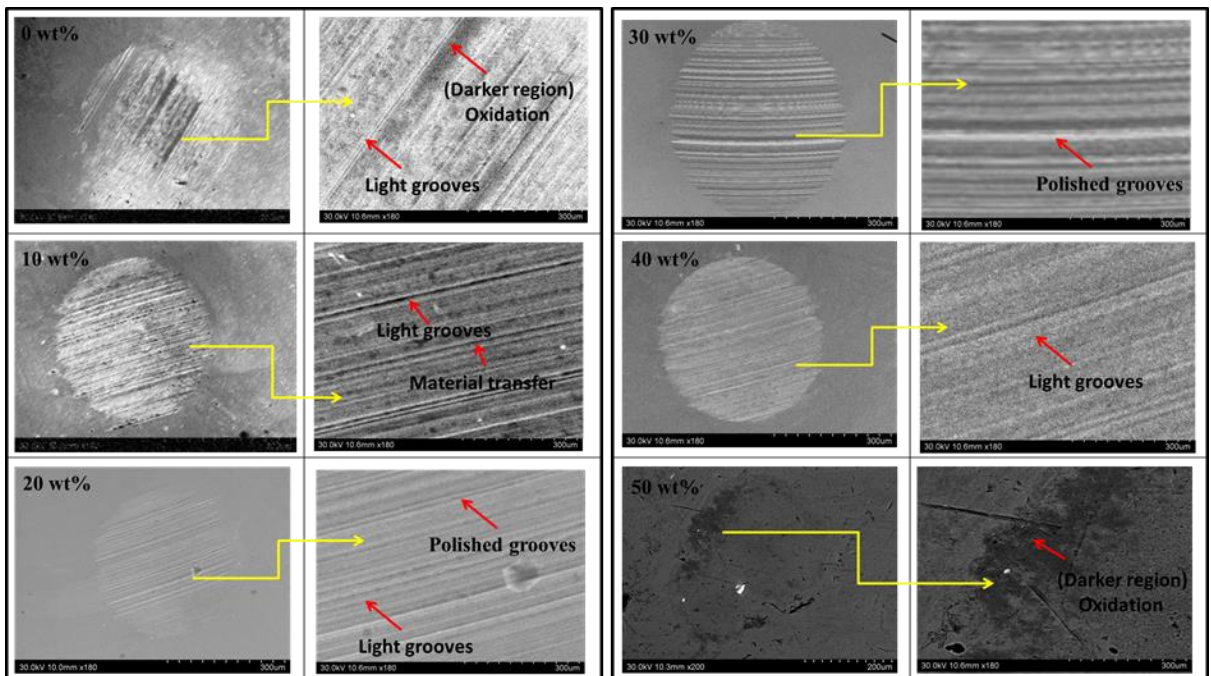


Fig. 4.22: Microscopic images of worn surface of stationary steel balls at various concentrations

4.5 Summary

In the present investigation, pin-on-disc sliding tests were carried out to determine the performance of the solid lubricant suspension in SAE 40 oil. Lubricating properties of solid lubricants are affected by different particle and concentration of additives in SAE 40 oil. Performance evaluation of solid lubricant characteristics highlights that it is essential to have high viscosity, optimal and correct concentration of solid lubricants in base oil. Test results revealed that friction coefficient increases with increase in applied load for all the considered environments. The analysis of wear morphology indicates that the suspension of solid lubricants decreases the rate of wear and results in a relatively smooth surface with fewer scars. The results obtained highlight that it is essential to have high viscosity and correct optimal concentration of a solid lubricant, which must be compatible with any other additives present, to obtain optimum beneficial effects. To elucidate the effect of particle size and concentration upon the lubricating effectiveness of MoS₂ solid lubricant, experimental set-up was developed to measure the lubricant film thickness at sliding interface. Continuous MoS₂ films have been observed with smaller particle size and lower concentration, among the considered, solid lubricants with 20%wt of MoS₂ in base oil provided better performance in terms of improving tribological properties and load carrying capacity. MoS₂ suspension with higher grain size (50 μm) provide higher wear values than that of MoS₂ with finer particles (10 μm). This tendency is more pronounced at higher load conditions and thus smaller particles are capable of handling high load conditions with effective lubrication conditions.

This work emphasizes the proper selection of solid lubricants, particle size and

as well as concentration of solid lubricant particles in base oil. Further, there is a need to analyze the machinability of hard-to-cut materials with the selected MoS₂ as solid lubricant at the contact surface between chip-tool-workpiece interfaces, which is discussed in chapter 5.

CHAPTER 5

ELECTROSTATIC HIGH VELOCITY SOLID LUBRICANT MACHINING SYSTEM FOR PERFORMANCE IMPROVEMENT OF TURNING Ti-6Al-4V ALLOY

5.1 Introduction

Turning is one of the widely used and efficient means of machining materials at relatively high rate. Advanced engineering materials like Ti-6Al-4V alloys find numerous applications in automobile and aerospace industries due to which machining of these difficult-to-cut materials has been a curious topic for manufacturing industries and scientific world. However, machining of Ti-6Al-4V alloy is extremely complex due to its high work hardening ratio, high chemical affinity and low thermal conductivity with most materials used as cutting tools that accelerate tool wear, poor surface quality and diminish productivity. Highly reactive nature of titanium alloys and high heat generated at tool-chip interface while machining causes the material to adhere to tool surface leads to excessive tool wear and reduce tool life. The high cutting forces acting in the shearing zone promote high friction with high heat generation and consequently develop high temperature that promotes tool wear. As lubricant delivered in the machining zone, the cutting fluid must be present at the chip-tool-workpiece interfaces and be active (preferably combining with the materials) to form layers with reduced shearing strength and friction.

The application of cutting fluid increases the thermal convection. The combination of these lubri-cooling actions reduces tool wear, improves surface quality and augments productivity. Abundant application of metalworking fluids may increase production cost and cause environmental and health damages, particularly when not properly managed. Effective cooling/lubrication in the machining zone are essential to improve friction and temperatures by efficient heat dissipation which increases surface quality and tool life. In order to reduce the high cost and mitigate the environmental burden associated with the use, treatment and disposal of cutting fluids, some new technologies have been sought to minimize or even avoid the use of cutting fluids in machining operations. These technologies include dry machining or machining with minimum quantity solid lubricant (MQSL).

It has been observed from research review that machining of difficult- to-cut materials like Ti-6Al-4V alloy causes high heat generation due to its poor thermal conductivity. It has also been revealed from the literature review that better cutting performance could be achieved when the lubricants penetrate quickly and effectively into the critical location i.e. tool-chip-workpiece interface in a short period of time [67-70]. Developments in modern tribology have recognized various solid lubricants with low cost and eco-friendly, which are capable to sustain and provide good lubricity over a wide range of temperatures.

In demanding the improvement of productivity and product quality of machining process, use of solid lubricant with thin film were suggested as one of the necessary alternative machining technique to apply lubricants effectively to the high temperature zone. Evolution in modern machining process has identified many solid lubricants with low cost and eco-friendly, which can able to withstand high temperatures and pressures. Development of advanced machining methods is one of

the alternatives in this direction to apply lubricants effectively to the high temperature cutting region. In this direction, in the present research work, the feasibility of a novel approach for developing a new generation of machining technique namely EHVSL experimental set-up shown in Fig. 5.1 has been envisaged with an aim to improve process performance and to eliminate the usage of cutting fluids during machining process.

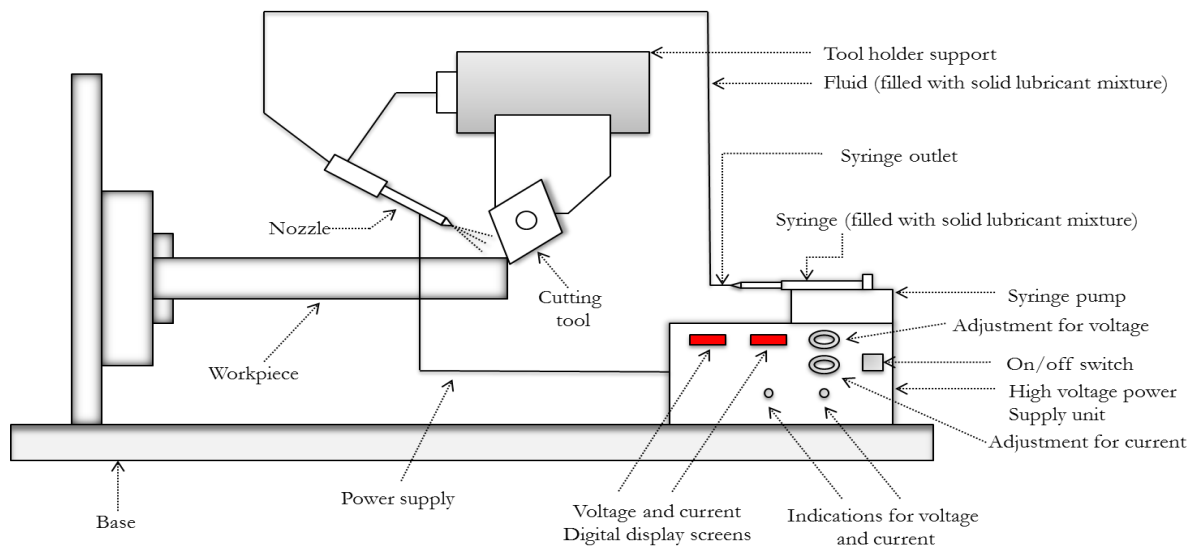


Fig. 5.1: Line diagram of developed electrostatic high velocity solid lubricant spray system

To investigate the role of developed EHVSL system, turning experiments were carried on Ti-6Al-4V alloy at varying feed rate, cutting speed and depth of cut considering surface roughness, cutting force and tool wear as performance indices. The detailed experimental procedure of EHVSL system is discussed in Chapter 3. A detailed comparison has also been made with the other cooling techniques MQSL, MQL, wet and dry cutting conditions using carbide cutting tool inserts with an objective to reduce the overall machining cost and improve machining performance. Efforts should be continued in this direction to control high heat generation during machining of Ti-6Al-4V alloy.

5.2 Results and discussions

During turning of titanium alloy, excess heat is generated at the (i) primary heat source from the a shearing zone, due to plastic deformation takes place, (ii) secondary heat source from a shearing zone along tool-chip interface and (iii) third source from rubbing zone along tool-workpiece interface. The performance of turning Ti-6Al-4V alloy under the developed EHVSL set-up are compared with the existing cooling techniques and has been assessed in terms of surface roughness, cutting force, and tool wear. Hence, in the present work, the experiments have been conducted to study the machining of Ti-6Al-4V alloy using MoS₂ as solid lubricants on the developed EHVSL spray system and compared the same with dry, wet, MQL and MQSL conditions.

5.2.1 Effect of EHVSL on cutting force

The machining force component is a crucial parameter during the evaluation of the performance of any machining process. Several parameters like workpiece material, tool material and its geometry and the presence of lubricant have a considerable effect on machining force, which helps to estimate the energy requirement of the machining process. During the machining process, the behaviour of average machining force components under considered environment with various cutting parameters is shown in Fig. 5.2-5.4. It was understood that cutting speed significantly influences the cutting force. The experimental results shown in Fig. 5.2-5.4 that at high-speed cutting conditions, the cutting force decreases causing reduction of shear strength at the machining zone. Due to the formation of thin solid lubricant film in the machining zone, good friction and wear reduction performance is

observed that reduces low shear strength of materials so that machining becomes easier.

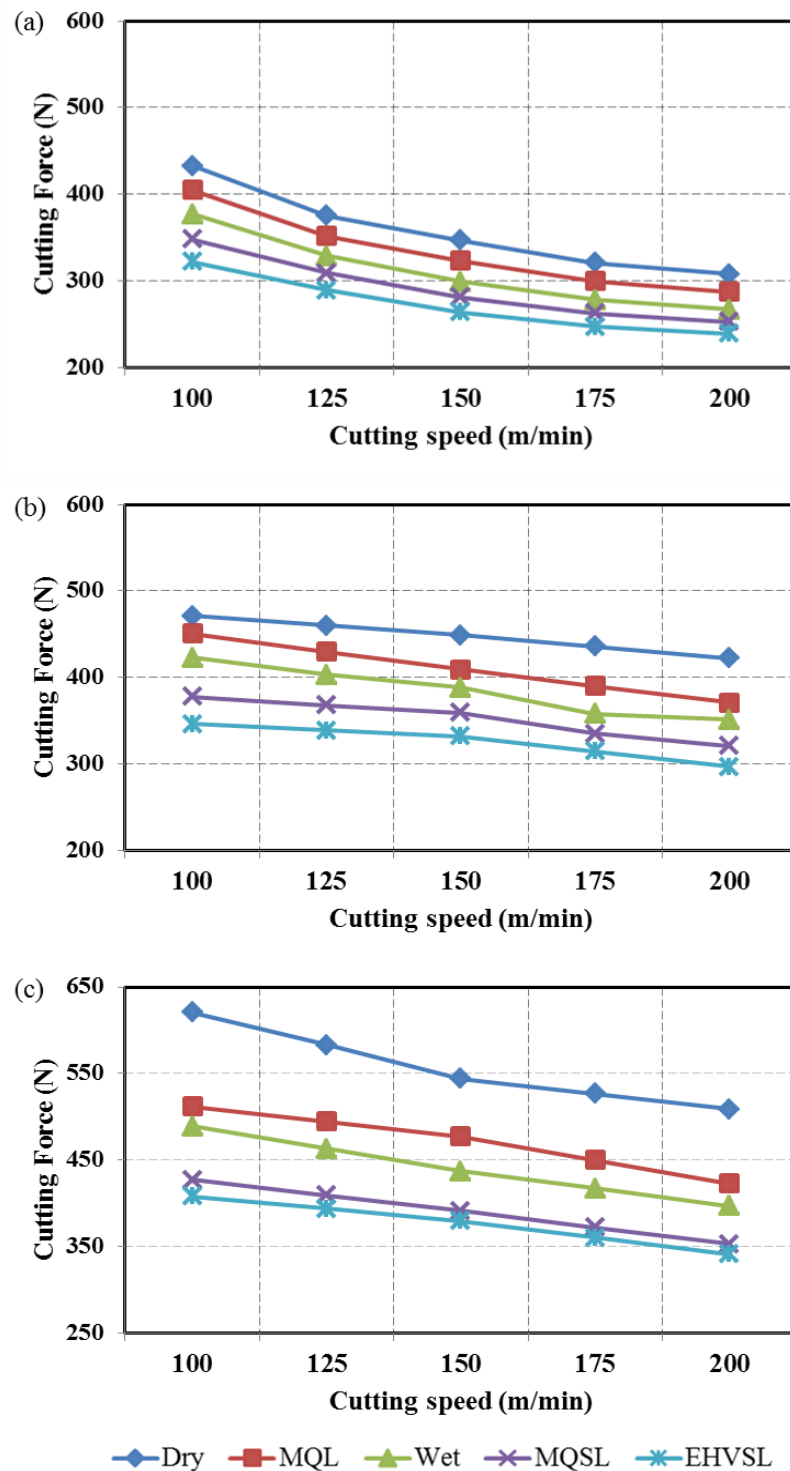


Fig. 5.2: Cutting force at cutting speed = 100, 150, 200 m/min, (a) Feed = 0.1, (b) Feed = 0.15, (c) Feed = 0.2 mm/rev under different environments (depth of cut = 0.5 mm)

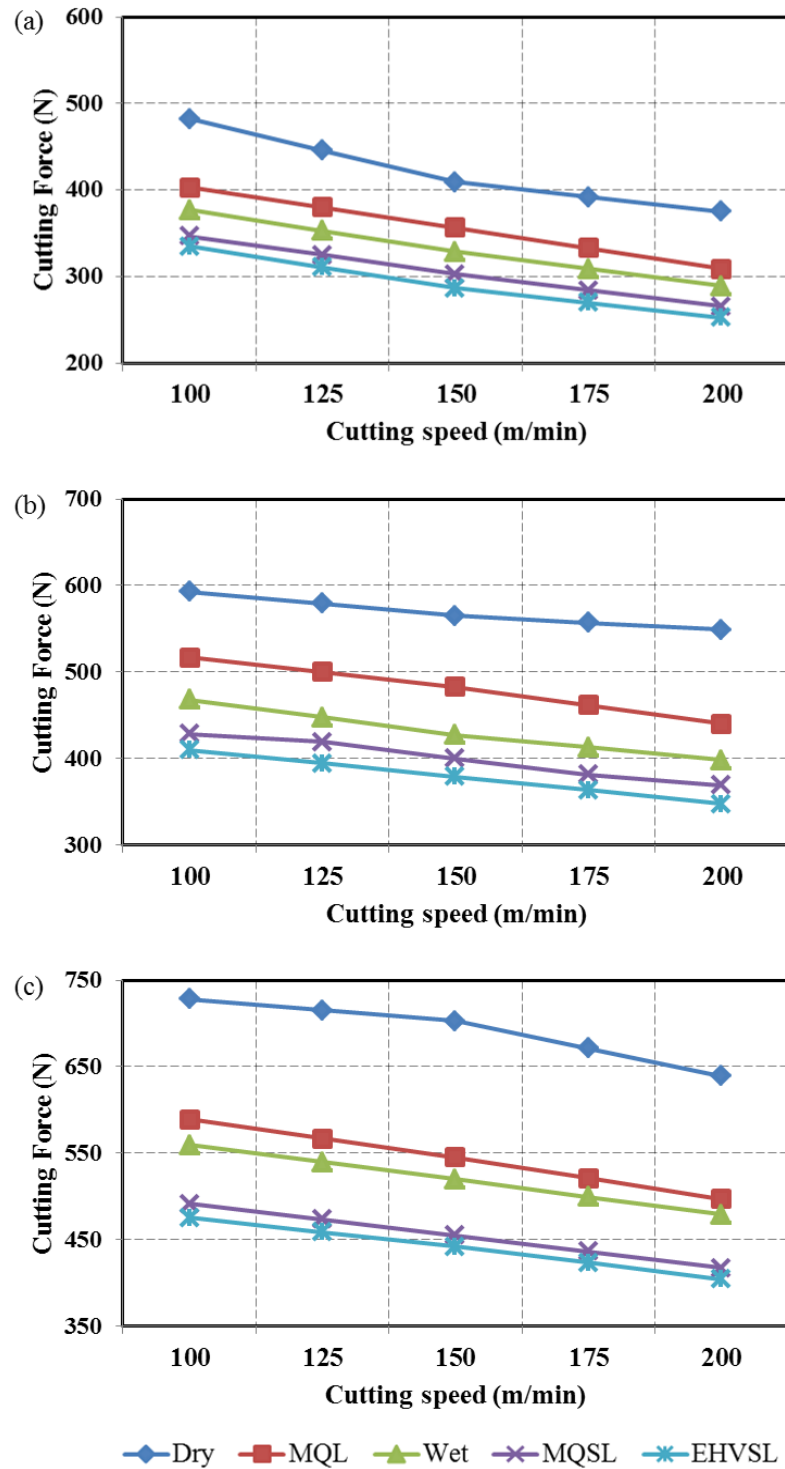


Fig. 5.3: Cutting force at cutting speed = 100, 150, 200 m/min, (a) Feed = 0.1, (b) Feed = 0.15, (c) Feed = 0.2 mm/rev under different environments (depth of cut = 1 mm)

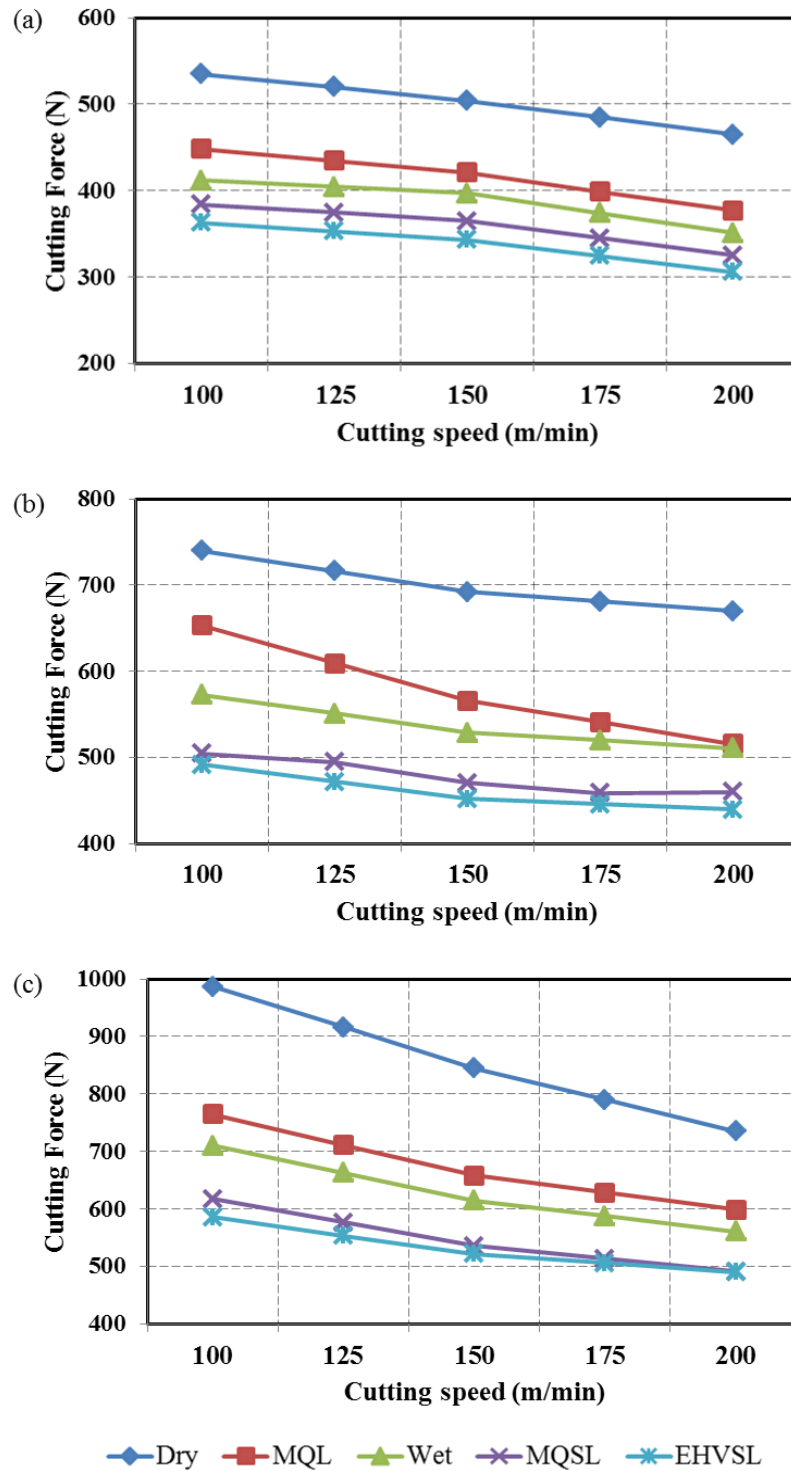


Fig. 5.4: Cutting force at cutting speed = 100, 150, 200 m/min, (a) Feed = 0.1, (b) Feed = 0.15, (c) Feed = 0.2 mm/rev under different environments (depth of cut = 1.5 mm)

The solid particles of layered solid lubricants shear easily under traction to yield low coefficient of friction. Upon further increase in the machining speed, the friction coefficients at the tool-chip zone on the cutting tool (at rake face) results in a decreased shear plane angle [6]. Therefore, cutting force decreases at high-speed condition. As a result, the cutting speed was found to be more significant effect in terms of inducing the machining force. Results also showed that machining force increases with increasing feed rate and depth of cut in the machining process. This is due to the fact that, increase in feed rate and depth of cut results in increased rate of plastic deformation at the primary shearing zone [147]. Considerable reduction of cutting force was observed during EHVS and MQS assisted machining condition as compared with dry, wet, and MQL machining conditions. The efficiency of the lubricant in minimizing the friction developing at the tool-chip-workpiece interface zone is realized by the reduction of cutting forces achieved with EHVS machining technique when compared with MQS, MQL, flood and dry lubricant cutting. From the obtained results it was observed that, dry machining is associated with enhanced friction, which leads to increased cutting temperatures, thereby increasing cutting force. The high cutting forces acting in the shearing zones promote high friction with high heat generation and consequently develop high temperature that accelerates tool wear. This could be, due to the absence of coolant in the hot-interface zone. Thus, the negligible amount of solid lubricants that can still reach the tool-chip interface zone seems to have a vital effect on reducing temperature. Whereas, during MQL process, it was observed that the lubricant cannot penetrate effectively into the tool-chip interface. The EHVS lubricants act predominantly and contribute to reduce the friction and the chip-tool-workpiece contact areas, allowing higher cutting speed, better surface finish and greater tool life. Compare to wet, dry, MQL and MQS

machining condition, the efficiency of lubricant in reducing the friction at the tool/workpiece/chip contact zone is evident by reduction in cutting force under EHVSL machining condition. Further, results revealed from the tested experiment that the cutting force reduced by 7%, 17%, 23% and 31% less cutting force were occurred during EHVSL cutting condition as compared with MQSL, wet, MQL and dry cutting conditions. The interactions at tool-chip and reduction in machining temperature in the vicinity of primary cutting edge where chips seize and tendency to form BUE are more predominant.

The turning performance of EHVSL system provides considerable improvement than MQSL system mainly due to better penetration of solid lubricant into the mating surface which provides higher lubrication characteristics between the chip-tool interface zone. Hence, from the obtained results it can be extracted that EHVSL system improves the surface quality of the machined surface and tool life by reducing the cutting force. This further leads to improvement in productivity. The significant reduction in cutting force strengthens the use of EHVSL system in manufacturing industries as the best alternative solution for effective reduction in friction forces between tool-workpiece interfaces.

Fig. 5.2, 5.3 and 5.4 shows the variation of depth of cut against the cutting force for different lubricant conditions. It is evident from the experimental results that increasing depth of cut results in increased cutting force in all the lubricant conditions considered. The greater the depth of cut larger the cross-sectional area of the uncut chip thickness and the volume of the deformed metal, consequently greater is the resistance of the material to chip formation and larger is the cutting force.

MoS₂ is used as coolants and is recognized to be good solid lubricant due to its significant reduction in friction generated between sliding components, which could significantly contribute to reduce cutting forces [65 & 99]. From the previous studies it was observed that MoS₂ (lamellar material) generally has good load carrying capacity with a corresponding low friction coefficient under sliding condition [18 & 95]. The considerable reduction of machining forces with the application of MoS₂ based machining is due to the formation of a thin film of lubricant that reduces shear strength of the material and temperature developed in the interface zone and making the machining easier [13 & 94]. Hence, an improvement in tool life and excellent surface quality products are achieved by minimizing the frictional force.

5.2.2 Effect of EHVSL on surface roughness

Surface roughness plays crucial role in the machining process and has significant impact on friction coefficient, wear, fatigue strength, lubrication, and corrosion resistance of the machined surface [148]. The degradation of surface quality often depends on the machining process and is influenced by various interdependent parameters during metal cutting process including selection of cutting conditions, lubricants and particularly the effectiveness of the cutting tool performance. Any improvement in tool-workpiece interaction by reducing the frictional effects on contact surfaces by proper supply of lubricants will affect the surface quality and as well as the tool performance to a greater level. The center line average (CLA) (R_a) parameter was measured in three different positions on Ti-6Al-4V alloy bar of 65 mm diameter machined surface under different environmental cutting conditions considered in this research work are represented in Fig. 5.5-5.7.

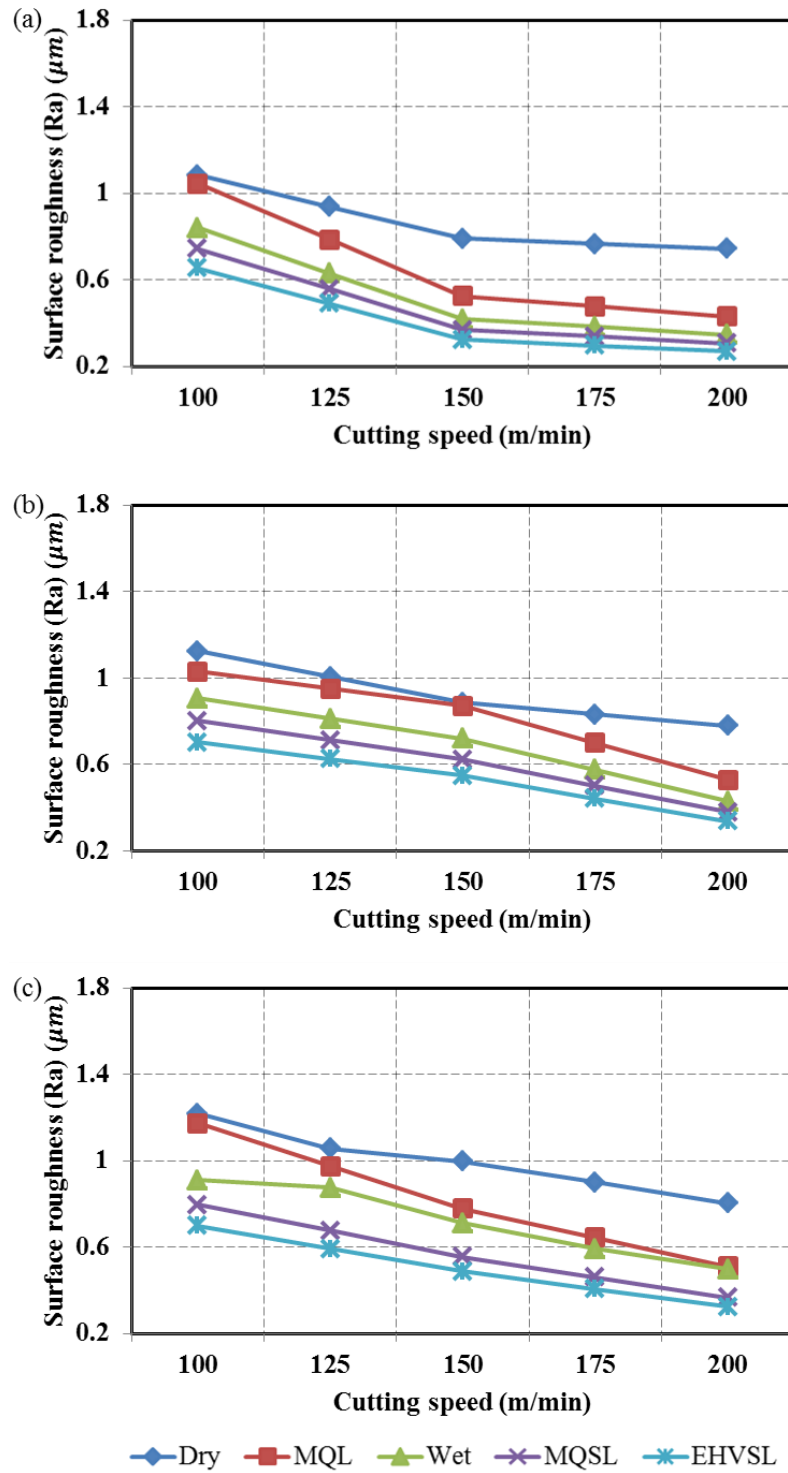


Fig. 5.5: Surface roughness at cutting speed = 100, 150, 200 m/min, (a) Feed = 0.1, (b) Feed = 0.15, (c) Feed = 0.2 mm/rev under different environments (depth of cut = 0.5 mm)

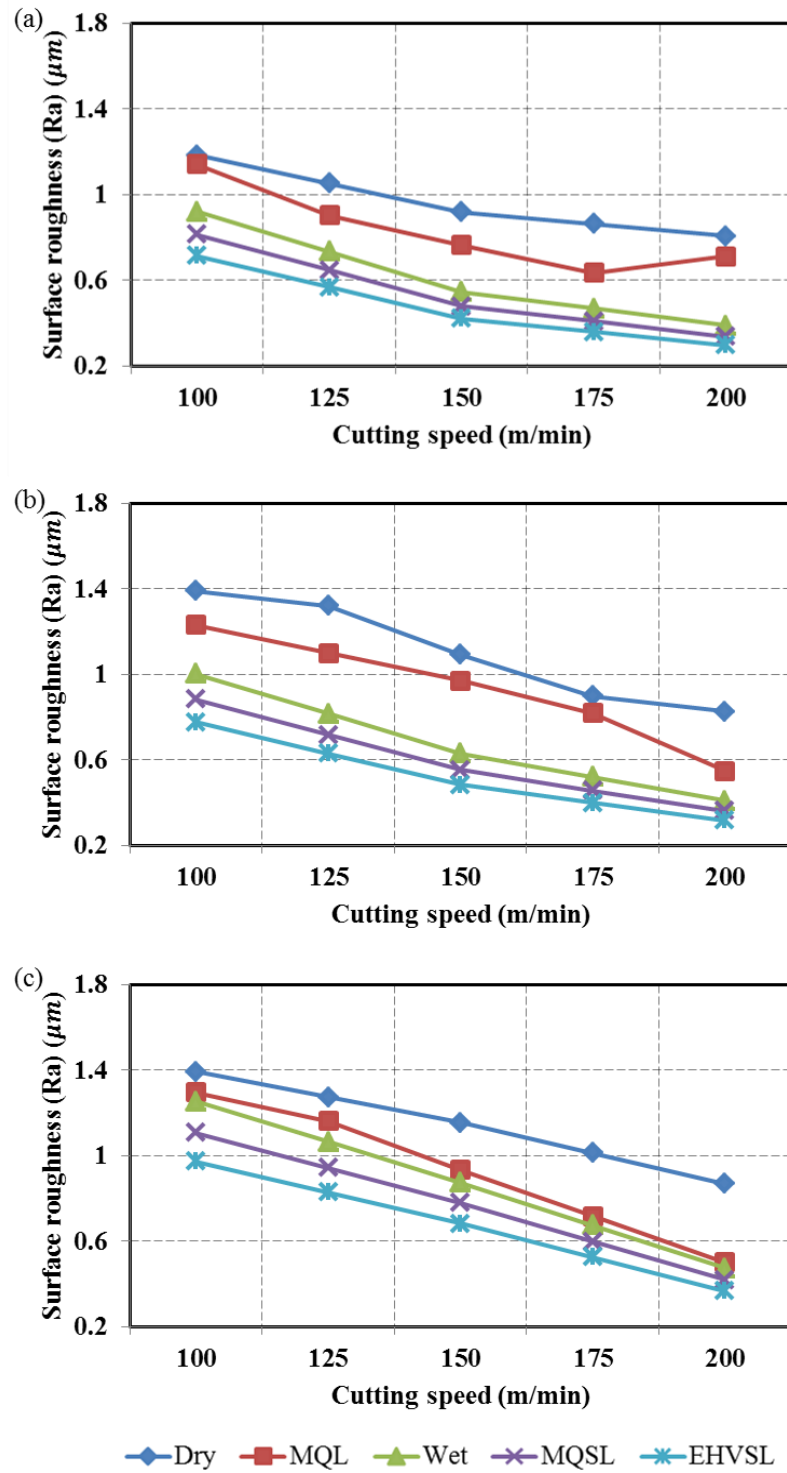


Fig. 5.6: Surface roughness at cutting speed = 100, 150, 200 m/min, (a) Feed = 0.1, (b) Feed = 0.15, (c) Feed = 0.2 mm/rev under different environments (depth of cut = 1 mm)

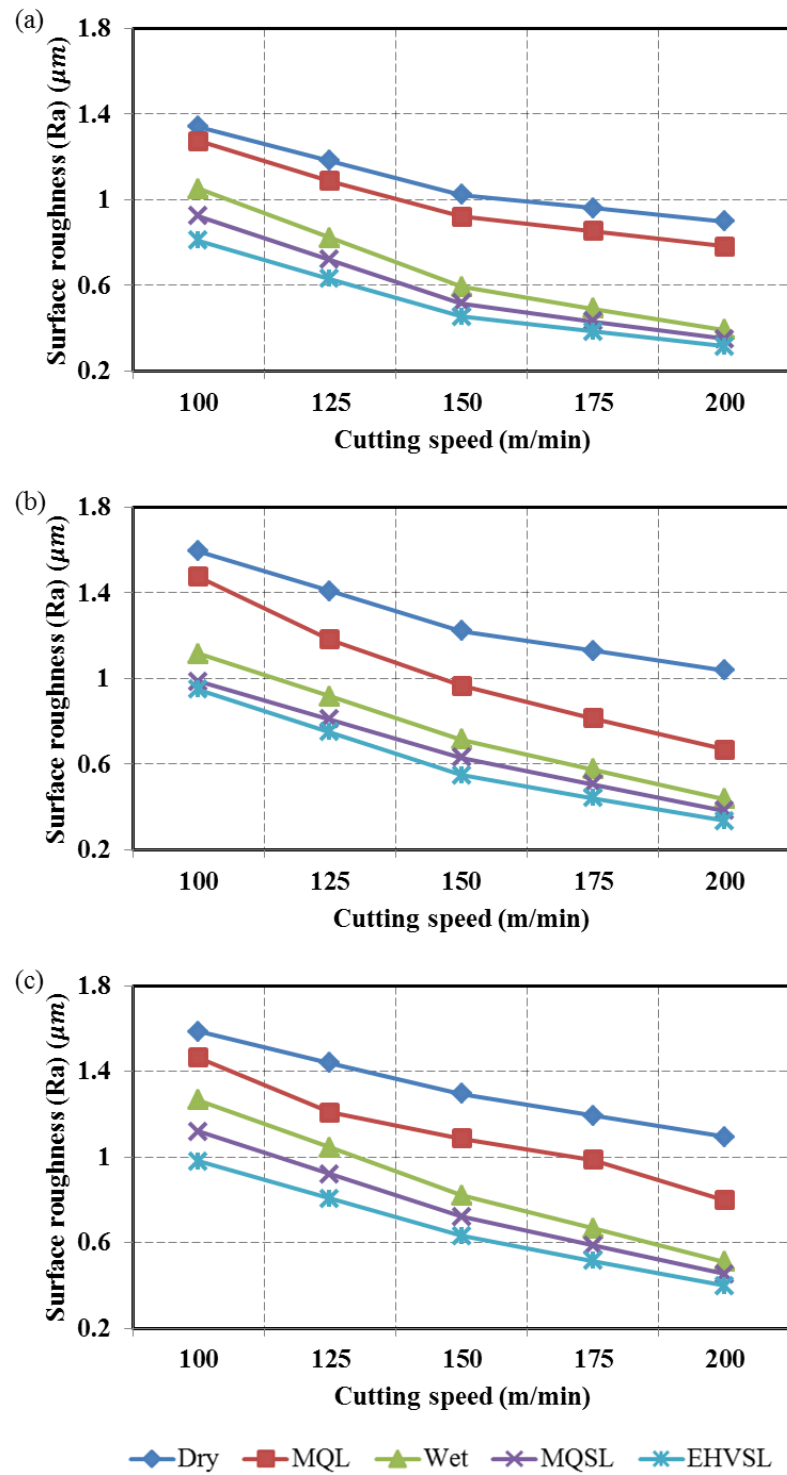


Fig. 5.7: Surface roughness at cutting speed = 100, 150, 200 m/min, (a) Feed = 0.1, (b) Feed = 0.15, (c) Feed = 0.2 mm/rev under different environments (depth of cut = 1.5 mm)

From Fig. 5.5-5.7 it was observed that in all the considered environments, at high cutting speed conditions better surface finish was observed on the workpiece owing to lower cutting force generated. It was also observed that at higher MRR condition surface finish increases. In addition, at higher cutting speed the BUE on cutting tool surface turn out to be less, chip breakage decreases, and hence the quality of the machined workpiece surface is achieved. It is predictable that at higher cutting speed condition chip removes easily from the workpiece resulting in a better surface finish of the workpiece. Further, results show that during EHVSL lubrication condition (shown in Fig. 5.5-5.7), surface roughness significantly improved by 11% in comparison with MQL assisted machining condition. It also leads to an average surface roughness of 25%, 40%, and 57% during EHVSL assisted machining conditions to compare to wet, MQL and dry cutting condition respectively. During EHVSL machining process, charged spray solid lubricant droplet particles effectively applied at chip-tool interface zone, form a thin lubricant film and adhered to the tool-chip interface effectively leading to process improvement at the contact surface. The lower surface roughness values achieved through EHVSL machining process can be attributed to the MoS₂ inherent lubricating properties and thereby reduce cutting temperatures generated, and further, preventing tool wear contribute to surface quality improvement. However, it is evident that lubricants with high viscous, high-velocity thin pulse jet system substantially improves the surface roughness primarily by delaying the deterioration of the auxiliary cutting tool edge due to abrasion, chipping and BUE formation.

Surface roughness has been observed to be lower at a depth of cut of 0.5 mm (Fig. 5.5). For values beyond i.e. 1 mm and 1.5 mm depth of cut, an increase in surface roughness values has been observed. The combination of high speed with low

depth of cut prevents the formation of BUE and thereby aids the process by yielding an improved surface quality [149]. The chatter tendency can be reduced with lower depth of cut. The direct influence of the depth of cut on surface roughness is not very little; however, the chatter may reduce the quality of the turned surface.

The high roughness values were observed during dry machining condition. During MQL process, it was observed that the evaporative mode is associated predominantly with high heat removal, which exhibits superior capability than the convective mode of heat transfer prevailing in conventional wet turning [32]. It was found that during EHVSL process, the MoS₂ solid lubricant particles supplied effectively to the rake face and flank face can firmly stick to the cutting tool and workpiece causing in the promotion of plastic flow on the back side of the chip due to Rebinder effect [18]. Close observation of crystal-lattice conceals that due to the presence of free electrons in MoS₂ particles the adhesion tendency is more to metal surfaces, resulting in low friction forces as compared to MQSL machining process. This was expected because sufficient lubricant with high-pressure was employed for proper lubrication in machining zone. In fact, reducing the interface temperature by cooling action and friction by lubrication action eventually result in improving the surface roughness [148].

Reddy et al. [69] suggested that minimizing the specific energy and cutting force results in increase in the surface quality and tool performance. Reddy and Rao [18] also studied that during the machining of medium carbon steel, an average surface roughness reduction of 23% was observed with MoS₂ solid lubricant when compared with wet cutting fluid and 43% reduction of surface roughness was observed in comparison to dry machining. Reddy and Yang [58] report that surface roughness decreases due to lubricating action of solid lubricant at high temperatures.

It was observed that the overall performance of application of solid lubricant was superior to MQL, wet, and dry in terms of improving the high heat generation, which minimizes deterioration of the cutting edge by chipping, BUE formation and abrasion.

5.2.3 Effect of EHVSL on tool wear

Tool flank wear has an imperative role in prompting the tool life and productivity of the machined surface. Increase in temperature at the machining zone strongly impair the physical properties associated with the cutting tool material and thus reduces the particle penetration ability, which further leads to influence the cutting tool performance [49 & 150]. Tool wear studies were performed to estimate the performance of EHVSL during machining of Ti-6Al-4V alloy at varying machining conditions. Fig. 5.8-5.10 shows the flank wear at different environmental conditions. It was observed that under the considered environment conditions, there is a steady increase in flank wear with cutting speed. Further, the flank wear was also found to be increasing with increase in feed rate and depth of cut. The results revealed (Fig. 5.8) that tool wear increases with increase in cutting speed, feed rate and depth of cut. The chips produced during cutting process slide on the rake face of the cutting tool. As the cutting speed in machining process increases, high cutting temperatures are developed at the tool-chip-workpiece interface causing adhesion between tool and workpiece material. Workpiece material was found to be adhered on the flank face of the cutting tool under high cutting parameter condition [94]. However, when comparing the conditions of lubrications used, application of MoS₂ solid lubricant with EHVSL supply system showed a significant improvement compared to MQSL, MQL, wet and dry cutting conditions.

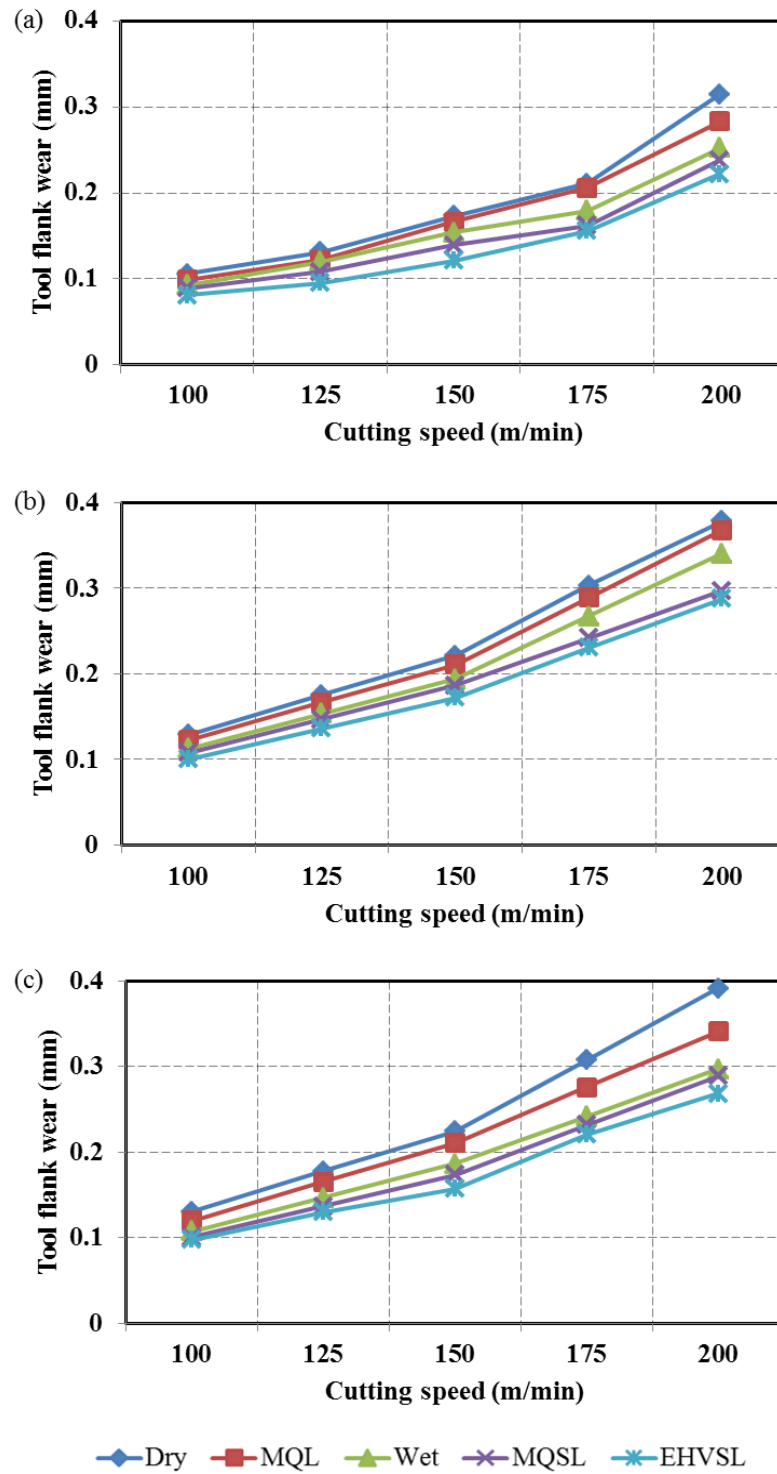


Fig. 5.8: Tool wear at cutting speed = 100, 150, 200 m/min, (a) Feed = 0.1, (b) Feed = 0.15, (c) Feed = 0.2 mm/rev under different environments (depth of cut = 0.5 mm)

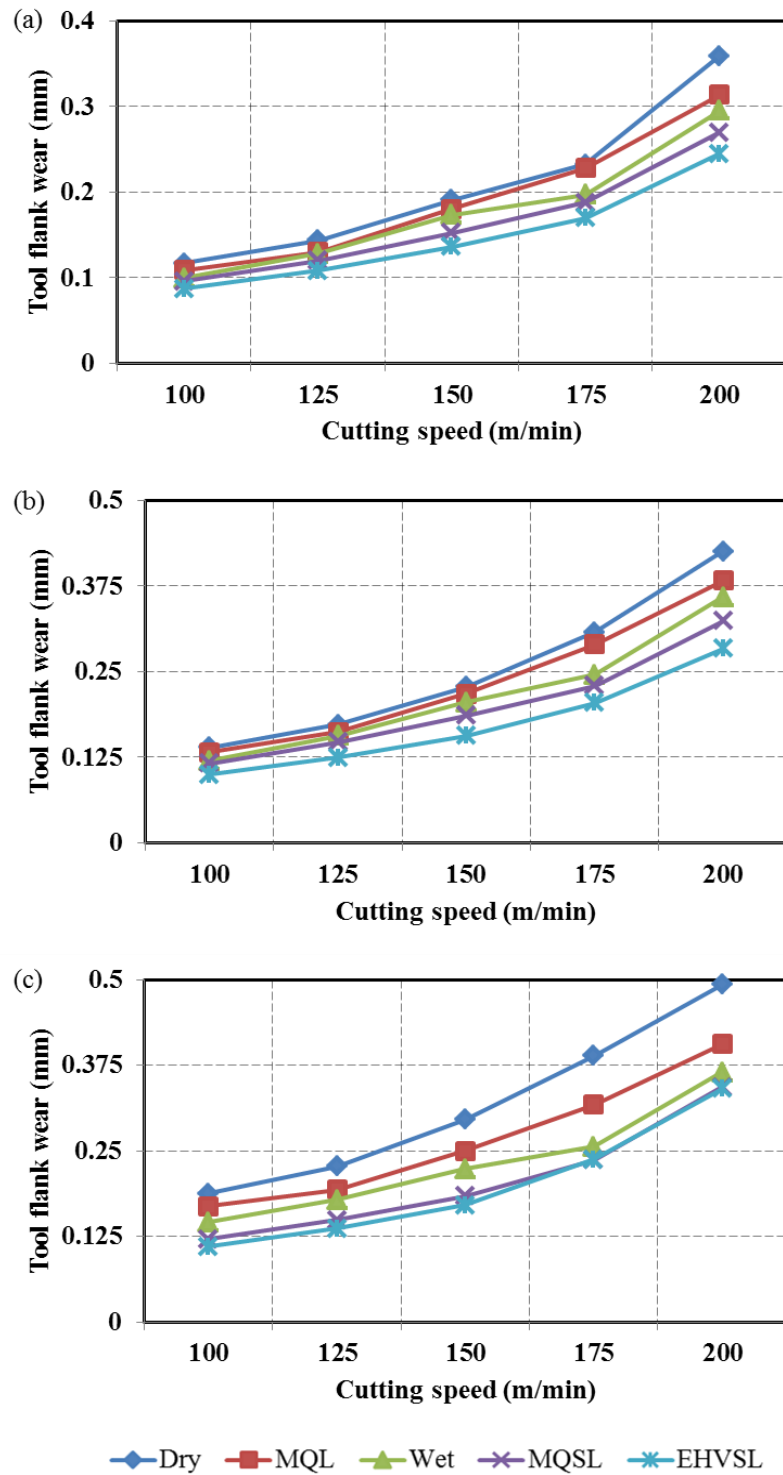


Fig. 5.9: Tool wear at cutting speed = 100, 150, 200 m/min, (a) Feed = 0.1, (b) Feed = 0.15, (c) Feed = 0.2 mm/rev under different environments (depth of cut = 1 mm)

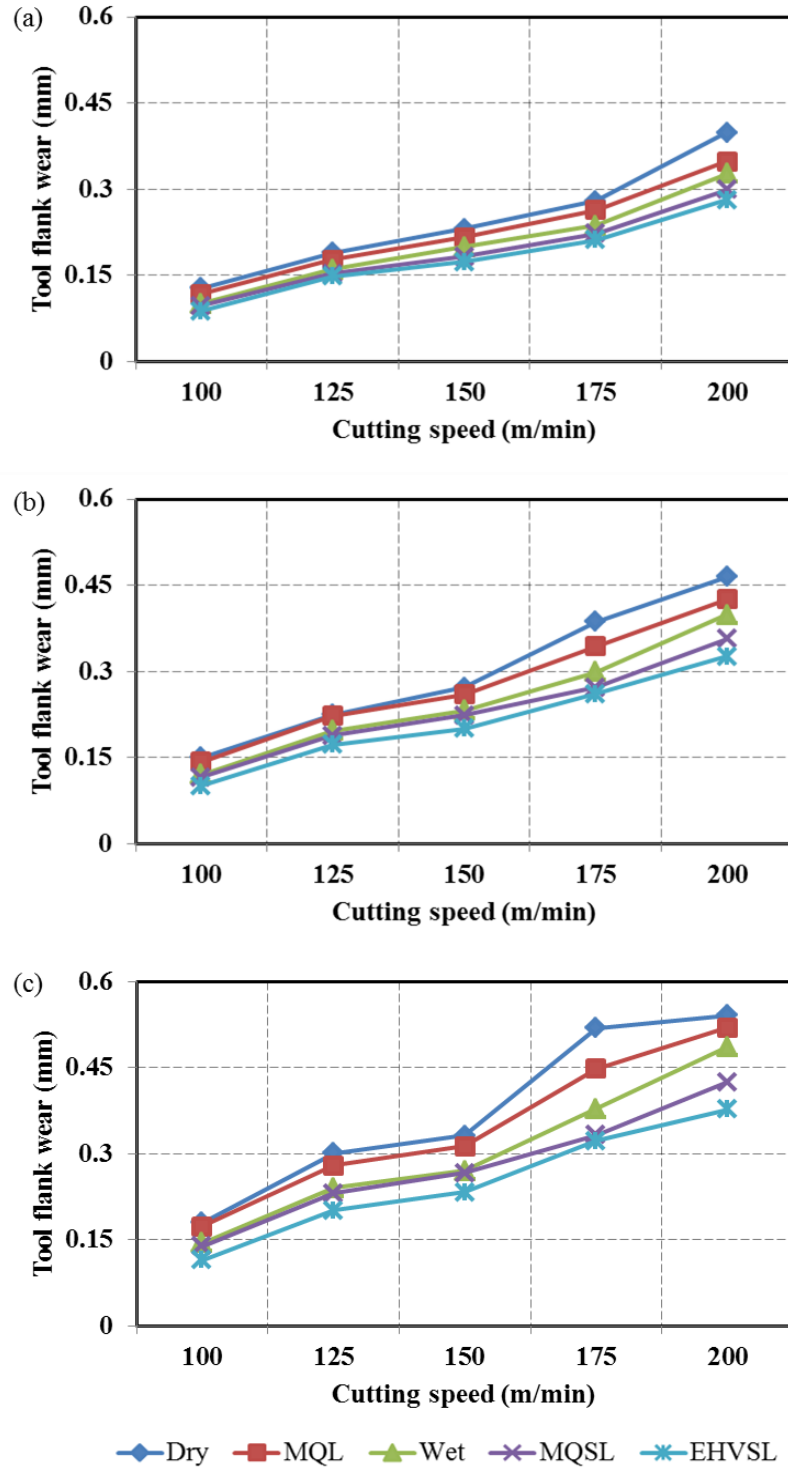


Fig. 5.10: Tool wear at cutting speed = 100, 150, 200 m/min, (a) Feed = 0.1, (b) Feed = 0.15, (c) Feed = 0.2 mm/rev under different environments (depth of cut = 1.5 mm)

Results revealed from Fig 5.8-5.10 that MoS₂ with developed EHVSL set-up leads to the reduction in tool flank wear by 9%, 12%, 18%, 23% compared to that of MQSL, wet, MQL and dry machining condition, respectively. This could be due to the reduced cutting forces and temperatures. This observation indicates that MoS₂ solid lubricant can be used as an effective coolant in the machining process. Further, the use of MQSL assisted machining showed no appreciable difference when compared with EHVSL condition. It has been observed that during EHVSL condition solid lubricant (MoS₂) melts and smears, forming a thin layer of lubricant at chip-tool-workpiece interface. This could probably be due to the good adhesion tendency of the solid lubricants near the machining zone with minimum plastic deformation by offering low friction coefficient and minimum shear resistance. High-pressure coolant systems were applied at the tool-chip-workpiece interface for adequate penetration and to change the thermo-mechanical conditions in the machining zone [55]. Examinations of the wear surfaces revealed that in all the testing environments, the presence of BUE at the cutting tool edge could be due to adhesion of machined workmaterial on the cutting tool surface. Workpiece material sticks to the flank face of the cutting tool under high cutting parameter conditions [141]. The wear occurring at the flank face of the cutting tool has been analysed using scanning electron microscope (SEM). Fig. 5.11-5.15 show details of the SEM analysis. In view of observation of great amount of adhesion of work materials on the tool surface, samples were embedded in hydrochloric acid (HCl) for 48 hrs to remove the adhered material and allow clear observation of worn areas.

Fig. 5.11-5.15 show details of the worn areas of the tools used with EHVSL, MQSL, wet, MQL and dry cutting conditions. From the study of Trent and Wright [151], wear mechanisms involved can be linked with the details of the worn areas of

the tools. The smooth worn areas seen on the surface of the tool indicate the existence of chemical wear at atomic levels. It is clear that attrition and abrasion depend more on active lubricant area [6]. Where as in the rougher portions of the worn area, due to attrition mechanism particles of the tool were plucked off. By observing the parallel ridges we can confirm the presence of abrasion wear mechanism. Because of the high temperature dependency of diffusion in comparison with attrition and abrasion, it can be concluded that cooling action is more important during machining of hard-to-machine material. The active lubricant area is the major factor on which attrition and abrasion depends. The superior performance of EHVSL is because of the combination of both the actions. From the Fig. 5.11, the presence of adhered MoS₂ on the tool surface shows clearly that the lubricant action is working.

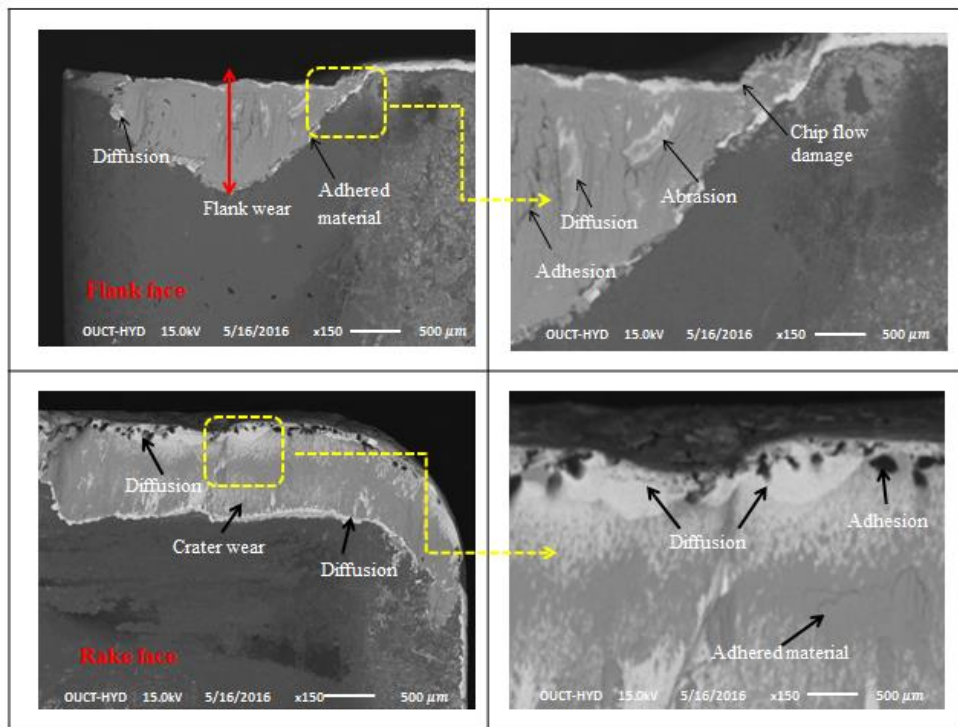


Fig. 5.11: SEM images of cutting tool in EHVSL machining condition at cutting speed 100 m/min

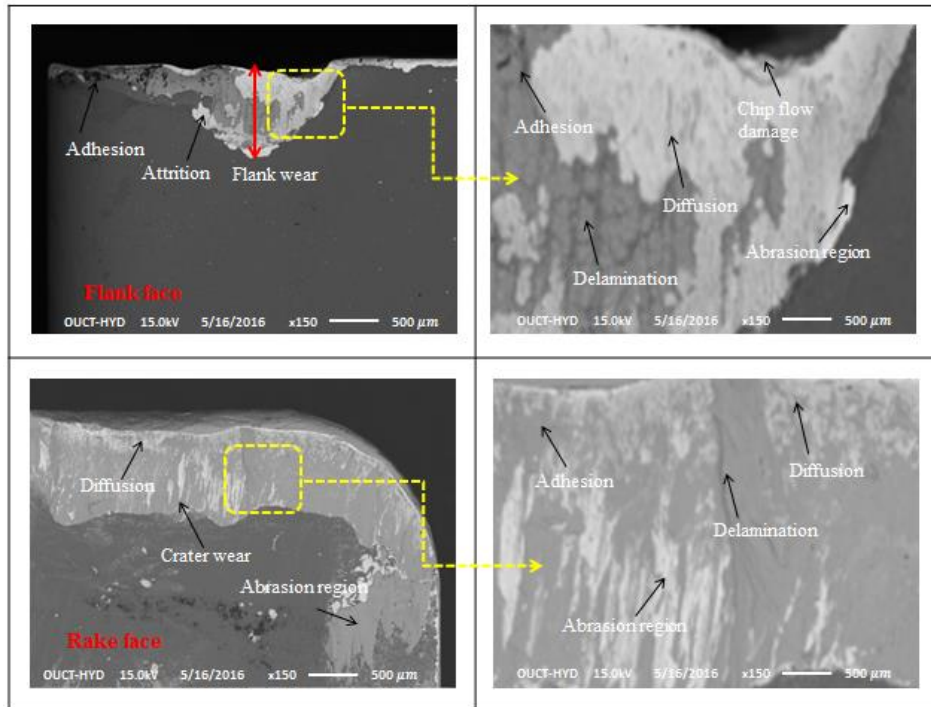


Fig. 5.12: SEM images of cutting tool in MQSL machining condition at cutting speed 100 m/min

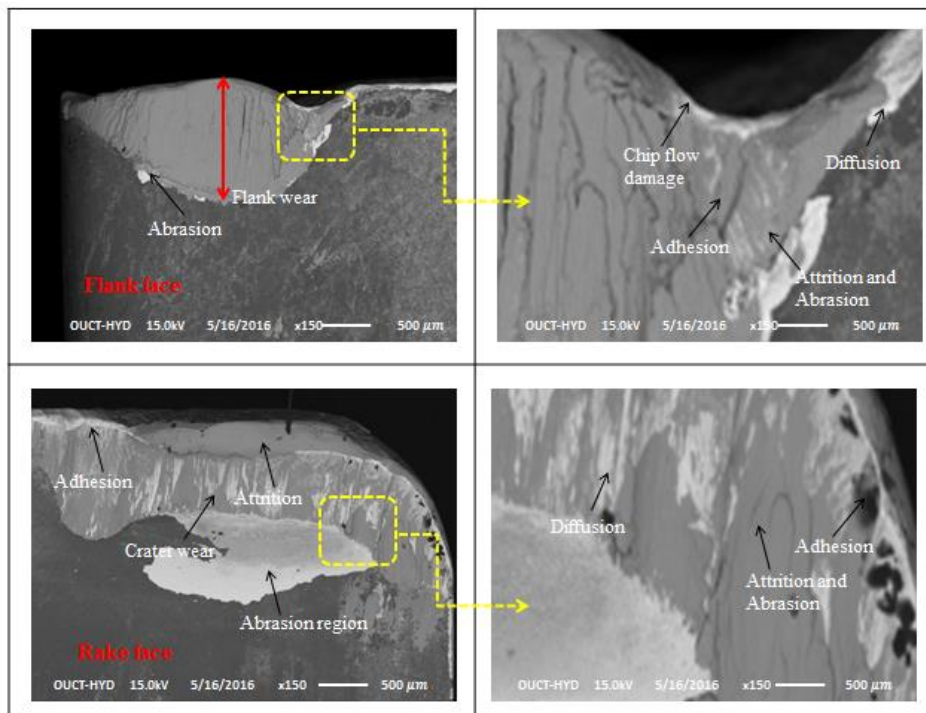


Fig. 5.13: SEM images of cutting tool in wet machining condition at cutting speed 100 m/min

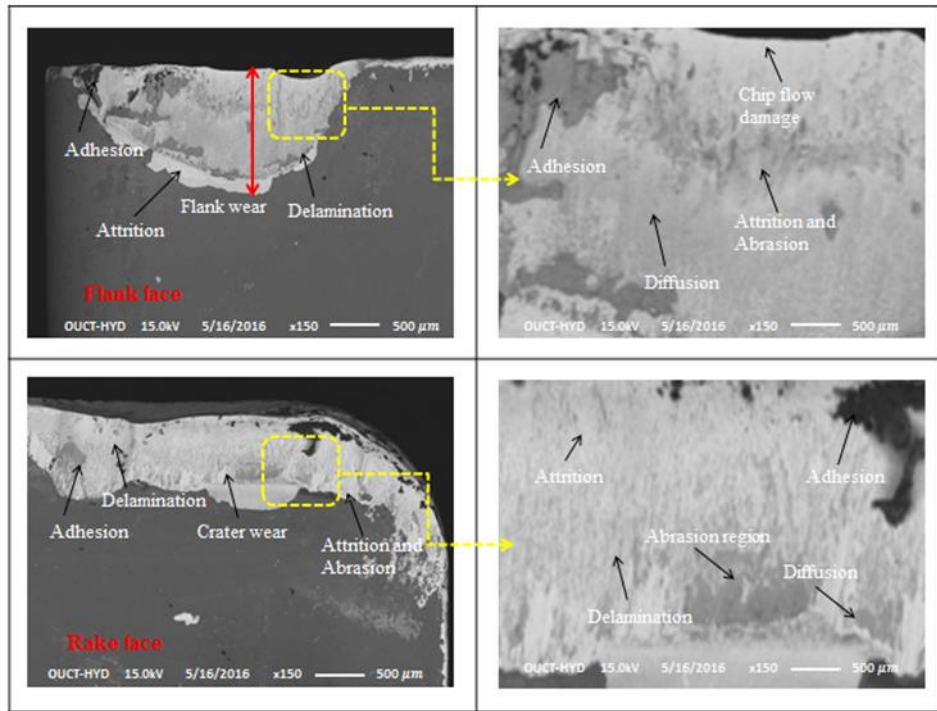


Fig. 5.14: SEM images of cutting tool in MQL machining condition at cutting speed 100 m/min

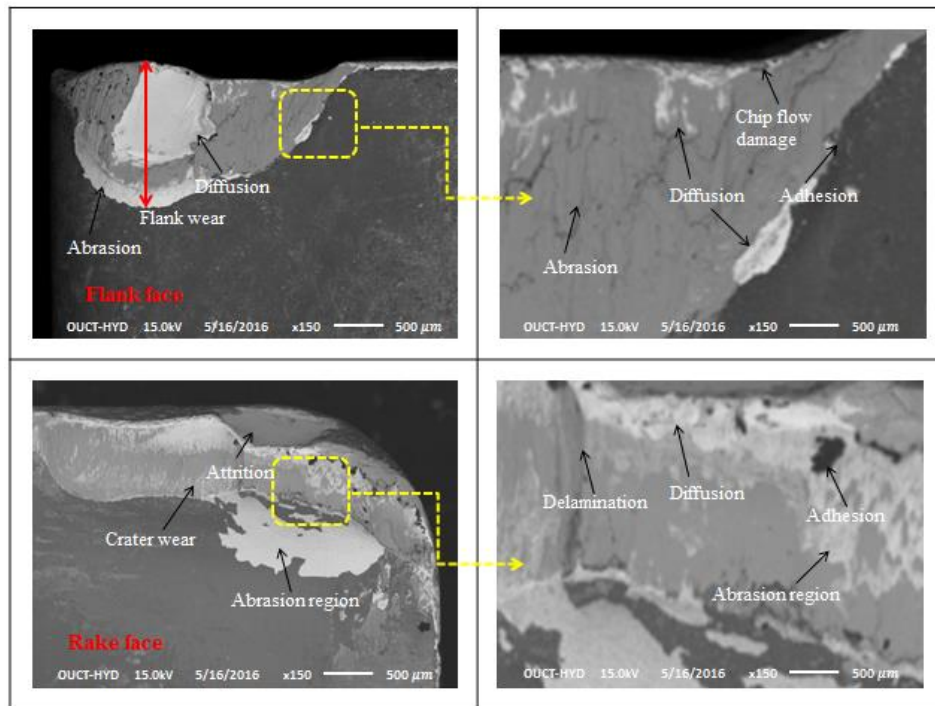


Fig. 5.15: SEM images of cutting tool in dry machining condition at cutting speed 100 m/min

5.2.4 Effect of chip thickness

The form of chip produced is a key factor in the cutting process as it significantly helps to estimate the heat generated and degree of deformation at tool-chip interface during turning process, which influences the quality of the workpiece surface and directly affects life of the cutting tool and eventually affecting the productivity. Chip thickness ratio (t_c/t) plays a crucial role in determining machinability of Ti-6Al-4V alloy, where 't_c' is stands for measured chip thickness and uncut chip thickness is denoted by 't'. Even minor changes can result in variations in surface finish, workpiece inaccuracy and reduced tool life during chip formation process. Moreover, to increase the productivity by improving the surface quality and tool life during machining of Ti-6Al-4V alloy, it is necessary to understand morphology of chip formation and its effect under dry and EHVSL machining conditions. The chips formed during the machining were collected at the completion of each experiment and their thickness was measured with the help of a tool maker's microscope. Fig. 5.16 shows the measured chip thickness at different speed and feed conditions. Experimental results suggest that reduction in friction at tool-workpiece interface is considerably high during EHVSL based machining when compared with dry machining condition. During EHVSL machining condition, chip thickness decreases due to temperature reduction at the tool-chip contact zone and the deterioration of tool rake angle by BUE formation and wear at the primary cutting edge is delayed is mainly because of reduction in coefficient of friction. At lower machining speed and feed rate, the chip thickness was found to be high. The plastic deformation zone becomes smaller when the cutting speed is increased. Chip thickness ratio was generally observed to be decreasing with increased cutting speed. Smaller contact regions and higher shear plane angles reduce the cutting forces [34].

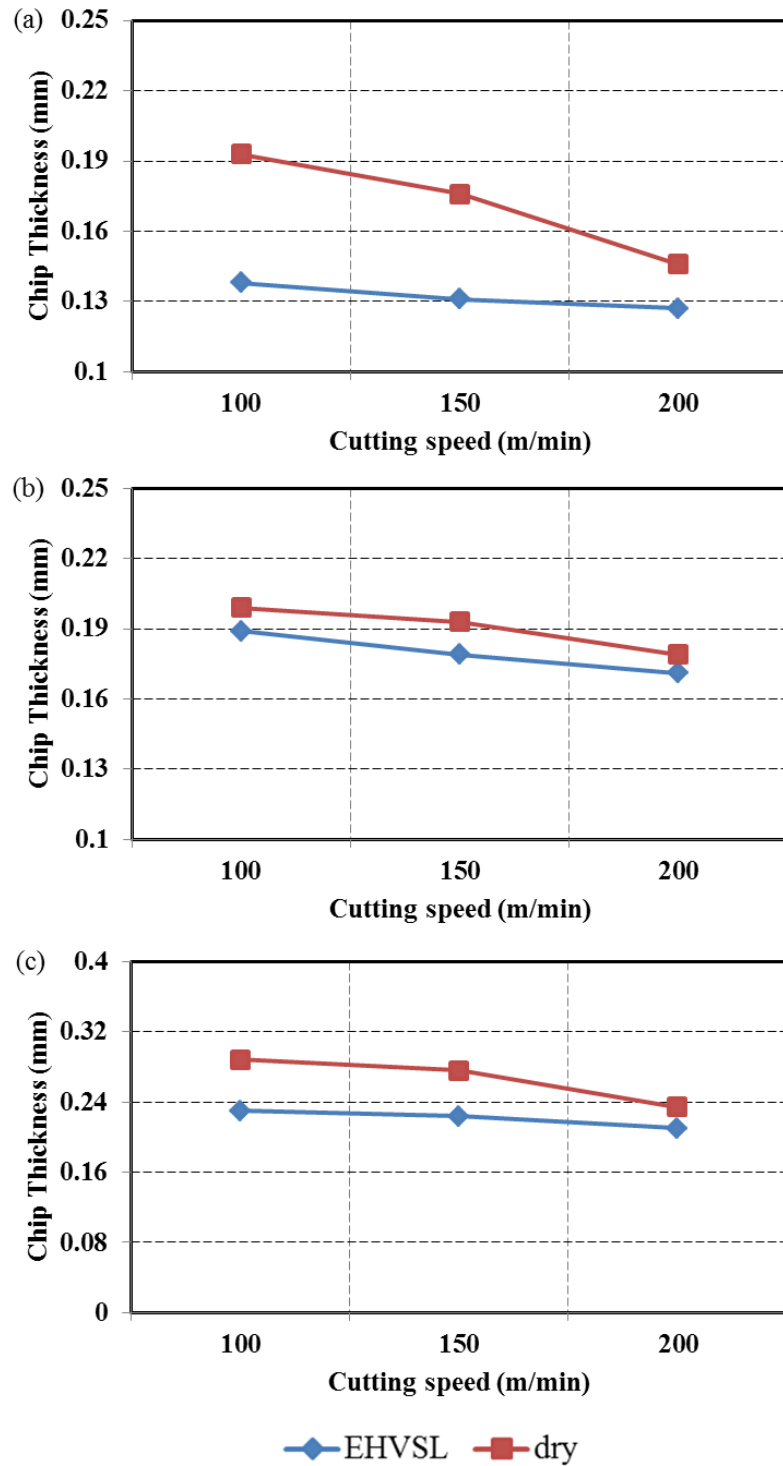


Fig. 5.16: Chip thickness at varying cutting speed = 100, 150, 200 m/min (a) Feed rate = 0.1 mm/rev, (b) Feed rate = 0.15 mm/rev, (c) Feed rate = 0.2 mm/rev under dry and EHVSL condition

It is clearly observed from Fig. 5.16 that at feed rate 0.1 mm/rev, there is a decrease in chip thickness as the cutting speed increases. This is due to the highly effective lubrication provided by EHVSL at high temperature zones. It was also observed that reduction in chip-thickness during EHVSL process causes lower cutting temperature and reduces the adhesion tendency between chip-tool-workpiece interface. Therefore, during high cutting speed condition small BUE with superior surface finish and chip thickness were found. Surface finish, cutting force variations and chip thickness ratio are affected beneficially using EHVSL when compared to MQSL, MQL, wet and dry machining.

5.3 Surface roughness estimation by Group Method of Data Handling (GMDH) technique for EHVSL machining condition

Turning is one of the most widely used and efficient means of machining materials at relatively high rate. Surface roughness in turning is an extremely complex phenomenon, influenced by a large number of variables, such as structural rigidity of the material, material properties of workpiece and cutting tool, cutting conditions, cutting temperature, lubricants used etc [152]. Surface finish is a common constraint that has to be considered in process improvement [148]. During process planning, it is very important to predict the machining conditions optimally to have good surface quality and to maintain dimensional accuracy of the workpiece. Productivity and part quality improvement in machining using modeling has been the important topic of research in the recent past. Apart from enhancing the economic utility of the machining, optimization helps to improve product quality to greater extents [153].

In recent years, the task to choose optimum cutting parameters to achieve minimum surface finish within the constraints of machining operations has become a

matter of high importance. A proper combination of cutting conditions must be selected to achieve better surface finish and MRR within shorter machining cycles [154]. Hence, to predict the surface roughness during cutting process, it is essential to model the same in an advanced manufacturing system.

It was observed from the literature review that one of the major problems encountered during regression analysis has been the necessity to clearly define and specify functional formulation [102-105]. The linear assumptions become invalid in all the considered cases and moreover, the occurrence of non-linearity in functional forms is infinite. The problem arises while estimating a dependent variable from measured variables. During such instances, though it is clear that few of the measured variables are to be considered, the way these variables are interrelated and their relative significance is unknown. In such cases, it is usually preferred to make use of the data to define the nature and parameter of the function [107-109]. This forms the motivation to develop newer self-organizing techniques in modeling like GMDH.

In 1966, Russian cyberneticist, A.G. Ivakhnenko introduced a technique called GMDH [19] for building an extremely complex higher-order regression polynomial. The idea of GMDH technique is to build an analytical function which would behave itself in such a way that the predicted value of the output would be as close as possible to its actual value. Over the years, it has found many applications in modeling and control, including some in the field of manufacturing. GMDH technique suits best for instructed and complex systems where the interest of the investigator solely lies in obtaining an input-output relationship of high order [107]. Moreover, this heuristic technique, unlike regression analysis, is not built on a solid foundation.

GMDH technique follows an approach where it uses a network like structure made of multiple layers to fit a higher degree polynomial. The typical GMDH network shown in Fig. 5.17 has four inputs and one output. Input is given to the network at the first layer. Nodes at the first hidden layer appropriately receive inputs X_1, X_2, X_3, X_4 distributed from the input layer. Individual nodes of each layer succeeding the initial input layer obtain two inputs which form the output for the nodes of the preceding layer sequence. Components that belong to input vector 'X' are first sent to the input units. These get appropriately distributed among the processing elements of the first hidden layer. The outputs obtained from these processing elements of the first hidden layer are input to the next consecutive layer, and so on. The output of the network obtained at the end is a single real number 'Y', where $Y=F(X)$. Each element of the GMDH network gives output in the form of a partial polynomial function of the two given inputs. All processing elements in k^{th} layer, except the initial layer have the below shown configuration (Fig. 5.18).

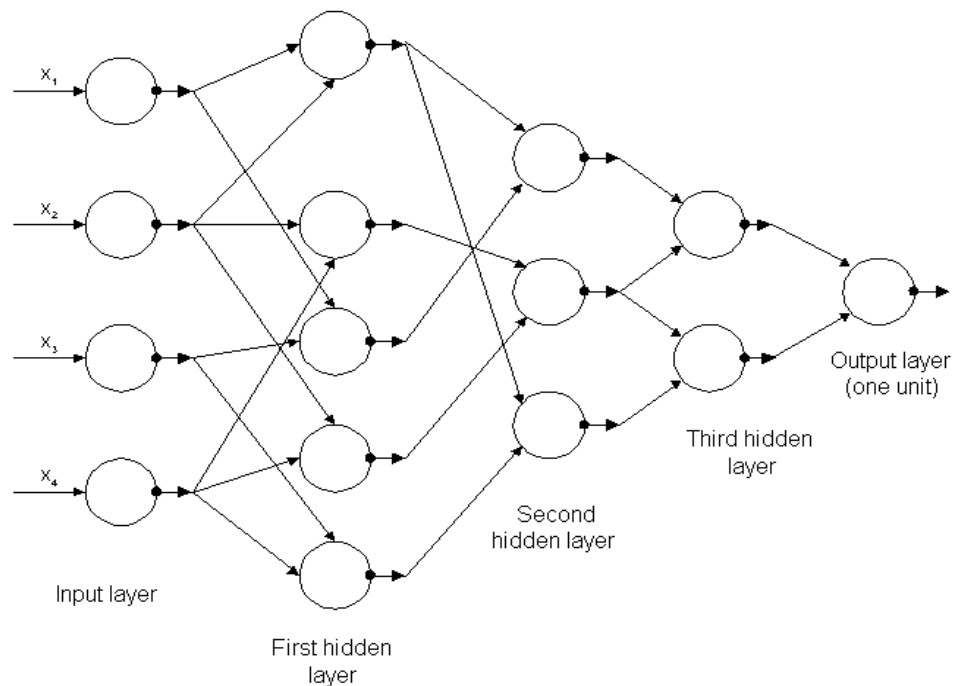


Fig. 5.17: Typical GMDH network

The output of the layer ‘k’ and processing element ‘m’ is given by a quadratic function. Training set data is used to determine the coefficients of the quadratic functions. All input combinations are taken twice at a time for evaluation. The self-organizing combinations allowed to pass to the next layer are terminated soon after an optimum level of complexity is attained by evaluating a criterion function chosen from the checking data set.

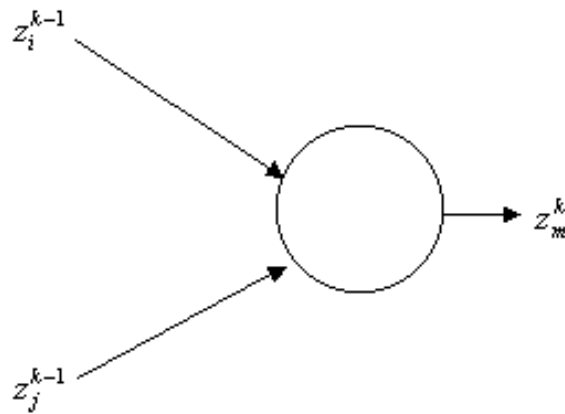


Fig. 5.18: GMDH network processing element ‘m’ of layer ‘k’

Different heuristic approaches used to assist the self-organization are presented below. Data having highest variance is input to the training set, the variance of i^{th} data point is given by,

$$D_i^2 = \sum_{j=1}^m (X_{ij} - X_j)^2 / \sigma_j^2 \text{-----}(5.1)$$

Where, D_i = measure of variance for i^{th} data point, σ_j = variance for j^{th} input variable, X_j = mean for j^{th} variable

$$\sigma_j^2 = (1/n) \sum_{i=1}^n (X_{ij} - X_j)^2 \text{-----}(5.2)$$

The algorithm is trained with the experimental data for GMDH network to learn the process. The experimental outcomes are divided into two separate sets; one being the training set, while the other being the testing set. The training set helps

GMDH to learn the process, while the testing set evaluates the performance of GMDH. By varying the proportion of data in the training set with different models can be created out of which best model can be selected, viz., 50%, 62.5% and 75%. The best model is considered from the given data percentages. Usually, variables considered for each layer may be taken as fixed number or a number that increases constantly. It is generally assigned with factorial increment in number of free variables existing in the previous level. For estimation, there are three different criterion functions can be considered mainly root mean square (RMS) or regularity criteria, unbiased criteria and combined criteria. For proper modeling, it is very important to choose the node selection criterion. Criterion function is one of the key features of GMDH which describes the model structure and the neurons which are allowed to proceed to the next layer. Regularity criterion is given by the equation

$$r_j^2 = \frac{\sum_{i=nt+1}^n (Y_i - Z_{ij})^2}{\sum_{i=nt+1}^n Y_i^2} \quad j = 1, 2, \dots, m(m-1)/2 \text{-----} (5.3)$$

The Unbiased criteria is given by

$$u_j^2 = \frac{\sum_{i=1}^n (Y_i - Z_{ij})^2}{\sum_{i=1}^n Y_i^2} \quad j = 1, 2, \dots, m(m-1)/2 \text{-----} (5.4)$$

Where Z_{ij} refers to the estimate of the i^{th} dependent variable using j^{th} equation. A combined criterion includes both unbiased and regularity criteria. Combined criteria is given by

$$C_j^2 = r_j^2 + u_j^2 \text{-----} (5.5)$$

In the present work all the three criterion functions have been taken for surface roughness estimation, with 50%, 62.5% and 75% of experimentation data in the training set. Attempts are made to identify the best available criterion and data

percentage in the training set for estimating surface roughness optimally based on different cutting conditions. Table 5.1 shows the machining performance of Ti-6Al-4V alloy under different cutting parameters. Input data used for GMDH surface roughness modeling for different machining conditions is shown in Fig. 5.19.

Table 5.1: Machining performance of Ti-6Al-4V alloy under different cutting parameters

Sl No	Cutting speed (v_c) (m/min)	Feed (f) (mm/rev)	Depth of cut (a_p) (mm)	Measured Surface roughness (R_a) (μm)
1	100	0.1	0.5	1.084
2	150	0.1	0.5	1.184
3	200	0.1	0.5	1.341
4	100	0.15	0.5	1.126
5	150	0.15	0.5	1.230
6	200	0.15	0.5	1.593
7	100	0.2	0.5	1.117
8	150	0.2	0.5	1.393
9	200	0.2	0.5	1.587
10	100	0.1	1	0.793
11	150	0.1	1	0.919
12	200	0.1	1	1.022
13	100	0.15	1	0.887
14	150	0.15	1	0.970
15	200	0.15	1	1.222
16	100	0.2	1	0.998
17	150	0.2	1	1.153
18	200	0.2	1	1.295
19	100	0.1	1.5	0.743
20	150	0.1	1.5	0.807
21	200	0.1	1.5	0.898
22	100	0.15	1.5	0.778
23	150	0.15	1.5	0.826
24	200	0.15	1.5	1.039
25	100	0.2	1.5	0.803
26	150	0.2	1.5	0.870
27	200	0.2	1.5	1.095

5.4 Comparison of predicted and measured surface roughness using GMDH

The estimated surface roughness results are presented in this section using GMDH. In designating the GMDH model, it is essential to determine the number of output and input layers. There is no theory that can be used to guide the selection of number of input nodes and the level of output estimation. The selection of the number of input nodes corresponds to the number of variables. The three criterion functions, for machining performances viz., regularity, unbiased and combined were tried out. All the three criterion functions can be used for prediction and the best criterion function can be selected. In the current study, 50% of the experimental data was considered for the number of data in the training set which was varied in steps of 12.5% up to 75%. Hence 50%, 62.5% and 75% of experimental data was considered in the training set. Input data for used GMDH surface roughness modelling for different cutting condition is shown in Fig. 5.19 (v_c , f , a_p , R_a). Fig. 5.19-5.22 shows the estimated surface roughness by GMDH for different data percentages.

```

Description about GMDH
03,27,14,0,0.0,1
3- NUMBER OF INDEPENDENT VARIABLES
27-NUMBER OF SETS
14- TRAINING SAMPLES TO BE TAKEN
0.0- NUMBER OF LEVELS
1- TYPE OF CRITERIA
(1 - REGULARITY, 2 - UNBIASED, 3 - COMBINED)
IN NUMBER OF LEVELS 0 FOR AUTOMATIC
*****
This is full factorial hard turning data for surface
roughness experimental results with cutting conditions
in the checking set
*****
03      27      14|      0      0.0      1
1.0837,100,0.1,0.5
1.1836,150,0.1,0.5
1.3406,200,0.1,0.5
1.1256,100,0.15,0.5
1.2304,150,0.15,0.5
1.5930,200,0.15,0.5
1.1170,100,0.2,0.5
1.3933,150,0.2,0.5
1.5865,200,0.2,0.5
0.7929,100,0.1,1
0.9193,150,0.1,1
1.0223,200,0.1,1
0.8869,100,0.15,1
0.9703,150,0.15,1
1.2215,200,0.15,1
0.9976,100,0.2,1
1.1533,150,0.2,1
1.2950,200,0.2,1
0.7434,100,0.1,1.5
0.8073,150,0.1,1.5
0.8980,200,0.1,1.5
0.7784,100,0.15,1.5
0.8255,150,0.15,1.5
1.0388,200,0.15,1.5
0.8033,100,0.2,1.5
0.8699,150,0.2,1.5
1.0951,200,0.2,1.5

```

Fig. 5.19: Input data for GMDH surface roughness model (R_a , v_c , f , a_p)

GMDH CONVERTED AFTER 1 GENERATION(S)				
MULTIPLE CORRELATION (SUMMED OVER TRAINING SET)= .85				
CASE NO.	OBSERVED VALUE	ESTIMATE	ERROR	PERCENT ERROR
1	.10837000E+01	.11208740E+01	-.37174340E-01	-.34303170E+01
2	.13406210E+01	.14741990E+01	-.13357760E+00	-.99638590E+01
3	.74343900E+00	.77632160E+00	-.32882570E-01	-.44230360E+01
4	.89802400E+00	.98956500E+00	-.91540930E-01	-.10193590E+02
5	.11170000E+01	.11208740E+01	-.38743020E-02	-.34684890E+00
6	.80339000E+00	.77632160E+00	.27068440E-01	.33692770E+01
7	.15865990E+01	.14741990E+01	.11240040E+00	.70843620E+01
8	.10951770E+01	.98956500E+00	.10561210E+00	.96433810E+01
9	.79298100E+00	.87186870E+00	-.78887640E-01	-.99482380E+01
10	.10223410E+01	.11551520E+01	-.13281140E+00	-.12990910E+02
11	.99761900E+00	.87186870E+00	.12575030E+00	.12605040E+02
12	.12950680E+01	.11551520E+01	.13991560E+00	.10803730E+02
13	.11836590E+01	.12573900E+01	-.73731300E-01	-.62291000E+01
14	.80735900E+00	.84279710E+00	-.35438120E-01	-.43893880E+01
15	.13933580E+01	.12573900E+01	.13596770E+00	.97582770E+01
16	.86998500E+00	.84279710E+00	.27187880E-01	.31250980E+01
17	.91937200E+00	.97336430E+00	-.53992270E-01	-.58727340E+01
18	.11533100E+01	.97336430E+00	.17994560E+00	.15602540E+02
19	.77840900E+00	.77632160E+00	.20874140E-02	.26816420E+00
20	.11256160E+01	.11208740E+01	.47416690E-02	.42125100E+00
21	.10388620E+01	.98956500E+00	.49297030E-01	.47452920E+01
22	.15930850E+01	.14741990E+01	.11888650E+00	.74626570E+01
23	.12215810E+01	.11551520E+01	.66428540E-01	.54379150E+01
24	.88696400E+00	.87186870E+00	.15095350E-01	.17019130E+01
25	.12304900E+01	.12573900E+01	-.26900290E-01	-.21861450E+01
26	.82550000E+00	.84279710E+00	-.17297090E-01	-.20953470E+01
27	.97032700E+00	.97336430E+00	-.30372740E-02	-.31301550E+00

MAXIMUM ERROR = .1799
STANDARD ERROR = .0164

Fig. 5.20: Regularity criteria output obtained while modeling surface roughness at 75% of data

GMDH CONVERTED AFTER 1 GENERATION(S)				
MULTIPLE CORRELATION (SUMMED OVER TRAINING SET)= .85				
CASE NO.	OBSERVED VALUE	ESTIMATE	ERROR	PERCENT ERROR
1	.10837000E+01	.11032450E+01	-.19545080E-01	-.18035510E+01
2	.13406210E+01	.14565690E+01	-.11594830E+00	-.86488510E+01
3	.74343900E+00	.78044920E+00	-.37010130E-01	-.49782340E+01
4	.89802400E+00	.99369220E+00	-.95668200E-01	-.10653190E+02
5	.11170000E+01	.11032450E+01	.13754960E-01	.12314200E+01
6	.80339000E+00	.78044920E+00	.22940870E-01	.28555090E+01
7	.15865990E+01	.14565690E+01	.13002970E+00	.81954980E+01
8	.10951770E+01	.99369220E+00	.10148480E+00	.92665230E+01
9	.79298100E+00	.88536980E+00	-.92388750E-01	-.11650820E+02
10	.10223410E+01	.11686530E+01	-.14631250E+00	-.14311510E+02
11	.99761900E+00	.88536980E+00	.11224920E+00	.11251710E+02
12	.12950680E+01	.11686530E+01	.12641450E+00	.97612280E+01
13	.11836590E+01	.11919270E+01	-.82678790E-02	-.69850180E+00
14	.80735900E+00	.79909030E+00	.82686540E-02	.10241610E+01
15	.13933580E+01	.11919270E+01	.20143120E+00	.14456530E+02
16	.86998500E+00	.79909030E+00	.70894660E-01	.81489520E+01
17	.91937200E+00	.93903130E+00	-.19659280E-01	-.21383380E+01
18	.11533100E+01	.93903130E+00	.21427860E+00	.18579450E+02
19	.77840900E+00	.78044920E+00	-.20401480E-02	-.26209200E+00
20	.11256160E+01	.11032450E+01	.22370930E-01	.19874390E+01
21	.10388620E+01	.99369220E+00	.45169770E-01	.43480050E+01
22	.15930850E+01	.14565690E+01	.13651570E+00	.85692680E+01
23	.12215810E+01	.11686530E+01	.52927490E-01	.43327050E+01
24	.88696400E+00	.88536980E+00	.15942450E-02	.17974180E+00
25	.12304900E+01	.11919270E+01	.38563130E-01	.31339650E+01
26	.82550000E+00	.79909030E+00	.26409690E-01	.31992350E+01
27	.97032700E+00	.93903130E+00	.31295720E-01	.32252750E+01

MAXIMUM ERROR = .2143
STANDARD ERROR = .0178

Fig. 5.21: Unbiased criteria output obtained while modeling surface roughness at 75% of data

GMDH CONVERTED AFTER 1 GENERATION(S)				
MULTIPLE CORRELATION (SUMMED OVER TRAINING SET)= .85				
CASE NO.	OBSERVED VALUE	ESTIMATE	ERROR	PERCENT ERROR
1	.10837000E+01	.11032450E+01	-.19545080E-01	-.18035510E+01
2	.13406210E+01	.14565690E+01	-.11594830E+00	-.86488510E+01
3	.74343900E+00	.78044920E+00	-.37010130E-01	-.49782340E+01
4	.89802400E+00	.99369220E+00	-.95668200E-01	-.10653190E+02
5	.11170000E+01	.11032450E+01	.13754960E-01	.12314200E+01
6	.80339000E+00	.78044920E+00	.22940870E-01	.28555090E+01
7	.15865990E+01	.14565690E+01	.13002970E+00	.81954980E+01
8	.10951770E+01	.99369220E+00	.10148480E+00	.92665230E+01
9	.79298100E+00	.88536980E+00	-.92388750E-01	-.11650820E+02
10	.10223410E+01	.11686530E+01	-.14631250E+00	-.14311510E+02
11	.99761900E+00	.88536980E+00	.11224920E+00	.11251710E+02
12	.12950680E+01	.11686530E+01	.12641450E+00	.97612280E+01
13	.11836590E+01	.11919270E+01	-.82678790E-02	-.69850180E+00
14	.80735900E+00	.79909030E+00	.82686540E-02	.10241610E+01
15	.13933580E+01	.11919270E+01	.20143120E+00	.14456530E+02
16	.86998500E+00	.79909030E+00	.70894660E-01	.81489520E+01
17	.91937200E+00	.93903130E+00	-.19659280E-01	-.21383380E+01
18	.11533100E+01	.93903130E+00	.21427860E+00	.18579450E+02
19	.77840900E+00	.78044920E+00	-.20401480E-02	-.26209200E+00
20	.11256160E+01	.11032450E+01	.22370930E-01	.19874390E+01
21	.10388620E+01	.99369220E+00	.45169770E-01	.43480050E+01
22	.15930850E+01	.14565690E+01	.13651570E+00	.85692680E+01
23	.12215810E+01	.11686530E+01	.52927490E-01	.43327050E+01
24	.88696400E+00	.88536980E+00	.15942450E-02	.17974180E+00
25	.12304900E+01	.11919270E+01	.38563130E-01	.31339650E+01
26	.82550000E+00	.79909030E+00	.26409690E-01	.31992350E+01
27	.97032700E+00	.93903130E+00	.31295720E-01	.32252750E+01

MAXIMUM ERROR = .2143
STANDARD ERROR = .0171

Fig. 5.22: Combined criteria output obtained while modeling surface roughness at 75% of data

The results obtained from GMDH network for various machining conditions were presented and discussed. Theoretical estimation of machining performances was carried out for Ti-6Al-4V alloy material using various machining conditions by GMDH technique and this estimation was carried out with single level and the least error of approximation and best-fit will be found at each level. Fig. 5.19-5.22 shows the estimated surface roughness by GMDH for Ti-6Al-4V alloy material for 75% of data set level for regularity, unbiased and combines criterion method. From Table 5.2, it was perceived that the surface roughness estimate obtained by regularity, unbiased and combined criterion correlates well with the evaluated surface roughness. An attempt was made to discover the preferable level of estimation. Recognizing of the best criterion, best percentage of data and the optimal level of estimation was based on the value of standard error of estimation. The independent variables considered for

the estimation were used as the input to the GMDH algorithm, which estimates surface roughness as a polynomial function of the supplied input.

Table 5.2: Measured and predicted surface roughness estimation for different criteria using GMDH for Ti-6Al-4V alloy

SI No	Measured Surface roughness (R_a) (μm)	Prediction of Surface roughness (R_a) data for different criteria		
		Regularity	Unbiased	Combined
1	1.084	1.107	1.087	1.088
2	1.184	1.141	1.177	1.177
3	1.341	1.313	1.316	1.396
4	1.126	1.057	1.125	1.087
5	1.230	1.258	1.170	1.118
6	1.593	1.582	1.582	1.647
7	1.117	0.976	1.065	1.067
8	1.393	1.373	1.359	1.526
9	1.587	1.593	1.572	1.566
10	0.793	0.800	0.809	0.817
11	0.919	1.062	0.932	0.909
12	1.022	1.002	1.063	1.134
13	0.887	0.873	0.893	0.862
14	0.970	0.892	0.990	0.967
15	1.222	1.078	1.121	1.179
16	0.998	1.071	0.982	0.984
17	1.153	1.112	1.157	1.158
18	1.295	1.268	1.272	1.348
19	0.743	0.760	0.707	0.676
20	0.807	0.706	0.769	0.771
21	0.898	0.902	0.890	0.886
22	0.778	0.899	0.789	0.769
23	0.826	0.813	0.831	0.802
24	1.039	0.917	0.953	1.003
25	0.803	0.810	0.835	0.827
26	0.870	0.856	0.876	0.845
27	1.095	1.119	1.099	1.092

Fig. 5.23 shows GMDH estimation of surface roughness from regularity criteria, for various percentages of data in the training set. At 75% of data, least error and best-fit was observed in the training set and least surface roughness error found

was $164 \mu\text{m}$ in training set at level auto level. Fig. 5.23 (a) shows GMDH estimation of surface roughness from various criteria for training set data of 50%.

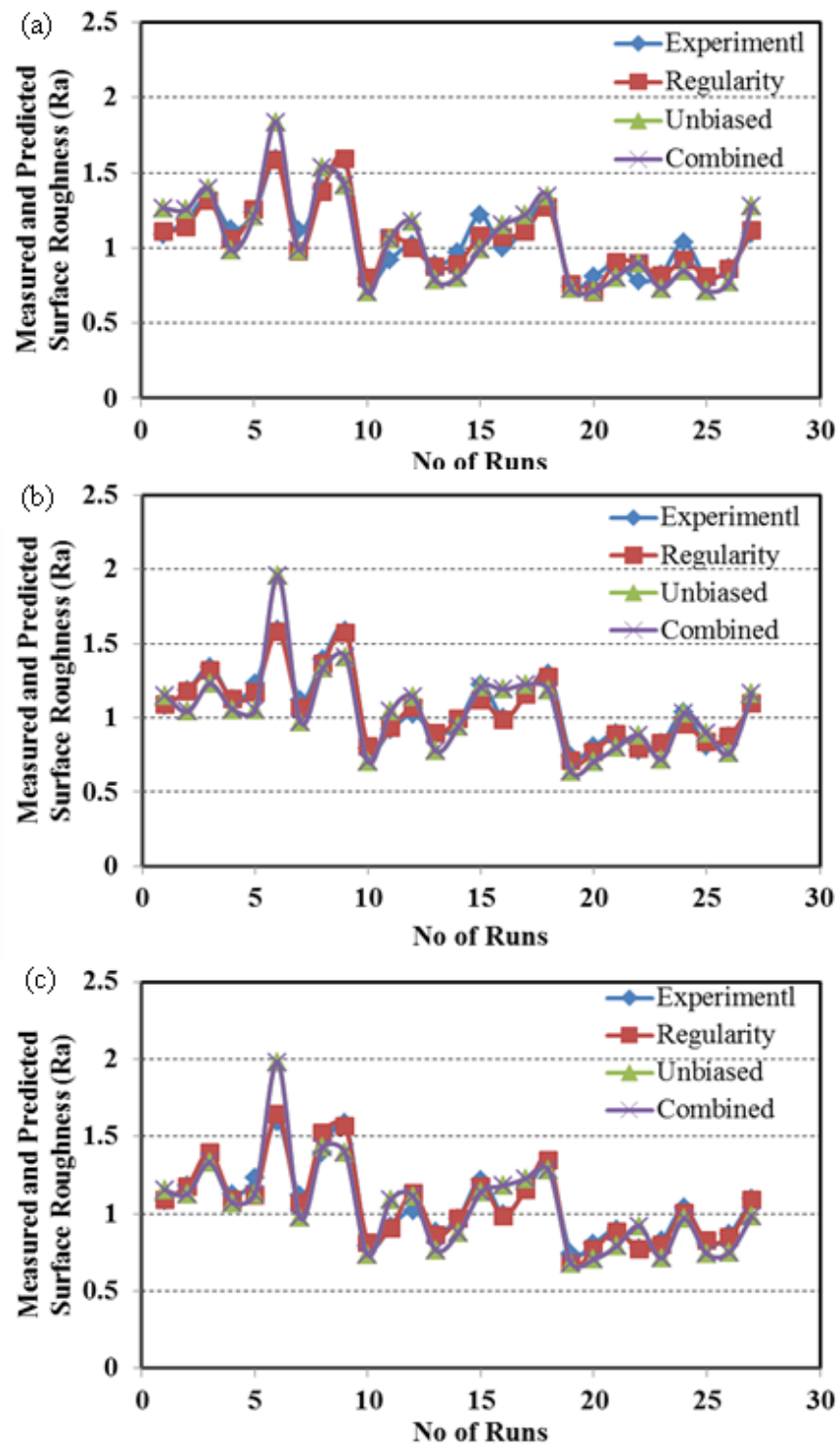
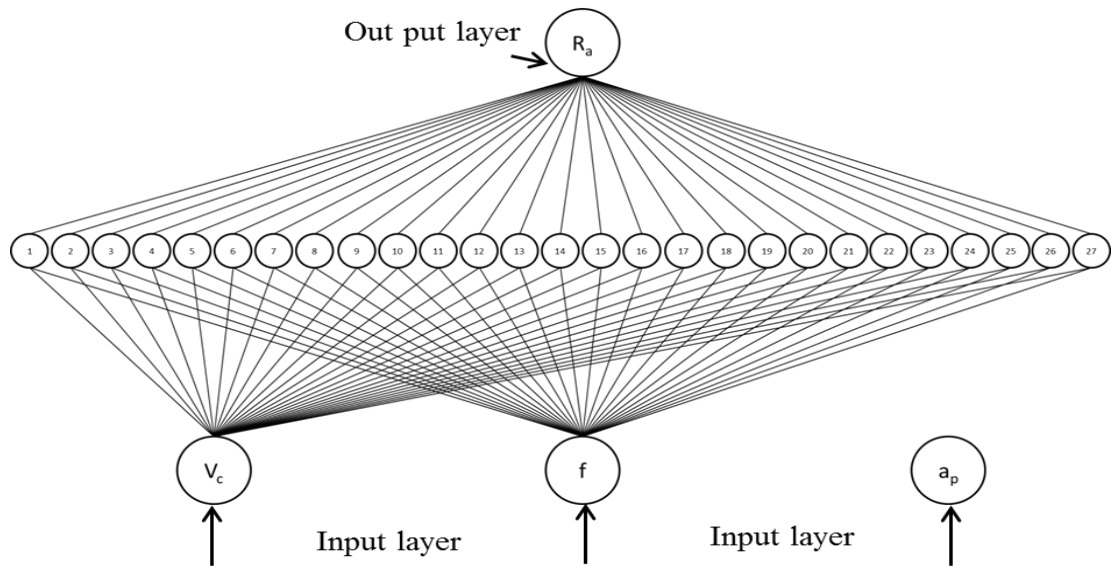


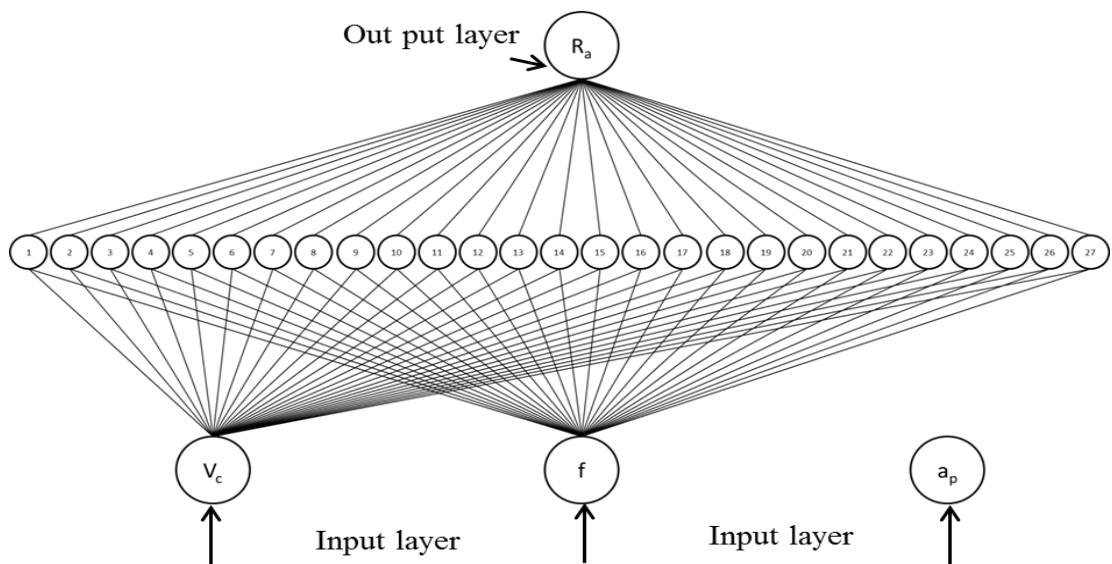
Fig. 5.23: Comparison of measured and predicted surface roughness at (a) 50%, (b) 62.5% and (c) 75% of experimental data in training set

It is clearly observed that the surface roughness estimation acquired by regularity criterion correlates well with the measured surface roughness when compared to unbiased and combined criteria. Fig. 5.23 shows GMDH estimation of surface roughness from regularity criteria for various percentages of data in the training set. At 75% of data least error and best-fit was observed in the training set. The least surface roughness error is $0.0164 \mu m$ for 75% of data in training set level in regularity criteria. Next least surface roughness standard error was observed in combined criteria ($0.0171 \mu m$). Due to the estimation of coefficient of the output quadratic functions is determined from the training set, it was perceived from the Fig. 5.23 that with the increase in the percentage of data in the training set, the estimation power of criterion also increases [107]. The self-organizing GMDH algorithm helps to learn the process better and make better estimation due to more number of experimental data in the training set [106]. From the study, it was observed that, with the increase in the percentage of data, minimum surface roughness values occurred at higher levels. For 50% of data in the training set, maximum surface roughness occurred at lower levels and 62.5% and 75% of data in training minimum surface roughness occurred at higher levels. Fig. 5.24-5.26 shows the diagrammatic representations of tree structure for estimation of surface roughness by regularity (Fig. 5.24), unbiased (Fig. 5.25) and combined (Fig. 5.26) criteria. The variables that enter into the final equation and the interactions among the variables can be clearly seen from the Fig. 5.24-5.26. It can be clearly observed from Fig. 5.24 and 5.25 that cutting speed and feed rate is having more effect followed by depth of cut. Compare to regularity and unbiased criteria there is no much effect on depth of cut. It is also clearly observed from Fig. 5.26, feed rate and depth of cut is having more effect than cutting speed.



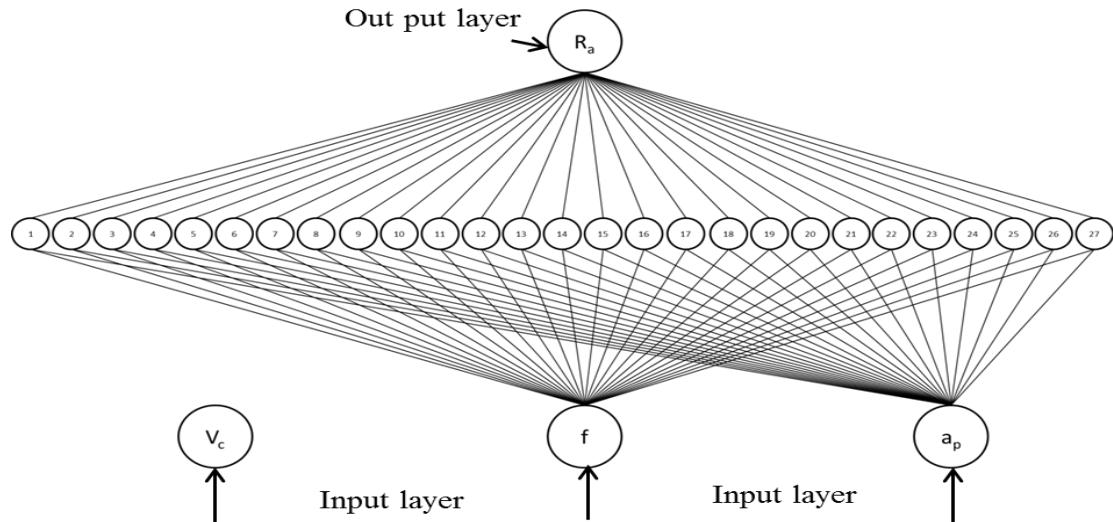
V_c = Cutting speed, f = Feed rate, a_p = depth of cut, R_a = Measured surface roughness

Fig. 5.24: Regularity criterion model for estimation of surface roughness at 75% data in the training set at different speed, feed depth of cut conditions



V_c = Cutting speed, f = Feed rate, a_p = depth of cut, R_a = Measured surface roughness

Fig. 5.25: Unbiased criterion model for estimation of surface roughness at 75% data in the training set at different speed, feed depth of cut conditions



V_c = Cutting speed, f = Feed rate, a_p = depth of cut, R_a = Measured surface roughness

Fig. 5.26: Combined criterion model for estimation of surface roughness at 75% data in the training set at different speed, feed depth of cut conditions

From the above results, it can be inferred that, with increase in the percentage of data in training set, the level of estimation in achieving improved surface roughness. This is because at higher levels, more combinations of inputs are used for estimation. Hence, estimation by GMDH depends on the combination of variables that the model selects and on the level at which it predicts. Based on the present work, it can be concluded that the regularity criterion functions well for the set of input variables for steady-state cutting conditions. The estimation ability of GMDH was better at higher cutting conditions than at lower cutting conditions, as the standard errors at higher conditions are very less. This implies that the data handling capability of this estimation method is high.

5.5 Summary

The current research work influences the novel methodology in developing EHVSLS assisted machining process to apply lubricants effectively to the machining

zone with a goal to improve the performance of machining process during turning of Ti-6Al-4V alloy. An outstanding outcome of the present research work is that the solid lubricants with low particle size and constant flow rate using electrostatic technique provides better performance compared to the existing machining techniques. The improved machinability by reducing friction at tool-workpiece interface results in better MRR without affecting the quality of the surface produced. Therefore, the present methodology appears to offer considerable benefits over other methods of machining Ti-6Al-4V alloy. This work also emphasizes that proper selection of solid lubricant is essential for making it an interesting alternative to eliminate cutting fluids in metal cutting and hence making the machining environmental friendly. The results obtained highlighted that it was essential to apply lubricants selectively to the machining zone with considered environmental requirements towards finding out an improved method for specific hard turning of Ti-6Al-4V alloy. As a result, it was shown that with the selected machining parameters and cooling/lubricant conditions, chip breakability is improved. The carried research work clearly demonstrates the cost effectiveness by abandonment of the cutting fluid and also at the same time improving economic, environmental and social performance with solid lubricants in the context of increasing industrialization. In the present study, also is introduced a GMDH method for modeling surface roughness as a function of the input parameters of cutting speed, feed rate and depth of cut. The GMDH algorithm provides an easy procedure of automatically and accurately modeling complex systems. To have a better understanding of cutting process, finite element modeling and simulation of orthogonal metal cutting process for Ti-6Al-4V alloy is developed and presented in chapter 6.

CHAPTER 6

FINITE ELEMENT MODELING AND SIMULATION OF MACHINING TI-6AL-4V ALLOY

The previous chapter presents experimental tests to understand the physical cutting process variables, such as, cutting force, surface roughness, tool wear etc., during machining of Ti-6Al-4V alloy under different environmental conditions. FE simulation of orthogonal metal cutting process of Ti-6Al-4V alloy is presented in this chapter. FEA have become widely used in research and industrial applications because of the advancements in computational techniques through machining simulation that significantly reduce the time-to-market and thus increase competitiveness. This chapter attempts to propose a J-C (Johnson-Cook) model with energy-based failure simulation method, developed using finite element method to predict cutting force and chip thickness during orthogonal turning of Ti-6Al-4V alloy. Use of finite element tool is aimed at giving a better understanding of cutting process presented in chapter 5 to see the accuracy of machining results, and to have a comparison of numerical predictions with experimental findings.

6.1 Introduction

The impetus in prognostic process engineering of machining process using FEM tool is due to its science-based approach in comprehending the physical cutting process variables. Finite element method provides an insight for further understanding of machining process, through predictive capability of machining parameters such as cutting force, cutting temperature and chip formation, etc. Further, application of FE tool in metal cutting simulation has great importance in predicting results that are

experimentally very difficult to be evaluated. Success and reliability of FE machining model are heavily dependent on accurate selection of material constitutive relation, friction parameters between the cutting tool and workmaterial contact, and simulation settings during FE modeling of machining process [157].

During machining of Ti-6Al-4V alloy, cutting edges wear rapidly because of poor thermal conductivity of titanium alloy and high chemical reactivity, results in higher temperature, and strong adhesion between the tool and workpiece. Chip segmentation by shear localization is an important characteristic which can be observed in a certain range of cutting speed during machining of titanium alloy. Also, it was observed that, chip separation by shear localization in certain range of cutting speed conditions [158]. Shivpuri et al. [159] observed that Ti-6Al-4V segmentation is produced by crack initiation and propagation in the primary shear zone by FE simulation results. In FE simulation process with change in input parameters like, workpiece and tool geometry, friction coefficient, constitutive equation, environment etc., for a particular simulation model can significantly affect the accuracy of prediction [158]. Wang et al. [135] studied the FE simulation using Oxley's predictive machining theory of Ti-6Al-4V alloy with different coolant supply strategy. Limited studies have been conducted on effect of point of cooling and lubrication orthogonal machining of Ti-6Al-4V alloy.

Cooling and lubrication methods during machining difficult-to-cut materials like Ti-6Al-4V alloys have a significant effect of frictional heat generation [110]. Numerous cutting force models have been developed to predict the cutting parameters on chip formation and are studied by using different FEM simulation parameters [112-116]. Many researchers have focused predominantly on dry machining condition, although lubricants are widely used in the machining process especially for

the difficult-to-cut materials for improving product quality and productivity. Metal cutting process involves high temperatures and strain rates, which make Johnson-Cook [115] material model the preferred material model that can simulate these exceptional conditions. It has been noticed that there are many parameters that could affect the resulting forces in metal cutting process, such as the workpiece material, tool geometry, feed rates, and cutting speeds and many other factors. The resulting force per unit area is called the cutting coefficients. Determining friction parameters at the tool-chip interface is one of the main problem in FE simulation of machining. The presence of coolant makes it extremely difficult to determine the friction coefficient at chip-tool interface. Some researchers used empirical models to estimate cutting coefficients [135]; while others used analytical models [3]. Many approaches have been used to predict the relation between these parameters and the resulting cutting coefficients.

Guang et al. [157] studied a series of FE simulations of high speed machining of Ti-6AL-4V alloy based on ductile failure criteria is carried out to compare the test results with chip morphology and cutting force. The results observed that the chip morphology and cutting force showed good agreement with the experiments results, results proving that the ductile failure criteria is suitable for titanium alloy in extremely high speed machining conditions. In addition, it was observed that FEM results under varying cutting conditions which shows good agreement with experimental results are proposed by modifying FE model such as critical failure criteria parameter. Therefore, a method which can be used to accurately simulate one kind of material at different cutting conditions needs to be developed.

In this chapter, the main focus of the present work is to study the effect of lubricant supply method on the cutting force and chip thickness. A FE analysis of

orthogonal machining of Ti-6Al-4V alloy is carried out using commercial FEA ABAQUS/Explicit software. In this study, J-C material model with energy-based failure criteria is used for FE simulation of Ti-6Al-4V alloy. During the simulation process, in order to predict experimental results, failure-energy parameter has been modified in first simulation condition, after that, the FE model is applied to other cutting conditions based on same energy-failure parameter.

6.2 Finite element model of orthogonal machining process

The present work outlines the development of 2D finite element model for orthogonal machining of Ti-6Al-4V alloy using commercial FEA ABAQUS/Explicit software. The FE model is composed of cutting tool and workpiece. To study the behaviour of Ti-6Al-4V alloy during the orthogonal machining process, Johnson-Cook's constitutive equation with a set of material constants is applied in the FE simulation process.

6.2.1 Modeling of workpiece and cutting tool materials

The research work deals with the FE simulation of the orthogonal machining of Ti-6Al-4V alloy workpiece material using a tungsten carbide cutting tool. In the present study, FE simulations are carried out by considering Ti-6Al-4V alloy and the obtained results are validated with the experimentally measured (Chapter 5) cutting force and chip thickness. A few preliminary simulations were performed in order to select the appropriate set of material constants. The Johnson-Cook model [120] is employed in this study to describe the flow stress properties of Ti-6Al-4V alloy workpiece material. The input requirements of the FEM simulation are shown in Fig 6.1. The thermal and mechanical properties of the workpiece and cutting tool used in the FEM simulation are listed in Table 6.1.

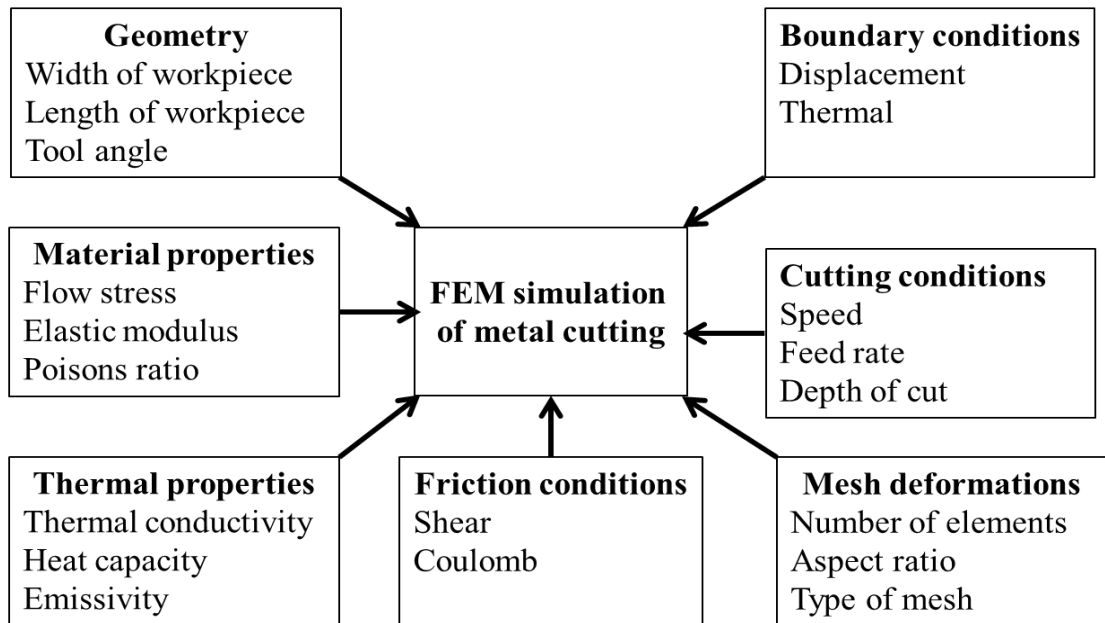


Fig. 6.1: Input requirements for the FE model

Table 6.1: Thermal and mechanical properties of workpiece and cutting tool used in FE simulations [134]

Material	Young's modulus (GPa)	Density (kg/m ³)	Poisson's ratio	Specific heat (J kg ⁻¹ °C ⁻¹)	Conductivity (W/(m°C))	Thermal expansion (µm.m/°C)
Ti-6Al-4V	109	4,430 (4.43e ⁻⁹)	0.34	3.9	17.2	25
Tungsten carbide insert	534	11,900 (11.9e ⁻⁹)	0.22	17.8	24	-

6.2.2 Constitutive model for work material

In FE simulation process, a constitutive material model is required to relate the strain rate, flow stress to strain and temperature. The Johnson-Cook [120] constitutive equation is employed to build the orthogonal FE model with material constant

obtained from literature review to study the behaviour of Ti-6Al-4V alloy during the machining process in dry and EHVSL environment conditions. This model describes flow stress as a product of high-temperature, strain and strain-rate dependent flow stress in FE simulation model. The J-C phenomenological constitutive model is successfully used for a variety of materials with different range of deformation temperature and strain-rate in finite element simulation modeling.

$$\bar{\sigma} = [A + B(\bar{\epsilon})^n] \left[1 + C \ln \left(\frac{\dot{\bar{\epsilon}}}{\dot{\bar{\epsilon}}_0} \right) \right] \left[1 - \left[\frac{T - T_r}{T_m - T_r} \right]^m \right] \text{-----} \quad (6.1)$$

Where ‘ $\bar{\sigma}$ ’ stands for flow stress, ‘A’ stands for yield stress at reference strain rate ($\dot{\bar{\epsilon}}_0$) and ‘ T_r ’ reference temperature (25°C), ‘B’ for coefficient of strain hardening, $\bar{\epsilon}$ for plastic strain, $\dot{\bar{\epsilon}}$ for strain rate and ‘ T_m ’ for melting temperature (1600°C).

Many researchers used J-C constitutive model for deformation behavior of metal alloys at high strain rate and temperatures, and identified the material constants from SHPB tests [141-146]. Among those, Lee and Lin [146] presented a J-C model for high temperature deformation behavior of a titanium alloy, Ti-6Al-4V; obtained from SHPB test results at a strain rate of 2000 s⁻¹, but, with temperature up to 1100°C. The J-C model parameter values which have been used to simulate the behaviour of Ti-6Al-4V alloy are specified in Table 6.2.

Table 6.2: Ti-6Al-4V material constants for J–C constitutive model [120]

J-C Model	A (MPa)	B (MPa)	C	m	n
Ti-6Al-4V	860	683	0.035	1	0.47

6.2.3 Damage model

The damage model is incorporated as a chip separation along with the material model in the damage zone in order to study the chip formation behavior in FEA machining process. Damage criterion is referred to as material state at onset of damage zone. The J-C model is used to model the failure model or damage evolution and predict failure in many engineering materials. The damage criteria is modeled in ABAQUS/Explicit and the damage parameter is defined as the ratio of sum of increments in the equivalent plastic strain $\Delta\bar{\epsilon}^p$ to the sum of fracture strain ϵ^f as shown in Eq. 6.2.

$$\omega_D = \sum \frac{\Delta\bar{\epsilon}^p}{\epsilon^f} \text{-----} \quad (6.2)$$

The fracture strain ϵ^f is expressed as follows [158]

$$\bar{\epsilon}_f = \left[D_1 + D_2 \exp\left(D_3 \frac{P}{\bar{\sigma}}\right) \right] \times \left[1 + D_4 \ln \frac{\dot{\epsilon}}{\dot{\epsilon}_0} \right] \times [1 + D_5 T^*] \text{-----} \quad (6.3)$$

$$T^* = \frac{T - T_0}{T_{melt} - T_0} \text{-----} \quad (6.4)$$

Where D_1, D_2, D_3, D_4, D_5 are material failure constants, ‘ T ’ is the current process temperature, ‘ T_0 ’ is the ambient temperature, ‘ T_{melt} ’ is the melting temperature of the workpiece, $\frac{P}{\bar{\sigma}}$ is the ratio of stress to von Mises stress, $\dot{\epsilon}_0$ is reference strain rate, $\dot{\epsilon}$ is the plastic strain rate.

The damage parameters are determined using tensile and torsion tests [158]. Material damage attributes to the complete damage of load carrying capacity which results from progressive degradation of material stiffness [158]. J-C damage model constants for Ti-6Al-4V alloy are listed in Table 6.3.

Table 6.3: J-C failure parameters for Ti-6Al-4V alloy [157]

J-C Model	D1	D2	D3	D4	D5
Ti-6Al-4V	-0.09	0.25	-0.5	0.014	3.87

During the FE simulation process, the energy based failure parameters is improved in one simulation condition in order to understand the different parameters (system parameters), later, the numerical analysis of turning tests is applied to other cutting processes based on same failure criteria to predict experimental results.

6.2.4 FE machining simulation procedure

The study by Ambati et al. [160] mainly concentrated on the cutting process simulation parameters. It was reported that the most influencing constituent in the process of cutting simulation is the size of element. To investigate the effect of mesh size on the cutting process simulation, FE analysis was carried out with adiabatic assumptions based on plastic deformation failure criterion. In the current study, the simulation model (based on ductile failure energy criterion) was created to keep the density of failure energy invariant, which makes the simulation results independent of the characteristic length. The FE simulation procedure is as shown by the flow chart in Fig. 6.2. Further, an attempt was made to modify failure energy criterion until the simulation results (cutting force and chip thickness) show a good agreement with the experimental results. The failure energy which is related with characteristic length ‘L’ is modified until the difference between the predicted and measured cutting forces is minimized.

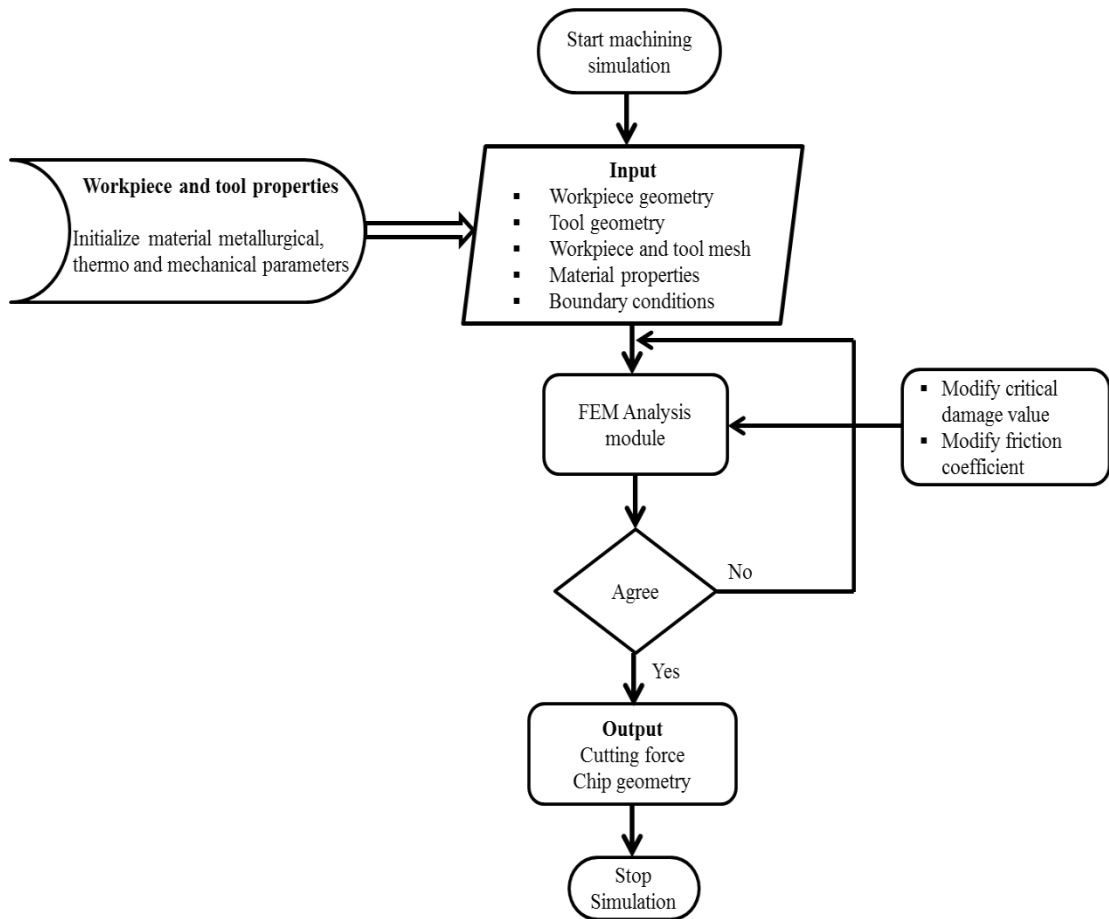


Fig. 6.2: Flow chart of FEA prediction model of Ti-6Al-4V alloy machining

6.2.5 FEA modeling and simulation of orthogonal turning

In order to validate orthogonal simulation model, the FE machining results with experimentally measured cutting force and chip thickness were compared and discussed. FE analysis of machining of Ti-6Al-4V alloy was made by using a J-C material model with an energy based ductile failure criteria. The geometry of the 2D orthogonal machining model is shown in Fig. 6.3. A typical refined mesh in the high deformation zone surfaces used at the initial geometry. It is defined in terms of feed rate (depth of cut) for dissimilar cutting conditions. Initially the workpiece is meshed with 12000 elements; the rigid tool is meshed and further divided into 1000 elements. The tool geometry consists of a 5° rake angle (γ) and 6° clearance angle (α).

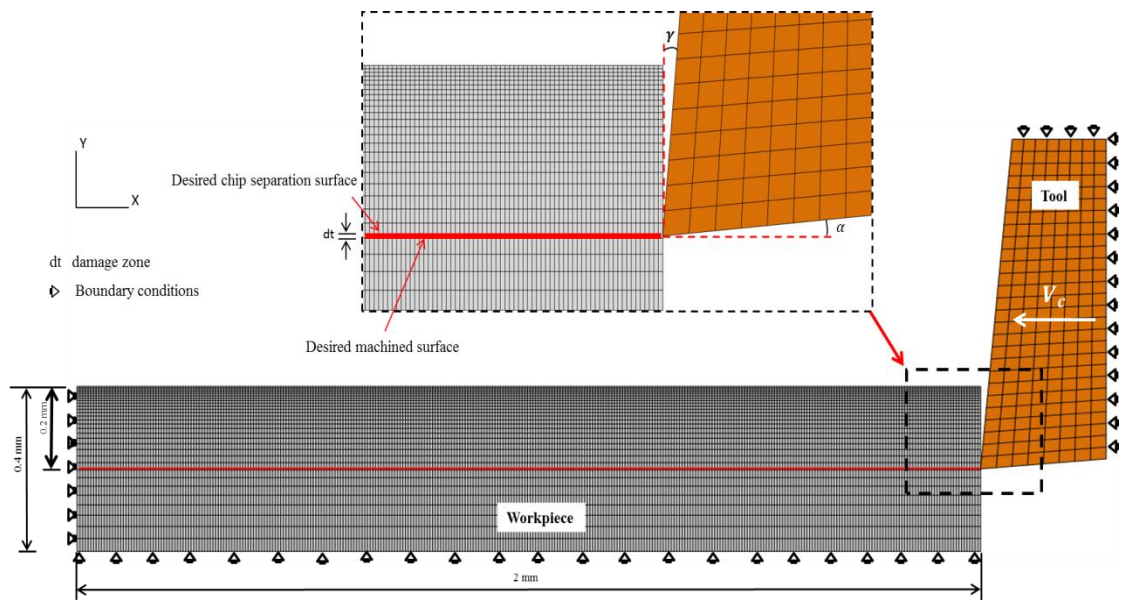


Fig. 6.3: The geometry of the 2D orthogonal cutting FE model

6.3 Simulation results and discussions

FEM simulation of machining process is proposed with same failure parameters in different cutting conditions (i.e. failure energy). The predicted results such as cutting forces, chip thickness when simulating the Ti-6Al-4V alloy machining process under dry and lubricant environments at different cutting conditions were compared with the experimental results.

6.3.1 Effect of cutting force

Determination of cutting force plays a vital role in the machining process in terms of estimation of cutting power consumption, which also enables selection of power sources during design of machine tools. Results obtained from the numerical simulation were validated by comparing with experimental results. Output parameters such as chip thickness and cutting force are helpful for making comparative analysis. Cutting force is chosen as the parameter for comparison between FE simulation and experimental results since internal output parameter, i.e. stress-strain distribution has

inherent complexities. The comparison between predicted cutting force and cutting force obtained by experiments, under lubricant condition for different speed and feed rate, is shown in Fig. 6.4. The variation in the cutting force has been shown in Fig. 6.4 to be related to the chip morphology. It is evident from Fig. 6.4 that the predicted cutting force shows approximately no deviation from the experimental results; increase in cutting force is attributed to increasing feed rate. This indicates that the J-C model with damage evaluation give an accurate and precise estimate of the flow behavior of Ti-6Al-4V alloy material under high strain rate condition and can be used to predictive process engineering to analyze the machining process.

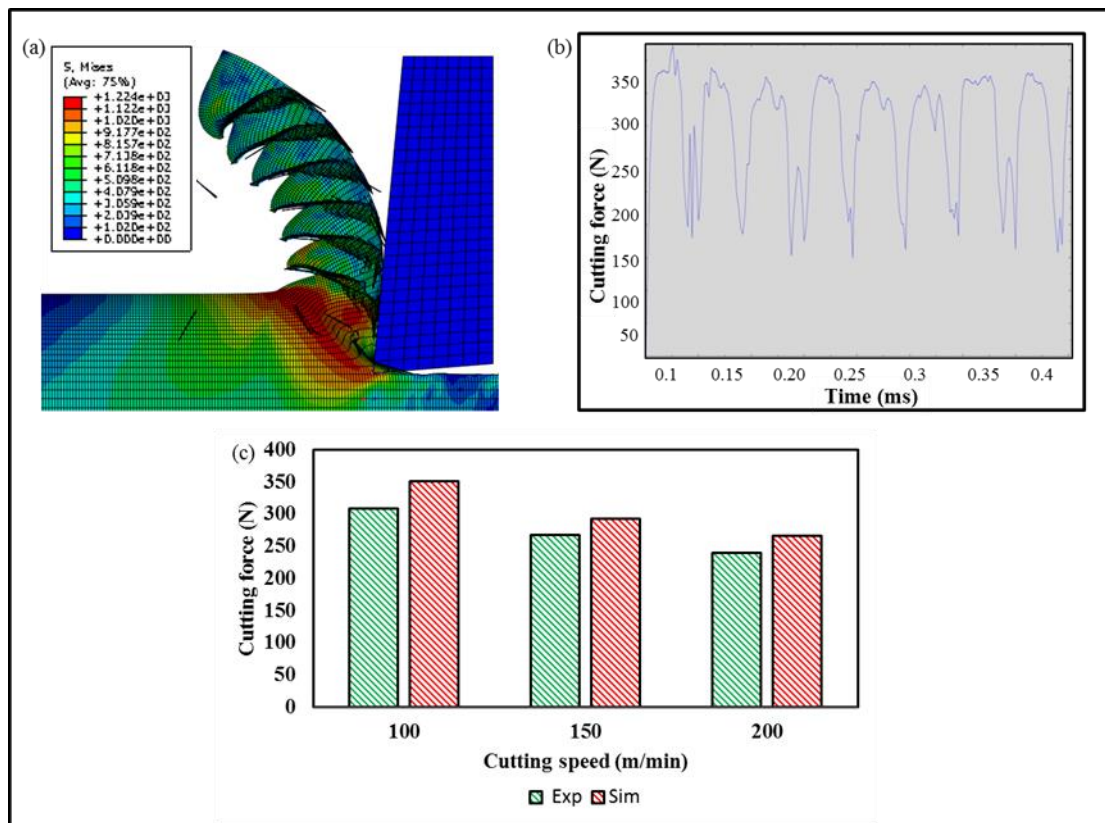


Fig. 6.4: FEM Simulation (a) chip formation (b) predicted cutting force under lubrication condition (c) comparison between experimental and simulation cutting force at different cutting speeds ($f = 0.1$ mm/rev)

It can be observed from the obtained results that the agreement between the measured and predicted results of cutting force when machining Ti-6Al-4V alloy under lubricant conditions is reasonably good as the relative error is low at all considered speed and feed conditions. It is observed that during lubrication condition yield saw teeth chips were formed; whereas in dry cutting condition wavy chips were formed. Despite, under dry condition, at cutting speed of 150 m/min, the estimated cutting force being larger from the experimental value; the prediction error observed is 14% compare with experimental results. It can be concluded here that the proposed FE machining simulation allows to predict accurate cutting forces and is helpful in better understanding of the physical cutting process variables and to relate the same with practical conditions of machining process before resorting to costly and time consuming experimental trials. Fig. 6.5 and Fig. 6.6 show the experimental and numerical predictions of the cutting force when machining Ti-6Al-4V alloy with lubricant condition at different cutting speeds and feed rate.

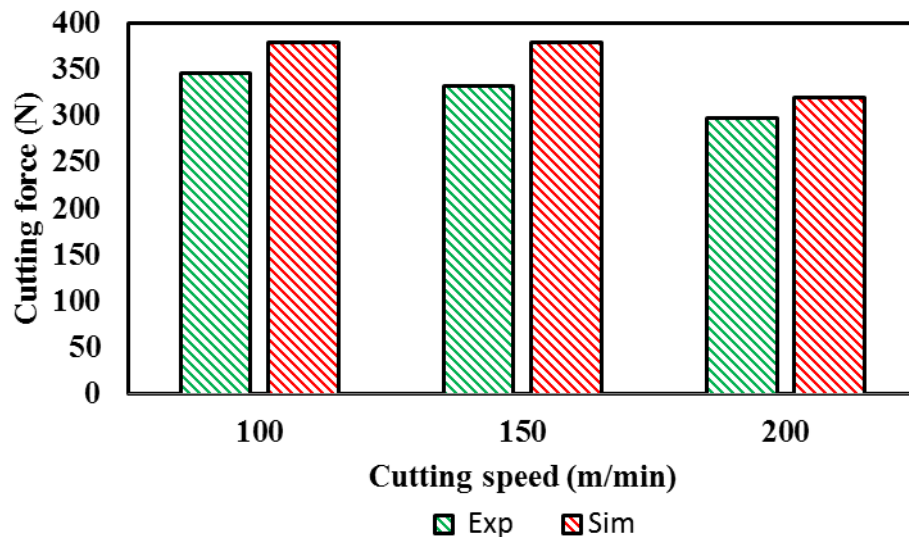


Fig. 6.5: Comparison of experimental and FE simulated cutting force during Ti-6Al-4V alloy machining under lubricant at different cutting speeds ($f = 0.15$ mm/rev)

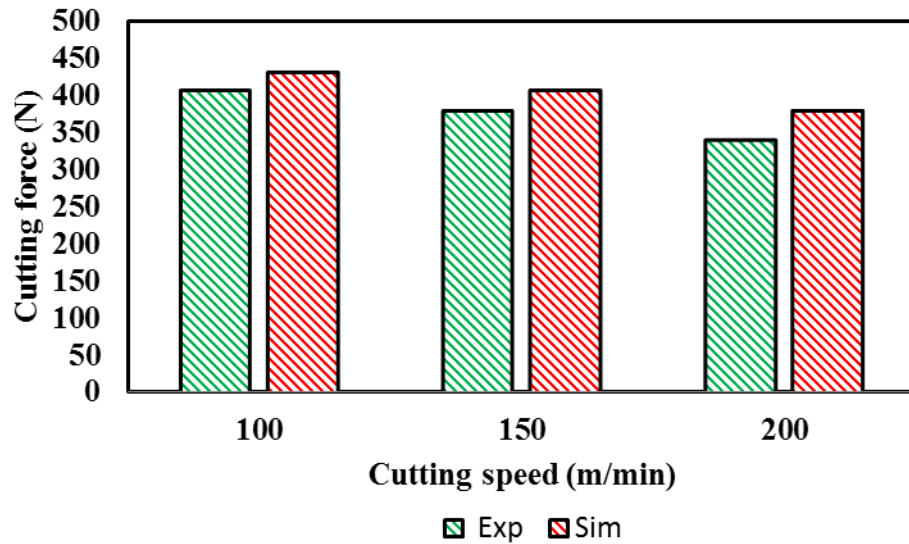


Fig. 6.6: Comparison of experimental and FE simulated cutting force during Ti-6Al-4V alloy machining under lubricant at different cutting speeds ($f = 0.2$ mm/rev)

Fig. 6.7 shows the overall distribution of equivalent von Mises stresses, von Mises equivalent strains and temperature distribution during the tool-workpiece interaction under lubricant condition. The type of chip formed depends largely on the distribution of strain. In the present study, from the Fig. 6.7 it is observed that strains are highly localized in the shear zone; therefore there is a uniform stress and strain over the entire chip formation. As the rate of heat generation is determined by strain rate, localized heating occurs due to plastic deformation in the shear plane [158]. Consequently, the high temperature near the tool tip begins to extend towards the chip free side in a highly localized zone. Chen et al. [157] observed that with the increase in the temperature in workpiece is one of the reason that cause residual stresses to become more tensile. It was observed during FE simulation of dry machining process that the maximum cutting temperature accomplished as 1000°C .

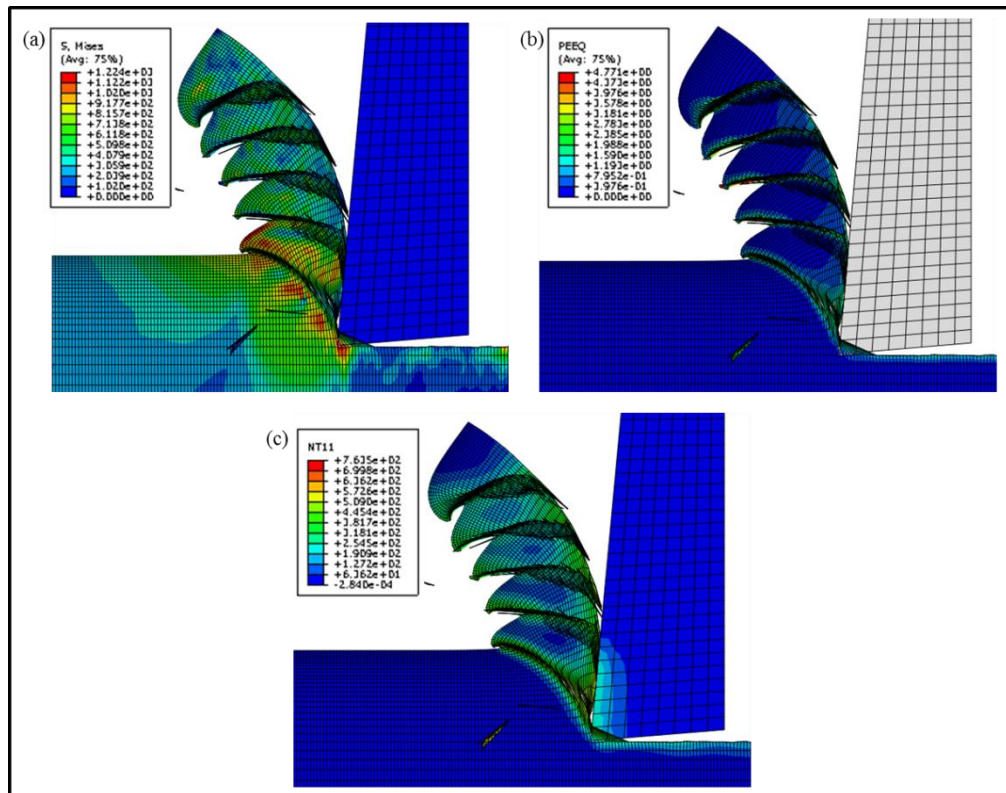


Fig. 6.7 Distribution of (a) stress (b) strain and (c) temperature under lubricant condition while machining Ti-6Al-4V alloy at $V_c=100$ m/min and $f = 0.1$ mm/rev

The simulation results indicate that the J-C material model and energy-based failure FE model used in this research has given a good prediction of cutting force under different cutting conditions. It can be concluded that the proposed FE model allows to accurately predict the cutting force, enhances the understanding of physical cutting process variables and to relate the same with practical conditions of machining process before resorting to costly and time consuming experimental trials. Fig. 6.8 shows the predicted cutting force under dry condition, and comparison between experimental and simulation cutting force cutting speed = 100 m/min at different feed rates (feed rate = 0.1 mm/rev). Comparison of predicted and measured cutting force under dry condition at different cutting speed and feed rate are shown in Fig. 6.9-6.10.

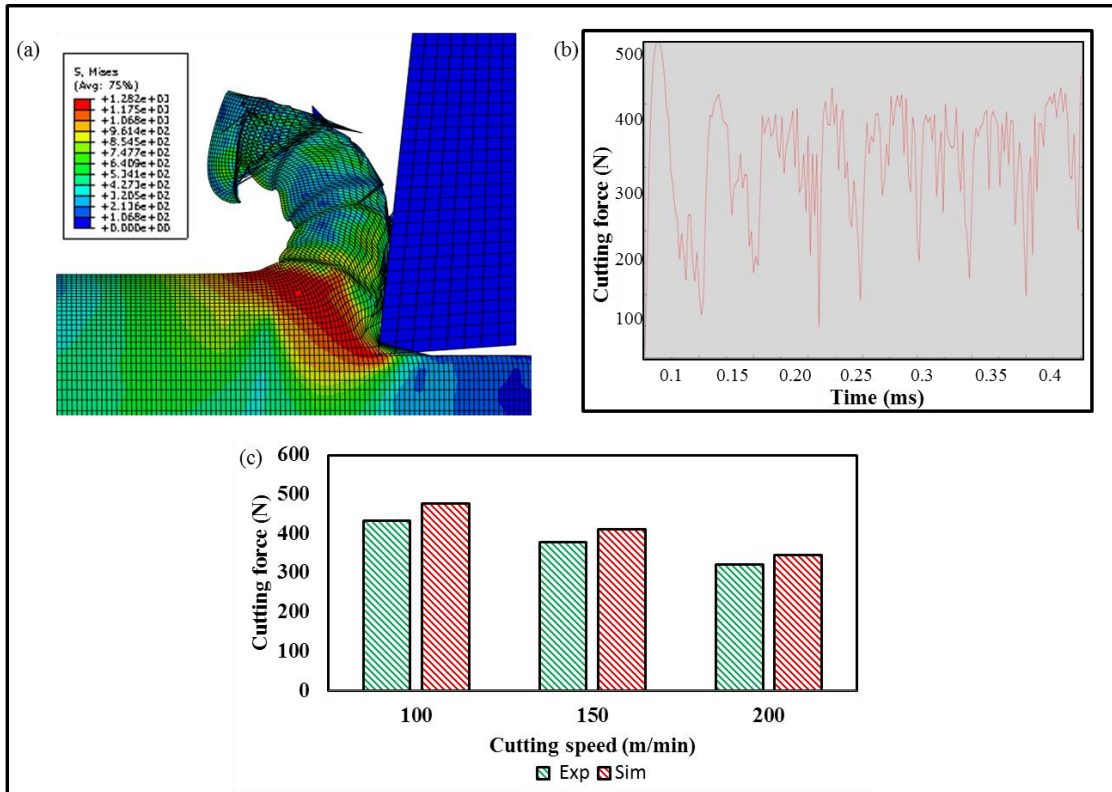


Fig. 6.8: FEM Simulation (a) chip formation (b) predicted cutting force under dry condition (c) comparison between experimental and simulation cutting force at different cutting speeds ($f = 0.1$ mm/rev)

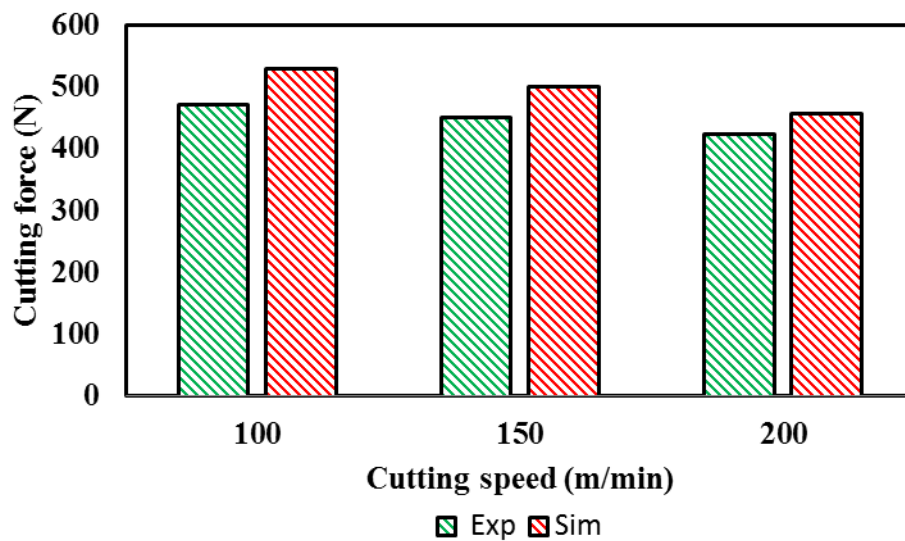


Fig. 6.9: Comparison of experimental and FE simulated cutting force during Ti-6Al-4V alloy machining under dry at different cutting speeds ($f = 0.15$ mm/rev)

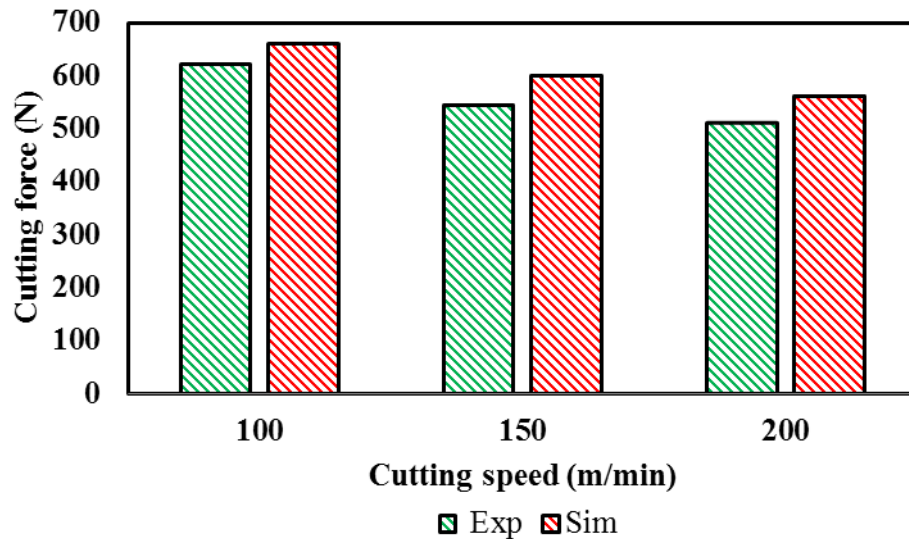


Fig. 6.10: Comparison of experimental and FE simulated cutting force during Ti-6Al-4V alloy machining under dry at different cutting speeds ($f = 0.2$ mm/rev)

Fig. 6.11 shows the overall distribution of equivalent von Mises stresses, von Mises equivalent strains and temperature distribution during the tool-workpiece interaction under lubricant condition. It was observed that when continuous chip is produced, the heat generated near the tool rake face is quite uniform; whereas in case of segmented chips produced the temperature along the rake face is not uniform. It was observed that the shear stress has a similar trend to decrease with increase in cutting speed. It was observed that the shear stress has a similar trend to decrease with increase in cutting speed. Fig. 6.11 shows that the temperatures increase gradually at the time of bulging of the chip segment but increases rapidly once the shear banding begins to form. The results revealed that as the cutting speed increases tool-chip contact temperature decreases in lubricant condition, whereas in dry condition cutting temperature increases gradually.

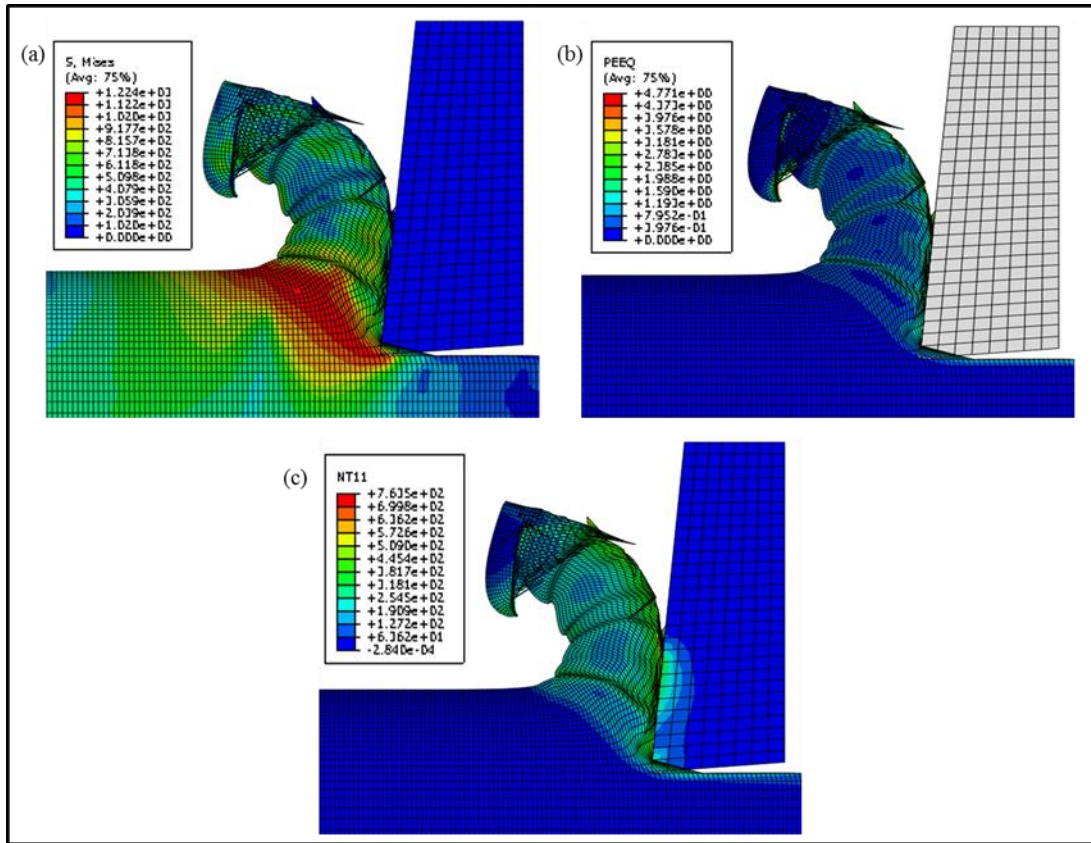


Fig. 11: Distribution of (a) stress (b) strain and (c) temperature under dry condition while machining Ti-6Al-4V alloy at $V_c=100$ m/min and $f = 0.1$ mm/rev

6.3.2 Effect of chip thickness

Chip thickness is another important parameter that can be readily monitored and measured. In the current research work, chip thickness was characterized by comparing the experimentally measured chip thickness with the FE simulation results. The comparison of predicted and experimental (Chapter 5) chip thickness when machining Ti-6Al-4V alloy with lubricant conditions at different cutting conditions is shown in Fig. 6.12-6.14. As shown in Fig. 6.12, the predicted and measured chip geometry parameters are similar when J-C model is considered. It is noticed that continuous chip thickness exists in both the simulated and experimental results during machining with dry and lubricant condition. Fig. 6.13-6.14 shows the comparison of experimental and FE simulated chip thickness during Ti-6Al-4V alloy machining

under lubricant condition. At low feed rate, the chip thickness is thinner. Further, in lubrication condition, another main function of cutting coolants is to carry the chips away from the cutting zone. Under the effect of lubricant spray process, it will remove chips within a short period of time, and it causes a large amount of heat to be taken away from chip-tool interface.

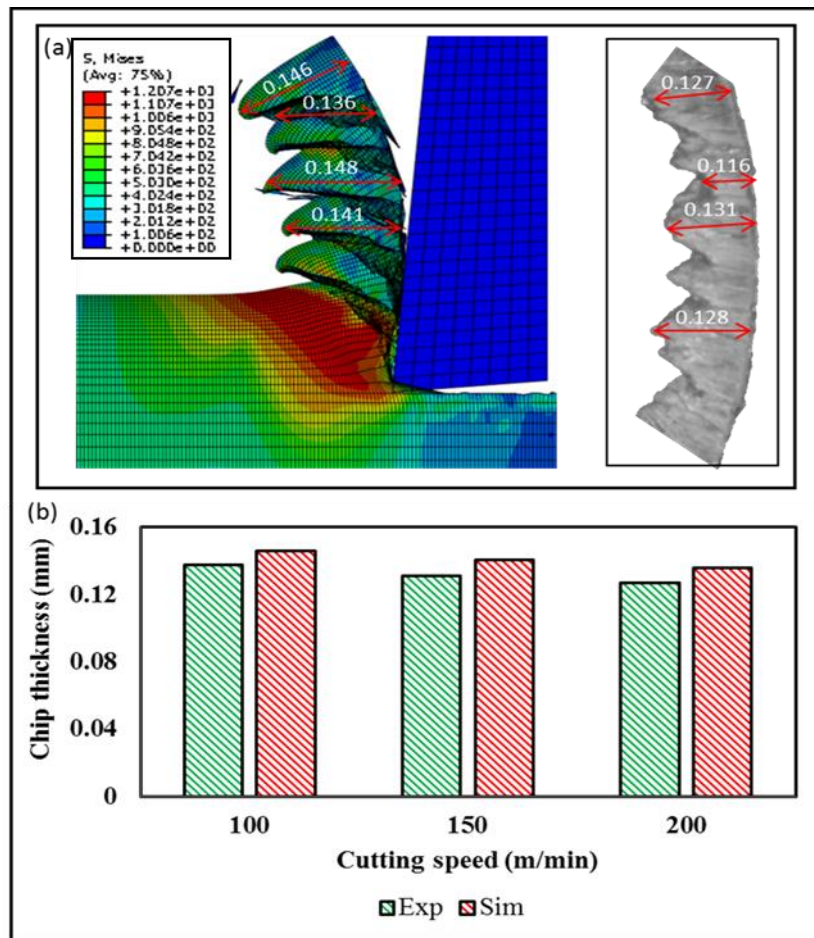


Fig. 6.12: (a) Comparison of simulated and experimental captured chip formation (b) comparison between experimental and simulation chip thickness under lubricant condition at different cutting speeds (cutting feed = 0.1 mm/rev)

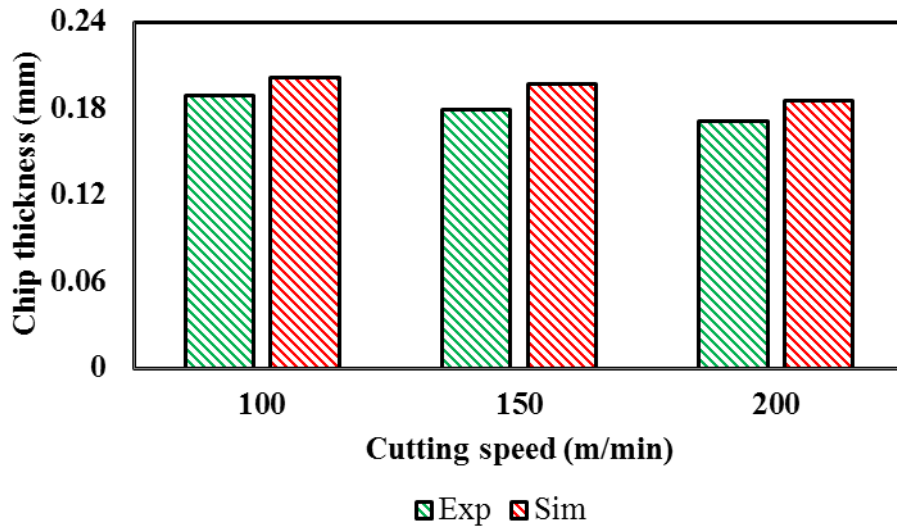


Fig. 6.13: Comparison of experimental and FE simulated chip thickness during Ti-6Al-4V alloy machining under lubricant condition at different cutting speeds ($f = 0.15$ mm/rev)

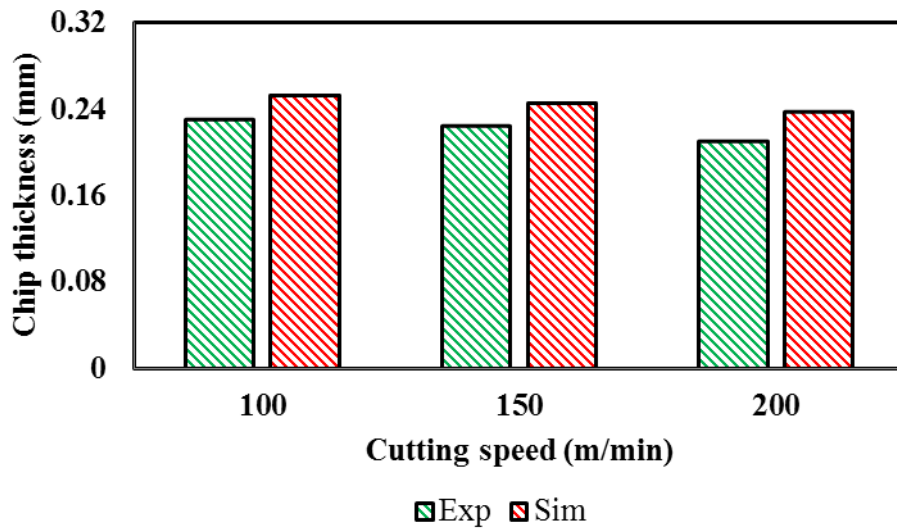


Fig. 6.14: Comparison of experimental and FE simulated chip thickness during Ti-6Al-4V alloy machining under lubricant condition at different cutting speeds ($f = 0.2$ mm/rev)

Further, the chips under higher cutting speed become more difficult to deform with the increase in chip thickness. It was observed from Fig. 6.15-6.17 that dry condition chip thickness gradually decreases with the increase in cutting speed at the

feed rate of 0.2 mm/rev. It is observed that during lubrication condition saw teeth type chips were formed; whereas in dry cutting condition wavy type chips were formed. Because at higher feed rate more cutting temperature is generated during machining process with increase in cutting speed within the same machining time, this higher cutting temperature may make chips to deform easily from workpiece. It is also observed that irregularity disappears gradually when increasing cutting speed and uncut chip thickness leading to asymptotic periodic oscillations [125].

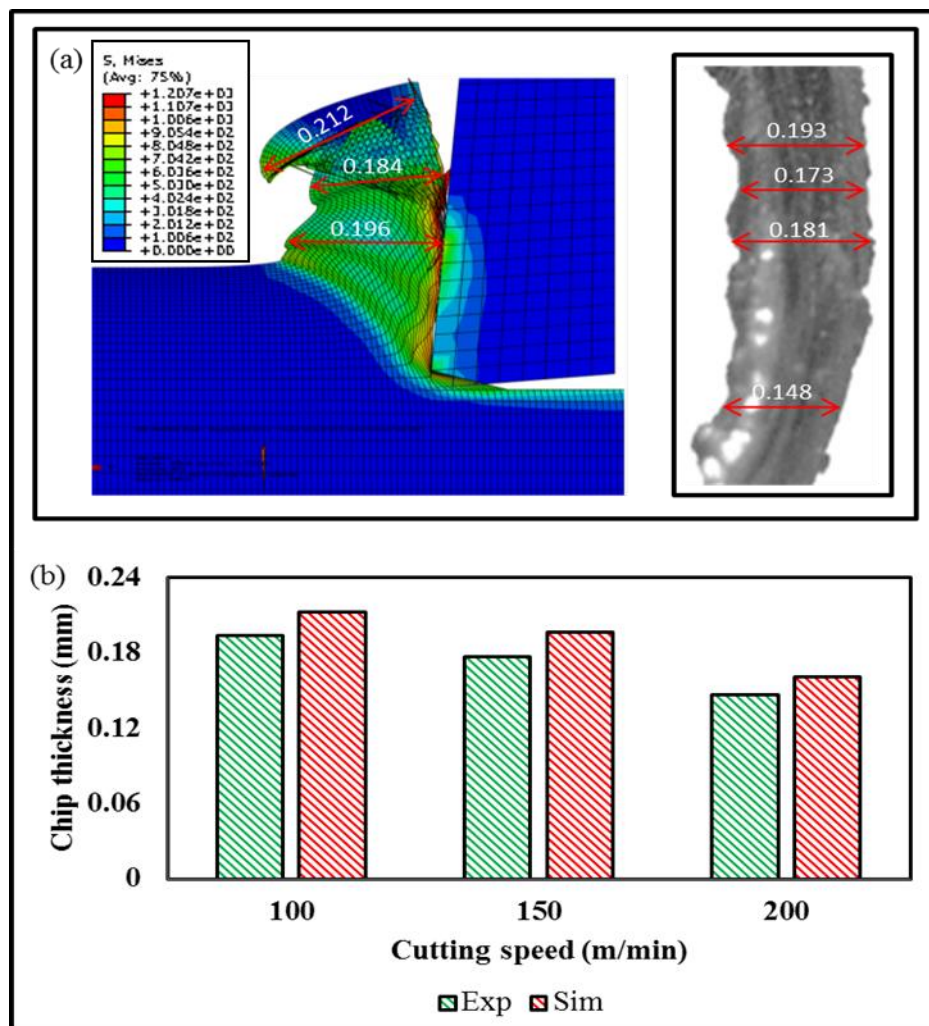


Fig. 6.15: (a) Comparison of simulated and experimental captured chip formation (b) comparison between experimental and simulation chip thickness under dry condition at different cutting speeds (cutting feed = 0.1 mm/rev)

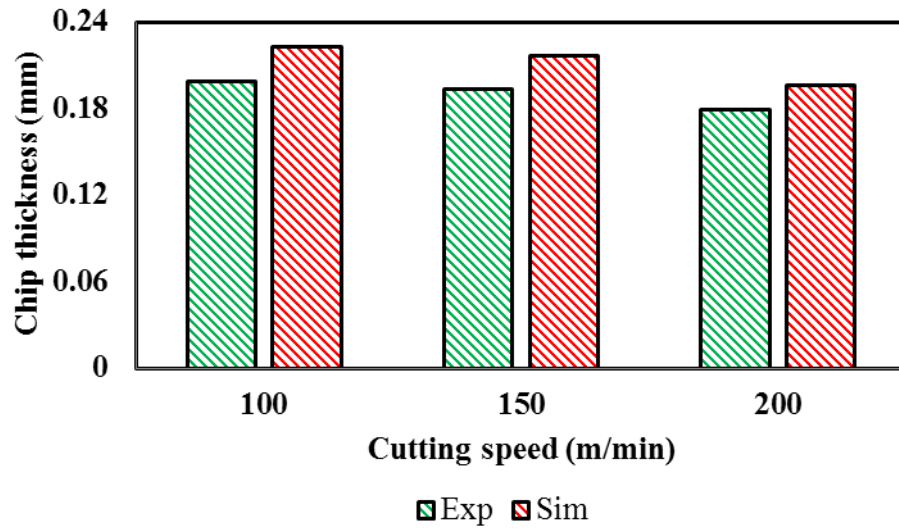


Fig. 6.16: Comparison of experimental and FE simulated chip thickness during Ti-6Al-4V alloy machining under dry condition at different cutting speeds ($f = 0.15$ mm/rev)

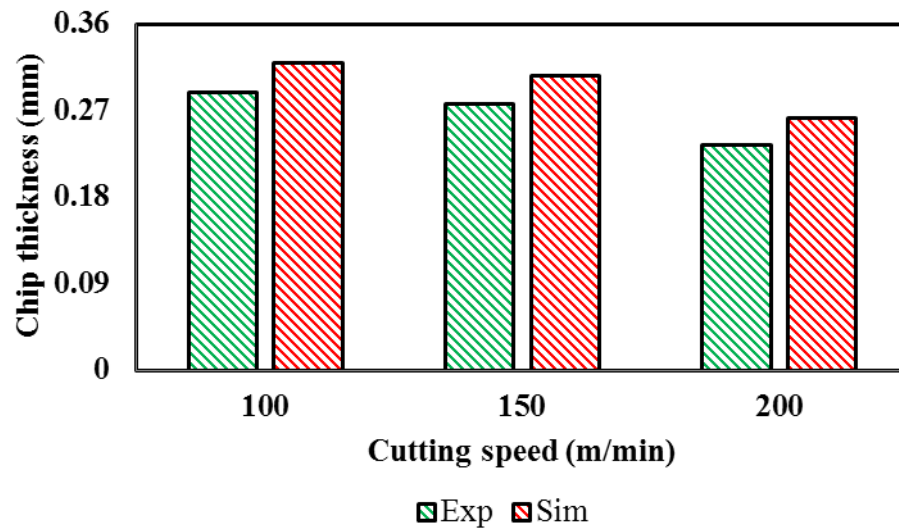


Fig. 6.17: Comparison of experimental and FE simulated chip thickness during Ti-6Al-4V alloy machining under dry condition at different cutting speeds ($f = 0.15$ mm/rev)

However, the good agreement obtained between the experimental and FE simulation results indicate that the proposed J-C model appears to be suitable for

studying the machining of Ti-6Al-4V. Finally, it results in decrease of chip thickness with the increase in cutting speed. Thus, it can be concluded that the proposed J-C model in this study can be employed to study the orthogonal machining process of Ti-6Al-4V alloy and to predict the actuality of the cutting force and chip thickness with satisfactory accuracy.

6.4 Summary

In the present chapter, machining simulations have been investigated under dry and lubrication at different cutting conditions. The FE simulation results obtained during machining of Ti-6Al-4V alloy in this section is useful in perspective the fundamental mechanism that may be liable for the formation of segmented chip formation. The variation of cutting force and chip thickness with different cutting speed and feed rates are investigated. The machining simulations of Ti-6Al-4V alloy have given detailed information of the cutting process. In the present study J-C material model with an energy based damage criteria is utilized to simulate the machining of Ti-6Al-4V alloy. The percentage error observed between the experimental and FE simulated results of cutting force is approximately 10% when machining with and without lubrication conditions. Further, for all the cutting conditions and with both machining environment, it was observed that the average chip thickness values from machining tests reasonably agree with the FE simulation results. Comparison between the experimental and estimated cutting force and chip thickness has been predicted with good accuracy.

CHAPTER 7

CONCLUSIONS AND FUTURE WORK

7.1 Summary

Machining of hard turning has received substantial attention due to its increasing use in various industrial applications. Research in this area is intended to improve the hard turning process so as to achieve the required conditions for best possible surface quality under given constraints. The current research work proposes novel methodology in developing electrostatic high velocity solid lubricant assisted machining process to apply lubricants effectively to the machining zone with a goal to improve the performance of machining process during turning of Ti-6Al-4V alloy. This research work addresses some of the problems associated with turning of Ti-6Al-4V alloy under different environmental conditions, and efforts have been made to study the influence of some of the critical factors such as cutting force, surface roughness and tool wear. The results would serve in understanding the process in a better way and provide inputs that can ensure better machining of Ti-6Al-4V alloy material. This was executed by conducting turning experiments over the recommended range of cutting parameters.

Chapter 1 is an introductory stage which briefly described about the current state of the research work.

Chapter 2 features review of literature related to the domain of current research and gaps are identified. This chapter covered the motivating factors behind this work and sets a path in the current direction.

Chapter 3 explained the complete fabrication of a novel experimental set-up to improve machining performance by eliminating the cutting fluid usage in

machining operation. It explains the improved methods by which solid lubricants can effectively be applied to machining zone. The investigation carried out to study the effect of optimum process parameters with the developed experimental set-up is reported in this chapter.

Chapter 4 covered tribological experiments (friction and wear) performed on various solid lubricant characteristics at different sliding conditions using pin-on-disc wear and friction monitor. It also investigated the tribological effect of particle size and concentration of MoS₂ solid lubricants. Development procedure of an experimental set-up to characterize the lubricant film behaviour between pin-disc interface is also explained in this chapter.

Chapter 5 is a detailed description about turning experiments conducted to study the performance of Ti-6Al-4V alloy with the developed EHVSL spray system set-up using MoS₂ as solid lubricant. During machining, heat is generated at the primary deformation zone and secondary deformation zone, but the temperature becomes maximum at the tool/chip interface. So, there is a need for controlling the cutting zone temperature within tolerable limits for achieving good machining performance. MoS₂ has been used as solid lubricants to reduce the friction between tool and workpiece, and thereby to reduce heat generation at tool and workpiece interface. A comparative performance analysis of MoS₂ assisted machining with MQSL, MQL, wet machining and dry machining experiments have been carried out in order to identify the ideal solid lubricant for machining Ti-6Al-4V alloy material. The surface roughness model was developed using cutting condition. The developed model has been compared using experimental data from turning of Ti-6Al-4V alloy. Estimation and comparison of machining performance was carried out using GMDH technique.

Chapter 6 focused on FEM simulation of deformation process of Ti-6Al-4V alloy during turning using Abaqus/Explicit 6.14 software. Further, for all cutting conditions and with both machining environment (EHVSL and dry), it is observed that the average chip thickness values from machining tests reasonably agree with FE simulation results. The predicted cutting forces are also found to be a good agreement with the experimental results.

7.2 Major contribution

The current research work influences the novel methodology in developing electrostatic high velocity solid lubricant assisted machining process to apply lubricants effectively to the machining zone with a goal to improve the performance of machining process during turning Ti-6Al-4V alloy. A significant outcome of this research work is that MoS₂ solid lubricants with low particle size and constant flow rate using electrostatic technique provide better performance compared to the existing machining techniques. Results obtained in the present work has been promising and highlighted the following important conclusions. Significant development has been made to reduce friction and wear with an optimum grain size and concentration of solid lubricant. An outstanding outcome of this research is that the solid lubricant with low particle size provided effective film thickness in comparison with higher particle size. Measured friction coefficient and wear rate results were plotted as a function of applied load for all lubrication conditions considered. In order to investigate the solid lubricant film thickness with respect to particle size, experiments were carried out on pin-on-disc tribometer. Estimation and comparison of machining performance were carried out using GMDH technique. Different models of GMDH were built by varying the number of data in the training set of 50%, 62.5% and 75% of the total data. The orthogonal turning of Ti-6Al-4V alloy is simulated with FEM based on the

constitutive model of Ti-6Al-4V alloy. The J-C model with an energy-based failure criterion is used to simulate the machining of Ti-6Al-4V alloy. The results obtained in the present work highlighted the following important conclusions.

- Performance evaluation of solid lubricant characteristics highlights that it is essential to have high viscosity, optimal and correct concentration of solid lubricants in base oil.
- Sliding properties have been improved with selected solid lubricants compared to dry sliding condition, however, solid lubricant suspension of MoS₂ (20%) in SAE 40 oil showed superior improvement of tribological properties compared to graphite (30%) and boric acid (30%).
- The non-polluting nature of solid lubricant is a clear distinctive advantage and is critical in making the choice for minimizing/eliminating the use of cutting fluid in various industries.
- Tribological tests results revealed that friction coefficient increases with increase in applied load for all considered environments. The analysis of wear morphology indicates that the suspension of solid lubricants decreases wear rate and results in a relatively smooth surface with fewer scars.
- It has been observed that the effectiveness of lubrication with solid lubricants will depend on the formation of a complete film protecting the surfaces. This formation surely will be processed by an orientation of the particles within the clearance between the sliding parts.
- MoS₂ suspensions with higher particle give higher wear values than that of MoS₂ with finer particles. This tendency is more pronounced at higher load conditions and thus smaller particles are capable of handling high load conditions with effective lubrication conditions.

- Continuous MoS₂ films have been observed with smaller particle size and lower concentration. Among the considered, lubricants 20% of MoS₂ in base oil provided better performance in terms of improvement in tribological properties and load carrying capacity.
- With the developed novel experimental set-up electrostatic high velocity solid lubricant (EHVSL) the concept of reducing or eliminating the use of cutting fluids in hard turning of Ti-6Al-4V has been successful with the application of MoS₂ as solid lubricant.
- Optimal process parameters of solid lubricant with developed experimental set-up provide the required amount of lubrication and cooling effect between tool and workpiece interface.
- The force component was drastically reduced in the domain of tested conditions. This substantial reduction can be attributed to the lattice layer structure of solid lubricants, which act as an effective lubricating film.
- To effectively supply MoS₂ solid lubricant particles and to considerably improve machining performance, EHVSL spray system is effective as an alternative technique compared to MQSL, MQL, flood cooling (wet) and dry machining process.
- Increase in the air pressure reduces size of the droplets and increases the number of lubricant droplets that lead to re-impinging of secondary droplets on the tool-workpiece interface. In turn the heat dissipation capability is reduced.
- The EHVSL technique has proved to be a versatile technique in terms of improving eco-friendly machining processes by reducing part cost, and quantity of lubricant. Product quality improvement has been achieved by effective penetration of lubricant into the rake face and flank face of the cutting tool.

- The overall machining performance during EHVSL technique was found to be superior to that of MQSL, MQL, wet, and dry turning, considering surface roughness, cutting force, tool wear as performance indices.
- The experimental results found that the chip thickness was less during MoS₂ assisted machining condition when compared to dry machining.
- Results from GMDH show that the regularity criteria function provides good estimation than the unbiased and combined criteria with least error of estimation and best fit was found for 75% of data in training set for surface roughness.
- The predicted chip morphology and cutting forces agree well with the experimental results, which indicates that even with variation of cutting speed, the energy-based damage failure criteria can give a good prediction for chip morphology and cutting force with same failure parameters.
- Comparison between the experimental and FEM simulation results shows that the cutting force and chip thickness have been predicted with good accuracy.

The results obtained highlighted that it was essential to apply lubricants selectively to the machining zone with considered environmental requirements towards finding out an improved method for specific hard turning of Ti-6Al-4V alloy. As a result, it was shown that with selected machining parameters and cooling/lubricant conditions, chip breakability is improved. The research work carried out clearly demonstrates cost effectiveness by abandonment of cutting fluid and, at the same time by improving economic, environmental and social performance with solid lubricants in the context of increasing industrialization.

7.3 Scope of future work

It would be interesting to continue the present investigation using various solid lubricants in order to standardize the performance of developed EHVSL spray system to further level, especially with different cutting tool and workmaterial groups.

Some possible ways to continue the research could be:

- To incorporate the parameters of tool geometry by considering rake angle, approach angle and nose radius along with cutting conditions to get combined influence of these parameters on cutting force, surface roughness, tool wear, and chip thickness during machining of hard-to-cut materials.
- A further improvement in process performance may be realized by introducing machining studies to characterize the thin fluid film in terms of its formation and the role of film thickness on the EHVSL spray system cooling and lubrication performance.
- In order to spread the application of developed EHVSL system machining studies with other hard to machine materials that experience similar machining performance related wear issues of titanium and its alloys (e.g. nickel-based alloys) to determine the potential breadth of application of this efficient cooling and lubrication system. Such a study could also reveal differences in mechanisms for different work materials.

References

- [1] E.O. Ezugwu, Z.W. Wang, Titanium alloys and their machinability - A review, *Journal of Materials Processing Technology*, 68 (1997), 262-274.
- [2] N.R. Dhar, M.W. Islam, S. Islam, M.A.H. Mithu, The influence of minimum quantity of lubrication (MQL) on cutting temperature, chip and dimensional accuracy in turning AISI-1040 steel, *Journal of Materials Processing Technology*, 171 (1) (2006), 93-99.
- [3] E.O. Ezugwu, Key improvements in the machining of difficult-to-cut aerospace super-alloys, *International Journal of Machine Tools and Manufacturing* 45 (2005), 1353–1367.
- [4] P.U.M. Reddy, M.Y. Ratnam, M.R Reddy, N.S.K. Reddy, Measurement and Analysis of Surface Roughness in WS₂ Solid Lubricant Assisted Minimum Quantity Lubrication (MQL) Turning of Inconel 718, *CIRP Procedia*, 40 (2016), 138-143.
- [5] S.I. Jaffery, P.T. Mativenga, Assessment of the machinability of Ti–6Al–4V alloy using the wear map approach, *International Journal of Advanced Manufacturing and Technology*, 40 (2009), 687-696.
- [6] A. Marques, N.S.K. Reddy, A.R. Machado, G.R. Kumar, J.S. Kumar, R.B.D. Silva, M.B. D. Silva, Performance assessment of MSQL: Minimum quantity solid lubricant during turning of Inconel 718, *Journal of Engineering Manufacture*, doi.org/10.1177/0954405415592128 (2015).
- [7] A.L. Baburao, A chip-tool interface lubrication technique for improvement in machinability of EN-31 steel, Aligarh Muslim University, PhD thesis report.
- [8] G.R. Kumar, N.S.K. Reddy, H.A. Kishawy, A Novel Technique to Achieve Sustainable Machining System, *Procedia CIRP*, 40 (2016), 31-34.
- [9] S. Vasim, Mist and microstructure characterization in end milling AISI 1018 steel using microlubrication, University of North Texas PhD thesis report.
- [10] B. Bhushan, *Modern Tribology Handbook*, CRC Press, New York, 2000.

- [11] H. Cohen, E.M. White, Metalworking fluid mist occupational exposure limits: a discussion of alternative methods, *Journal of Occupational and Environmental Hygiene*, 3 (2009), 501-507.
- [12] M. Lahres, P. Müller-Hummel, O. Doerfel, Applicability of different hard coatings in dry milling aluminium alloys, *Surface and Coatings Technology*, 91 (1-2) (1997), 116-121.
- [13] K. Sorby, K. Tonnessen, High pressure cooling of face-groove operations in Ti-6Al-4V, *Journal of Engineering Manufacture*, 220 (2006), 1621–1627.
- [14] K.A. Venugopal, S. Paul, A.B. Chattopadhyay, Tool wear in cryogenic turning of Ti-6Al-4V alloy, *Cryogenics*, 47 (2007), 12–18.
- [15] M. Rukosuyev, C.S. Goo, M.B.G. Jun, Understanding the effects of the system parameters of an ultrasonic cutting fluid application system for micro-machining, *Journal of Manufacturing Processes*, 12 (2010), 92–98.
- [16] A.V. Gopal, P.V. Rao, Performance improvement of grinding of SiC using graphite as a solid lubricant, *Materials and Manufacturing Processes* 19 (2) (2004) 177–186.
- [17] D. Mukhopadhyay, S. Banerjee, N.S.K. Reddy, Investigation to study the applicability of solid lubricant in turning AISI 1040 steel, *Transactions of the ASME*, 129 (2007), 520-526.
- [18] N.S.K. Reddy, P.V. Rao, Experimental investigation to study the effect of solid lubricants on cutting forces and surface quality in end milling, *International Journal of Machine Tools Manufacture*, 46 (2006), 189-198.
- [19] P.A. Viktor, *Tribology of Metal Cutting*, Mechanical Tribology, New York: Marcel Dekker, pp. 307-346, 2004.
- [20] T. Ozel, T. Altan, Modeling of high speed machining processes for predicted tool forces stresses and temperatures using FEM simulations, in: *Proceedings of the CIRP International Workshop on Modeling of Machining Operations*, Atlanta, GA, 1998.
- [21] T. Walker, *The MQL Hand Book*, Unist Inc. V1.0.3

- [22] D. Dudzinski, A. Devillez, A. Moufki, A review of developments towards dry and high speed machining of Inconel 718 alloy. *International Journal of Machine Tool Manufacture*, 44 (2004), 439-456.
- [23] N.A. Abukhshim, P.T. Mativenga, M.A. Sheikh, Heat generation and temperature prediction in metal cutting: A review and implications for high speed machining. *International Journal of Machine Tools and Manufacture*, 46 (2006), 782-800.
- [24] R.S. Pawade, S.S. Joshi, P.K. Brahmankar, Effect of machining parameters and cutting edge geometry on surface integrity of high-speed turned Inconel 718. *International Journal of Machine Tools and Manufacture*, 48 (2008), 15-28.
- [25] Sulzer, Product life cycle, Sulzer technical review, 1 (2013) 1-36.
- [26] M.C. Shaw, *Metal Cutting Principles*, 2nd edition, Oxford University Press, New York, (2005), 267-290.
- [27] I. Korkut, M.A. Donertas, The Influence of Feed Rate and Cutting Speed on The Cutting Forces, Surface Roughness and Tool-chip Contact Length during Face Milling, *Materials and Design*, 28 (1) (2007), 308-312.
- [28] P. Donguk, A. Patrica, Stewart, B.C. Joseph, Determinants of Exposure to Metalworking Fluid Aerosols: A Literature Review and Analysis of Reported Measurements, *Annals of Occupational Hygiene*, 53 (3) (2009), 271-288.
- [29] C. Howard, M.W. Eugene, Metalworking Fluid Mist Occupational Exposure Limits: A Discussion of Alternative Methods, *Journal Of Occupational And Environmental Hygiene*, 3 (9) (2006), 501-507.
- [30] F.S. Wisley, D.E. Anselmo, Á.R. Machado, Application of Cutting Fluids in Machining Processes, *Journal of the Brazilian Society of Mechanical Sciences*, 23 (2) (2001), doi.org/10.1590/S0100-73862001000200009.
- [31] D.P. Adler, W.W-S Hii, D.J. Michalek, J.W. Sutherland, Examining the Role of Cutting Fluids in Machining and Efforts to Address Associated Environmental/Health Concerns, *International Journal of Journal Machining Science and Technology*, 10 (1) (2006), 25-58.
- [32] A. Shokrani, V. Dhokia, S.T. Newman, Environmentally conscious machining of difficult-to-machine materials with regard to cutting fluids, *International Journal of Machine Tools and Manufacture*, 57 (2012), 83-101.

- [33] A.R. Machado, A.M. Abrão, R.T. Coelho, Theory of materials machining. 2nd ed. São Paulo, SP: Editora Edgar Blucher, 2011.
- [34] V.S. Sharma, Manu Dogra, N.M. Suri, Cooling techniques for improved productivity in turning, *International Journal of Machine Tools and Manufacture*, (2009) 435–453.
- [35] E.O. Bennett, Water based cutting fluids and human health, *Tribology International*, 16 (3) (1983), 133-136.
- [36] A.T. Simpson, M. Stear, J.A. Groves, M. Piney, S.D. Bradley, S. Stagg, B. Crook, Occupational Exposure to Metalworking Fluid Mist and Sump Fluid Contaminants, *The Annals of Occupational Hygiene*, 47 (1) (2003), 17-30.
- [37] H.S.E Books, Health Surveillance of Occupational Skin Diseases, MS 24, HSE Books, London, 1991.
- [38] M.M.A. Khan, M.A.H. Mithu, N.R. Dhar, Effects of minimum quantity lubrication on turning AISI 9310 alloy steel using vegetable oil based cutting fluid, *Journal of Materials Processing Technology*, 209 (2009) 5573–5583.
- [39] V. Jegatheesan, J.L. Liow, L. Shu, S.H. Kim and C. Visvanathan, The need for global coordination in sustainable development, *Journal of Cleaner Production*, 17 (7) (2009), 637-643.
- [40] F. Jovane, H. Yoshikawa, L. Alting, C.R. Boer, E. Westkamper, D. Williams, The incoming global technological and industrial revolution towards competitive sustainable manufacturing, *CIRP Annals - Manufacturing Technology*, 57 (2008), 641–659.
- [41] K. Weinert, I. Inasaki, J.W. Sutherland, T. Wakabayashi, Dry machining and minimum quantity lubrication, *CIRP Annals-Manufacturing Technology*, 2004, 53(2), 511-537.
- [42] J. StevenSkerlos, F. KimHayes, F. Andres Clarens, Fu Zhao, Current advances in sustainable metalworking fluids research, *Current Advances in Sustainable Metalworking Fluids Research*, 1 (1-2) (2008), 1-28.
- [43] Anselmo Eduardo Diniz, Ricardo Micaroni, Cutting conditions for finish turning process aiming: the use of dry Cutting, *International Journal of Machine Tools and Manufacture*, 42 (2002), 899-904.

- [44] P.S. Sreejith, B.K.A. Ngoi, Dry machining: Machining of the future, *Journal of Materials Processing Technology*, 101 (2000), 287-291.
- [45] F. Klocke, G. Eisennblatter, Dry cutting, *CIRP Annals - Manufacturing Technology*, 46 (2) (1997), 519-526.
- [46] N.S.K. Reddy and P.V. Rao, Selection of an optimal parametric combination for achieving better surface finish in end milling using genetic algorithms, *International Journal of Advanced Manufacturing Technology*, 28(5-6) (2006), 463-473.
- [47] B.C. Schramm, H. Scheerer, H. Hoche, E. Broszeit, E. Abele, C. Berger, Tribological properties and dry machining characteristics of PVD-coated carbide inserts, *Surface & Coatings Technology*, 188-189 (2004), 623-629.
- [48] P.U.M. Reddy, N.S.K. Reddy, Experimental investigation to study the effect of electrostatic micro-solid lubricant-coated carbide tools on machinability parameters in turning, *Proc IMechE Part B: Journal of Engineering Manufacture (SAGE)*, DOI: 10.1177/0954405414530903.
- [49] A. Attanasio, M. Gelfi, C. Giardini, C. Remino, Minimal quantity lubrication in turning: Effect on tool wear, *Wear*. 260 (2006) 333–338.
- [50] M. Rahman, A.S. Kumar, Mansoor-ul-salam, Evolution of minimal quantity of lubricant in end milling, *International Journal of Advanced manufacturing Technology*, 18 (2001), 235-241.
- [51] Z.J.F. Zhoua, H. Zhanga, Y. Wangb, W.J. Sutherland, Optimization of machining parameters considering minimum cutting fluid consumption, *Journal of Cleaner production*, 108 (Part A) (2015), 183-191.
- [52] G. Byrne, E. Scholta, Environmentally clean machining processes – a strategic approach, *CIRP Annals - Manufacturing Technology*, 42(1) (1993), 471–474.
- [53] A. Filipovic, D.A. Stephenson, Minimum quantity lubrication (MQL) applications in automotive power-train machining, *Machining Science and Technology: An International Journal*, 10 (1) (2006), 3-22.
- [54] A.S. Varadarajan, P.K. Philip, B. Ramamoorthy, Investigations on hard turning with minimal cutting fluid application (HTMF) and its comparison with dry and

- wet turning, *International Journal of Machine Tools and Manufacturing*, 42 (2002) 193–200.
- [55] A.R. Machado, J. Wallbank, The effects of a high pressure coolant jet on machining, *Journal of Engineering Manufacturing* 208 (1994) 29–38.
- [56] F. Klocke, G. Eisennblatter, Dry cutting, *CIRP Annals - Manufacturing Technology*, 46 (2) (1997), 519-526.
- [57] L.M. Barczak, A.D.L. Batako, M.N. Morgan, A Study of Plane Surface Grinding under Minimum Quantity Lubrication (MQL) conditions, *International Journal of Machine Tools and Manufacture*, 50 (11)(2010), 977-985.
- [58] N.S.K. Reddy, M. Yang, Development of an electro static lubrication system for drilling of SCM 440 steel, *Journal of Engineering Manufacture*, 224 (2) (2010), 217-224.
- [59] M.J. NurulAdlina, T. Kamaleshwaran, M. AhamdFairuz, I.A. Azwan, A study of surface roughness & surface integrity in drilling process using various vegetable-oil based lubricants in minimum quantity lubrication, *Australian Journal of Basic and Applied Sciences*, 8 (15) (2014), 191-197.
- [60] A.E. Diniz, A.J. Oliveira, Optimizing the use of dry cutting in rough turning steel operations, *International Journal of Machine Tools & Manufacture*, 44 (2004), 1061–1067.
- [61] C.P. Priarone, M. Robiglio, L. Settineri, V. Tebaldo, Milling and turning of titanium aluminides by using minimum quantity lubrication, *Procedia CIRP*, 24 (2014), 62-67.
- [62] Z.A. Zailani, R. Hamidon, M.S. Hussin, The influence of solid lubricant in machining parameter of milling operation. *International Journal of Engineering Science and Technology*, 3 (2011), 5221–5226.
- [63] P.V. Krishna, R.R. Srikant, D.N. Rao, Experimental investigation to study the performance of solid lubricants in turning of AISI1040 steel, *Journal of Engineering Tribology*, 224 (2010), 1273–1281.
- [64] B. Rahmati, A.A.D. Sarhan, M. Sayuti, Morphology of surface generated by end milling AL6061-T6 using molybdenum disulphide (MoS₂) nano-lubrication in end milling machining. *Journal of Clean Production*, 66 (2013), 685–691.

- [65] S. Dilbag, P.V. Rao, Performance improvement of hard turning with solid lubricants, *International Journal of Advanced Manufacturing Technology*, *International Journal of Advanced Manufacturing Technology*, 38 (2008) 529–535.
- [66] T. Obikawa, Y. Kamata, Y. Asano, Micro-liter lubrication machining of Inconel 718, *International Journal of Machine Tools and Manufacture*, 48 (2008), 1605–1612.
- [67] S.D. Deshmukh, S.K. Basu, Significance of solid lubricants in metal cutting, *Proceedings of 22nd All India Manufacturing Technology, Design and Research, (AIMTDR), Chennai, 2006*, 156-162.
- [68] P.V. Krishna, R.R. Srikant, D.N. Rao, Experimental investigation on the performance of nanoboric acid suspensions in SAE-40 and coconut oil during turning of AISI 1040 steel, *International Journal of Machine Tools & Manufacture*, 50 (10) (2010), 911-916.
- [69] N.S.K. Reddy, P.V. Rao, Performance improvement of end milling using graphite as a solid lubricant, *Journal Materials and Manufacturing Processes*, 20 (2005), 673–686.
- [70] H. Singh, I.B. Gulati, Tribological behaviour of base oil and their separated fractions, *Wear* 147 (1991) 207–218.
- [71] D.D. Fuller, *Theory and Practice of Lubrication for Engineers*, Wiley, New York, 1956.
- [72] I. Iliuc, *Tribology of Thin Layers*, Tribology Series Four, Elsevier, New York, 1980.
- [73] E.W. Roberts, Thin solid lubricant films in space, *Tribology International*. 23 (2) (1990) 95–104.
- [74] W. Gisser, H.A. Jehn, *Advanced Techniques for Surface Engineering*, Kluwer Academic Publishers, London, 1992.
- [75] C.H. Alexander, C. Nath, Characterization of fluid film produced by an atomization based cutting fluid (ACF) spray system during machining, *ASME 2013 International Manufacturing Science and Engineering Conference MSEC2013-1187* (2013) 1-10.

- [76] D. Dowson, History of Tribology, Second ed. Longman, New York, 1979.
- [77] T. Matthew Siniawski, N. Saniei, J. Pfaendtner, Tribological degradation of two vegetable-based lubricants at elevated temperatures, *Lubrication Science*, 24 (3) (2007) 167–179.
- [78] P.U.M. Reddy, N.S.K. Reddy, Investigation on wear behavior of electrostatic micro-solid lubricant coatings under dry sliding conditions ASME proceedings Design Materials and Manufacturing, IMECE2012-87201 (2012) 2105-2110.
- [79] N.H. Jayadas, K.P. Nair, G.A. Kumar, Tribological evaluation of coconut oil as an environment-friendly lubricant, *Tribology International*, 40 (2007) 350-354.
- [80] H. Singh, I.B. Gulati, Tribological behaviour of base oil and their separated fractions, *Wear*, 147 (1991) 207-218.
- [81] D.D. Fuller, Theory and practice of lubrication for engineers, Wiley, New York, 1956.
- [82] E.W. Roberts, Thin solid lubricant films in space, *Tribology International*, 23 (2) (1990) 95-104.
- [83] J.B. Wilfried, Some investigations on the influence of particle size on the lubricating effectiveness of molybdenum disulfide, *ASLE Transactions*, 15 (1971) 24-27.
- [84] H. Huang, An investigation on tribological properties of graphite nanosheets as oil additive, *Wear*, 261 (2) (2007) 140-144.
- [85] R.R. Sahoo, K.B. Sanjay, Deformation and friction of MoS₂ particles in liquid suspensions used to lubricate sliding contact, *Thin solid films*, 518 (2010) 5995-6005.
- [86] W.J. Bartz, Solid lubricant additives-effect of concentration and other additives on anti-wear performance, *Wear*, 17 (5-6) (1971) 421-432.
- [87] S. Odi-Owel, B.J. Roylance, The effect of solid contamination on the wear and critical failure load in a sliding lubricated contact, *Wear* 112 (1986) 239-255.
- [88] C. Zhao, The influence of solid additives on the tribological properties of lubricants, PhD thesis, University of Hertfordshire, Hatfield, UK, 2013.

- [89] P. Guoliang, G. Qiang, D. Jian, Z. Weidong, W. Xiaoming, Tribological behaviors of graphite/epoxy two-phase composite coatings, *Tribology International*, 43 (2010) 1318-1325.
- [90] L. Rapoport, Tribological properties of WS₂ nanoparticles under mixed lubrication, *Wear*, 255 (7) (2003) 785-793.
- [91] D.Y. Guo Chen, W. Chen, Z. Zhen, Effects of solid lubricants on hard turning. Ann. in: *Proceedings of the 2nd International Conference on Electronic and Mechanical Engineering and Information Technology*, (2012) 1147–1149.
- [92] A.H. Battez, R. González, D. Felgueroso, Wear prevention behaviour of nanoparticle suspension under extreme pressure conditions, *Wear*, 263 (7-12) (2007) 1568-1574.
- [93] Y. Epshteyn, J.R. Thomas, Molybdenum disulfide in lubricant applications a review, Presented at the 12th lubricating grease conference NLGI India, 28-30 (2010) 1-12.
- [94] D.N. Rao, P.V. Krishna, The influence of solid lubricant particle size on machining parameters in turning, *International Journal of Machine Tools & Manufacture*, 48 (2008), 107-111.
- [95] M.R. Richardo, M.B.D. Silva, A.R. Machado, W.F. Sales, The effect of application of cutting fluid with solid lubricant in suspension during cutting of Ti-6Al-4V alloy, *Wear*, 332-333 (2015) 762-771.
- [96] N.S.K. Reddy, N. Mohammed, The influence of solid lubricant for improving tribological properties in turning process, *Lubrication science*, 23 (2011) 49-59.
- [97] L.N. Sentyurikhina, G.A. Lutsenko, Milling of Molybdenum Disulfide and Graphite in impact-rebound mills, *Chemistry and technology of fuels and oils* 16 (2) (1980) 103-106.
- [98] M.J. Devine, E.R. Lamson, L. Stallings, Molybdenum disulfide diester lubricating grease, *Journal of national lubricating grease institute* 2005.
- [99] G.R. Kumar, N.S.K. Reddy, Tribological studies to analyze the effect of solid lubricant particle size on friction and wear behaviour of Ti-6Al-4V alloy, *Surface and Coating Technology*, 308 (2016), 203-212.

- [100] S. Ruhaidah, S. Puteh, A Time Series Forecasting Model Using Group Method Of Data Handling (GMDH),
- [101] S.Y. Liang, D.A. Dornfeld, Tool wear detection using the time series analysis of acoustic emission. Transactions of the ASME, Journal of Engineering, 110 (1989), 199-205.
- [102] G. Ugrasen, H.V. Ravindra, G.V. Naveen Prakash, Estimation of Machining Performances of P-20 Material in Wire Electric Discharge Machining using Group Method Data Handling Technique, 5th International & 26thAIMTDR 2014, IIT Guwahati, India, 537:1-6.
- [103] S.N. Mukherjee, S.K. Basu, Multiple regression analysis in evaluation of tool wear, International Journal of Machine Tool Design and Research, 7 (1), (1967), 15-21.
- [104] C.G. Onwubolu, P. Buryan, F. Lemke, Modeling tool wear in end-milling using enhanced GMDH learning networks, The International Journal of Advanced Manufacturing Technology, 39 (11) (2008), 1080-1092.
- [105] H.V. Ravindra, M. Raghunandan, Y.G. Srinivasa, R. Rishnamurthy, Tool wear estimation by group method of data handling in turning, International Journal of Production Research, 32 (6) (1994), 1295-1312.
- [106] T. Yoshida, K. Nagasaka, Y. Kita, Fumio Hashimoto, Identification of a grinding wheel wear equation of the abrasive cut-off by the modified GMDH, International Journal of Machine Tool Design and Research, 26 (3) (1986), 283-292.
- [107] G. Ugrasen, H.V. Ravindra, G.V. Naveen Prakash, R. Keshavamurthy, Comparison of Machining Performances Using Multiple Regression Analysis and Group Method Data Handling Technique in Wire EDM of Stavax Material, Procedia Materials Science, 5 (2014), 2215-2223.
- [108] R. Keshavamurthy, G. Ugrasen, R. Manasa, G. Narasimha, Estimation of Tribological Behavior of Al2024-TiB2 In Situ Composite Using GMDH and ANN, Applied Mechanics and Materials, 592-594 (2014), 1310-1314.
- [109] G. Ugrasen, H.V. Ravindra, G.V. Naveen, R. Keshavamurthy, Comparison of machining responses using multiple regression analysis and group method data

- handling technique of EN-19 material in WEDM, *Applied Mechanics and Materials*, 592-594 (2014), 97-101.
- [110] G. Onwubolu, *GMDH and implementation in C*, Imperial College Press, World Scientific Publishing Singapore, 2015.
- [111] Y.M. Zuhair Abu-Kheil, *System identification using Group Method of Data Handling, (GMDH)*, PhD Thesis report (2005).
- [112] Ozel, Tugrul, E. Zeren, Finite element modeling of stresses induced by high speed machining with round edge cutting tools, *ASME 2005 International Mechanical Engineering Congress and Exposition. American Society of Mechanical Engineers*, 2005.
- [113] M.R. Vaziri, M. Salimi, M. Mashayekhi, Evaluation of chip formation simulation models for material separation in the presence of damage models, *Simulation Modelling Practice and Theory*, 19 (2011), 718-733.
- [114] N. Banerjee, A. Sharma Development of a friction model and its application in finite element analysis of minimum quantity lubrication machining of Ti-6Al-4 V, 238 (2016), 181-194.
- [115] E.A. Flores-Johnson, S. Luming, G. Irene, G.D. Nguyen, Numerical investigation of the impact behavior of bioinspired nacre-like aluminum composite plates, *Composites Science and Technology*, 96 (2014), 13-22.
- [116] O. Kienzle, D.B.V. Krafft, *Leistungen an Spanenden Werkzeugen Werkzeugmaschinen, Z-VDI*, 94 (1995), 299-302.
- [117] M.E. Merchant, Basic Mechanics of the Metal Cutting Process, *Journal of Applied Mechanics*, 11 (1944), 168-175.
- [118] Y. Huang, S.Y. Liang, Modeling of Cutting Forces Under Hard Turning Conditions Considering Tool Wear Effect, *Journal of Manufacturing Science and Engineering*, 127 (2005), 262-270.
- [119] X. Lai, H. Li, C. Li, Z. Lina, J. Nib, Modelling and Analysis of Micro Scale Milling Considering Size Effect, Micro Cutter Edge Radius and Minimum Chip Thickness, *International Journal of Machine Tools & Manufacture*, (2008), 1– 14.

- [120] W.S. Lee, C.F. Lin, High-temperature deformation behaviour of Ti6Al4V alloy evaluated by high strain-rate compression tests, *Journal of Materials Processing Technology* 75 (1–3) (1998): 127–136.
- [121] K. Maekawa, T. Shirakashi, E. Usui, Flow stress of low carbon steel at high temperature and strain rate (Part 2), *Bull. Japan. Soc. Prec. Engr.* 17 (3) (1983) 167–172.
- [122] J. Rech, Y.C. Yen, M.J. Schaff, H. Hamdi, T. Altan, K.D. Bouzakis, Influence of cutting edge radius on the wear resistance, *Wear* 259 (2005) 1168–1176.
- [123] P.J. Arrazola, *Modélisation Numérique de la Coupe: Étude de Sensibilité des Paramètres et Identification du Frottement entre Outil-Copeau*, Ph.D. Thesis, E.C. Nantes, France, 2003.
- [124] T.O. Zel, Influence of friction models on finite element simulations of machining, *International Journal of Machine Tools and Manufacture* 46 (5) (2006) 518–530.
- [125] L. Filice, F. Micari, S. Rizzuti, D. Umbrello, A critical analysis on the friction modelling in orthogonal machining, *International Journal of Machine Tools and Manufacture* 47 (3–4) (2007) 709–714.
- [126] P.L.B. Oxley, *The mechanics of machining: An analytical approach to assessing machinability*, Ellis Horwood Limited, Chichester, (1989), UK.
- [127] G.R. Johnson, W.H. Cook, A constitutive model and data for metals subjected to large strains, high strain rates and high temperatures, *Proceedings of 7th International Symposium Ball*, Hague, The Netherlands, (1983) 541–547.
- [128] F.J. Zerilli, R.W. Armstrong, Dislocation-mechanics-based constitutive relations for material dynamics calculations, *Journal of Applied Physics*, 61 (1987), 1816–1825.
- [129] E. Usui, H. Takeyama, A photoelastic analysis of machining stresses, *ASME Journal of Engineering for Industry*, 82 (1960), 303–308.
- [130] B. Banerjee, The mechanical threshold stress model for various tempers of AISI 4340 steel”, *International Journal of Solids and Structures*, 44 (2007), 834–859.
- [131] J. Litonski, Plastic flow of a tube under adiabatic torsion, *Bulletin of Academy of Pol. Science, Ser. Sci. Tech.*, XXV (1977), 7.

- [132] K. Maekawa, T. Shirakashi, E. Usui, Flow stress of low carbon steel at high temperature and strain rate (Part 2)–Flow stress under variable temperature and variable strain rate, *Bulletin of Japan Society of Precision Engineering*, 17 (1983), 167–172.
- [133] T. Ozel, E. Zeren, Material Flow Stress and Tool-Chip Interfacial Friction Properties by Using Analysis of Machining, *Journal of Manufacturing Science Engineering*, 128 (1) (2006), 119.
- [134] D. Umbrello, Finite element simulation of conventional and high speed machining of Ti6Al4V alloy, *Journal of Materials Processing Technology* 196 (1–3) (2008): 79-87.
- [135] Z.G. Wang, M. Rahman, Y.S. Wang, Study on orthogonal turning of titanium alloys with different coolant supply strategies.
- [136] N.S.K. Reddy, M. Nouari, M. Yang, Development of electrostatic solid lubrication system for improvement in machining process performance, *International Journal of Machine Tools and Manufacture*, 50 (2010), 789–797.
- [137] S.W. Li, Y.P. Wang, Y. Wang, H.L. Kui, R.B. Zhou, An electrostatic atomization to save fuel and reduce emissions, *Automotive Engineering*, 23 (2001), 283–286.
- [138] C. Ghanshyam, S. Bagchi, P. Kapur, Optimization of spray parameters in the fabrication of SnO₂ layers using electrostatic assisted deposition technique, *Journal of Electrostatics*, 71 (2013), 71:68–76.
- [139] S.E. Law, Agricultural electrostatic spray application a review of significant research and development during the 20th century, *Journal of Electrostatics* 51-52 (2001), 25–42.
- [140] X. Liu, W.J. Xu, J. Sun, Experimental research on the dry electrostatic cooling assisted machining for hardened steel, *Advanced Material Research* 189-193 (2011), 3026–30.
- [141] S. Singh, B.C. O’Neill, A.W. Bright, A parametric Study of Electrostatic Powder Coating, *Journal of Electrostatics*, 4 (4) (1978), 325-334.
- [142] S. Singh, Charging Characteristics of Some Powders used in Electrostatic Coating, *IEEE Transactions on Industry Applications*, IA-17 (1) (1980), 121-124.

- [143] A. Gomez, K. Tang, Charge and fission of droplets in electrostatic sprays, *Physics of Fluids*, 404 (6) (1994); doi: <http://dx.doi.org/10.1063/1.868037>.
- [144] I. Iliuc. *Tribology of thin layers*, Tribology series four. Elsevier: New York, 1980.
- [145] P.V. Krishna, D.N. Rao, Performance evaluation of solid lubricants in terms of machining parameters in turning, *International Journal of Machine Tools & Manufacture*, 48 (2008), 1131-1137.
- [146] A. Cambiella, J.M. Benito, C. Pazos, J. Coca, M. Ratoi, H.A. Spikers, The effect of emulsifier concentration on the lubricating properties of oil-in-water emulsions, *Tribology Letters* 22 (2006), 53–65.
- [147] P.V. Krishna, R.R. Srikant, D.N. Rao, Solid lubricants in machining, *Proceedings of the Institution of Mechanical Engineers, Part J: Journal of Engineering Tribology*, 225 (4) (2011), 213-227.
- [148] N.E. Karkalos, N.I. Galanis, A.P. Markopoulos, Surface roughness prediction for the milling of Ti–6Al–4V ELI alloy with the use of statistical and soft computing techniques, *Measurement*. 90 (2016) 25-35.
- [149] S. Kalpakjain, *Manufacturing Process for Engineering Materials*, 3rd Edition, Addison-Wesley Longman Inc., 1997, California.
- [150] Z.Q. Liu, X. J. Cai, M. Chen, Q.L. An, Investigation of cutting force and temperature of end milling Ti-6Al-4V with different minimum quantity lubricant lubrication (MQL) parameters, *Journal of Engineering Manufacturing Part: B*. 225 (2011) 1273-1279.
- [151] E.M. Trent, P.K. Wright, *Metal Cutting*, 4th ed., Butterworth-Heinemann, Boston, MA, 2000.
- [152] N.S.K. Reddy, P.V. Rao, A Genetic Algorithmic Approach for Optimization of Surface Roughness Prediction Model in Dry Milling, *Machining Science and Technology (Taylor and Francis)*, 9(1), 63-84, 2005.
- [153] T.G.A. Raj, Analysis and optimization of machining process using evolutionary algorithms, Cochin University of Science and Technology, PhD thesis report, 2012.
- [154] N.S.K Reddy, P.V. Rao, Selection of optimum tool geometry and cutting conditions using a surface roughness prediction model for end milling,

- International Journal of Advanced Manufacturing Technology, 26 (11-12) (2005), 1202- 1210.
- [155] Tom Pepinsky, Jennifer Tobin, Introduction to Regression and Data Analysis, Stat Lab Introduction to Regression and Data Analysis Workshop, 2003.
- [156] P.Y. Chao, P.M. Ferreira, C.R. Liu, Applications of GMDH-type Modeling in Manufacturing, Journal of Manufacturing Systems, 7 (3), 241-253.
- [157] G. Chen, C. Ren, X. Yang, X. Jin, T. Guo, Finite element simulation of high-speed machining of titanium alloy (Ti-6Al-4V) based on ductile failure model, The International Journal of Advanced Manufacturing Technology, 56 (9) (2011), 1027-1038.
- [158] A. Priyadarshini, K. Surjya, K.A.K. Samantaray, Finite element modeling of chip formation during orthogonal machining, PhD Tesis report.
- [159] J. Hua, R. Shivpuri, Prediction of chip morphology and segmentation during the machining of titanium alloys, Journal of Material Processing Technology, 150 (2004), 124-133.
- [160] R. Ambati, H. Yuan, FEM mesh-dependence in cutting process simulation, International, Journal of Advanced Manufacturing Technology, 53 (1) (2011), 313-323.

LIST OF PUBLICATIONS

International Journals

1. Rakesh Kumar Gunda, Suresh Kumar Reddy Narala, Evaluation of Friction and Wear Characteristics of Electrostatic Solid Lubricant at Different Sliding Conditions, Surface and Coatings Technology (Elsevier). (Accepted for publication) (IF: 2.589)
2. Rakesh Kumar Gunda, Suresh Kumar Reddy Narala, Electrostatic high velocity solid lubricant machining system for performance improvement of turning Ti-6Al-4V alloy, Journal of Engineering Manufacture (SAGE) (2017). (IF: 1.366)
3. Rakesh Kumar Gunda, Narala Suresh Kumar Reddy, Tribological Studies to Analyze the Effect of Solid Lubricant Particle Size on Friction and Wear Behaviour of Ti-6Al-4V alloy, Surface and Coatings Technology (Elsevier), 308 (2016), 203-212. (IF: 2.589)
4. Rakesh Kumar Gunda, Narala Suresh Kumar Reddy, H.A. Kishawy A Novel Technique to Achieve Sustainable Machining System, Procedia CIRP (Elsevier), 40, 30-34, (2015).
5. A. Marques, Suresh Kumar Reddy Narala, A.R. Machado, Rakesh Kumar Gunda, Saravan Kumar Josyula, R.B. Da Silva, M.B Da Silva, Performance assessment of MQSL: Minimum quantity solid lubricant during turning of Inconel 718, Journal of Engineering Manufacture (SAGE), 231 (7), 1144-1159 (2015). (IF: 1.366)

Publications in International conference proceedings

1. Rakesh Kumar Gunda, Suresh Kumar Reddy Narala, Evaluation of Friction and Wear Characteristics of Electrostatic Solid Lubricant at Different Sliding Conditions, 44th International Conference on Metallurgical Coatings and Thin Films (ICMCTF), (24th-28th April 2017), San Diego, California, USA.
2. Rakesh Kumar Gunda, Suresh Kumar Reddy Narala, New Cooling Approach for Tool Life Improvement with Minimal Quantity Solid Lubricant Machining of Ti-6Al-4V Alloy, 6th International & 27th All India Manufacturing Technology,

Design and Research Conference (AIMTDR-2016), Pune, India.

3. J. Sravan Kumar, G. Rakesh Kumar and N. Suresh Kumar Reddy, A Study for Selection of Cutting Parameters in Turning Process using Decision Making Method, 2014, International Conference on Advance Research and Innovations in Mechanical, Material Science, Industrial Engineering and Management (ICARIMMIEM-2014), Warangal, India.

Publications in National conference proceedings

1. Rakesh Kumar Gunda, Suresh Kumar Reddy Narala, Tribological Studies of Solid Lubricants on Ball-on-Disc Tribometer, Proceedings of 2nd DPLC Conference, BITS-Pilani Hyderabad Campus, Hyderabad, India.
2. Syed Adil, Rakesh Kumar G, N Suresh Kumar Reddy, Study of Tribological Characteristics of Tungsten Carbide and EN-31 Steel Combination under Different Environmental Conditions, Proceedings of 2nd DPLC Conference 2016, BITS-Pilani Hyderabad Campus, Hyderabad, India.
3. Bhasker Reddy Marri, Meghana M, Rakesh Kumar Gunda, Suresh Kumar Reddy Narala, Optimization of Milling Using Simulated Annealing and Artificial Neural Networks, Proceedings of 2nd DPLC Conference, BITS-Pilani Hyderabad Campus, Hyderabad, India.

BIOGRAPHY OF THE CANDIDATE

Name of the candidate	Rakesh Kumar G
ID. No.	2013PHXF0009H
Academic credentials	<ul style="list-style-type: none">• Ph.D. (pursuing from BITS-Pilani, Hyderabad Campus)• M.Tech in Design Engineering (KITS Warangal)• B.Tech in Mechanical Engineering (BIET, Ibrahimpatnam)• Intermediate in M.P.C (Sri Ramabadra Jr Collage, Hyderabad)• SSC, Ramnagar High School (Ramnagar, Hyderabad)
Personal details	Residential address: H.No: 1-7-630/31, Gemini Colony Ramnagar, Hyderabad – 500020 Contact Number: +91-9491883193 Email address: kumarrakeshgunda@gmail.com

BIOGRAPHY OF THE SUPERVISOR

Name of the Supervisor	Dr. SURESH KUMAR REDDY NARALA
Designation and address	Associate Professor, Department of Mechanical Engineering, BITS, Pilani, Hyderabad Campus
Experience (years)	17
Number of publications	Journals –25
	International Conferences –14
Number of citations	581
Sponsored projects	1. Performance evaluation of various coated drills based on wear and hole quality in dry drilling (Sponsor: Oerlikon Balzers) (Jan 2008 to Nov 2008)
	2. BITS-SG Project on “Development of novel coated tools for green machining”, Rs.11,80,000 (2011-2013).
	3. CSIR project on “Development of ES nano-solid lubricant coated tools for sustainable machining”, Rs.18,52,000. (2012-2015).
	4. DST project on “Novel minimal SLM application method for performance improvement in turning”, Rs. 40,16,174. (2013-2017).
	5. ISR project on “Studies related to control of porosity in casting”, Rs. 8,03,000 (2016-2019).
	6. DRDL project on “Novel Casting Approach to Improve Quality of Aluminum Alloy Casting: Hybrid Ultrasonic Assisted Bottom Pour Stir Casting Process”, Rs. 9,84,500 (2017-2020)
No. of PhD students completed	1
No. of Ph.D. students under in-progress	4

